

**SYNTHESIS, CHARACTERIZATION AND
ANTICANCER ACTIVITY OF
2-PYRIDINEFORMAMIDE DERIVED
THIOSEMICARBAZONES**



A THESIS SUBMITTED TO THE
CENTRAL DEPARTMENT OF CHEMISTRY
INSTITUTE OF SCIENCE AND TECHNOLOGY
TRIBHUVAN UNIVERSITY
NEPAL

FOR THE AWARD OF
DOCTOR OF PHILOSOPHY
IN CHEMISTRY

BY
BHUSHAN SHAKYA
MAY 2016

This page intentionally left blank

**SYNTHESIS, CHARACTERIZATION AND
ANTICANCER ACTIVITY OF
2-PYRIDINEFORMAMIDE DERIVED
THIOSEMICARBAZONES**



A THESIS SUBMITTED TO THE
CENTRAL DEPARTMENT OF CHEMISTRY
INSTITUTE OF SCIENCE AND TECHNOLOGY
TRIBHUVAN UNIVERSITY
NEPAL

FOR THE AWARD OF
DOCTOR OF PHILOSOPHY
IN CHEMISTRY

BY
BHUSHAN SHAKYA
MAY 2016

DECLARATION

This thesis entitled “**Synthesis, Characterization and Anticancer Activity of 2-Pyridineformamide Derived Thiosemicarbazones**” which is being submitted to Central Department of Chemistry, Institute of Science and Technology (IOST), Tribhuvan University, Nepal for the award of the degree of Doctor of Philosophy (Ph.D.), is a research work carried out by me under the supervision of Prof. Dr Paras Nath Yadav, Central Department of Chemistry, Tribhuvan University, Nepal.

This research work embodied in it is original and has not been submitted earlier in part or full in this or any other form to any university or institute, here or elsewhere, for the award of any degree.

.....

Bhushan Shakya

RECOMMENDATION

This is to recommend that **Bhushan Shakya** has completed Ph.D. thesis entitled “**Synthesis, Characterization and Anticancer Activity of 2-Pyridineformamide Derived Thiosemicarbazones**” for the award of Doctor of Philosophy (Ph.D.) in **Chemistry** under my supervision. To my knowledge, this work has not been submitted for any other degree.

He has fulfilled all the requirements laid down by the Institute of Science and Technology (IOST), Tribhuvan University, Kirtipur for the submission of the thesis for the award of Ph.D. degree.

.....

Dr. Paras Nath Yadav
Supervisor
Professor
Central Department of Chemistry
Tribhuvan University
Kirtipur, Kathmandu,
Nepal

May, 2016

त्रिभुवन विश्वविद्यालय
TRIBHUVAN UNIVERSITY
विज्ञान तथा प्रविधि अध्ययन संस्थान
Institute of Science and Technology



कीर्तिपुर, काठमाडौं, नेपाल ।
Kirtipur, Kathmandu, NEPAL.

रसायन शास्त्र केन्द्रीय विभाग
CENTRAL DEPARTMENT OF CHEMISTRY

पत्र संख्या:

Ref. No.:

CERTIFICATE OF APPROVAL

29/5/ 2016

On the recommendation of Prof. **Dr. Paras Nath Yadav**, this Ph. D. thesis work submitted by **Bhushan Shakya**, entitled “**Synthesis, Characterization and Anticancer Activity of 2-Pyridineformamide Derived Thiosemicarbazones**” is forwarded by Central Department Research Committee (CDRC) to the Dean, Institute of Science and Technology, Tribhuvan University.

Dr. Megh Raj Pokhrel
Professor,
Head,
Central Department of Chemistry
Tribhuvan University
Kirtipur, Kathmandu
Nepal

ACKNOWLEDGEMENTS

First and foremost, I would like to express my heartfelt thanks to my supervisor, Prof. Dr. Paras Nath Yadav for his inspiring guidance, generosity, encouragement and interminable supportive nature throughout the course of the research and in the preparation of this thesis.

Special thanks go to my friends: Dr. Suresh Awale, University of Toyama, Japan for biological materials, anticancer screenings and HRFAB mass spectral analysis, Dr. Krishna Gopal Dongol, NK Chemicals Pte. Ltd., Singapore for providing some of the necessary chemicals and Dr. Rajendra Kumar Shakya, Wayne State University, USA for IR and NMR measurements. I am very much thankful to the authorities of IIT, Madras, India for elemental analysis.

I deeply acknowledge the Head of Central Department of Chemistry Prof. Dr. Megh Raj Pokharel for providing all the available facilities in the Department. I owe to Prof. Dr. Rameshwar Adhikari and Prof. Dr. Amar Prasad Yadav for their help. My great appreciation and thanks also to all teaching and non-teaching staffs of Central Department of Chemistry for their kind co-operation and timely support during the tenure of my research work.

I would like to thank University Grants Commission of Govt. of Nepal for partial financial support for this research. I would also like to thank Amrit Science Campus, Thamel for permitting the study leave.

I appreciate my friends Prof. Dr. Pawan Raj Shakya, Dr. Gyan Hari Aryal, Dr. Nootan Bhattarai, Dr. Krishna Kattel, Rom Nath Baral, Paras Mani Yadav, my seniors Dr. Jageet Kaur, Dr. Bindra Shrestha, colleagues Dr. Sharmila Pradhan, Dr. Rajesh Pandit, Dr. Netra Lal Bhandari, Shanta Pokharel Bhattarai and Harish Chandra Subedi for their warm support and being there to boost up my confidence.

I also remember well wishers and all those persons who helped me directly or indirectly for preparation of this thesis.

Finally my parents deserve special mention for everything they have done for me. I can never forget my beloved brothers and sisters for their invaluable support and prayers. I have no words to express my feelings to my wife Samjhana, daughter Nairatma and son Achal for infinite love, patience, understanding and providing the comfort and support necessary to sustain the human psyche during the whole period of intense labour needed to complete this task.

.....
Bhushan Shakya

May, 2016

ABSTRACT

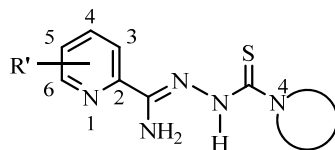
Cancer is the leading cause of death worldwide and is presently responsible for about 25% of deaths in developed countries and for 13% of deaths in developing countries. A suitable and well established target for cancer therapy is Ribonucleotide Reductase (RR), the key enzyme involved in reduction of ribonucleotides into deoxyribonucleotides during DNA synthesis. Heterocyclic Thiosemicarbazones (HCTs) are the most potent inhibitor of RR. Many HCTs have been synthesized and are found to be active against selected cell lines resistant to the clinically used drugs hydroxyurea and gemcitabine. There is need to improve the potency of drugs in clinical use and search for the new and more effective drug candidates.

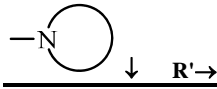
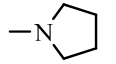
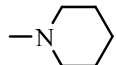
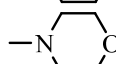
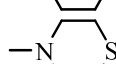
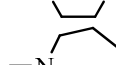
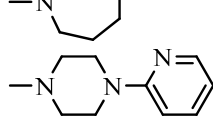
In this research work a series of 2-pyridineformamide thiosemicarbazones with variations in pyridyl ring and *N*(4)-substitution were synthesized through transamination reaction and characterized by partial elemental analysis, IR, ¹H- and ¹³C-NMR spectroscopic techniques and HRFAB mass spectrometry.

The synthesized compounds were evaluated for their anticancer activity against HeLa human cervical cancer cell line and also against PANC-1 human pancreatic cancer cell line utilizing antiausterity strategy. All the compounds exhibited potent cytotoxic activity. The compounds showed less potency against HeLa cells than the positive control paclitaxel. Conversely they exhibited potency higher than the controls paclitaxel and gemcitabine against PANC-1 cells under nutrient-deprived conditions. The potency of all compounds against PANC-1 cells under nutrient-deprived conditions was comparable with that of positive control arctigenin and nine of these compounds (compound no. **1**, **6**, **7**, **12**, **13**, **17**, **21**, **22** and **23**) were found to exhibit more potent preferential cytotoxicity than arctigenin.

Morphological assessment of *N'*-(4-(pyridin-2-yl)piperazine-1-carbonothioyl)picolinohydrazonamide (compound **6**) showed a dramatic alteration in the PANC-1 cell morphology in ethidium bromide (EB)/acridine Orange (AO) staining assay. It was found to induce apoptosis against PANC-1 cells which was further supported by annexin-V (AV)/propidium iodide (PI) fluorescence imaging assay.

The present study indicated that 2-pyridineformamide thiosemicarbazones can be considered as powerful antiausterity agents for the development of therapeutics against deadly pancreatic cancers.



	Compounds			
	H-	4-Me	5-F	6-Me
	1	7	13	18
	2	8	-	19
	3	9	14	20
	4	10	15	21
	5	11	16	22
	6	12	17	23

Key words : Heterocyclic thiosemicarbazone, Anticancer activity, Ribonucleotide reductase, 2-Pyridineformamide thiosemicarbazone, Pancreatic cancer, Elemental analysis, FTIR spectroscopy, NMR spectroscopy, HRFAB mass spectrometry, Preferential cytotoxicity, Nutrient starvation, Anti-austerity agents, Apoptosis.

TABLE OF CONTENTS

	Page No.
Title Page	i
Declaration	ii
Recommendation	iii
Certificate of Approval	iv
Acknowledgements	v
Abstract	vii
Table of Contents	ix
List of Abbreviations	xv
List of Symbols	xvii
List of Tables	xviii
List of Figures	xx
List of Schemes	xxv

CHAPTER 1

1. INTRODUCTION	1
1.1 General overview of thiosemicarbazones	2
1.1.1 Classification of thiosemicarbazones	4
1.1.1.1 Mono-thiosemicarbazones	5
1.1.1.2 Bis-thiosemicarbazones	5
1.1.1.3 Di-thiosemicarbazones	5
1.1.2 Synthetic procedures of thiosemicarbazones	6
1.1.3 α -(N)-Heterocyclic thiosemicarbazones	6
1.1.4 Isomerism of thiosemicarbazones	7
1.1.5 Coordination properties	9
1.2 Rationale	12
1.3 Objectives	13

3.1.3 Tubulin interactive agents	36
3.1.4 Hormonal agents	36
3.2 Anticancer activity of thiosemicarbazone	36
3.2.1 Ribonucleotide reductase	37
3.2.2 Ribonucleotide reductase reaction	38
3.2.3 Inhibition of RR activity	41
3.2.4 Other possible mechanisms	43

CHAPTER 4

4. MATERIALS AND METHODS	44
4.1 Materials	44
4.1.1 Biological materials	44
4.1.2 Cancer cell lines and cell culture	45
4.2 Methods and instrumentation.....	45
4.2.1 Melting point determination	45
4.2.2 Elemental analysis	46
4.2.3 Infrared spectroscopy	46
4.2.4 Nuclear magnetic resonance spectroscopy	46
4.2.5 Mass spectrometry	46
4.3 Synthesis of 2-pyridineformamide derived thiosemicarbazones	46
4.3.1 Synthesis of precursors	46
4.3.1.1 Synthesis of 2-(methyl(phenyl)carbamothioylthio)acetic acid	46
4.3.1.2 Synthesis of <i>N</i> -methyl- <i>N</i> -phenylhydrazinecarbothioamide ..	47
4.3.1.3 Synthesis of <i>N</i> (4)- ring incorporated thiosemicarbazide	48
4.3.2 General procedure for synthesis of <i>N</i> (4)-ring incorporated thiosemicarbazones	50
4.4 Cell viability assay against HeLa cells	65
4.5 Preferential Cytotoxic Activity against PANC-1 Cancer Cells in Nutrient-Deprived Medium	66
4.6 Morphological assessment of cancer cells	66
4.7 Western blot analysis	67
4.8 Annexin V/PI staining assay	67

CHAPTER 5

5. RESULTS AND DISCUSSION	68
5.1 Synthesis, characterization and biological activity of 2-pyridine-formamide <i>N</i> (4)-ring incorporated thiosemicarbazones	68
5.1.1 General discussions.....	68
5.1.2 Spectral studies.....	69
5.1.2.1 IR spectra.....	69
5.1.2.2 NMR spectra.....	71
5.1.2.3 Mass spectrometry.....	77
5.1.3 Biological activity of 2-pyridineformamide <i>N</i> (4)-ring incorporated thiosemicarbazone	78
5.1.3.1 Antineoplastic activity against HeLa cervical cancer cell line	78
5.1.3.2 Preferential cytotoxic activity against panc-1 human pancreatic cancer cell line in nutrient-deprived medium ..	81
5.1.3.3 Morphological assessment of cancer cells.....	84
5.1.3.3.1 Ethidium bromide/Acridine orange staining assay....	84
5.1.3.3.2 Western blot analysis.....	86
5.1.3.3.3 Annexin V/Propidium iodide staining assay.....	87
5.1.4 Conclusion.....	88
5.2 Synthesis, characterization and biological activity of 4-Methyl-2-pyridineformamide <i>N</i> (4)-ring incorporated thiosemicarbazones	89
5.2.1 General discussions.....	89
5.2.2 Spectral studies.....	90
5.2.2.1 IR spectra.....	90
5.2.2.2 NMR spectra.....	92
5.2.2.3 Mass spectrometry.....	96
5.2.3 Biological activity of 4-Methyl-2-pyridineformamide <i>N</i> (4)-ring incorporated thiosemicarbazone	97
5.2.3.1 Antineoplastic activity against HeLa cervical cancer cell line	97
5.2.3.2 Preferential cytotoxic activity against panc-1 human pancreatic cancer cell line in nutrient-deprived medium	98

5.2.4 Conclusion	99
5.3 Synthesis, characterization and biological activity of 5-Fluoro-2-pyridineformamide <i>N</i> (4)-ring incorporated thiosemicarbazones	101
5.3.1 General discussions	101
5.3.2 Spectral studies	102
5.3.2.1 IR spectra	102
5.3.2.2 NMR spectra	104
5.3.2.3 Mass spectrometry	108
5.3.3 Biological activity of 5-Fluoro-2-pyridineformamide <i>N</i> (4)-ring incorporated thiosemicarbazone	109
5.3.3.1 Antineoplastic activity against HeLa cervical cancer cell line	109
5.3.3.2 Preferential cytotoxic activity against panc-1 human pancreatic cancer cell line in nutrient-deprived medium	110
5.3.4 Conclusion	111
5.4 Synthesis, characterization and biological activity of 6-Methyl-2-pyridineformamide <i>N</i> (4)-ring incorporated thiosemicarbazones	112
5.4.1 General discussions	112
5.4.2 Spectral studies	113
5.4.2.1 IR spectra	113
5.4.2.2 NMR spectra	115
5.4.2.3 Mass spectrometry	119
5.4.3 Biological activity of 6-Methyl-2-pyridineformamide <i>N</i> (4)-ring incorporated thiosemicarbazone	119
5.4.3.1 Antineoplastic activity against HeLa cervical cancer cell lines	119
5.4.3.2 Preferential cytotoxic activity against panc-1 human pancreatic cancer cell line in nutrient-deprived medium	121
5.4.4 Conclusion	122

CHAPTER 6

6. CONCLUSION AND RECOMMENDATIONS	123
6.1 Conclusion	123
6.2 Recommendation for further work	124

CHAPTER 7	
7. SUMMARY	125
REFERENCES	130
APPENDICES	152
Appendix A IR spectra (A1 – A19)	152
Appendix B NMR spectra (B1 – B30)	164
Appendix C Mass spectra (C1- C18)	190
LIST OF PUBLICATIONS	201
LIST OF PRESENTATIONS	202

LIST OF ABBREVIATIONS

Anal. Calcd.	Analytical Calculated
¹³ C NMR	Carbon Nuclear Magnetic Resonance
¹ H NMR	Proton Nuclear Magnetic Resonance
3-AP	3-Aminopyridine-2-Carboxaldehyde Thiosemicarbazone
3-HP	3-Hydroxypyridine-2-Carboxaldehyde Thiosemicarbazone
ADP	Adenosine Diphosphate
AO	Acridine Orange
ApT	2-Acetylpyridine Thiosemicarbazone
ATP	Adenosine Triphosphate
BpT	2-Benzoylpyridine Thiosemicarbazones
CDCl ₃	Deuterated Chloroform
CDP	Cytidine Diphosphate
Cu-ATSM	Diacety-2,3-bis(4- <i>N</i> -methyl-3-thiosemicarbazonato)copper(II) complex
dATP	Deoxyadenosine Triphosphate
DFO	Desferrioxamine
dGTP	Deoxyguanosine Triphosphate
DMEM	Dulbecco's Modified Eagle's Medium
DMF	Dimethyl Formamide
DMSO- <i>d</i> ₆	Deuterated Dimethyl Sulphoxide
DNA	Deoxyribonucleic Acid
dNDP	2'-Deoxyribonucleoside Diphosphate
Dp44mT	Di-2-Pyridylketone-4,4-Dimethyl-3-Thiosemicarbazone
DpT	Di-2-Pyridylketone Thiosemicarbazones
dTTP	Deoxythymidine Triphosphate
EB	Ethidium Bromide
ELISA	Enzyme-Linked Immunosorbent Assay
FAD	Flavin Adenine Dinucleotide
GDP	Guanosine Diphosphate
GR	Glutathione reductase
GrxR	Glutaredoxin reductase
GSH	Glutathione

GSSG	Oxidized Glutathione
HCT	Heterocyclic Thiosemicarbazone
HeLa	Human Cervical Cancer Cell Line
HIV	Human Immunodeficiency Virus
HR-FAB MS	High Resolution Fast Atom Bombardment Mass Spectrometry
HSV	Herpes Simplex Virus
Hz	Hertz (NMR)
IR	Infrared
IUPAC	International Union of Pure and Applied Chemistry
mL	Millilitre
mp	melting point
MDR1	Multidrug Resistance Protein
MHz	Mega Hertz (NMR)
MTT	3-(4,5-Dimethylthiazol-2-yl)-2,5-Diphenyltetrazolium Bromide
NADPH	Nicotinamide Adenine Dinucleotide Phosphate
NBpT	2-(3'-Nitrobenzoyl)pyridine Thiosemicarbazones
NDM	Nutrient Deprived Medium
PANC-1	Human Pancreatic Cancer Cell Line
PBS	Phosphate Buffered Saline
ppm	parts per million
PS	Phosphatidylserine
PVDF	Polyvinylidene Difluoride
rNDP	Ribonucleoside Diphosphate
ROS	Reactive Oxygen Species
RR	Ribonucleotide Reductase
TB	Tuberculosis
TrxR	Thioerdoxin reductase
TSC	Thiosemicarbazone
UDP	Uridine diphosphate
UV	Ultraviolet
WST	Water soluble tetrazolium

LIST OF SYMBOLS

%	Percentage
δ	bending vibration (IR) ; Chemical shift (NMR)
ρ	Deformation vibration
μ	micro
ν	Stretching vibration
$^{\circ}\text{C}$	Degree Celsius
br s	broad singlet (NMR)
d	doublet (NMR)
dd	doublet of doublet (NMR)
h	Hour
IC_{50}	Maximal concentration to cause 50% inhibition of activity
J	Spin-Spin Coupling Constant (NMR)
M	Moles per litre
m	Multiplet (NMR); Medium Intensity (IR)
PC_{50}	Concentration at which 50% cell died preferentially in NDM
s	Singlet (NMR); Strong intensity (IR)
t	triplet (NMR)
w	Weak intensity (IR)

LIST OF TABLES

	Page No.
Table 5.1 Physical properties of compounds 1-6	68
Table 5.2 Elemental analysis data of compounds 1-6	69
Table 5.3 Diagnostic bands in the IR spectra of compounds 1-6	70
Table 5.4 ¹ H NMR spectral assignments for the compounds 1 – 6	72
Table 5.5 ¹³ C NMR spectral assignments for the compounds 1 – 6	76
Table 5.6 Mass spectrometric data of compounds 1-6	78
Table 5.7 IC ₅₀ values of compounds 1-6 against HeLa.....	81
Table 5.8 Preferential cytotoxicity data of compounds 1-6 against PANC-1 ..	84
Table 5.9 Physical properties of compounds 7-12	89
Table 5.10 Elemental analysis data of compounds 7-12	90
Table 5.11 Diagnostic bands in IR spectra of compounds 7-12	91
Table 5.12 ¹ H NMR spectral assignments for the compounds 7 – 12	92
Table 5.13 ¹³ C NMR spectral assignments for the compounds 7– 12	94
Table 5.14 Mass spectrometric data of compounds 7-12	96
Table 5.15 IC ₅₀ values of compounds 7-12 against HeLa	98
Table 5.16 Preferential cytotoxicity data of compounds 7-12 against PANC-1..	98
Table 5.17 Physical properties of compounds 13-17	101
Table 5.18 Elemental analysis data of compounds 13-17	102
Table 5.19 Diagnostic bands in IR spectra of compounds 13-17	102

Table 5.20 ^1H NMR spectral assignments for the compounds 13 – 17	104
Table 5.21 ^{13}C NMR spectral assignments for the compounds 13– 17	106
Table 5.22 Mass spectrometric data of compounds 13-17	108
Table 5.23 IC_{50} values of compounds 13-17 against HeLa.....	110
Table 5.24 Preferential cytotoxicity data of compounds 13-17 against PANC-1	110
Table 5.25 Physical properties of compounds 18-23	112
Table 5.26 Elemental analysis data of compounds 18-23	113
Table 5.27 Diagnostic bands in the IR spectra of compounds 18-23	114
Table 5.28 ^1H NMR spectral assignments for the compounds 18 – 23	115
Table 5.29 ^{13}C NMR spectral assignments for the compounds 18– 23	117
Table 5.30 Mass spectrometric data of compounds 18-23	119
Table 5.31 IC_{50} Values of Compounds 18-23 against HeLa	121
Table 5.32 Preferential cytotoxicity data of compounds 18-23	121

LIST OF FIGURES

		Page No.
Figure 1.1	Structures of antitumor thiosemicarbazones	2
Figure 1.2	Structures of (a) Thiacetazone (b) Marboran	2
Figure 1.3	General structure of thiosemicarbazone	3
Figure 1.4	Other semicarbazone derivatives	3
Figure 1.5	Structural arrangement of thiosemicarbazone skeleton	4
Figure 1.6	Tautomeric forms of thiosemicarbazone	4
Figure 1.7	General structure of mono-thiosemicarbazone	5
Figure 1.8	General structure of bis(thiosemicarbazone)	5
Figure 1.9	General structure of di-thiosemicarbazone	5
Figure 1.10	Structures of α -(<i>N</i>)-Heterocyclic thiosemicarbazones	7
Figure 1.11	Different isomeric forms of α -(<i>N</i>)-pyridyl TSCs	8
Figure 1.12	Neutral and Anionic forms of thiosemicarbazone ligand	9
Figure 1.13	Canonical anionic forms of thiosemicarbazone ligand	9
Figure 1.14	Increased coordination possibilities (a) due to additional donor atom (b) by formation of <i>S</i> -alkyl derivatives	10
Figure 1.15	Sites for structural modifications of α (<i>N</i>)-heterocyclic thiosemicarbazones	12
Figure 1.16	General structure of synthesized thiosemicarbazones	13
Figure 2.1	Structures of antitrypanosomal thiosemicarbazones	14

Figure 2.2	Thiosemicarbazones as inhibitors of <i>cruzain</i>	15
Figure 2.3	Structural formula of chimeras of thiosemicarbazones and ferroquine	17
Figure 2.4	Examples of antitubercular thiosemicarbazones and isoniazid	19
Figure 2.5	Structures of antifungal thiosemicarbazones and fluconazole..	20
Figure 2.6	Structures of some thiosemicarbazones tested for anti-HIV activity	22
Figure 2.7	Structure of thiosemicarbazones which are active/inactive against L1210 leukemia in mice	23
Figure 2.8	Effect of modifications in the side chain of isoquinoline-1-carboxaldehyde thiosemicarbazone on the tumor-inhibiting potency in mice bearing Sarcoma 180 ascites cells	24
Figure 2.9	Structures of NT series	26
Figure 2.10	Structures of DpT series	26
Figure 2.11	Structures of BpT series	27
Figure 2.12	Structures of the ApT series	28
Figure 2.13	Structures of IQ-1 and MAIQ-1	29
Figure 2.14	Structures of the QT series	29
Figure 2.15	Some clinically used anti-cancer drugs containing a quinoline scaffold	30
Figure 2.16	Chemical structures of the 2-pyridineformamide thiosemicarbazones	31
Figure. 2.17	Structure Cu-ATSM	32

Figure 2.18	Structural representation of Gallium(III) complexes of 2-acetylpyridine thiosemicarbazone	33
Figure 2.19	Antiausterity strategy in anticancer drug discovery	34
Figure 3.1	Model of ribonucleotide reductase from <i>E. coli</i>	37
Figure 3.2	Reduction of ribonucleotides to deoxyribonucleotides by ribonucleotide reductase	38
Figure 3.3	Catalytic mechanism for the ribonucleotide reductase reaction	39
Figure 3.4	Regulation of ribonucleotide reductase by deoxynucleoside triphosphate	41
Figure 3.5	Addendal Ligand blocking model	42
Figure 5.1	IR spectrum of compound 1	71
Figure 5.2	<i>E</i> , <i>Z</i> and <i>Z'</i> geometrical isomers and <i>cis</i> , <i>trans</i> conformers of compound 1	73
Figure 5.3	¹ H NMR spectrum (400 MHz, DMSO- <i>d</i> ₆) of compound 6 ...	73
Figure 5.4	¹ H-COSY Spectrum (400 MHz, DMSO- <i>d</i> ₆) of compound 6 ...	74
Figure 5.5	¹ H NMR spectrum (400 MHz, CDCl ₃) of compound 1	75
Figure 5.6	¹ H NMR spectrum (400 MHz, DMSO- <i>d</i> ₆) of compound 1	75
Figure 5.7	¹³ C NMR Spectrum (100MHz, DMSO- <i>d</i> ₆) of compound 6	77
Figure 5.8	¹³ C NMR Spectrum (100MHz, DMSO- <i>d</i> ₆) of compounds 1 ...	77
Figure 5.9	HRFABMS of compound 1	78
Figure 5.10	Principle of the cell viability detection with Cell Counting Kit-8	79
Figure 5.11	Antineoplastic activity of the compounds 1-6 against HeLa cervical cancer cell line	80

Figure 5.12	Preferential cytotoxic activity of compounds 1-6 , Arctigenin, Gemcitabin and Paclitaxel against the PANC-1 human pancreatic cancer cell line in nutrient deprived medium (NDM) and Dulbecco's modified Eagle medium (DMEM)	82
Figure 5.13	Structures of Arctigenin, Paclitaxel and Gemcitabine	84
Figure 5.14	Fluorescent [ethidium bromide (EB)/acridine orange (AO)] and phase contrast images of PANC-1 cells at 24 h	85
Figure 5.15	Western blot of the effect of compound 6 for 4 h against Akt, pAkt, pro-caspase 3, and cleaved-caspase	86
Figure 5.16	Fluorescent [Annexin v (AV)/propidium iodide (PI)] and phase contrast images of PANC-1 cells treated with 1 μ M of compound 6 in NDM and incubated for 12 h.	87
Figure 5.17	IR spectrum of compound 7	91
Figure 5.18	^1H NMR spectrum (400 MHz, DMSO- d_6) of compound 9	92
Figure 5.19	^1H NMR spectrum (400 MHz, CDCl_3) of compound 7	93
Figure 5.20	^1H NMR spectrum (400 MHz, DMSO- d_6) of compound 7	94
Figure 5.21	^{13}C NMR Spectrum (100MHz, DMSO- d_6) of compound 9	95
Figure 5.22	^{13}C NMR Spectrum (100MHz, DMSO- d_6) of compounds 7 ...	95
Figure 5.23	HRFABMS of compound 9	96
Figure 5.24	Antineoplastic activity of the compounds 7-12 against the HeLa cervical cancer cell line	97
Figure 5.25	Preferential cytotoxic activity of compounds 7-12 against the PANC-1 human pancreatic cancer cell line in nutrient deprived medium (NDM)) and Dulbecco's modified Eagle medium (DMEM)	99

Figure 5.26	IR spectrum of compound 15	103
Figure 5.27	¹ H NMR spectrum (400 MHz, DMSO- <i>d</i> ₆) of compound 15	104
Figure 5.28	¹ H NMR spectrum (400 MHz, CDCl ₃) of compound 13	105
Figure 5.29	¹ H NMR spectrum (400 MHz, DMSO- <i>d</i> ₆) of compound 13	106
Figure 5.30	¹³ C NMR Spectrum (100MHz, DMSO- <i>d</i> ₆) of compound 15 ...	107
Figure 5.31	¹³ C NMR Spectrum (100MHz, DMSO- <i>d</i> ₆) of compounds 13 ..	107
Figure 5.32	HRFABMS of compound 15	108
Figure 5.33	Antineoplastic activity of the compounds 13-17 against the HeLa human cervical cancer cell line	109
Figure 5.34	Preferential cytotoxic activity of compounds 13-17 against the PANC-1 human pancreatic cancer cell line in nutrient deprived medium (NDM)	111
Figure 5.35	IR spectrum of compound 22	114
Figure 5.36	¹ H NMR spectrum (400 MHz, DMSO- <i>d</i> ₆) of compound 22	115
Figure 5.37	¹ H NMR spectrum (400 MHz, CDCl ₃) of compound 18	116
Figure 5.38	¹ H NMR spectrum (400 MHz, DMSO- <i>d</i> ₆) of compound 18 ...	116
Figure 5.39	¹³ C NMR Spectrum (100MHz, DMSO- <i>d</i> ₆) of compound 22 ...	118
Figure 5.40	¹³ C NMR Spectrum (100MHz, DMSO- <i>d</i> ₆) of compounds 18 ..	118
Figure 5.41	HRFABMS of compound 22	119
Figure 5.42	Antineoplastic activity of compounds 19-24 against the HeLa cervical cancer cell line	120
Figure 5.43	Preferential cytotoxic activity of compounds 18-23 against the PANC-1 human pancreatic cancer cell line in nutrient deprived medium (NDM)	122

LIST OF SCHEMES

	Page no.
Scheme 1.1 General method for synthesis of thiosemicarbazone	3
Scheme 1.2 Synthetic procedures of <i>N</i> (4)-substituted thiosemicarbazones..	6
Scheme 1.3 Different modes of coordination of monothiosemicarbazone with metal	11
Scheme 3.1 RR inhibition mechanisms of α -(<i>N</i>)-thiosemicarbazones	42
Scheme 4.1 Synthesis of 2-(methyl(phenyl)carbamothioylthio)acetic acid..	47
Scheme 4.2 Synthesis of <i>N</i> -methyl- <i>N</i> -phenylhydrazinecarbothioamide	47
Scheme 4.3 Synthesis of <i>N</i> (4)- ring incorporated thiosemicarbazide	48
Scheme 4.4 Synthesis of 2-pyridineformamide <i>N</i> (4)-ring incorporated thiosemicarbazone	50

1. INTRODUCTION

Cancer, the leading cause of death worldwide, is presently responsible for about 25% of deaths in developed countries and for 13% of deaths in developing countries. International Agency for Research on Cancer (IARC) estimated 14.1 million new cancer cases and 8.2 million cancer-related deaths in 2012, whereas 12.7 million and 7.6 million, respectively, in 2008. By 2035, the number of new cancer cases is projected to grow to 24 million.¹

The most common types of treatment for cancer include surgery, chemotherapy and radiation therapy. Chemotherapy is the use of chemicals to kill the cancer cells or stop them from growing. A suitable and well-established target for cancer therapy is Ribonucleotide Reductase (RR) the key enzyme involved in reduction of ribonucleotides into deoxyribonucleotides during DNA synthesis, because it is highly expressed in tumor cells.²

Heterocyclic Thiosemicarbazones (HCTs) are one of the most potent inhibitor of RR activity.³ Brockman *et al.*⁴ first reported anticancer activity of HCT in 1956 revealing antileukemic activity of pyridine-2-carboxaldehyde thiosemicarbazone (Fig. 1.1, a) in mice bearing the L1210 leukemia. Further studies evinced that an α -(N)-heterocycle is essential for biological activity.⁵ These α -(N)-heterocyclic thiosemicarbazones are several orders of magnitude more effective than hydroxyurea, the first clinically applied RR inhibitor.⁶ It has been demonstrated that 3-Hydroxypyridine-2-carboxaldehyde thiosemicarbazone (3-HP) (Fig. 1.1, c) are active against leukemia L1210, Ehrlich ascites carcinoma, lymphoma L5178Y, the Lewis lung carcinoma, and adenocarcinoma 755.⁷ 5-Hydroxypyridine-2-carboxaldehyde thiosemicarbazone (5-HP) (Fig. 1.1, c) was the first compound of HCT series that entered phase I clinical trials.⁸ Currently the most promising thiosemicarbazone as antitumor agent is 3-aminopyridine-2-carboxaldehyde thiosemicarbazone (3-AP, Triapine), (Fig. 1.1, d) which entered several phase I and phase II clinical trials.⁹⁻¹³

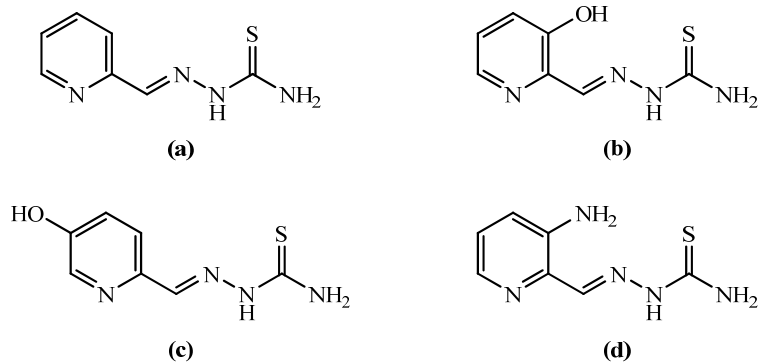


Figure 1.1: Structures of antitumor thiosemicarbazones (a) Pyridine-2-carboxaldehyde thiosemicarbazone, (b) 3-Hydroxypyridine-2-carboxaldehyde thiosemicarbazone (c) 5-Hydroxypyridine-2-carboxaldehyde thiosemicarbazone, (d) Triapine

In 1946 Domagk *et. al.* first reported the antibacterial properties of Thiosemicarbazones (TSCs) against *Mycobacterium. tuberculosis*.¹⁴ One of the member of this class of compound *p*-acetamidobenzaldehyde thiosemicarbazone, commercially available as thiacetazone (Fig. 1.2, a) has been widely used for treatment of tuberculosis.¹⁵ Thiosemicarbazones were also the first compounds found to have antiviral activity (against vaccinia virus)^{16,17} and the member, *N*-methylisatin- β -thiosemicarbazone (Marboran) (Fig. 1.2, b), entered in clinical treatment of smallpox.¹⁸

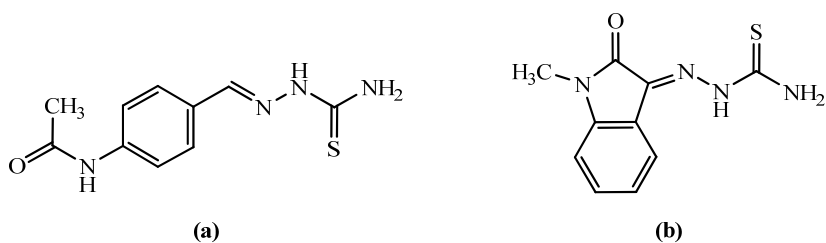
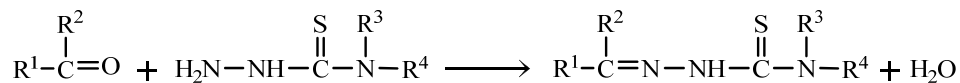


Figure 1.2: Structures of (a) Thiacetazone (b) Marboran

1.1 General overview of Thiosemicarbazones

Thiosemicarbazones (TSCs) are compounds of considerable interest because of their variable bonding modes, promising biological implications, structural diversity, and ion-sensing ability.¹⁹⁻²¹

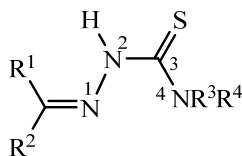
TSCs are synthetic compounds, usually obtained by condensation of thiosemicarbazide with a suitable aldehyde or ketone (Scheme 1.1).



Scheme 1.1: General method for synthesis of thiosemicarbazone

It is named by adding the class name thiosemicarbazone after the name of aldehyde or ketone condensed with the thiosemicarbazide.²²

The structure of TSCs and numbering of its atoms according to IUPAC is shown in Fig. 1.3.



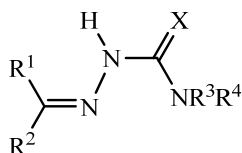
$\text{R}^1, \text{R}^2 = \text{H}, \text{alkyl}, \text{aryl}$ or heterocyclic group

$\text{R}^3, \text{R}^4 = \text{H}, \text{alkyl}, \text{aryl}, \text{heterocyclic}$ group or part of a cyclic system.

Figure 1.3: General structure of thiosemicarbazone

When R^2 is heterocyclic like pyridine an additional functionality is also included to give *N,N,S* donors. When R^3 and R^4 of the thioamide group are part of a cyclic system, a ring incorporated thiosemicarbazone is formed.

TSCs and analogous derivatives are shown in Fig. 1.4.



$\text{X} = \text{O}$, Semicarbazone

$\text{X} = \text{Se}$, Selenosemicarbazone

$\text{X} = \text{NH}$, Guanylylhydrozone

Figure 1.4: Other semicarbazone derivatives

In solid state, the $\text{C}=\text{N}-\text{NH}-\text{CS}-\text{N}$ backbone of TSC, is usually in an approximately planar arrangement with the S atom *trans* to azomethine N. (configuration *E*, Fig. 1.5, a). The planar configuration is due to extensive electron delocalization throughout the thiosemicarbazone moiety. This arrangement is adopted most probably because the *trans* arrangement puts the amine and azomethine nitrogen atoms in relative positions more suitable for intramolecular hydrogen bonding. In fact, TSCs, in which the amine group is fully substituted, crystallize with the S atom *cis* to the azomethine N (*Z*-

configuration; Fig. 1.5, b).²³ The usual *E*-configuration of unsubstituted TSCs is not likely to change by substitution of the hydrazinic H. However, TSCs adopt the *Z* form (Fig 1.5, c, R = alkyl) when the S atom is substituted.

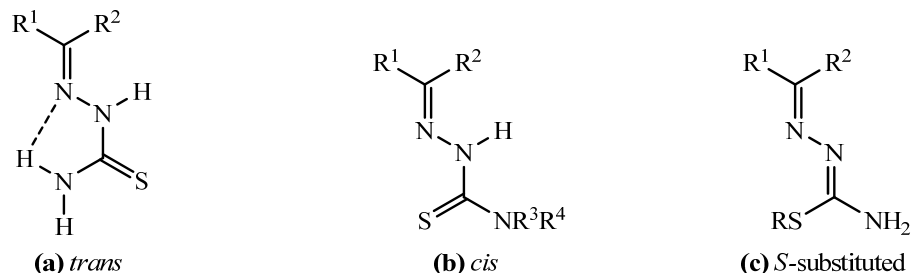


Figure 1.5: Structural arrangement of thiosemicarbazone skeleton

TSCs are extensively delocalized systems, especially when aromatic radicals are bound to the azomethine carbon atom.²⁴

Presence of NH-C=S group in TSCs can bring about thione-thiol tautomerism. In solution TSCs exist as an equilibrium mixture of *thione* (Fig 1.6, a) and *thiol* (Fig. 1.6, b) forms.

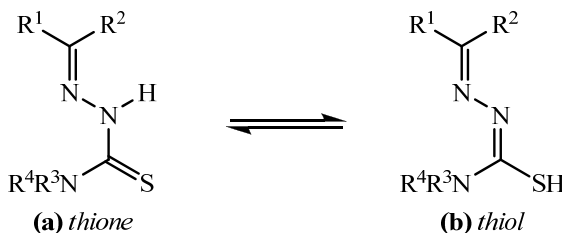


Figure 1.6: Tautomeric forms of thiosemicarbazone

In the thiol form, there is an effective conjugation along the thiosemicarbazone skeleton thus giving rise to an effective electron delocalization along the moiety. Hetero aromatic substituents on the skeleton can further enhance the delocalization of electron cloud and hence generate new potential sites for coordination.

1.1.1 Classification of thiosemicarbazones

Thiosemicarbazones are basically Schiff bases and are broadly classified as mono-thiosemicarbazones, bithiosemicarbazones and dithiosemicarbazones.

1.1.1.1 Mono-thiosemicarbazones

Monothiosemicarbazone consists one thiosemicarbazone moiety. It is formed when the parent carbonyl compound and the thiosemicarbazide are taken in 1:1 ratio.

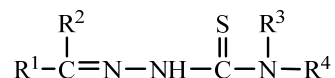


Figure 1.7: General structure of mono-thiosemicarbazone

1.1.1.2 Bis-thiosemicarbazones

Bis-thiosemicarbazone is a dimeric structure generally containing two thiosemicarbazone moieties connected by their imine nitrogens to a two carbon skeleton. It is formed when ketoaldehyde, dialdehyde or diketone is condensed with appropriate thiosemicarbazide in 1:2 ratio. Bis-thiosemicarbazone (Fig. 1.8) was first synthesized by Bahr in 1955.²⁵

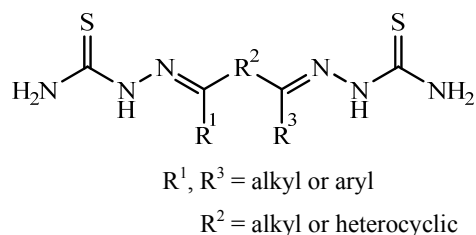


Figure 1.8: General structure of bis(thiosemicarbazone)

1.1.1.3 Di-thiosemicarbazones

Dithiosemicarbazone is a dimeric structure generally containing two thiosemicarbazone moieties consisting of two mono-thiosemicarbazone moieties connected by their amide nitrogen atoms to an aliphatic or aromatic spacer (Fig. 1.9).

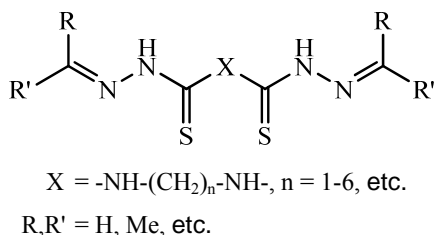
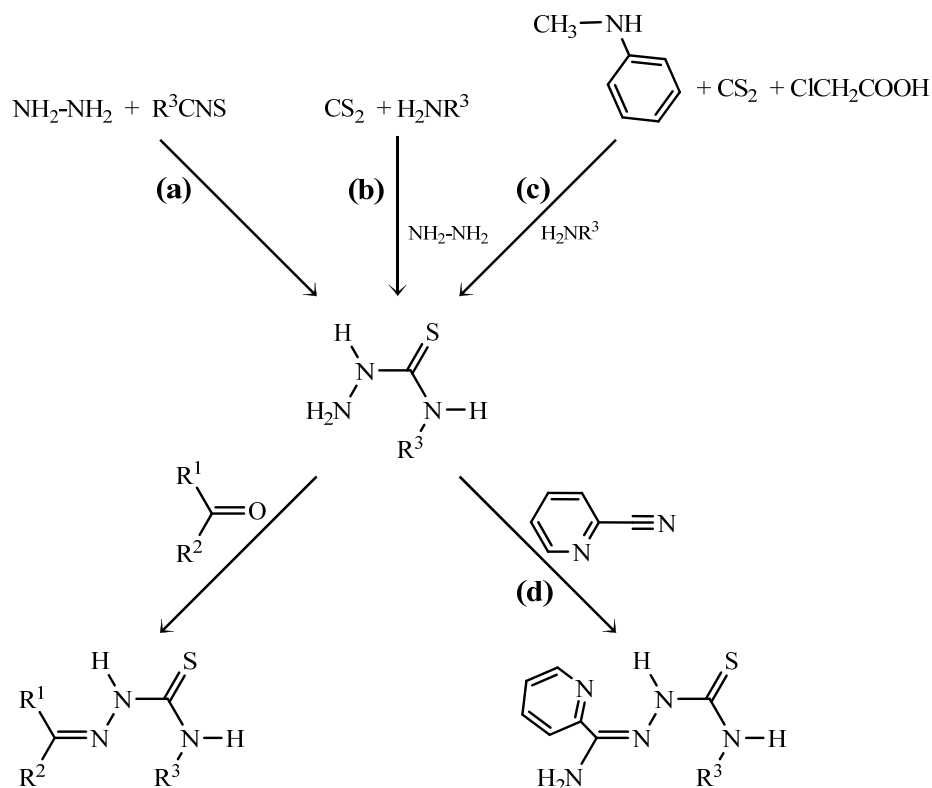


Figure 1.9: General structure of di-thiosemicarbazone

1.1.2 Synthetic procedures of thiosemicarbazones

Thiosemicarbazones, in general, are obtained by the condensation of corresponding thiosemicarbazide with aldehydes or ketones. The thiosemicarbazides used in the synthesis can be obtained by a series of synthetic procedures. For example, by the treatment of hydrazine hydrate with isothiocyanates (Scheme 1.2, a) or by the reaction of amines with carbon disulphide followed by the addition of hydrazine hydrate (Scheme 1.2, b)²⁶ or by transamination of 4-methyl-4-phenyl-3-thiosemicarbazide (Scheme 1.2, c).²⁷ However, an alternative method of synthesis involves the use of nitrile as starting material.²⁸ In this case, the resulting TSC contains an additional amino group (Scheme 1.2, d), which gives improved water solubility. This in turn can improve the biological activity of these compounds.²⁹



Scheme 1.2: Synthetic procedures of *N*(4)-substituted TSCs

1.1.3 α -(*N*)-Heterocyclic thiosemicarbazones

α -(*N*)-Heterocyclic TSCs are the compounds in which the thiosemicarbazone side-chain is attached to α -position to a heterocyclic ring (Fig. 1.10). In these compounds

the aromatic ring can enter into the π - π interaction with biomolecules modifying the biological activity.³⁰

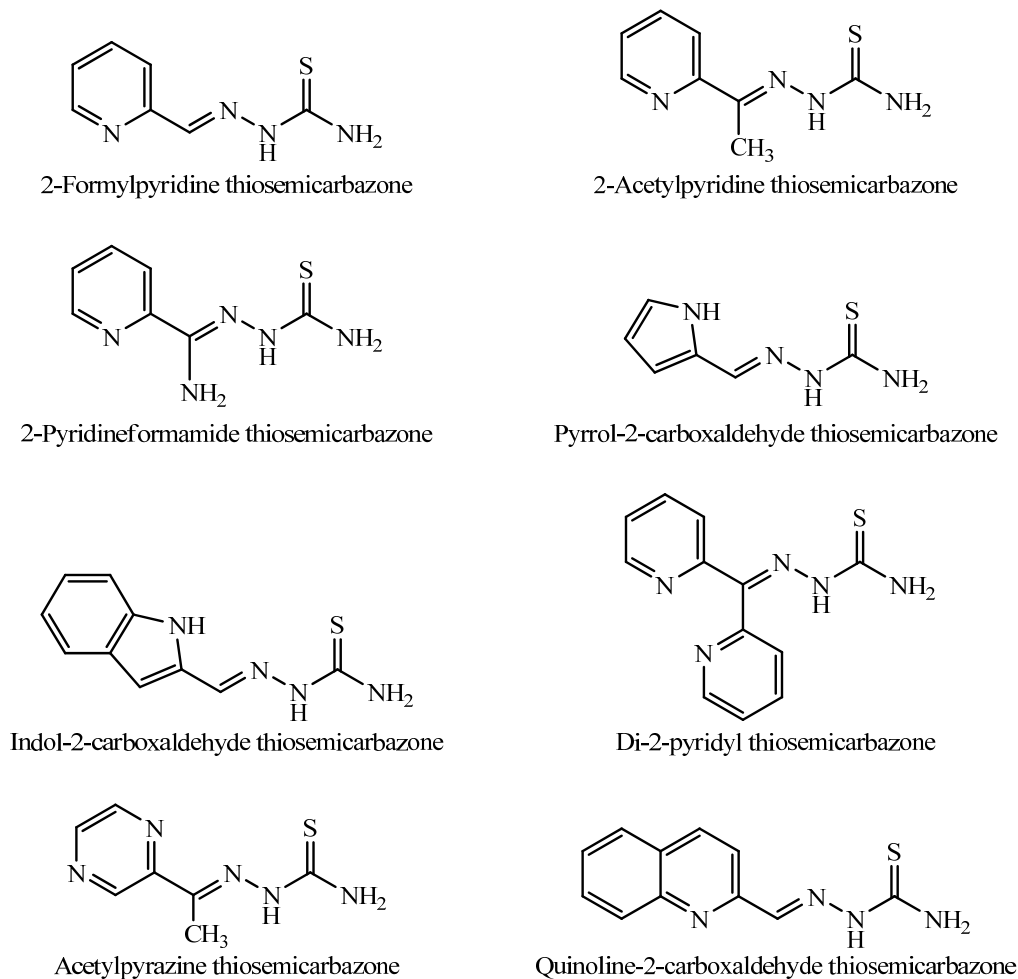


Figure 1.10: Structures of α -(*N*)-Heterocyclic TSCs

1.1.4 Isomerism of thiosemicarbazones

For the TSCs, in general, two geometrical isomers, *viz.* *E* and *Z*, about the imine double bond are possible. However, when the thiosemicarbazone side-chain is attached to α position to a heterocyclic ring, such as in α -(*N*)-pyridyl TSCs, at least four different structural modifications (Fig 1.11) are possible depending on the disposition of substituents about the C=N bond and thioamide (NHC=S) group:

- E* with respect to the imine function of the thiosemicarbazone without hydrogen bonding to the pyridyl nitrogen.³¹
- Hydrogen bonding to the pyridyl nitrogen by *N*(3)H, *Z* with respect to the imine function of the thiosemicarbazone and *Z* with respect to the *N*(3) – *C*(8) bond.³¹⁻³³

- (c) Hydrogen bonding to the pyridyl nitrogen by the $N(3)H$, Z with respect to the imine function of the thiosemicarbazone, but E with respect to the $N(3) - C(8)$ bond.³²
- (d) The bifurcated E' tautomer in which the $N(3)$ hydrogen has shifted to the imine nitrogen, $N(2)$, and is hydrogen bonding to both the pyridyl nitrogen and sulphur of the thiosemicarbazone moiety (the three donor atoms $N(1)$, $N(2)$ and $S(1)$ are all on the same side of the TSC backbone).^{31,34}

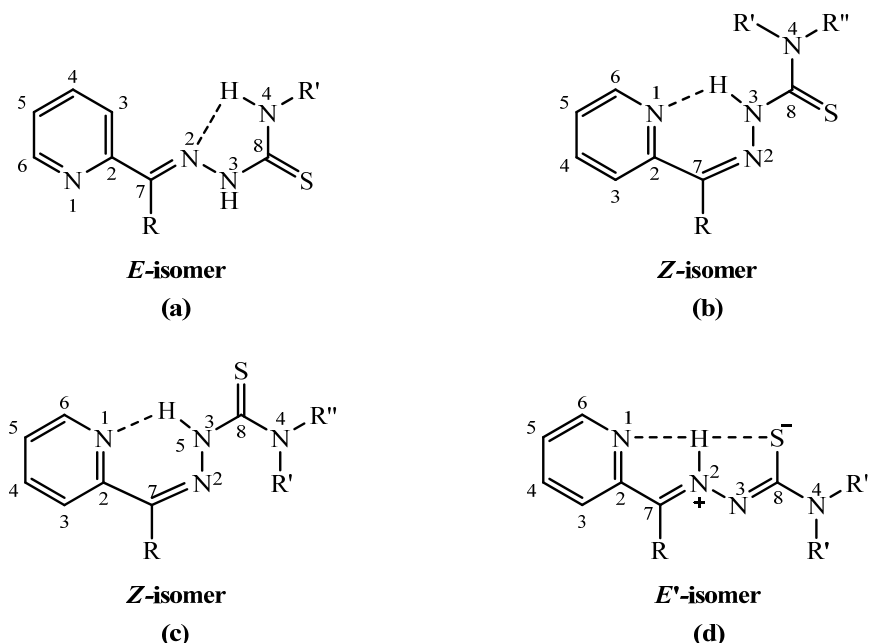


Figure 1.11: Different isomeric forms of α -(N)-pyridyl TSCs **(a)** E (anti, anti $N(3)$ -protonated form) **(b)** Z (syn, syn $N(3)$ -protonated form) **(c)** Z (syn, anti $N(3)$ -protonated form) and **(d)** E' (syn, syn $N(2)$ -protonated form)

The electronic influence of the group attached to $C(7)$ is crucial in dictating the conformation and tautomeric form. The electron-donating group such as methyl raise the proton affinity of $N(2)$ and favour E isomer, whereas electron-withdrawing group, such as pyridyl and phenyl favour the Z isomer (Fig. 1.11, b and c) where $N(3)$ is protonated and H-bonded to $N1$.^{35,36} Similarly, the corresponding 2-pyridineformamide TSCs, where an electron donating primary amino group bonded to $C(7)$ instead of a methyl group and $N(4)$ bears no H-atoms, the molecule is converted to the E' (syn, syn) tautomeric form where the labile proton resides on $N(2)$ [rather than $N(3)$] where it is H-bonded to the pyridyl N-atom and S atom (Fig. 1.11, d).^{37,38}

In solution the solvent affects the isomeric distribution and two or more forms may be present as evinced by NMR.³⁹ The chemical shift of the thioamide proton on the *N*(3) is diagnostic of the isomeric form. An important structural determinant is the intramolecular hydrogen bonding that involves either *N*(3) or *N*(4) in the formation of hydrogen bond to give *Z* or *E* isomer, respectively (Fig. 1.11, a, b and c).⁴⁰ The formation of hydrogen bonds between solvent molecules and *N*(4)H is favoured by solvents with high donor number and it results in stabilization of the *E* isomer. On the other hand, the *Z* isomer is stabilized by the intramolecular $N(3)H \cdots N_{\text{pyridine}}$ bond in solvents with low donor number.⁴¹

The lipophilicity of TSCs is strongly correlated with biological activity and may be readily tuned by variations of the substituents R, R', and R".^{39,42,43} With these variations the solubility properties of the compound will also be affected. Because of its polar structure the zwitterionic *E'* form should be more hydrophilic than either the *E* or *Z*.³⁹

1.1.5 Coordination Properties

TSCs are versatile ligands in both neutral (Fig. 1.12, a) and anionic (Fig. 1.12, b) forms.

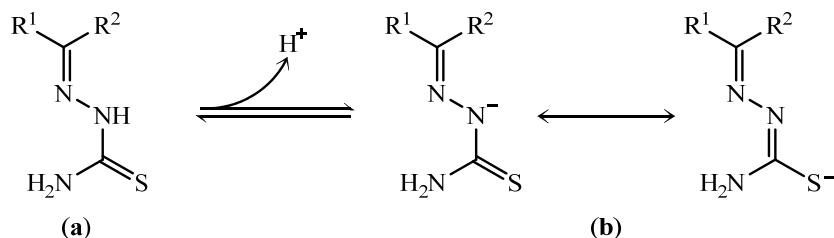


Figure 1.12: Neutral and anionic forms of thiosemicarbazones ligand

The anion is usually in *Z*-configuration and is usually represented in the canonical thiol form. (Fig. 1.13, a and b) though proton lost by the anions formally belongs to the hydrazinic –NH group.¹⁹

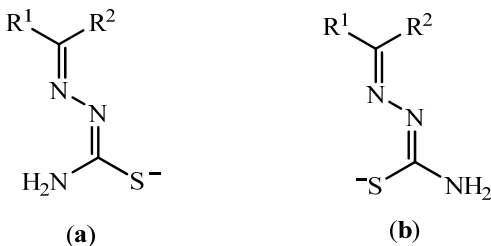


Figure 1.13: Canonical anionic forms of TSC ligand

The presence of a N,N,S tridentate "soft donor" coordination system determines the ability of TSCs to chelate metal ions and allows the thiosemicarbazone ligands to bind Fe,^{44,45} Cu, Zn, and other transition metals.⁴⁶

The coordination possibilities can be modified by introducing substituents on backbone donor atoms (e.g., by the formation of *S*-alkyl derivatives; (Fig. 1.14, a) and can be increased when the substituents R¹ and/or R² include additional donor atoms (Fig. 1.14, b).¹⁹

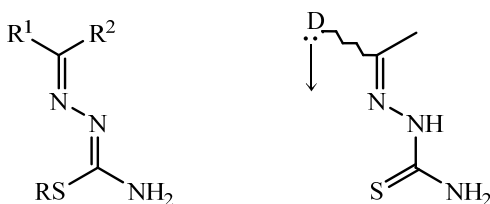
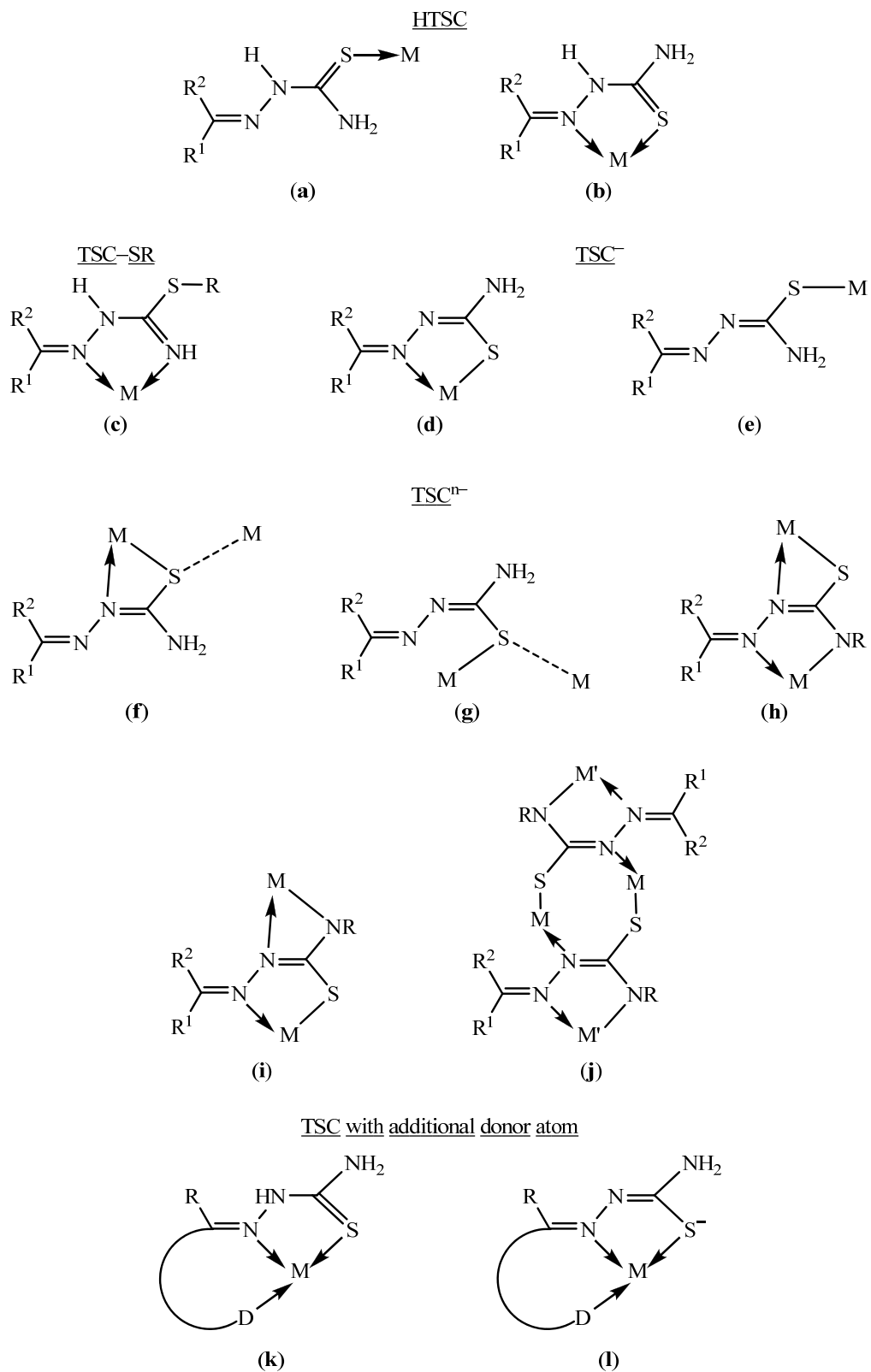


Figure 1.14: Increased coordination possibilities (a) by formation of *S*-alkyl derivatives (b) due to additional donor atom

It can act as mono, bi or tridentate ligands binding to metal ions *via* different donor atoms. TSC behaves as a monodentate ligand bonding only through the sulphur atom. (Scheme 1.3, a and d) while complexing in *E* configuration. TSCs coordinate as bidentate ligands *via* azomethine nitrogen and thione/thiol sulfur atom. (Scheme 1.3, b, c and e). They will coordinate in a tridentate manner when an additional coordination functionality is present in the proximity of the donating centers, either in the neutral molecule (Scheme 1.3, k) or in the monobasic anion formed by loss of hydrogen (Scheme 1.3, l).⁴⁷

The three possible donor atoms, N_{pyr} , $N(1)$ and S , must adopt the *E'* conformation, with all three donor atoms *syn* with respect to each other (Scheme 1.2, k), for binding a single metal center in a tridentate fashion. On deprotonation the resulting negative charge resides mostly on the S donor atom (Scheme 1.2, l) this enhances the ability of the TSC to stabilize metals in higher oxidation states.⁴⁸⁻⁵⁰

The different coordination modes of monothiosemicarbazones are summarized in Scheme 1.3.

Scheme 1.3: Different modes of coordination of monothiosemicarbazone with metal¹⁹

1.2 RATIONALE

Anticancer chemotherapy is nowadays a very active field of research. Over expression of the RR is associated with malignant transformation and cancer metastasis. Therefore, RR has been listed as a promising target in cancer therapy. The modification of the structure of the HCT is found to significantly affect the activity of thiosemicarbazone. The HCTs skeleton can be modified around four positions, Fig. 1.15: (i) the heterocyclic ring, (ii) the substituent on the carbonyl moiety (iii) the *N*(4)-substituents on the thiosemicarbazone moiety and (iv) metal chelation and hydrogen bonding area.

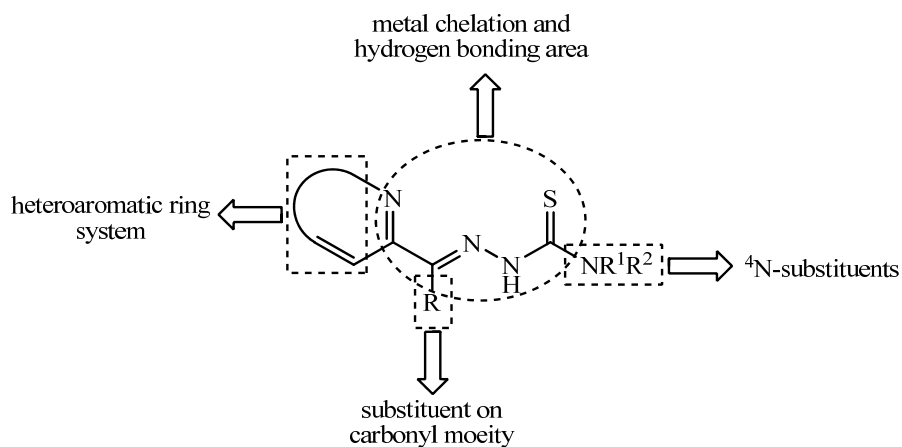


Figure 1.15: Sites for structural modifications of α -(N)-heterocyclic thiosemicarbazones.

Much effort has been devoted to structural variations of the thiosemicarbazones for achieving the ultimate goal of medicinal applications. Many HCTs have been synthesized and are found to be active against selected cell lines resistant to hydroxyurea and gemcitabine. There is need to improve the drugs already in clinical use and search for the new and more effective ones. Further the extreme insolubility of most thiosemicarbazones in water causes difficulty in the oral administration in clinical practice. The solubility of thiosemicarbazone can be increased by introducing an additional amino group. 2-Pyridineformamide thiosemicarbazones contain an additional amine group where the thiosemicarbazone moiety is attached to an amide carbon rather than an aldehyde or ketone carbon. Thiosemicarbazones of such a functionality could provide a series of compounds with greater pharmaceutical promise than previously studied.

1.3 OBJECTIVES

The objectives of the present study are:

- i. Synthesis of a series of 2-pyridineformamide derived thiosemicarbazones of the general structure shown in Fig. 1.16.

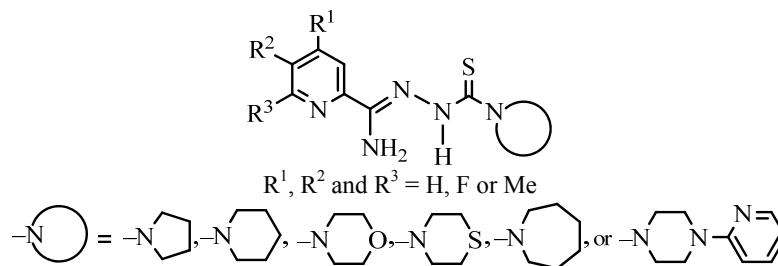


Figure 1.16: General structure of synthesized thiosemicarbazones

- ii. Characterization of the synthesized compounds.
- iii. Evaluation of the anticancer activity of the characterized compounds.

2. LITERATURE REVIEW

2.1 Bioactivity of Thiosemicarbazones

Thiosemicarbazones and their metal complexes have been widely explored because of their versatile biological activity and prospective use as drugs.⁵¹ TSCs and their metal complexes have antitumor,⁵ antifungal,⁵² antibacterial,⁵³ antimalarial,⁵⁴ antifilarial,⁵⁵ antiviral,⁵⁶ and anti-HIV,⁵⁷ activities. The biological activity of TSCs depends on the parent aldehyde or ketone⁵⁸ and related with the *N,N,S* tridentate nature of the systems.⁵⁹ It has been observed that the presence of a bulky group at the at the *N*(4) position of the thiosemicarbazone moiety greatly enhances the activity.⁶⁰⁻⁶²

2.1.1 Antiprotozoal Activity

Thiosemicarbazones are useful ligands for the building of metal complexes with a wide variety of biological targets, including protozoan parasites because they are endowed with the unique capacity of metallic co-ordination, semi-labile, chemically stable, and synthetically treatable-features which make them suitable for performing structure–activity relationships (SAR) studies.^{40,63-66} In the context of TSCs, the most studied parasitic diseases are trypanosomiasis and malaria.

2.1.1.1 Antitrypanosomal Activity

Wilson *et al.* first reported on *in vitro* and *in vivo* antitrypanosomal activities of TSCs in 1974.⁶⁷ The most effective compounds from the reported series are **a** and **b** (Fig. 2.1). The *in vitro* biological evaluation of 2-acetylpyridine TSCs (Fig. 2.1. c-f) against *Trypanosoma rhodesiense* was reported by Casero *et al.* in 1980.⁶⁸ In both studies, it was suggested that inhibition of protein may be the cause of marked antitrypanosomal activities of TSCs.

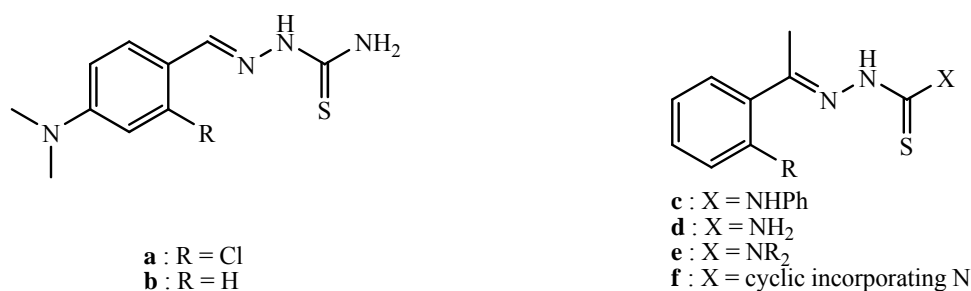


Figure 2.1: Structures of antitrypanosomal thiosemicarbazones

A series of TSCs displaying significant activities against cruzain, the cysteine protease of *Trypanosoma cruzi* were identified by Du *et al.*⁶⁹ The compound **a** (Fig. 2.2) was found to be the most active TSC.⁷⁰ Captivated by these observations, a series of compounds analogous to **a** were synthesized and evaluated for their ability to inhibit cysteine proteases (Fig. 2.2).⁷¹ Compound **b** and **c** were found to inhibit cruzain effectively without activity against the cognate protease. Following this study a second series of TSCs were synthesized and evaluated against *Trypanosoma cruzi* and *T. brucei* which resulted in novel TSCs displaying greater trypanocidal activity.⁷²⁻⁷⁴ The growing interest in TSCs as potential antitrypanosomal agents is further illustrated by the report of Porcal *et al.*⁷⁵

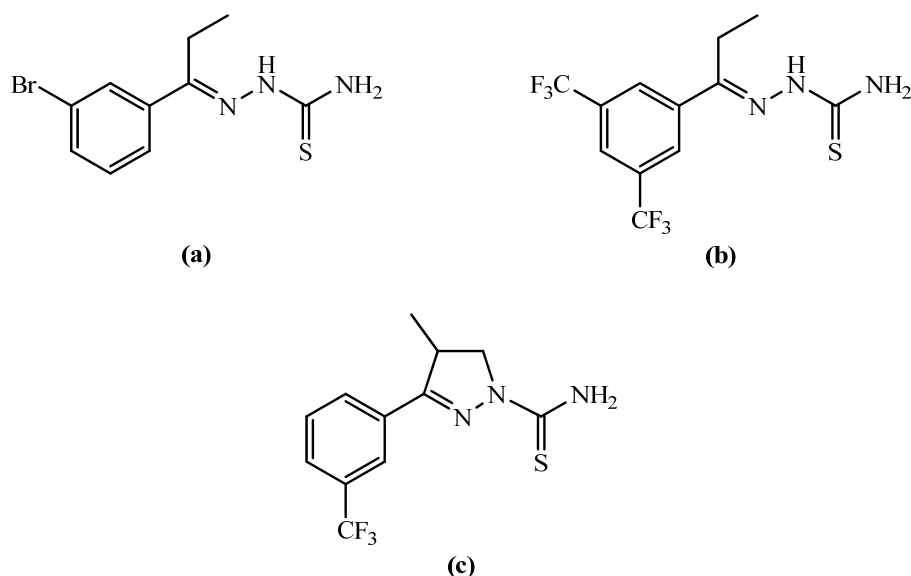


Figure 2.2: Thiosemicarbazones as inhibitors of *cruzain*

Palladium complexation was found to result in increased activity against *T. cruzi* as evident from the report on activity of 5-nitrofuryl-3-acroleine thiosemicarbazone palladium(II) complexes that showed higher *in vitro* growth inhibition activity than nifurtimox, the most efficient drug in clinical use.⁷⁶ The studies of Pérez-Rebolledo *et al.*⁷⁷ proved that *N*(4)-substituted-4-nitroacetophenone thiosemicarbazones and their copper(II) complexes were as active as the clinical reference drugs nifurtimox. Vieites *et al.*^{78,79} further reported that platinum complexes of 5-nitrofuraldehyde containing thiosemicarbazones were more potent in anti-trypanosomal activity than the reference nifurtimox. All these studies suggest that the trypanocidal mechanism of action is probably mainly due to the inhibition of parasite growth through a dual pathway involving production of toxic free radicals by thiosemicarbazone bioreduction and

metal complex-DNA interaction.^{80,81} Trypanothione reductase could be a further target as reported by Otero *et al.*⁷⁶ In a recent report by Lessa *et al.*⁸² Sb(III) complexes of pyridine-derived TSCs exhibited more potent activity than the reference drugs benzimidazole and nifurtimox against the epimastigote and trypomastigote forms of *Trypanosma cruzi*.

2.1.1.2 Antimalarial Activity

In 1979, Klayman *et al.*⁸³ demonstrated the antimalarial activity of an extensive series of TSCs against *Plasmodium berghei* in mice. Initially, it was observed that the *N*(4) monosubstituted analogue (Fig. 2.1, c) cured mice at doses below 200 mg/kg/day. However, further investigation revealed that the activity was enhanced when *N*(4) is disubstituted (Fig. 2.1,e) or incorporated into a medium-sized (i.e., six- or seven-membered) monocyclic or bicyclic system (Fig. 2.1, f).⁶⁰ This led to extensive investigations into antimalarial properties of TSCs.

Recently, Biot *et al.*^{84,85} synthesized chimeras of thiosemicarbazones and ferroquine (Fig. 2.3) and studied their antimalarial activity against four strains of the malaria parasite *Plasmodium falciparum* and against the parasitic cysteine protease falcipain-2. They started with the thiosemicarbazones of known potent antimalarial activity,⁸⁶ which were previously neglected because of the heavy side effects and inserted a ferroquine, another molecule also reported to have antimalarial properties.⁸⁴ The studies suggested that the aminoquinoline thiosemicarbazone part may be the major contributor to the antimalarial activity. The chimeras of thiosemicarbazones and ferroquine analogues were observed to be most active derivatives against all strains of *P. falciparum*, but in some cases the corresponding organic derivatives were also found to be equally active. The antimalarial activity of 3,4-dichloroacetophenone TSC and 3,4-dichloropropiophenone TSC and their Pd(II) complexes against *P. falciparum* strains 3D7 (chloroquine sensitive) and K1 (Chloroquine and pyrimethamine resistant) was reported by Chellan *et al.*⁸⁷ More recently, Khaney *et al.*⁸⁸ reported *in vitro* antiplasmodial assays of the dendritic ferrocenyl TSCs against *P. falciparum* and revealed that dendritic TSCs displayed improved antiplasmodial activity possibly due to their enhanced accumulation in the infected erythrocytes.

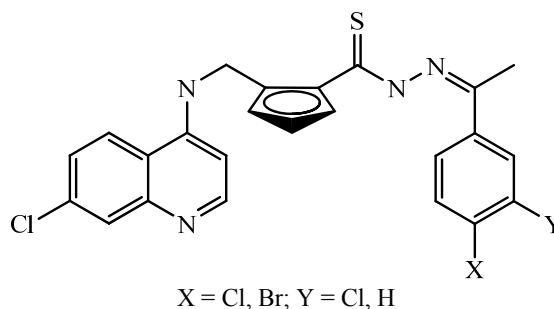


Figure 2.3: Structural formula of chimeras of thiosemicarbazones and ferroquine⁸⁵

2.1.2 Antibacterial Activity

In the assessment of the antibacterial activity of sixty five 2-acetylpyridine thiosemicarbazones and related compounds using clinical isolates of nine bacterial genera, Dobek *et al.* reported that these compounds were able to significantly inhibit *Neisseria gonorrhoeae*, *Neisseria meningitidis*, *Staphylococcus aureus*, *Streptococcus faecalis* and group D *Enterococcus* but were less active against the gram-negative bacilli viz., *Pseudomonas*, *Klebsiella-Enterobacter*, *Shigella*, *Escherichia coli*, and *Proteus*.⁵³ Similar results were obtained with thiosemicarbazones of 2-acetylquinoline and 1- and 3-acetylisquinoline.⁸⁹ Moreover, a series of 2-(α -hydroxyacetyl)pyridine thiosemicarbazones exhibited potent inhibitory activity against penicillin-sensitive as well as penicillin-resistant *N. gonorrhoeae*, against *N. meningitides*, and *S. aureus* while being less toxic to the host than the corresponding 2-acetylpyridine thiosemicarbazones.⁹⁰ 2-Acetylpyridine-1-oxide thiosemicarbazones were also found to be active against *N. gonorrhoeae*, *N. meningitidis*, *S. aureus* and *S. faecalis* but these compounds were found to be ineffective against the gram-negative enteric cultures and the *Pseudomonas* isolates.⁹¹ Pt(II) complexes of 2-acetylpyridine thiosemicarbazone also found to have complete lethal effect on gram-positive bacteria while the same complexes showed no bactericidal effect against gram-negative bacteria.⁹² 2-Formylpyridine thiosemicarbazones and their oxovanadium(IV) complexes were reported to exhibit powerful *in vitro* antibacterial activity towards *E. coli*.⁹³ On the other hand growth of gastritis-causing bacteria *Helicobacter pylori* was found to be inhibited by Bi(III) complexes with derivatives of tropolones and thiosemicarbazones.⁹⁴ Aryl thiosemicarbazones were also found to display good activity against *Aeromonas hydrophilia* and *Salmonella typhimurium*.⁹⁵ Limited antibacterial activity has also been reported with thiosemicarbazones and

thiocarbohydrazones of 1-adamantyl 2-pyridylketone and 1-adamantyl methyl ketone.⁹⁶

2.1.2.1 Antitubercular Activity

For the first time, in the mid 1940s, Domagk *et al.*¹⁴ reported that some TSCs of cyclic aldehydes and ketones exhibited antitubercular activities *in vitro*. Hoggart *et al.*⁹⁷ studied the antitubercular activity of a series of semi and thiosemicarbazones and reported that marked activity against acute *Mycobacterium tuberculosis* in mice was limited to the thiosemicarbazones of substituted benzaldehydes or heterocyclic aldehydes with highest activity observed when substituted at para position. Subsequent investigations by a number of workers have shown other TSCs to be antimycobacterial.⁹⁸⁻¹⁰⁰

p-Acetamidobenzaldehyde thiosemicarbazone, also known as Thiacetazone (Fig. 2.4, a) is the most widely used drug for treatment of tuberculosis.^{101,102} However, it suffers from a range of side effects and the development of resistance to the drug by the organism. So, it was recommended to use in combination with other antitubercular drugs (*e.g.* isoniazid, Fig. 2.4, b).¹⁰³ Inspired from the clinical success of thiacetazone more TSCs were studied for antitubercular activity^{53,104-108} and this led to the development of compounds **c** and **d** (Fig. 2.4) which were more active than compound **a** *in vitro* and *in vivo* against *Myocobacterium avium*.¹⁰⁹

The structure–activity study in a series of *N*(4)-substituted 2-acetylpyridine thiosemicarbazones suggested that antimycobacterial activity of these compounds depends on an optimum hydrophobicity, which in turn controls their rate of entry into the bacterial cell.¹¹⁰

In 2010, Pavan *et al.*¹¹¹ found that compounds **c**, **d** and **e** (Fig. 2.4) were more active and less toxic than some drugs commonly used in the treatment of tuberculosis.

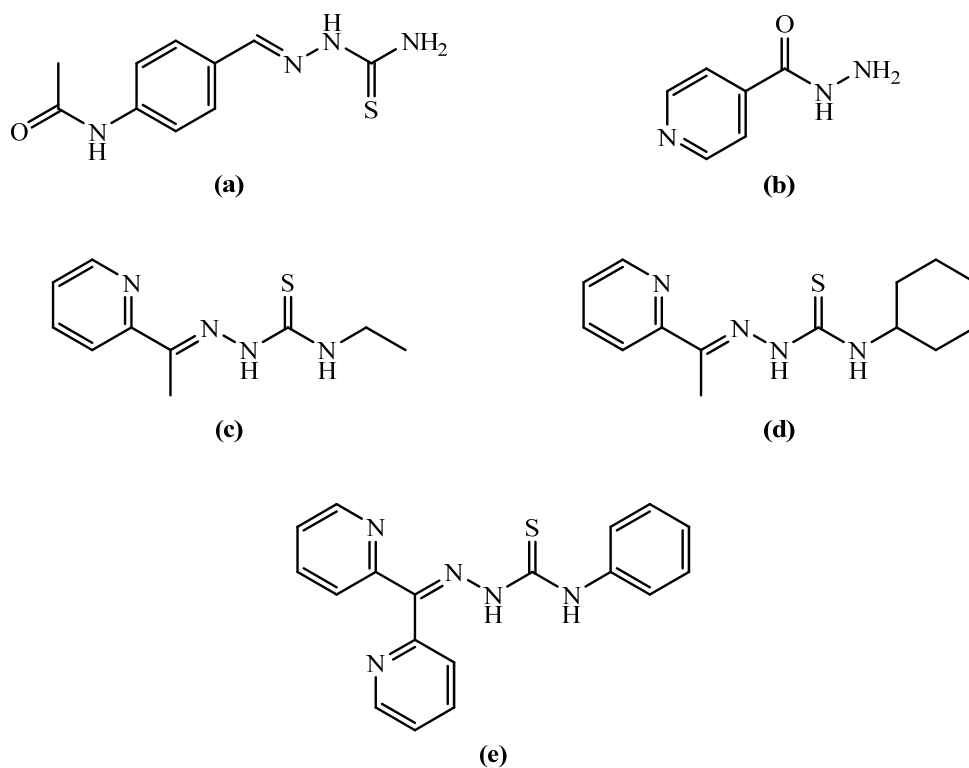


Figure 2.4: Examples of antitubercular thiosemicarbazones and isoniazid

2.1.3 Antifungal Activity

As early as 1960, a number of TSCs having aliphatic and aromatic substituents were tested for antifungal activity against *Chaetomium globosum* and *Aspergillus niger*. Of the thiosemicarbazones tested, 9-undecenal thiosemicarbazone appeared to be effective for complete inhibition of both organisms at 10 ppm, the lowest concentration used.¹⁰² The screening for antifungal activity of *p*-anisaldehyde TSC (Fig. 2.5 a) and pyridine-2-aldehyde TSC (Fig. 2.5 b) and their metal complexes against *Alternaria sp.*, *Paecilomyces sp.*, *Pestalotia sp.* revealed that the corresponding metal complexes were far more active compared to the free TSC ligand.¹¹²

Antifungal activity of pyridine-2-carbaldehyde, pyridine-3-carbaldehyde thiosemicarbazones and their metal complexes against *Candida albicans* and *Aspergillus fumigatus* were studied. The pyridine-2-carbaldehyde derivative was found to be more active than its 3-analogue, but the activity of the latter increased on coordination.¹¹³ Furthermore, *N*(4)-alkyl-, *N*(4)-dialkyl-2-acetylpyridine thiosemicarbazones as well as their Cu(II) complexes and Ni(II) complexes were found to show marked inhibitory activity against growth of *Aspergillus niger* with the Cu(II)

complexes being more active than Ni(II) complexes.^{114,115} However, Ni(II) complexes were found to be relatively more active than Cu(II) complexes when screened against *Paecilomyces variotii*.¹¹⁶ The Zn(II) complex of the *N*(4)-methyl derivative of 2-acetylpyridine thiosemicarbazone as well as *N*(4) substituted 2-benzoylpyridine thiosemicarbazones and its Cu(II) complexes also showed activity against both *A. niger* and *P. variotii*.^{117,118} Moreover, dinuclear Ni(II) complexes of *N*(4) substituted 2-hydroxyacetophenone thiosemicarbazones displayed considerable activity against *P. variotii* but not against *A. niger*.¹¹⁹

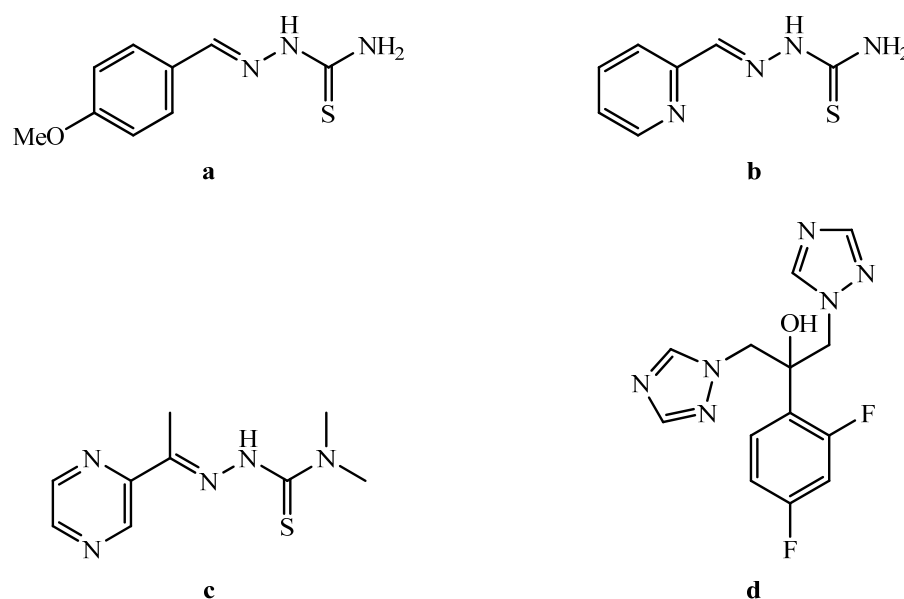


Figure 2.5: Structures of antifungal thiosemicarbazones and fluconazole

Recently, Opletlová *et al.*¹²⁰ studied the antifungal activity of acetylpyrazine TSCs against *C. albicans*, *C. tropicalis*, and *T. asahii* and reported that compound **c** (Fig. 2.5) exhibited most potent activity with comparable efficacy to the clinically used agent, **fluconazole** (Fig. 2.5 d). This compound also exhibited greater potency against *C. krusei*, *C. glabrata*, *A. fumigatus*, *A. corymbifera*, and *T. mentagrophytes* than fluconazole.

2.1.4 Antiviral Activity

The antiviral activity of thiosemicarbazones was first reported in 1950 by Hamre *et al.* with the observation that benzaldehyde thiosemicarbazone, its *p*-acetamido analogue and their *N*(4)-isobutyl derivatives were active against vaccinia virus in mice.¹⁶

Thompson *et al.*¹²¹ then explored the antiviral activity of TSCs containing phenyl, thiophenyl, pyridinyl, quinolinyl or isatinyl groups in the mice inoculated with virus by the cerebral route and compounds given orally. This led to the emergence of isatin 3-thiosemicarbazones.¹²² The notable example of a successful commercial TSC drug is *N*-methyl- β -isatin TSC, better known as methisazone (Marboran®, Fig. 1.2 b), which was used to treat smallpox.¹²³ In addition, marboran has also been used to treat individuals infected with the Herpes Simplex Virus (HSV).⁵⁶ Similarly, other studies have shown that 4',4'-diethyl derivatives of methisazone inhibit replication of Moloney leukemia virus by interfering with the early phase of viral life cycle¹²⁴ and that of human immunodeficiency virus (HIV) by a significant selective inhibition of HIV structural protein synthesis.¹²⁵

The first report on anti-herpes virus activity of a substituted thiosemicarbazone was from Sidwell *et al.* in 1969.¹²⁶ From the evaluation of a series of purine analogs as antiviral agents they demonstrated that purine-6-carboxaldehyde thiosemicarbazone was effective in suppressing both the cytopathic effect and the titers of human cytomegalo virus. The effect of heterocyclic thiosemicarbazones against HSV was examined by Brockman *et al.*¹²⁷ However, Shipman *et al.*¹²⁸ in 1981 evaluated the inhibitory activity of a series of thiosemicarbazones derived from 2-acetylpyridine, 2-acetylquinoline and 1-acetylquinoline against type 1 and type 2 herpes simplex virus and reported the selective antiviral activity against HSV-1 and HSV-2.⁵⁶ The results of study of the effects of 2-acetylpyridine thiosemicarbazones on mammalian and HSV-RR supported the hypothesis that the HSV-induced RR is an important target for the design of antiviral drugs.¹²⁹

Mishra *et al.*⁵⁷ evaluated menthone thiosemicarbazone, (Fig. 2.6, a) for the first time, against the human immunodeficiency virus (HIV) types 1 and 2 in which the compounds revealed a marked antiviral activity. It was found that thiosemicarbazones with chlorobenzene substituents at the *N*(4) position revealed the highest activity among the various (\pm)-3-menthone thiosemicarbazones. Bal *et al.*¹³⁰ reported a promising anti-HIV 1 activity for a series of isatin β -thiosemicarbazone derivatives (Fig. 2.6, b).

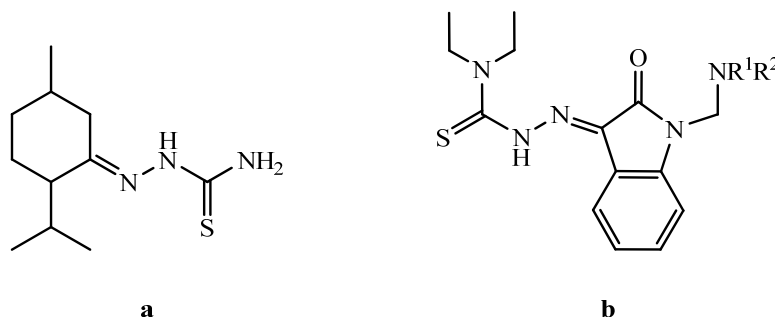


Figure 2.6: Structures of some TSCs tested for anti-HIV activity

2.1.5 Antitumor Activity

The antitumor effects of TSCs was first reported by Brockman *et al.*⁴ In 1963, French *et al.*¹³¹ formulated hypotheses about the mode of action of α -N-heterocyclic TSCs and this stipulated further investigations into these compounds for biological benefits.

2.1.5.1 Development of Thiosemicarbazones as Antitumor Agents

2.1.5.1.1 Hydroxypyridine-2-Carboxaldehyde Thiosemicarbazone and Older Generation Thiosemicarbazones

The antitumor activity of thiosemicarbazones was discovered in 1956, with the observation that pyridine-2-carboxaldehyde TSC (Fig. 2.7, a) showed antileukemic activity in mice.⁴ In that study it was also reported that the analogous compounds 3-formylpyridine TSC (Fig. 2.7, b) and 4-formylpyridine TSC (Fig. 2.7, c) as well as *p*-acetamidobenzaldehyde TSC (Fig. 2.7, d), *p*-nitrobenzaldehyde TSC (Fig. 2.7, e), quinoline-4-carboxaldehyde TSC (Fig. 2.7, f), indole-3carboxaldehyde TSC (Fig. 2.7, g), and TSCs derived from 2-furaldehyde, 2-thenaldehyde and 2-pyrrolaldehyde (Fig. 2.7, h) show no significant effect on the life span of the mice. Further studies on thiosemicarbazones with different formyl heterocycles confirmed the assumption that all compounds with other donor set than *N,N,S* are inactive.⁵ Hence the minimum requirement for biological activity is a heterocyclic nitrogen in α -position to the thiosemicarbazide side chain.

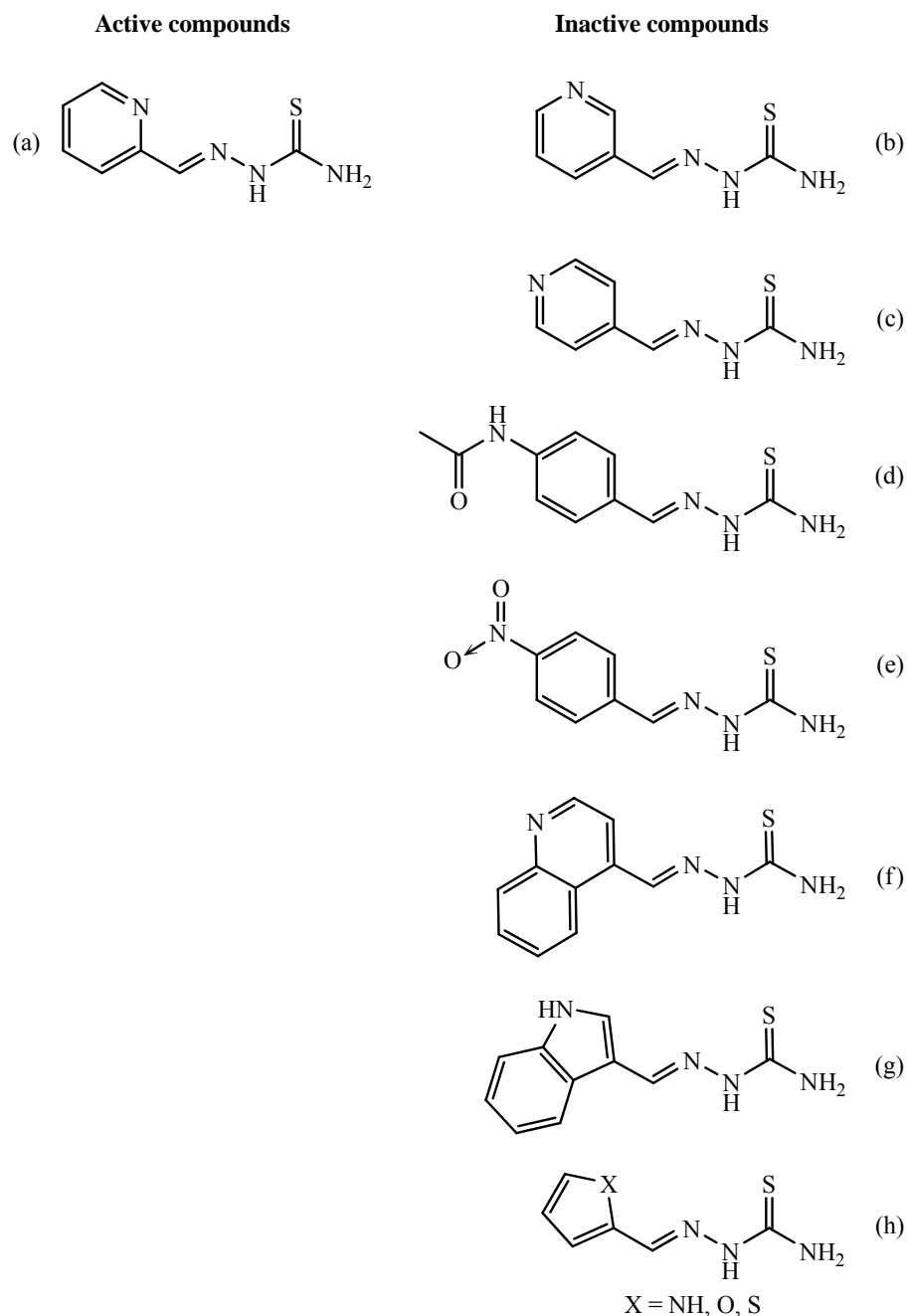


Figure 2.7: Structure of thiosemicarbazones which are active/inactive against L1210 leukemia in mice. The study of a series of isoquinoline-1-carboxaldehyde thiosemicarbazone (Fig. 2.8, a) derivatives in mice bearing Sarcoma 180 ascites cells showed that 1-acetylisquinoline thiosemicarbazone (Fig. 2.8, b) and isoquinoline-1-carboxaldehyde guanylhydrazone (Fig. 2.8, c) are the most active derivatives, but with reduced tumor-inhibiting potency as compared to isoquinoline-1-carboxaldehyde thiosemicarbazone. This study further revealed that replacement of the thiosemicarbazide side chain by semicarbazide (Fig. 2.8, d), *N*(2)-methyl thiosemicarbazide (Fig. 2.8, e), *S*-

methylthiosemicarbazide (Fig. 2.8, f) or 1-formylthiosemicarbazide (Fig. 2.8, g) results in the loss of activity.¹³²

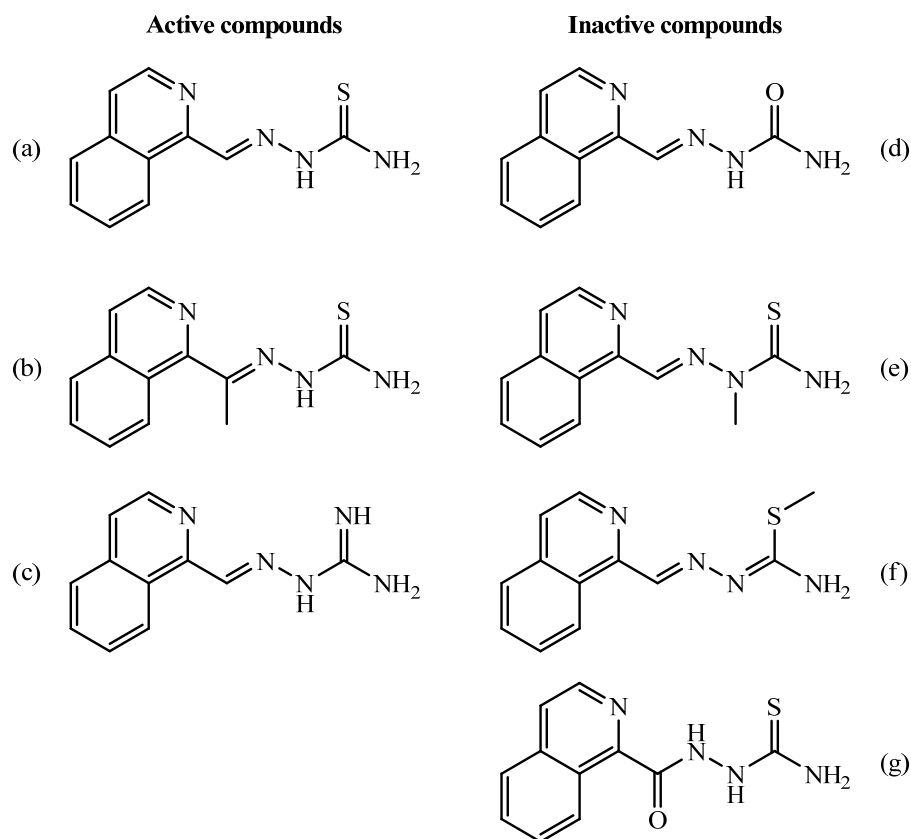


Figure 2.8: Effect of modifications in the side chain of isoquinoline-1-carboxaldehyde thiosemicarbazone on the tumor-inhibiting potency in mice bearing Sarcoma 180 ascites cells

These structure-activity studies led to the development of pyridine-2-carboxaldehyde TSc (Fig. 2.7, a) and isoquinoline-1-carboxaldehyde TSC (Fig. 2.8, a). Extensive studies by French *et al.*^{133,134} and Creasy *et al.*¹³⁵ identified that the most promising candidate was 5-hydroxypyridine-2-carboxaldehyde thiosemicarbazone (Fig. 1.1 b), which was further evaluated in clinical trials. However, because of severe side effects and short half life in patients (due to rapid inactivation *via* formation and subsequent elimination of the *O*-glucuronide conjugate) it has been withdrawn.^{8,136} These early investigations revealed that the anti-tumor activity of thiosemicarbazones was associated with their ability to deprive iron from RR.^{137,138}

2.1.5.1.2 3-AP and Ribonucleotide Reductase Inhibition

Sartorelli *et al.* synthesized a series of 4-methyl, 3-amino, 5-amino and 5-nitro substituted derivatives that are resistant to glucuronidation and rapid elimination.^{139,140} Among them the amino substituted compounds showed higher potency compared to 5-hydroxypyridine-2-carboxaldehyde thiosemicarbazone when tested in mice bearing L1210 leukemia. For further evaluation in clinical trials, 3-aminopyridine-2-carboxaldehyde thiosemicarbazone (Triapine, 3-AP) (Fig. 1.1 d) was selected.¹³⁹ 3-AP markedly inhibited the proliferation of L1210 leukemia cell both *in vitro* and *in vivo* as well as inhibiting the growth of murine M109 lung carcinoma and human A2780 ovarian carcinoma xenograft in mice.^{141,142} Subsequent studies by Chaston *et al.*¹⁴³ demonstrated that the 3-AP-Fe complex was redox active, leading to ascorbate oxidation, hydroxylation of benzoate, plasmid DNA degradation, as well as glutathione depletion and DNA degradation in cultured tumor cells. A later study by Shao *et al.*² suggested that the FeII-3-AP complex was a more effective RR inhibitor than the free ligand, in agreement with the previous studies. Shao and colleagues showed that the cytotoxic effect of 3-AP was the result of both ROS-mediated quenching of the tyrosyl radical in the R2 subunit of RR, rendering the enzyme inactive, as well as the toxic effects of ROS on proteins.² Earlier studies also showed that the Fe complex of similar monothiosemicarbazones inhibit RR more effectively than the free ligand.¹⁴⁴

2.1.5.1.3 2-Hydroxy-1-naphthylaldehyde-3-thiosemicarbazones (NT) series

The low antiproliferative activity observed with thiosemicarbazones analogous to 2-pyridylcarboxaldehyde isonicotinoyl hydrazone (PCIH) suggested that the antitumor activity may be mostly conferred by the thiosemicarbazide moiety of HCTs instead of 2-pyridylcarboxaldehyde.^{145,146} With this observation further structurally modified new series of thiosemicarbazones known as 2-hydroxy-1-naphthylaldehyde-3-thiosemicarbazone (NT) (Fig. 2.9) were synthesized. In these studies 2-hydroxy-1-naphthylaldehyde-3-thiosemicarbazone (NT), 2-hydroxy-1-naphthylaldehyde-4-methyl-3-thiosemicarbazone (N4mT), and 2-hydroxy-1-naphthylaldehyde-4,4-dimethyl-3-thiosemicarbazone (N44mT) demonstrated greater ability to inhibit the growth of neoplastic cells compared with a range of normal cells.¹⁴⁷ It was observed that as the substituents on the terminal nitrogen atom of the thiosemicarbazide became

increasingly lipophilic, the compounds lost antiproliferative activity. For instance, replacing methyl groups with phenyl substituents resulted in a marked decrease in antiproliferative activity.¹⁴⁷

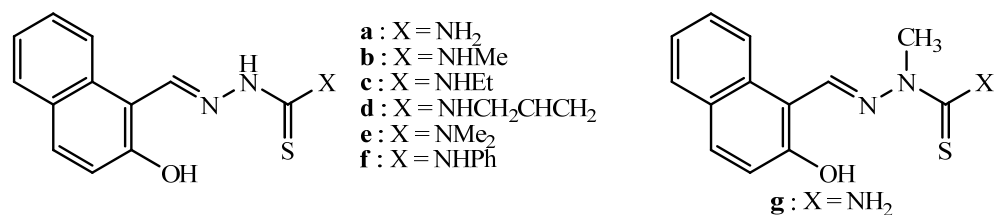


Figure 2.9. Structures of NT series¹⁴⁷

2.1.5.1.4 Di-2-pyridylketone Thiosemicarbazones (DpT) series

Although 3-AP has shown some promises, it has serious side effects including hypoxia and methemoglobinemia.¹⁴⁸ To overcome these problems and encouraged by the promising activities of the aroylhydrazones (NT series) and early thiosemicarbazones even more effective compounds known as the DpT series have been designed (Fig. 2.10).¹⁴⁹ The design of the DpTs, (Fig. 2.10, a – f) was based on the high activity of triapine and the aroylhydrazones belonging to the class of 2-pyridylketone isonicotinoyl hydrazone (PKIH).^{143,150} One of the most active compounds in this series was di-2-pyridylketone-4,4-dimethyl-3-thiosemicarbazone (Dp44mT) (Fig. 2.10, e) which was more effective than desferrioxamine (DFO) in both entering cells and inducing iron release and preventing iron uptake from transferin.¹⁴⁹ This compound showed high anti-proliferative activity *in vitro* against a variety of cancer cell lines, including murine *M109* lung cell line, SK-N-MC neuroepithelioma cell line, SK-Mel-28 melanoma cell line and MCF-7 breast cancer cell line.^{40,149-151} When administered intravenously, Dp44mT (Fig. 2.10 e) markedly inhibited human and murine tumour xenograft growth in mouse models,¹⁵²⁻¹⁵⁴ with tumour weight reduced to 8% compared to the control at a dosage of 0.4 mg/kg.¹⁵¹ However, increasing the dosage to 0.75 mg/kg over 2 weeks induced cardiac fibrosis in nude mice.⁴⁰

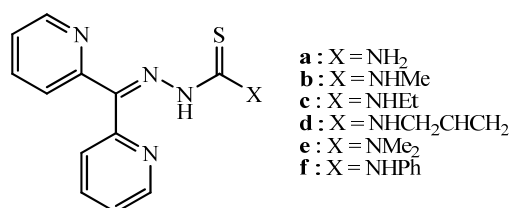


Figure 2.10. Structures of DpT series¹⁵⁵

In addition to the ability of Dp44mT to effectively induce cellular iron-deprivation *in vitro*, initial studies revealed that the iron complex was redox-active within cells.^{42,149} Hence, it was proposed that the antitumor activity of these compounds relates both to their ability to bind intracellular iron and to form redox-active iron complexes that generate cytotoxic ROS.^{42,156}

2.1.5.1.5 2-Benzoylpyridine Thiosemicarbazones (BpT) and 2-(3'-Nitrobenzoyl)pyridine Thiosemicarbazones (NBpT) series

In order to address the issue of cardiac fibrosis in nude mice induced by the DpTs,¹⁵¹ new series of 2-benzoylpyridine thiosemicarbazones (BpT) (Fig. 2.11, a - f) and 2-(3'-nitrobenzoyl)pyridine thiosemicarbazones (NBpT) (Fig. 2.11, g - l) were synthesized with structural modifications of DpT.¹⁵⁷ This structural modification involved the addition of a phenyl ring in place of the non-coordinating 2-pyridyl group. The rationale for this change was that it could increase the lipophilicity of the ligands as well as to enhance the redox activity of the ligand-iron complex *via* removal of an electron-withdrawing pyridyl ring.¹⁵⁷ Both series of chelator analogues were shown to have selective anti-tumor activity *in vitro* and *in vivo* with the most potent compound being Bp4eT (Fig. 2.11, c).⁴³ Importantly, these compounds were found to be effective *via* the intravenous or oral routes.^{152,154,158} Structure-activity relationship analysis showed that substitution with hydrophobic groups enhanced anti-proliferative activity in comparison to hydrophilic parent compounds BpT (Fig. 2.11, a) and NBpT (Fig. 2.11, g).¹⁵⁷ Additionally, these thiosemicarbazones were more stable in plasma and are advantageous over aldehyde-derived aroylhydrazones (PCIH series) which undergo hydrolysis of the hydrazone bond.¹⁵⁹

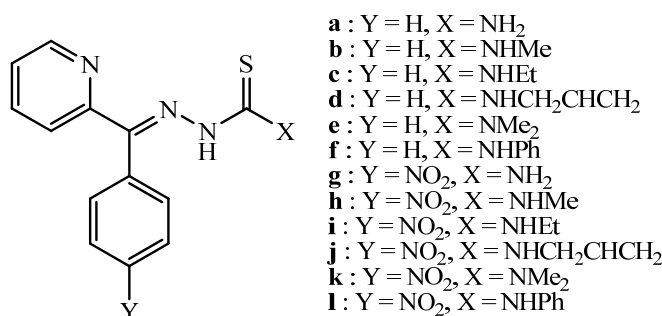


Figure 2.11. Structures of BpT series¹⁵⁷

The iron coordination, chelation efficacy and redox activity of BpT and NBpT series have also been investigated. The enhanced iron efflux induced by these chelators was

attributed to their higher lipophilicity in comparison to the DpT ligands, leading to improved membrane permeability. Although, the incorporation of an electron-withdrawing group (-NO₂) lowered the redox potential of the NBpT-iron complexes, no increase was observed in their anti-proliferative activity due to hindrance from the nitrophenyl group.¹⁵⁷

These findings suggest that the combination of benzoylpyridine and thiosemicarbazone results in an effective backbone structure for the further development of potent iron chelators for anti-cancer treatment.

2.1.5.1.6 2-Acetylpyridine Thiosemicarbazones (ApT)

With the demonstration that the DpT, BpT and NBpT series exhibit antiproliferative activity through redox cycling,^{42,149} an attempt was made to examine the effect of substituents at the imine carbon on antitumor and redox activity. This led to the development of the 2-acetylpyridine thiosemicarbazone (ApT) series (Fig. 2.12, a - f). To generate this series, one of the electron-withdrawing pyridine rings of the DpT scaffold was replaced by an electron-donating methyl group.⁴⁰ Out of the six ApT chelators synthesized, four of those demonstrated potent anti-proliferative activity in human SK-N-MC neuroepithelioma cell lines and also demonstrated iron chelation efficacy similar to the DpT and BpT series.³⁹ In this series ApT (Fig. 2.12, a) was the least effective probably due the fact that it is the most hydrophilic compound of the series. More importantly, the ApT chelators were able to effectively mobilise intracellular ⁵⁹Fe and inhibit ⁵⁹Fe uptake in tumour cells.^{39,40} These results demonstrated that the nature of the substituent at the imine carbon of the thiosemicarbazone scaffold has a significant effect on the anti-proliferative activity and Fe^{III/II} redox potentials. Hence, this series of compounds could be considered as a potential anti-tumour agent for the treatment of cancers.

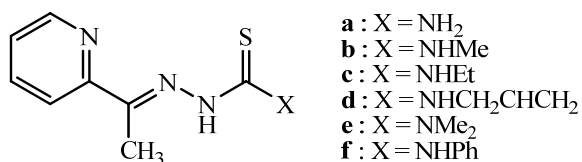


Figure 2.12: Structures of the ApT series³⁹

2.1.5.1.7 Quinoline Thiosemicarbazones (QT)

French and Blanz⁵ synthesized 1-formylisoquinoline TSC (IQ-1, Fig. 2.13, a) to continue the investigation on anticancer activity of HCTs and subsequently Agrawal¹⁶⁰ and others extended the studies by fabricating a variety of structurally modified compounds of this class. A number of IQ-1 derivatives proved to be more active against transplanted animal tumors and less toxic to the host than 2-formylpyridine TSC. Among the most potent inhibitors of RR in this class of agents was the 4-methyl-5-amino derivative (MAIQ-1, Fig. 2.13, b), which was specifically designed to incorporate increased water solubility coupled with potent inhibitory activity for RR and therapeutic properties.¹⁶⁰

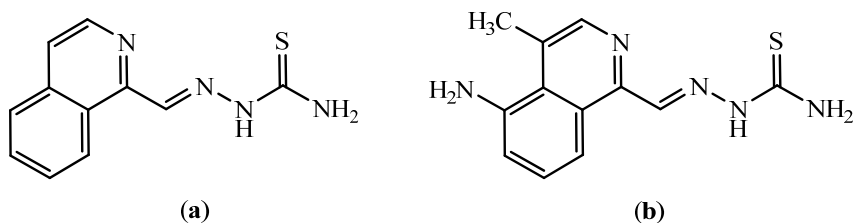


Figure 2.13: Structures of IQ-1 and MAIQ-1

More recent studies have led to the development of quinoline thiosemicarbazone (QT) series (Fig. 2.14, a - l).¹⁶¹ The compounds were designed to contain a quinoline scaffold (as in clinically used anti-cancer drugs e.g., camptothecin (Fig. 2.15, a) derivatives, topotecan (Fig. 2.15, b) and irinotecan (Fig. 2.15, c)^{162,163} in order to investigate their effect on iron uptake, iron mobilization and anti-proliferative activity against tumor cell lines.

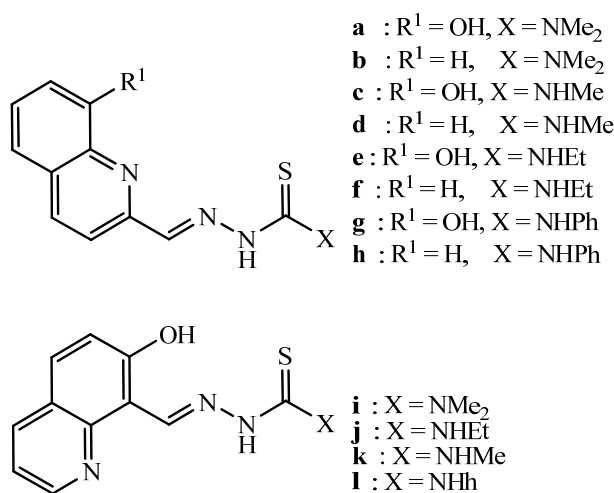


Figure 2.14: Structures of the QT series¹⁶¹

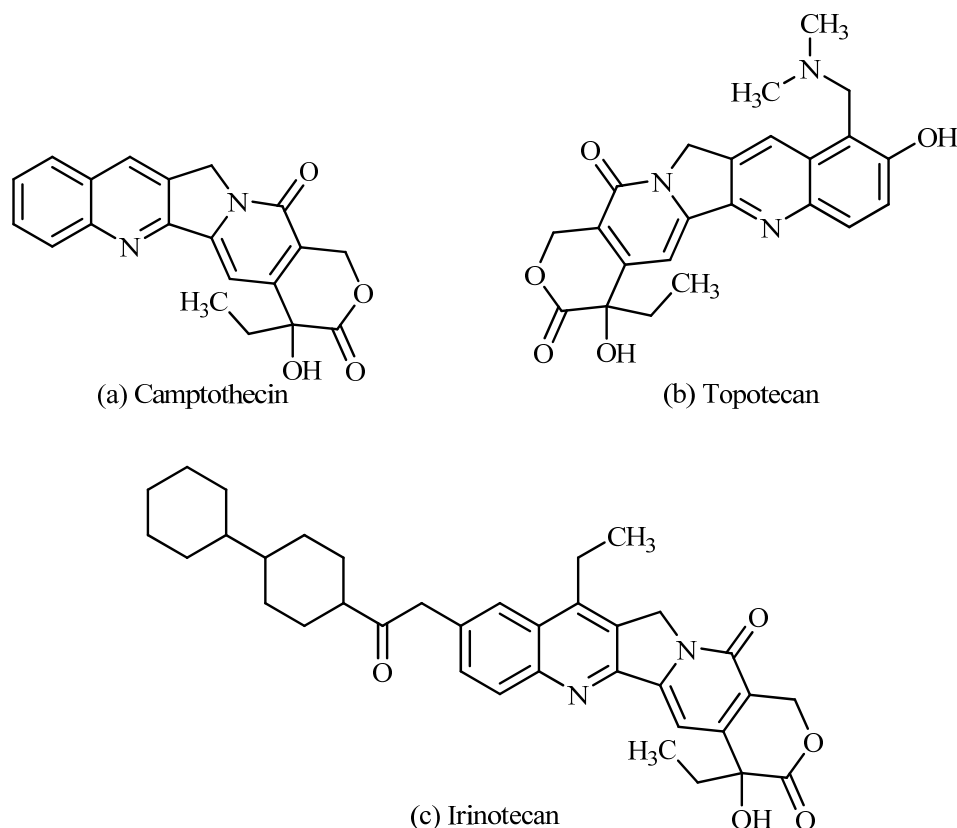


Figure 2.15: Some clinically used anti-cancer drugs containing a quinoline scaffold

In first series (Fig. 2.14, a - h), the four-atom moiety ($N=C-C=N$), which is found in the DpTs and BpTs is maintained. In contrast, in second series, (Fig. 2.15, i - l), this moiety was extended ($N=C-C-C=N$), while a five-atom fragment construct ($N=C-C-C-OH$) similar to NT was preserved. Several analogs of the two series of QTs acted similarly to Dp44mT with marked prevention of cellular iron uptake and promotion of iron mobilization.^{42,149,151}

All the QTs of second series (Fig. 2.15, i - l) demonstrated moderate anti-cancer activity in SK-N-MC cells, while only one member of first series (Fig. 2.15, b) showed appreciable anti-proliferative effects. The QT series demonstrated selective anti-proliferative activity againsts neo-plastic cells over normal cells.^{149,151,157} In general, the QT series were less efficient as anti-proliferative agents than their precursors, namely the BpT and DpT series.^{149,151,157,158}

2.2. Biological Activity of 2-Pyridineformamide Thiosemicarbazones

Although a variety of *N*(4)-substituted α (N)-HCTs and their metal complexes were reported to possess substantial *in vitro* activity against various human tumor lines,^{118,164-166} they exhibited less promising *in vivo* activity due to the lack of solubility in aqueous solutions. The attempt to enhance the water solubility of thiosemicarbazones and their complexes led to development of a series of 2-pyridineformamide TSCs in which the TSC moiety is attached to an amide carbon rather than an aldehyde or ketone carbon.¹⁶⁷ The rationale behind this is that the resulting TSC contains an additional amino group which could give improved water solubility that in turn can improve biological activity. Further this NH₂ functionality could decrease drug toxicity.²⁹

Mendes *et al.*^{168,169} reported that 2-pyridineformamide thiosemicarbazones and their tin(IV) complexes were effective as antimicrobials against the growth of *Candida albicans*, *Salmonella typhimurium*, and *Pseudomonas aeruginosa*, and were highly active against malignant glioblastoma. These thiosemicarbazones and their tin(IV) complexes proved to be more potent as cytotoxic agents than cisplatin. 2-Pyridineformamide thiosemicarbazone (H2AmD4), its *N*(4)-methyl (H2Am4Me) and *N*(4)-ethyl (H2Am4Et) derivatives (Fig. 2.16) and their iron(III) complexes presented toxicity against *Artemia salina* at low concentrations.¹⁷⁰ Copper(II) complexes of methyl, ethyl and phenyl derivatives of 2-pyridineformamide are also found to be active against *A. salina*.¹⁷¹ Since the toxicity against *A. salina* bioassay has a good correlation with cytotoxic activity in human solid tumors, these compounds present potential pharmacological applications.

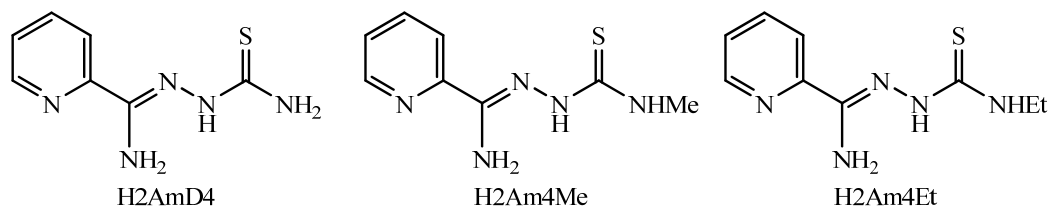


Figure 2.16: Chemical structures of the 2-pyridineformamide thiosemicarbazones

Mendes *et al.* tested a series of 2-pyridineformamide-derived thiosemicarbazones and their gallium(III) complexes against several isolates of pathogenic *Cryptococcus* strains. On complexation the antifungal activity significantly increased, suggesting

coordination to gallium (III) to be an interesting strategy for the antifungal dose reduction.^{172,173}

2.3. Enzyme modelling

The active centres of several metalloenzymes such as hydrogenases, xanthine oxidase and nitrogenase are found to be comprised of transition metal complexes of ligands containing sulphur and nitrogen donor centres.¹⁷⁴ Valuable information to understanding the functions of different enzymes at the molecular level have been derived from synthesis, characterization and structure and reactivity studies of such complexes with *N*, *S* and *N*, *N*, *S* donor sets.¹⁷⁵ Model complexes for the active sites of metalloenzymes with mixed N/S donor centres such as nitrile hydratase have been synthesized using bis-thiosemicarbazones because they also have an N₃S donor set.¹⁷⁶ One of the recent area of interest is the active sites of carbon monoxide hydrogenase, acetyl coenzyme synthase A, etc.

2.4. Radiolabelling and image sensing

In the modern clinical environment, *in vivo* molecular imaging plays a vital role in drug discovery. There are two general techniques used to produce diagnostic images, single photon emission computed tomography (SPECT) utilizing gamma-emitting isotopes, and positron emission tomography (PET) utilizing positron-emitting isotopes.

Being fluorescent (bis-thiosemicarbazonato)copper complexes are found to be useful in radiolabelling and are hence suitable for diagnostic imaging of Alzheimer's.^{177,178} Because of their hypoxic selectivity, certain copper bis-thiosemicarbazones, for example diacety-2,3-bis(4-*N*-methyl-3-thiosemicarbazonato) copper(II) complex (Cu-ATSM) (Fig. 2.17) have been used as PET agents to image tissue hypoxia and as vehicles for the delivery of radioactive copper isotopes to tumors or leukocytes.¹⁷⁹⁻¹⁸⁴

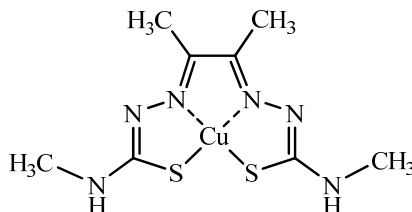


Figure 2.17: Structure Cu-ATSM

Ga(III) complexes of 2-acetylpyridine thiosemicarbazones (Fig. 2.18), a convenient source of γ -ray emitters, are found to exhibit profound antiviral and antitumor activity with energy, which make them useful for medical diagnostic agent.^{185,186}

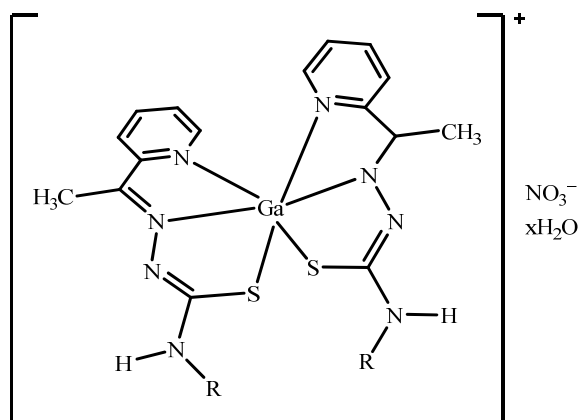


Figure 2.18: Structural representation of Gallium(III) complexes of 2-acetylpyridine thiosemicarbazone

2.5. Antiausterity strategy

The genetic and epigenetic alterations of the cells cause unregulated growth of cancer cells and there is insufficient and inappropriate vascular supply to the newly formed cells. As a result, the demand of cancer cells for essential nutrients as well as oxygen always exceeds the supply.¹⁸⁷⁻¹⁸⁹ However, cancer cells show an inherent tolerance to nutrient starvation by changing their energy metabolism.¹⁹⁰ Pancreatic cancer cell lines, such as PANC-1, AsPC-1, BxPC-1, and KP-3, exhibit marked tolerance and survive for prolonged periods of time even under extremely nutrient-starved conditions.¹⁹⁰ Thus, it was hypothesized that tolerance to nutrient starvation might be a part of the biological response to insufficient blood supply. Elimination of this tolerance to nutrient starvation has been recognized as a novel biochemical approach for cancer therapy and the development of drugs that specifically target the resistance of tumor cells to nutrient starvation has been termed the antiausterity therapeutic strategy.¹⁹⁰⁻¹⁹²

The screening of agents for anticancer activity in the anti-austerity strategy is quite different from the conventional method. In conventional method the activity of a sample is studied by testing its cytotoxicity in nutrient rich medium. If it is cytotoxic it may act as anticancer agent. If it not toxic then it is not considered as anticancer

agent (Fig. 2.19). However, in anti-austerity strategy, the sample which is not toxic in nutrient rich medium is tested for its cytotoxicity in nutrient deprived medium (NDM). If it is cytotoxic then it can be a potential preferentially cytotoxic candidate. The advantage of anti austerity agents against conventional anticancer agents is that these agents targets tumor microenvironment directly and does not cause toxicity to the normal cells.

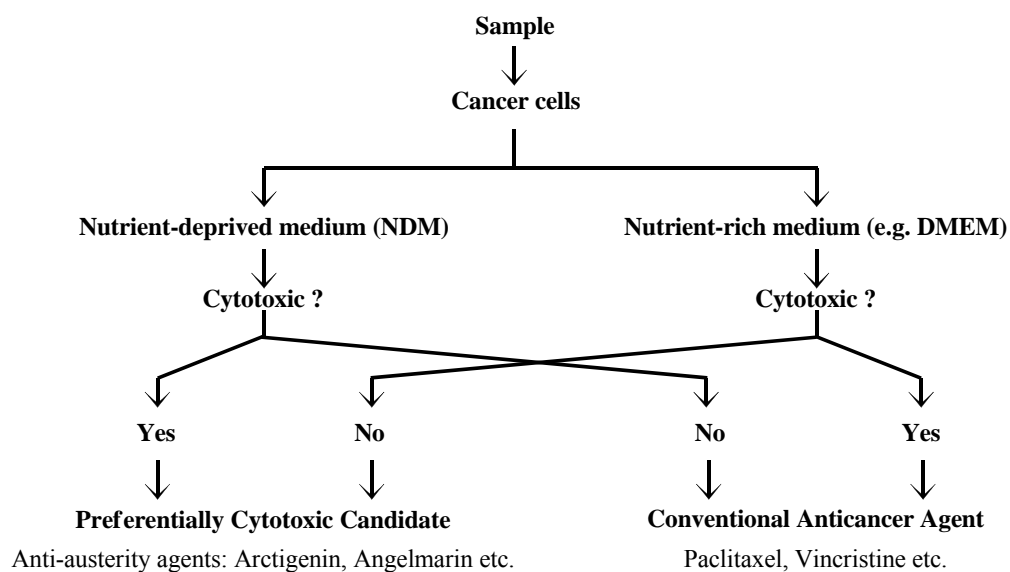


Figure 2.19: Antiausterity strategy in anticancer drug discovery

3. MECHANISM OF ACTION OF THIOSEMICARBAZONE AS AN ANTICANCER AGENT

3.1 Types of cancer chemotherapy drugs and their mode of action

On the basis of the mechanism of action current cancer chemotherapeutic agents can be classified into following categories:¹⁹³

3.1.1 Antimetabolites

These are structurally similar to natural metabolites and are able to disrupt nucleic acid synthesis either by falsely substituting for biosynthetic precursors of DNA/RNA or by inhibition of normal precursor biosynthesis. Examples of this type of chemotherapeutic drugs are as follows:

- a. **Folate Antagonist:** Inhibit dihydrofolate reductase. e.g., methotrexate
- b. **Pyrimidine Antagonist:** Inhibit thymidylate synthetase, e.g., fluorouracil; and those which inhibit DNA polymerase e.g., cytarabine.
- c. **Purine Antagonist:** Inhibit interconversion of purine nucleotide. e.g., 6-mercaptopurine and 6-thioguanine.
- d. **Ribonucleotide Reductase Antagonist:** which inhibit ribonucleotide reductase. e.g., hydroxyurea, thiosemicarbazones such as triapine etc.

3.1.2 DNA interactive agents

These agents alter DNA structure so as to interfere with its template function for replication. This includes –

- a. **Alkylating agents:** e.g., mechlorethamine, cyclophosphamide, isosfamide, chlorambucil, mephalan, busulfan, nitrosoureas and thio-TEPA
- b. **DNA strand-breaking agents:** e.g., cisplatin, carboplatin and oxaliplatin, imatinib
- c. **DNA intercalating antibiotics:** e.g., bleomycin, mitomycin C, actinomycin D, daunorubicin, doxorubicin and idarubicin.
- d. **Intercalating topoisomerase II inhibitors:** e.g., mitoxantrone, amonafide, ellipticine.

- e. **Non-intercalating topoisomerase II inhibitors:** e.g., etoposide, teniposide, and topoisomerase I inhibitors; camptothecin analogues such as topotecan, irinotecan.

3.1.3 Tubulin interactive agents

These agents are essentially mitotic inhibitors and act by interfering with the cellular mechanism of mitosis thus interfering with protein synthesis. It includes;

- a. **Antitubulin:** bind tubulin and destroy spindle to produce mitotic arrest e.g., vinca alkaloids such as vincristine, vinblastin, vinorelbine, paclitaxel, docetaxel.
- b. **Agents influencing amino acid supply:** e.g., L-asparaginase.

3.1.4 Hormonal agents

These agents are often natural or synthetic hormonal substances such as steroids, steroid analogs or hormone-like compounds which interact with hormone receptors to reduce tumors whose growth are sensitive to hormonal controls. It includes:

- a. **Estrogens and estrogen antagonistic drugs** e.g., ethinylestradiol, fofestrol, SERM-tamoxifene.
- b. **Androgens and androgen antagonistic drugs** e.g., flutamide and bicalutamide.
- c. **Progestogen drug** e.g., hydroxyprogesterone acetate.
- d. **Gonadotropin-releasing hormone inhibitors** e.g., nafarelin, triptorelin.
- e. **Aromatase inhibitors** e.g., letrozole and anastrozole.

3.2 Anticancer Activity of Thiosemicarbazones

Among the various areas in which TSC compounds are being explored, the most promising one is their anticancer activity. Currently, RR inhibition,¹²⁷ topoisomerase II inhibition,¹⁹⁴ mitochondria disruption,¹⁴⁹ reactive oxygen species (ROS) production,² and, more recently, a multidrug resistance protein (MDR1) inhibition^{195,196} are the major notable effects associated with the anticancer activity of TSCs.

3.2.1 Ribonucleotide Reductase

The antitumor activity of TSCs was revealed in their ability to inhibit ribonucleotide reductase (RR), the enzyme that catalyzes the synthesis of deoxyribonucleotides, the building blocks of DNA from their ribonucleotide precursors. In fact, TSCs are the most potent known inhibitors of this enzyme, both in cell-free assays and in intact tumor cells³ and are several orders of magnitude more effective than hydroxyurea, the first clinically applied ribonucleotide reductase inhibitor.^{6,59} RR is produced at the transition from the G1 to the S phase of the cell cycle as a prerequisite for DNA replication and is highly expressed in tumor cells, making it a site of vulnerability to be targeted by antitumor agents.¹⁹⁹ Mammalian (class Ia) ribonucleotide reductase is composed of an α_2 homodimer (two identical R1 subunits) and a β_2 homodimer (two identical R2 subunit). The R1 subunit contains the active site as well as two allosteric control sites. This subunit includes the catalytically active centre consisting of redox-active cysteines that are regenerated by the action of thioredoxin and the R2 subunit contains a tyrosyl radical and a diiron center which are essential for initiation of the nucleotide reduction process at the active site in R1.²⁰⁰ The R1 and R2 subunits together form the catalytically active enzyme.

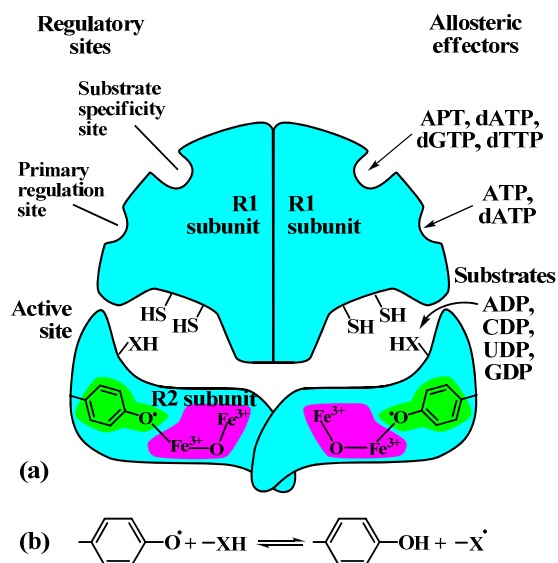


Figure 3.1: Model of ribonucleotide reductase from *E. coli*^{197,198} (a) Subunit structure. The function of the two regulatory sites is explained in Fig. 3.3. Each active site contains two thiols and a group (-XH) that can be converted into a an active-site radical; this group is probably the -SH of Cys-439, which functions as a thiyl radical. (b) The tyrosyl radical functions to generate the active-site radical (-X[•]), which is used in the mechanism shown in Fig. 3.2.

3.2.2. Ribonucleotide reductase reaction

Ribonucleotide reductase (RR) is a multifunctional enzyme that contains redox-active thiol groups for the transfer of electrons during reduction reactions. In the process of reducing the ribonucleoside diphosphate (rNDP) to a 2'-deoxyribonucleoside diphosphate (dNDP), RR becomes oxidized. RR is reduced in turn, by either thioredoxin or glutaredoxin. (Fig. 3.2) The ultimate source of the electrons is NADPH. The electrons are shuttled through a complex series of steps involving enzymes that regenerate the reduced forms of thioredoxin or glutaredoxin. These enzymes are thioredoxin reductase and glutathione reductase respectively.²⁰¹

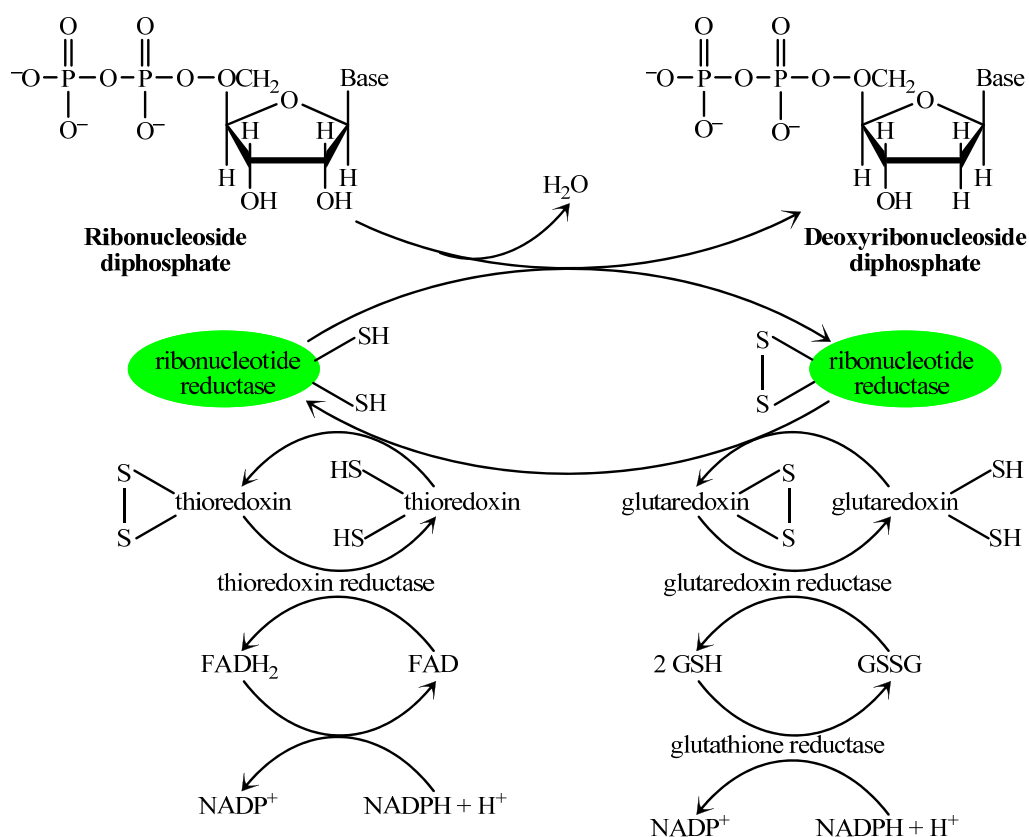


Figure 3.2: Reduction of ribonucleotides to deoxyribonucleotides by Ribonucleotide reductase.¹⁹⁸

The enzyme RR in *E. coli* and most eukaryotes is a dimer, with subunits designated R1 and R2 (Fig. 3.1). At each active site, R1 contributes two sulphhydryl groups required for activity and R2 contributes a stable tyrosyl radical. The R2 subunit also has a binuclear iron (Fe³⁺) cofactor that helps generate and stabilize the tyrosyl radicals (Fig. 3.1). The tyrosyl radical is too far from the active site to interact directly with the site, but it generates a thiyl radical of a cysteine residue which starts the substrate turnover cycle (Fig. 3.3).

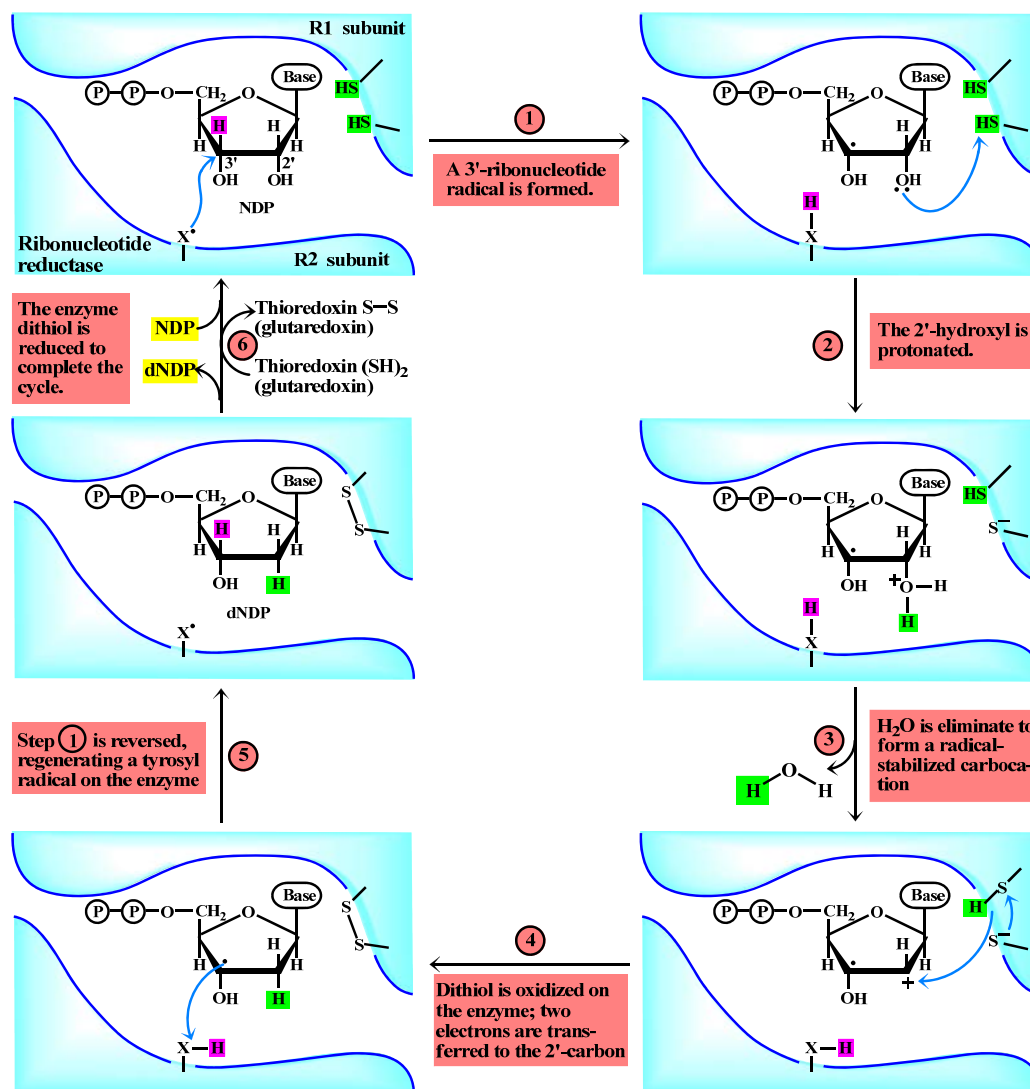


Figure 3.3: Catalytic mechanism for the ribonucleotide reductase reaction¹⁹⁸

In the first step, the thyl radical abstracts a hydrogen atom from C-3' of the generating a substrate radical at C-3'. Subsequently the radical at C-3' promotes the release of the OH⁻ from the C-2' carbon atom. Protonated by a second cysteine residue, the departing OH⁻ leaves as a water molecule and a 2'-ketyl radical is formed (state 3). Then a hydride ion is transferred from a third cysteine residue to complete the reduction of the C-2' position, generates a disulfide radical anion, and reform a C-3 radical (state 5). In the last step, this C-3' radical recaptures the same hydrogen atom originally abstracted by the first cysteine residue, and the deoxyribonucleotide is free to leave the enzyme. R2 provides an electron to reduce the thyl radical. The disulfide bond generated in the enzyme's active site is then reduced by a specific disulfide containing protein, such as thioredoxin, to regenerate the active enzyme.¹³⁸

To complete the overall reaction, the oxidized thioredoxin generated by this process is reduced by NADH in a reaction catalyzed by thioredoxin reductase.

Three classes of RR have been reported. Their mechanisms (where known) generally confirm to the scheme in Fig. 3. 3, but they differ on the identity of the group supplying the active-site radical and in the cofactors used to generate it. The *E. coli* enzyme (class I) requires oxygen to regenerate the tyrosyl radical if it is quenched, so this enzyme functions only in an aerobic environment. Class II enzymes, found in other microorganisms, have 5'-deoxyadenosylcobalamin rather than a binuclear iron center. Class III enzymes have evolved to function in an anaerobic environment. *E. coli* contains a separate class III RR when grown anaerobically; this enzyme contains an iron-sulfur cluster (structurally distinct from the binuclear iron center of the class I enzyme) and requires NADPH and *S*-adenosylmethionine for activity. It uses nucleoside triphosphates rather than nucleoside diphosphates as substrates. The evolution of different classes of RR for production of DNA precursors in different environments reflects the importance of this reaction in nucleotide metabolism.

Regulation of *E. coli* RR is unusual in that not only its *activity*, but its *substrate specificity* is regulated by the binding of effector molecules. Each R1 subunit has two types of regulatory site (Fig. 3.1). One type affects overall enzyme activity and binds either adenosine triphosphate (ATP), which activates the enzyme, or deoxyadenosine triphosphate (dATP), which inactivates it. The second type alters substrate specificity in response to the effector molecule—ATP, dATP, deoxythymidine triphosphate (dTTP), or deoxyguanosine triphosphate (dGTP) — that is bound there (Fig. 3.4). When ATP or dATP is bound, reduction of Uridine diphosphate (UDP) and cytidine diphosphate (CDP) is favored. When dTTP or dGTP is bound, reduction of guanosine triphosphate (GDP) or adenosine diphosphate (ADP), respectively, is stimulated. The scheme is designed to provide a balanced pool of precursors for DNA synthesis. ATP is also a general activator for biosynthesis and ribonucleotide reduction. The presence of dATP in small amounts increases the reduction of pyrimidine nucleotides. An oversupply of the pyrimidine dNTPs is signaled by high levels of dTTP, which shifts the specificity to favour the reduction of GDP. High levels of dGTP, in turn, shift the specificity to ADP reduction, and high levels of dATP shut the enzyme down. These

effectors are thought to induce several distinct enzyme conformations with altered specificities.¹⁹⁸

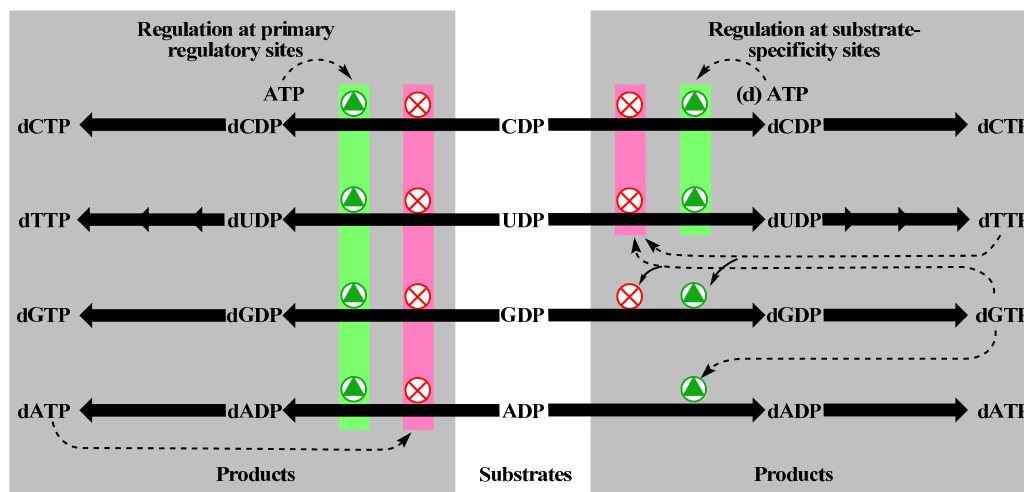


Figure 3.4: Regulation of ribonucleotide reductase by deoxynucleoside triphosphate¹⁹⁸

▲ = stimulation of enzyme activity, ⊗ = inhibition or stimulation of enzyme activity

The overall activity of the enzyme is affected by binding at the primary regulatory site (left). The substrate specificity of the enzyme is affected by the nature of the effector molecule bound at the second type of regulatory site, the substrate-specificity site (right). The diagram indicates inhibition or stimulation of enzyme activity with the four substrates.

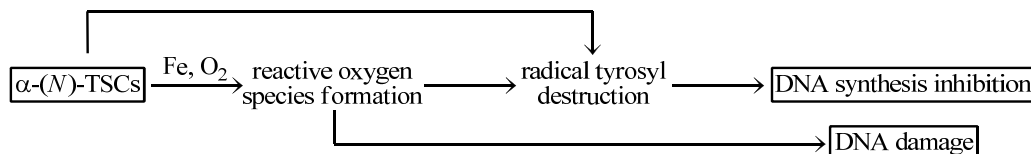
3.2.3. Inhibition of RR activity

Inhibitors of the RR are classified by their mode of interference with the enzyme functions:²

- (i) Free-radical scavengers (*e.g.*, hydroxyurea, trimidox, didox, etc.) that destroy the tyrosyl radical directly.
- (ii) Iron chelators (*e.g.*, triapine, pyridoxal isonicotinoyl hydrazone (PIH) or desferrioxamine, HCTs, etc.) that remove iron from or prevent incorporation of iron into the metal binding site thereby quenching the tyrosyl radical indirectly or inhibiting its formation,
- (iii) Nucleotide and nucleoside analogues (*e.g.*, gemcitabine, cladribine, fludarabine, cytarabine, azido-CDP, etc.) that interfere with substrate binding, and

- (iv) Gallium salts and complexes which inhibit the activity of the R2 subunit by competing with iron for its binding site and hence destabilizing the tyrosyl radical due to the inability to change the oxidation state.²⁰²

The α -(*N*)-heterocyclic TSCs are known iron chelators and as such can bind intracellular iron and/or damage the non-heme iron-stabilized tyrosyl free radical and thus inhibit the catalytic function of RR (Scheme 3.1).²⁰³



Scheme 3.1: RR inhibition mechanisms of α -(*N*)-TSCs

French *et al.*, first proposed an addendal ligand blocking model (Fig. 3.6) for inhibition of RR activity.²⁰⁴

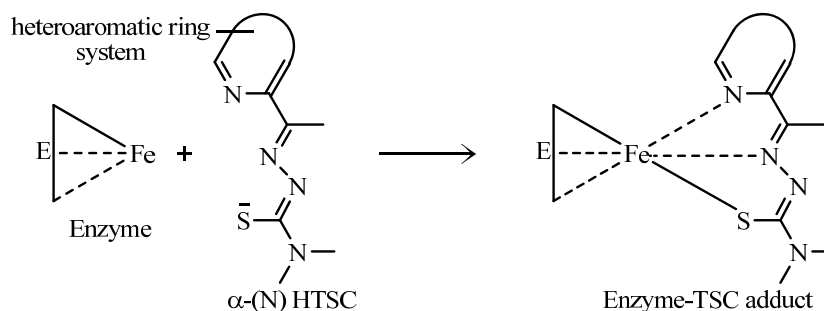


Figure 3.5: Addendal Ligand blocking model

TSC chelators enter cells and bind iron forming redox-complexes which decrease the glutathione/oxidized glutathione (GSH/GSSG) ratio, glutathione reductase (GR) and glutaredoxin reductase (GrxR) activity. These complexes also decrease thioerdoxin reductase (TrxR) activity, causing an increase in thioredoxin (Trx) oxidation. Both the GSH-Grx and Trx systems are crucial for the reduction of RR, which generates deoxyribonucleoside 5'-diphosphates (dNDPs) for DNA synthesis.²⁰⁵

Early reports suggested that the RR-inhibiting activity of α -(*N*)-heterocyclic TSCs is presumably due to their iron-chelating properties – (i) by binding iron at the active site of enzyme or (ii) by preformation of an iron chelate which then inhibits the enzyme by directly destroying the tyrosyl radical in the R2 subunit, implying that iron complexes might actually be the active species. The latter hypothesis was supported

by the observation that the preformed iron chelates are more potent inhibitors of RR in the absence of additional iron than the uncomplexed TSCs, but any interaction restricted to the iron site of the enzyme is unable to explain the partially protective effects observed with thioredoxin and small dithiol compounds.²⁰⁶⁻²⁰⁸ It was then proposed that preformed iron(III) chelates are readily reduced in blood or in the presence of thiols to the ferrous form^{144,185,207} which is able to destroy the tyrosyl radical of the enzyme by one-electron reduction in an oxygen-requiring reaction.²⁰⁸ Recent studies have demonstrated that inhibition of RR may also occur by depleting iron pools critical for enzyme activity.²¹⁰⁻²¹² More recently, the observation that 3-AP (Triapine) induces iron-dependent free radical damage, thereby behaving distinctly different from classic iron-chelating drugs such as desferrioxamine has supported the assumption that the activity of α -(*N*)-heterocyclic TSCs is not solely based on their iron-chelating properties.¹⁴³

3.2.4. Other possible mechanisms

One of another possible mechanism of the anticancer properties of thiosemicarbazones is the alkylation of thiol residues of topoisomerase-II-DNA complexes, leading to stabilization of these cleavage complexes.²¹³ Recent evidence has also pointed to the redox effects of the Triapine®-Fe³⁺ complex. Studies with copper-chelated thiosemicarbazones have shown that these complexes were capable of depleting GSH and forming reactive oxygen species (ROS), thereby inducing cell death.²¹⁴

4. MATERIALS AND METHODS

4.1. Materials.

The precursors for the synthesis of TSCs were either prepared by using organic protocols or purchased from commercial sources. 2-Cyanopyridine, 4-methyl-2-cyanopyridine, 5-fluoro-2-cyanopyridine, 6-methyl-2-cyanopyridine, thiomorpholine, 2-pyridyl piperazine, hexamethyleneimine were purchased from Aldrich and used as received. *N*-Methyl aniline and sodium chloroacetate were purchased from Himedia, CS₂ from Merck, sodium hydroxide, hydrochloric acid, ethanol, morpholine, piperidine, pyrrolidine, and acetonitrile from Qualigens and were used as received. Methanol was purchased from Fisher scientific and used after distillation.

Conventional anti-cancer agents, gemcitabine and paclitaxel were purchased from Sigma-Aldrich Co. (St. Louis, MO). Each reagent was dissolved in DMSO as a 10 mM stock solution and stored at -30 °C until use. Dilution of the test at a desired concentration was done before the treatment. Dulbecco's phosphate-buffered saline (D-PBS) was purchased from Nissui Pharmaceutical (Tokyo, Japan). Dulbecco's modified Eagle's medium (DMEM) was purchased from Wako Pure Chemical (Osaka, Japan). Sodium bicarbonate, potassium chloride, magnesium sulfate, sodium dihydrogen phosphate, potassium dihydrogen phosphate, sodium chloride, and phenol red were purchased from Wako Pure Chemical. 2-[4-(2-Hydroxyethyl)-1-piperazinyl]ethanesulfonic acid (HEPES) was purchased from Dojindo (Kumamoto, Japan). Fetal bovine serum (FBS) was from Nichirei Biosciences (Tokyo, Japan). The antibiotic antimycotic solution was from Sigma-Aldrich, Inc. (St. Louis, MO). WST-8 cell counting kit was from Dojindo. Cell culture flasks and 96-well plates were obtained from Falcon Becton Dickinson Labware (BD Biosciences, San Jose, CA). Nutrient deprived medium (NDM) was prepared following the procedure described by Izuishi *et al.*¹⁹⁰ Rabbit polyclonal antibodies to Akt, phosphorylAkt (S⁴⁷³), caspase 3 was purchased from Cell Signaling Technology (Danvers, MA). A rabbit polyclonal antibody to Glyceraldehyde 3-phosphate dehydrogenase (β -GAPDH) was purchased from GeneTex (Irvine, CA, USA). Horseradish peroxidase (HRP)-labeled goat polyclonal anti-rabbit immunoglobulins, HRP-labeled rabbit polyclonal anti-goat immunoglobulins and HRP-labeled goat polyclonal anti-mouse immunoglobulins were purchased from DakoCytomation (Glostrup, Denmark).

4.1.1 Cancer Cell Lines and Cell Culture

Cell lines used: HeLa and PANC-1

4.1.1.1 The HeLa human cervical cancer cell lines were obtained from the American Type Culture Collection (ATCC, Rockville, MD). These cell lines were maintained in standard DMEM supplemented with 2mM L-glutamine, 10% FBS, 100 IU/ml of penicillin and 100 µg/ml of streptomycin. The cells were maintained at 37 °C in a humidified atmosphere of 5% CO₂.

4.1.1.2 The PANC-1 human pancreatic cancer cell lines were purchased from Riken BRC cell bank. These cell lines were maintained in standard DMEM 10% FBS supplement, 0.1% NaHCO₃, and 1% antibiotic antimycotic solution. The medium was routinely changed after every 3 days and cells were passaged by trypsinisation (using 0.2 mg/mL trypsin solution) at approximately 80% confluence. Nutrient deprived medium (NDM) was prepared as follows: CaCl₂ (1M) (0.6 mL), Fe(NO₃)₃.9H₂O (0.5 mg), KCl (200 mg), MgSO₄.7H₂O (100 mg), NaCl (3.2 g), NaHCO₃ (350 mg), NaH₂PO₄ (62.5 mg), phenol red (7.5mg), 1M HEPES buffer (12.5 mL) and MEM vitamin solution (5 mL) (Lonza, UK) were dissolved in double distilled H₂O (final volume 500 mL). The pH was adjusted to 7.2 using an aqueous saturated solution of NaHCO₃. The medium was sterile filtered and stored at - 4°C.

4.2 Methods and Instrumentation.

The synthesized compounds were characterized by Elemental analysis, Melting point, IR, NMR, and HR-FAB mass analysis.

4.2.1 Melting Point Determination

Melting points of the compounds were determined by using Philip Harris melting point apparatus and were uncorrected.

4.2.2 Elemental Analysis (EA).

Elemental analyses were performed on a Perkin-Elmer CHN-2400 at IIT Madras, India.

4.2.3 Infrared Spectroscopy (IR).

Infrared spectra were measured from 4000 to 400 cm^{-1} using KBr pellets on a Tensor 27 FTIR-Spectrophotometer from BRUKER at Wayne State University, USA. The samples were prepared as pellets with oven dried KBr using a dye and a hydraulic press. The data collection was made by Optics User Software (OPUS) version 5.0.

4.2.4 Nuclear Magnetic Resonance Spectroscopy (NMR).

^1H NMR and ^{13}C NMR spectroscopy were used for analysis of the synthesized TSCs. NMR spectra were recorded at room temperature on 400 MHz Varian Mercury instruments at Wayne State University, USA.

4.2.5 Mass Spectrometry (MS).

High resolution fast atom bombarding mass spectrometry (HRFAB-MS) measurements were carried on a JEOL JMS-AX505HAD mass spectrometer in university of Toyama, Japan. Glycerol was used as matrix.

4.3 Synthesis of 2-pyridineformamide derived thiosemicarbazones

4.3.1. Synthesis of precursors

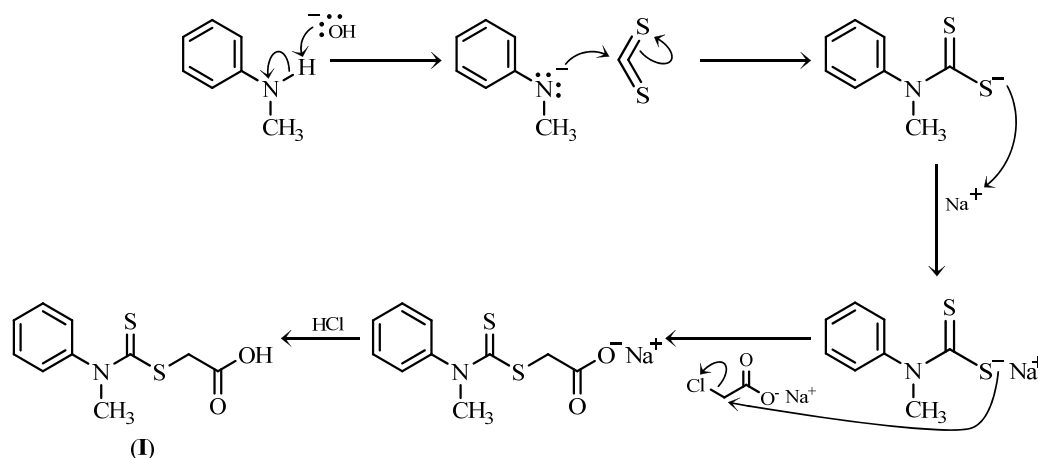
The precursors were synthesized by the facile method developed by Scovill.²⁷

4.3.1.1 Synthesis of 2-(methyl(phenyl)carbamothioylthio)acetic acid (I)

2-(Methyl(phenyl)carbamothioylthio)acetic acid (I) was synthesized by a modification of the method of Holmberg and Psilanderheilm.²¹⁵ It is an addition reaction involving the addition of *N*-methylaniline and sodium chloroacetate to carbon disulphide.

A mixture consisting of 12.0 mL (15.2 g, 200 mmol) of CS_2 and 21.6 mL (21.2 g, 200 mmol) of *N*-methylaniline was treated with 250 mL of NaOH solution (8.4 g, 210 mmol) and stirred at room temperature for 4 h until the organic layer disappeared. The straw coloured solution was then treated with sodium chloroacetate (23.2 g, 200 mmol) and allowed to stand for 17h at room temperature. The solution was acidified with conc. HCl (25 mL) to yield the buff coloured precipitate of 2-

(methyl(phenyl)carbamothioylthio)acetic acid (**I**), which was separated by filtration and then dried in oven at 40-45 °C. Scheme 4.1 shows the mechanistic pathway of the reaction.

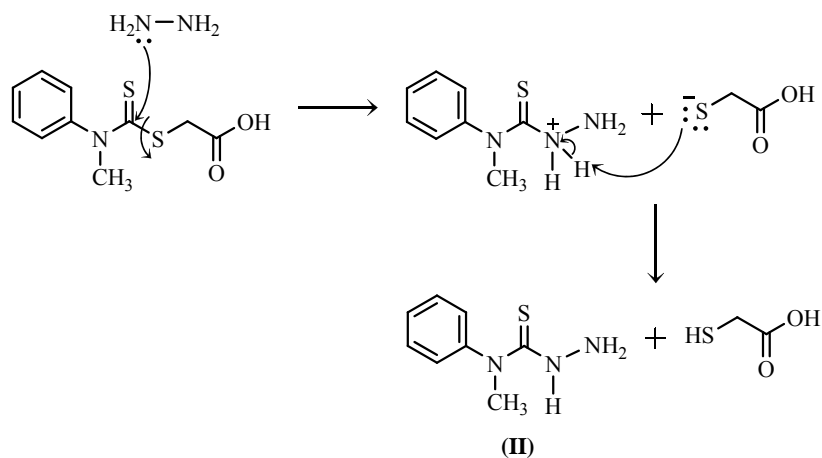


Scheme 4.1 Synthesis of 2-(methyl(phenyl)carbamothioylthio)acetic acid

Yield: 82% (39.7g); mp 197-198°C.

4.3.1.2. Synthesis of *N*-methyl-*N*-phenylhydrazinecarbothioamide (**II**)

N-Methyl-*N*-phenylhydrazinecarbothioamide (**II**) was synthesized by an improved method of Stanovnik and Tisler.²¹⁶ Here, the dithiocarbamate group is replaced by hydrazine leading to the formation of the thiosemicarbazide (Scheme 4.2).



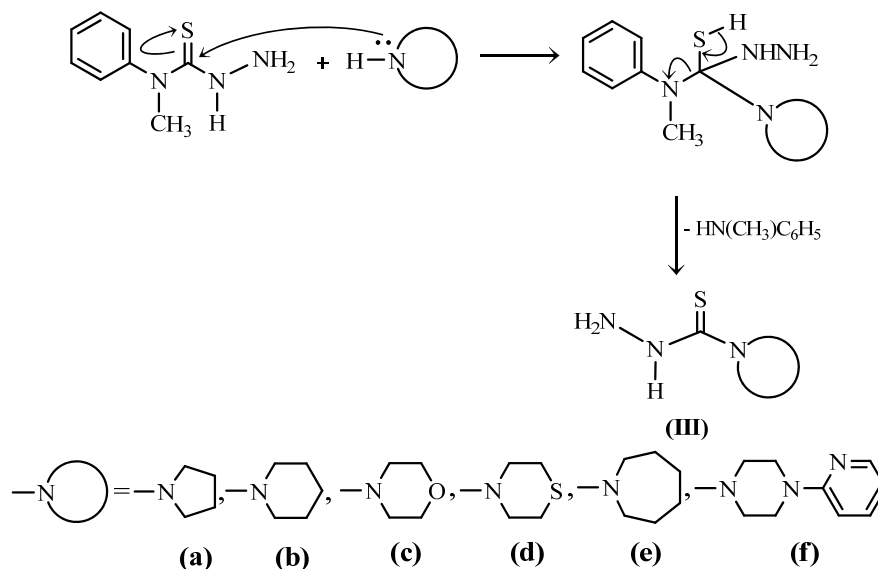
Scheme 4.2 Synthesis of *N*-methyl-*N*-phenylhydrazinecarbothioamide

A solution of 17.7 g (73.3 mmol) of 2-(methyl(phenyl)carbamothioylthio)acetic acid (**I**) was treated with 98% hydrazine hydrate (20 mL) and water (10 mL), and heated on water bath at 85°C. Crystals began to separate after 3 min. Heating was continued

for additional 22 min. The crystals were separated by filtration, washed with water and dried. It was then recrystallized in the mixture of EtOH (50 mL) and water (25 mL) to obtain stout colourless rods of *N*-methyl-*N*-phenylhydrazinecarbo-thioamide (**II**). Yield: 81% (10.8 g); mp 124-125°C.

4.3.1.3. Synthesis of *N*(4)-ring incorporated thiosemicarbazide (**IIIa-g**)

The required thiosemicarbazides were synthesized by the method transamination as described by Scovill.²⁷ This was done by transamination reaction for which the mechanism may be depicted as follows (Scheme 4.3). A secondary amine like *N*-methylaniline serves as a better leaving group for a more nucleophilic amine like pyrrolidine, piperidine etc. The transamination proceeds by the standard addition elimination mechanism. Nucleophilic addition of an amine to the thiocarbonyl group produces a tetrahedral intermediate. Elimination of *N*-methylaniline from this intermediate reforms the thiocarbonyl group resulting in a new *N*⁴-substituted thiosemicarbazide.



Scheme 4.3 Synthesis of *N*(4)-ring incorporated thiosemicarbazide

Pyrrolidine-1-carbothiohydrazide (IIIa). A solution of 1.00 g (5.52 mmol) of *N*-methyl-*N*-phenylhydrazinecarbothioamide (**II**) in MeCN (5 mL) was treated with 392 mg (5.52 mmol) of pyrrolidine and heated under reflux for 15 min. The resulting solution was cooled to 4 °C in refrigerator for 2 h, the crystals separated were

collected and washed with MeCN. It was then recrystallized in EtOH and dried in oven at 40-45 °C. This afforded 556 mg (69%) of pyrrolidine-1-carbothiohydrazide (**IIIa**), mp 172-173 °C.

Piperidine-1-carbothiohydrazide (IIIb). A solution of 1.00 g (5.52 mmol) of *N*-methyl-*N*-phenylhydrazinecarbothioamide (**II**) in MeCN (3 mL) was treated with 470 mg (5.52 mmol) of piperidine and heated under reflux for 2h. The resulting solution was cooled to 4 °C in refrigerator for overnight., the crystals separated were collected and then recrystallized in benzene and dried in oven at 40-45 °C. This afforded 344 mg (39%) of piperidine-1-carbothiohydrazide (**IIIb**), mp 95-96 °C.

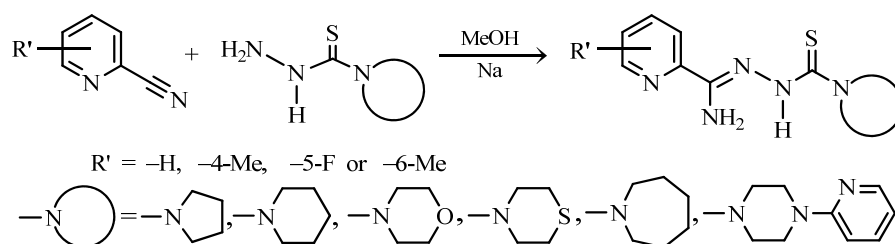
Morpholine-4-carbothiohydrazide (IIIc). A solution of 1.00 g (5.52 mmol) of *N*-methyl-*N*-phenylhydrazinecarbothioamide (**II**) in MeCN (5 mL) was treated with 481 mg (5.52 mmol) of morpholine and heated under reflux for 45 min. The resulting solution was cooled to 4 °C in refrigerator for 45 min., the crystals separated were collected and washed with MeCN. It was then recrystallized in MeOH and dried in oven at 40-45 °C. This afforded 466 mg (52%) of morpholine-1-carbothiohydrazide (**IIIc**), mp 175-176 °C.

Thiomorpholine-4-carbothiohydrazide (IIIId). A solution of 1.00 g (5.52 mmol) of *N*-methyl-*N*-phenylhydrazinecarbothioamide (**II**) in MeCN (5 mL) was treated with 570 mg (5.52 mmol) of thiomorpholine and heated under reflux for 45 min. The resulting solution was cooled to 4 °C in refrigerator for 45 min., the crystals separated were collected and washed with MeCN. It was then recrystallized in MeOH and dried in oven at 40-45 °C. This afforded 575 mg (59%) of thiomorpholine-1-carbothiohydrazide (**IIIId**), mp 149-150 °C.

Azepane-1-carbothiohydrazide (IIIe). A solution of 1.00 g (5.52 mmol) of *N*-methyl-*N*-phenylhydrazinecarbothioamide (**II**) in MeCN (5 mL) was treated with 547 mg (5.52 mmol) of hexamethyleneimine and heated under reflux for 45 min. The resulting solution was cooled to 4 °C in refrigerator for 30 min., the crystals separated were collected and recrystallized in MeOH and dried in oven at 40-45 °C. This afforded 462 mg (48%) of azepane -1-carbothiohydrazide (**IIIe**), mp 114-116 °C.

4-(2-Pyridyl)piperazine-1-carbothiohydrazide (III_f). A solution of 1.00 g (5.52 mmol) of *N*-methyl-*N*-phenylhydrazinecarbothioamide (**II**) in MeCN (5 mL) was treated with 901 mg (5.52 mmol) of 2-pyridylpiperazine and heated under reflux for 45 min. The resulting solution was cooled to 4 °C in refrigerator for 30 m., the crystals separated were collected and washed with MeCN. It was then recrystallized in EtOH and dried in oven at 40-45 °C. This afforded 652 mg (50%) of 4-(2-pyridyl)piperazine -1-carbothiohydrazide (**III_f**), mp 184-185 °C.

4.3.2. General procedure for synthesis of 2-pyridineformamide N(4)-ring incorporated Thiosemicarbazones²¹⁷

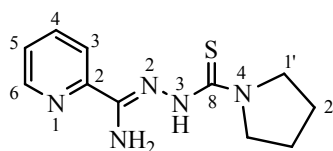


Scheme 4.4. Synthesis of 2-pyridineformamide *N*(4)-ring incorporated thiosemicarbazone

Sodium (0.092 g, 4.0 mmol) was added to dried methanol (25 mL),²¹⁸ and stirred until complete dissolution was achieved. 2-Cyanopyridine or substituted 2-cyanopyridine (24.9 mmol) was then added. The mixture was stirred for 30 min. The *N*(4)-disubstituted thiosemicarbazide (24.9 mmol) was then added in small portions over a period of 1 h. A further quantity of methanol (25 mL) was added and the mixture was heated under reflux for a minimum of 4 h. Slow evaporation of the methanol produced the crystals of the desired product (Scheme 4.4).

4.3.2.1 *N'*-(Pyrrolidine-1-carbonothioyl)picolinohydrazoneamide (**1**)

2-Cyanopyridine (2.592 g, 24.9 mmol) was reduced in the presence of thiosemicarbazide (**III_a**) (3.616 g, 24.9 mmol) through general procedure and *N'*-(pyrrolidine-1-carbonothioyl)picolinohydrazoneamide (**1**) was obtained.

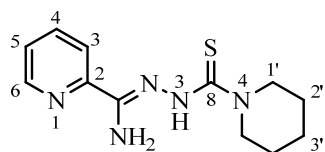


(1)

Yield: 46%. mp 159-160 °C. HRFABMS: m/z 250.11096 $[M + H]^+$ (calcd for $C_{11}H_{16}N_5S$, 250.11264). Elemental analysis: Calcd for $C_{11}H_{15}N_5S$; C, 52.99; H, 6.06; N, 28.09; S, 12.86%; Found; C, 53.45; H, 5.69; N, 27.72%. IR ν_{max} in KBr (selected bands) : cm^{-1} 3389 (m), 3260 (m), 3216 (m), 1672 (s), 1597 (s), 1579 (s), 1465 (s), 1428 (s), 1090 (m), 849 (m), 635 (m). 1H NMR (400 MHz, $CDCl_3$) : δ ppm 12.95 (1H, br. s., HN-), 8.61 (1H, br. s., H-6), 7.99 (1H, d, $J = 8.1$ Hz, H-3), 7.80 (1H, br. s., H-4), 7.39 (1H, br. s., H-5), 6.61 (2H, br. s., NH_2), 3.78 (4H, br. s., H-1'), 1.92 (4H, br. s., H-2'). 1H -NMR (400 MHz, $DMSO-d_6$) : δ ppm 12.55, 9.23 (1H, br. s, HN-, *E* and *Z'* geometrical isomers), 8.55, 8.74 (1H, d, $J = 4.9$ Hz, H-6, *E* and *Z'* geometrical isomers), 8.01, 8.10 (1H, m, H-3, *E* and *Z'* geometrical isomers), 7.84, 8.06 (1H, br d, $J = 6.5$ Hz, H-4, *E* and *Z'* geometrical isomers); 7.42 (br s), 7.61 (1H, dd, $J = 6.5$ Hz, $J = 4.9$ Hz, H-5, *E* and *Z'* geometrical isomers); 6.76 (2H, br. s., NH_2); 3.55, 3.73 (4H, br s, H-1', *E* and *Z'* geometrical isomers); 1.83 (4H, br s, H-2'). ^{13}C NMR (100 MHz, $DMSO-d_6$) : δ ppm 176.5 (C-8), 150.3 (C-6), 144.6 (C-2), 143.8 (C-7), 138.7 (C-4), 126.8 (C-5), 121.4 (C-3), 48.6 (C-1'), 25.2 (C-2').

4.3.2.2 *N'*-(Piperidine-1-carbonothioyl)picolinohydrazonamide (2)

2-cyanopyridine (2.592 g, 24.9 mmol) was reduced in the presence of thiosemicarbazide (**IIIb**) (3.965 g, 24.9 mmol) through general procedure and *N'*-(piperidine-1-carbonothioyl)picolinohydrazonamide (**2**) was obtained.



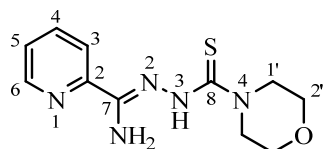
(2)

Yield: 21%. mp 154-155 °C. HRFABMS: m/z 264.13186 $[M + H]^+$ (calcd for $C_{12}H_{18}N_5S$, 264.12829). Elemental analysis: Calcd for $C_{12}H_{17}N_5S$; C, 54.73; H, 6.51; N, 26.59. S, 12.18%. Found; C, 55.27; H, 6.26; N, 26.83%. IR ν_{max} in KBr (selected bands) : cm^{-1} 3411 (m), 3263 (m), 3219 (m), 1667(s), 1601 (s), 1582 (s), 1473 (s), 1425 (s), 1074 (m), 884 (m), 636 (m). 1H NMR (400 MHz, $DMSO-d_6$) : δ ppm 12.69 (1H, br s, HN-), 8.75 (1H, br d, $J = 4.9$ Hz, H-6), 8.10 (1H, d, $J = 8.1$ Hz, H-3), 8.06 (1H, dd, $J = 8.1, 6.5$ Hz, H-4), 7.61 (1H, dd, $J = 6.5, 4.9$ Hz, H-5), 3.83 (4H, t, $J = 4.9$ Hz, H-1'), 1.57 (2H, br s, H-3'), 1.44 (4H, br s, H-2'). ^{13}C NMR (100 MHz, $DMSO-d_6$)

: δ ppm 178.7 (C- 8), 150.2 (C-6), 144.1 (C-2), 143.4 (C-7), 138.7 (C-4), 126.8 (C-5), 121.5 (C-3), 47.4 (C-1'), 26.2 (C-2'), 25.3 (C-3').

4.3.2.3 *N'*-(Morpholine-1-carbonothioyl)picolinohydrazonamide (3)

2-cyanopyridine (2.592 g, 24.9 mmol) was reduced in the presence of thiosemicarbazide (**IIIc**) (4.015 g, 24.9 mmol) through general procedure and *N'*-(morpholine-1-carbonothioyl)picolinohydrazonamide (**3**) was obtained.

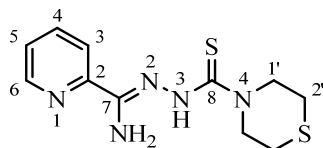


(3)

Yield: 60%. mp 173-175 °C. HRFABMS: m/z 266.10846 $[M + H]^+$ (calcd for $C_{11}H_{16}ON_5S$, 266.10756). Elemental analysis: Calcd for $C_{11}H_{15}ON_5S$; C, 49.79; H, 5.70; N, 26.39. S, 12.08%. Found; C, 50.29; H, 5.58; N, 26.10%. IR ν_{max} in KBr (selected bands) : cm^{-1} 3403 (m), 3276 (m), 3231 (m), 1670(s), 1605 (s), 1583 (s), 1460 (s), 1431 (s), 1025 (m), 892 (m), 627 (m); 1H NMR (400 MHz, DMSO- d_6) : δ ppm 12.55 (1H, br s, HN-), 8.77 (1H, d, $J = 5.7$ Hz, H-6), 8.14 (1H, d, $J = 7.3$ Hz, H-3), 8.09 (1H, br d, $J = 7.3$ Hz, H-4), 7.64 (1H, dd, $J = 7.3, 5.7$ Hz, H-5), 3.81 (4H, br s, H-2'), 3.56 (4H, br s, H-1'). ^{13}C NMR (100 MHz, DMSO- d_6) : δ ppm 179.1 (C-8), 150.3 (C-6), 145.2 (C-2), 144.4 (C-7), 138.7 (C-4), 127.1 (C-5), 121.7 (C-3), 66.7 (C-2'), 47.2 (C-1').

4.3.2.4 *N'*-(Thiomorpholine-1-carbonothioyl)picolinohydrazonamide (4)

2-cyanopyridine (2.592 g, 24.9 mmol) was reduced in the presence of thiosemicarbazide (**III d**) (4.415 g, 24.9 mmol) through general procedure and *N'*-(thiomorpholine-1-carbonothioyl)picolinohydrazonamide (**4**) was obtained.



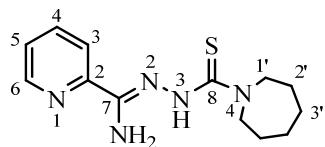
(4)

Yield: 59%. mp 162-163 °C. HRFABMS: m/z 282.08509 $[M + H]^+$ (calcd for $C_{11}H_{16}N_5S_2$, 282.08472). Elemental analysis: Calcd for $C_{11}H_{15}N_5S_2$; C, 46.95; H,

5.37; N, 24.89. S, 22.79%. Found; C, 47.21; H, 5.03; N, 24.62%. IR ν_{\max} in KBr (selected bands) : cm^{-1} 3404 (m), 3275 (m), 3234 (m), 1669(s), 1604 (s), 1584 (s), 1461 (s), 1428 (s), 959 (m), 861 (m), 628 (m); ^1H NMR (400 MHz, $\text{DMSO-}d_6$) : δ ppm 12.57 (1H, br s, HN-), 8.77 (1H, d, $J = 4.9$ Hz, H-6), 8.14 (1H, d, $J = 7.3$ Hz, H-3), 8.08 (1H, m, H-4), 7.63 (1H, d, $J = 4.9$ Hz, H-5), 4.17 (4H, br s, H-1'), 2.52 (4H, br s, H-2'). ^{13}C NMR (100 MHz, $\text{DMSO-}d_6$) : δ ppm 178.9 (C-8), 151.1 (C-6), 145.8 (C-2), 145.2 (C-7), 139.5 (C-4), 127.8 (C-5), 122.4 (C-3), 49.9 (C-1'), 27.4 (C-2').

4.3.2.5 *N'*-(Azepane-1-carbonothioyl)picolinohydrazoneamide (5)

2-cyanopyridine (2.592 g, 24.9 mmol) was reduced in the presence of thiosemicarbazide (**IIIe**) (4.315 g, 24.9 mmol) through general procedure and *N'*-(azepane-1-carbonothioyl)picolinohydrazoneamide (**5**) was obtained.

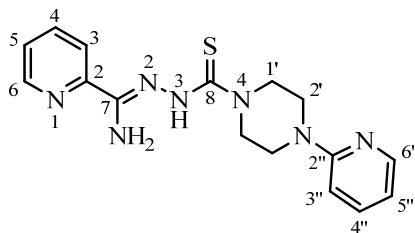


(5)

Yield: 24%. mp 153-155 °C. HRFABMS: m/z 278.14220 $[\text{M} + \text{H}]^+$ (calcd for $\text{C}_{13}\text{H}_{20}\text{N}_5\text{S}$, 278.14394). Elemental analysis: Calcd for $\text{C}_{13}\text{H}_{19}\text{N}_5\text{S}$; C, 56.29; H, 6.90; N, 25.25. S, 11.56%. Found; C, 56.77; H, 6.63; N, 25.59%. IR ν_{\max} in KBr (selected bands) : cm^{-1} : 3424 (m), 3229 (m), 3131 (m), 1673(s), 1595 (s), 1585 (s), 1476 (s), 1413 (s), 1097 (m), 861 (m), 631 (m); ^1H NMR (400 MHz, $\text{DMSO-}d_6$) : δ ppm 12.71 (1H, br s, HN-), 8.75 (1H, br d, $J = 4.1$ Hz, H-6), 8.09 (1H, d, $J = 8.1$ Hz, H-3), 8.06 (1H, dd, $J = 8.1, 6.5$ Hz, H-4), 7.60 (1H, dd, $J = 6.5, 4.1$ Hz, H-5), 3.81 (4H, br s, H-1'), 1.69 (4H, br s, H-3'), 1.45 (4H, br s, H-2'). ^{13}C NMR (100 MHz, $\text{DMSO-}d_6$) : δ ppm 178.3 (C-8), 150.3 (C-6), 144.6 (C-2), 143.6 (C-7), 138.6 (C-4), 126.7 (C-5), 121.3 (C-3), 48.6 (C-1'), 28.4 (C-2'), 27.1 (C-3').

4.3.2.6 *N'*-(4-(Pyridin-2-yl)piperazine-1-carbonothioyl)picolinohydrazoneamide (6)

2-cyanopyridine (2.592 g, 24.9 mmol) was reduced in the presence of thiosemicarbazide (**IIIf**) (4.339 g, 24.9 mmol) through general procedure and *N'*-(4-(pyridin-2-yl)piperazine-1-carbonothioyl)picolinohydrazoneamide (**6**) was obtained.

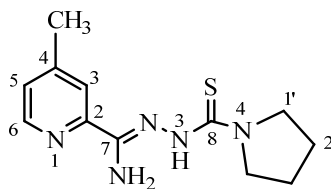


(6)

Yield: 45%. mp 151-152 °C. HRFABMS: m/z 342.15103 $[M + H]^+$ (calcd for $C_{16}H_{20}N_7S$, 342.15008). Elemental analysis: Calcd for $C_{16}H_{19}N_7S$; C, 56.28; H, 5.61; N, 28.72. S, 9.39%. Found; C, 56.67; H, 5.38; N, 28.41%. IR ν_{max} in KBr (selected bands) : cm^{-1} 3418 (w), 3277 (w), 3229 (m), 1673(s), 1602 (s), 1566 (s), 1462 (s), 1427 (s), 1020 (m), 877 (m), 628 (m); 1H NMR (400 MHz, DMSO- d_6) : δ ppm 12.59 (1H, br s, HN-), 8.77 (1H, d, $J = 5.7$ Hz, H-6), 8.16 (1H, d, $J = 7.3$ Hz, H-3), 8.14(1H, d, $J = 5.7$ Hz, H-6''), 8.08 (1H, d, $J = 7.3$ Hz, H-4), 7.64 (1H, dd, $J = 6.5, 5.7$ Hz, H-5), 7.53 (1H, dd, $J = 8.9, 6.5$ Hz, H-4''), 6.85 (1H, d, $J = 8.9$ Hz, H-3''), 6.64 (1H, dd, $J = 6.5, 5.7$ Hz, H-5''), 3.96 (4H, br s, H-1'), 3.48 (4H, br s, H-2'). ^{13}C NMR (100 MHz, DMSO- d_6) : δ ppm 179.9 (C-8), 160.5 (C-2''), 151.3 (C-6), 149.0 (C-6''), 146.0 (C-2), 145.4 (C-7), 139.7 (C-4), 138.9 (C-4''), 128.0 (C-5), 122.6 (C-3), 114.4 (C-5''), 108.6 (C-3''), 47.0 (C-1'), 46.0 (C-2').

4.3.2.7 4-Methyl- N' -(pyrrolidine-1-carbonothioyl)picolinohydrazoneamide (7)

2-cyano-4-methylpyridine (2.942 g, 24.9 mmol) was reduced in the presence of thiosemicarbazide (**IIIa**) (3.616 g, 24.9 mmol) through general procedure and 4-methyl- N' -(pyrrolidine-1-carbonothioyl)picolino hydrazoneamide (**8**) was obtained.



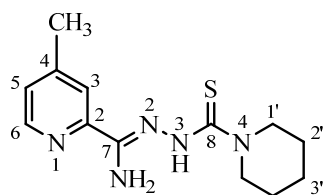
(7)

Yield: 24%. mp 164-166 °C. HRFABMS: m/z 264.12711 $[M + H]^+$ (calcd for $C_{12}H_{18}N_5S$, 264.12829). Elemental analysis: Calcd for $C_{12}H_{17}N_5S$; C, 54.73; H, 6.51; N, 26.59. S, 12.18%. Found; C, 55.14; H, 6.18; N, 26.79.%. IR ν_{max} in KBr (selected bands) : cm^{-1} 3419 (m), 3263 (m), 3143 (m), 1674(s), 1608 (s), 1589 (s), 1464 (s), 1433 (s), 1102 (m), 843 (s), 616 (m); 1H NMR (400 MHz, CDCl $_3$ - d_6) : δ ppm 12.94 (1H, br s, HN-), 8.47 (1H, br s, H-6), 7.77 (1H, br s, H-3), 7.26 (1H, br s, H-5), 6.62

(2H, br s, NH_2); 3.75 (4H, br s, H-1'), 2.45 (3H, br s, CH_3), 1.93 (4H, br s, H-2'); ^1H -NMR (400 MHz, $\text{DMSO-}d_6$) : δ ppm 12.52, 9.12 (1H, br s, HN-, *E* and *Z'* geometrical isomers), 8.41, 8.59 (1H, H-6, *E* and *Z'* geometrical isomers), 7.85, 7.99 (1H, m, H-3, *E* and *Z'* geometrical isomers), 7.27, 7.45 (1H, H-5, *E* and *Z'* geometrical isomers); 6.74 (2H, br s, NH_2): 3.55, 3.23 (4H, br s, H-1', *E* and *Z'* geometrical isomers); 1.83 (4H, br s, H-2'). ^{13}C NMR (100 MHz, $\text{DMSO-}d_6$) : δ ppm 178.6 (C-8), 150.1 (C-2), 148.8 (C-7), 143.9 (C-4), 138.7 (C-6), 126.5 (C-5), 118.7 (C-3), 47.4 (C-1'), 26.1 (C-2'), 24.6 (CH_3).

4.3.2.8 4-Methyl-*N'*-(piperidine-1-carbonothioyl)picolinohydrazoneamide (8)

2-cyano-4-methylpyridine (2.942 g, 24.9 mmol) was reduced in the presence of thiosemicarbazide (**IIIb**) (3.965 g, 24.9 mmol) through general procedure and 4-methyl-*N'*-(piperidine-1-carbonothioyl)picolino hydrazoneamide (**8**) was obtained.

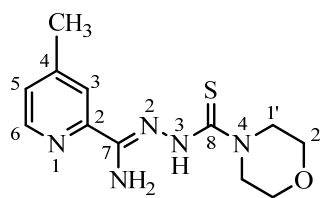


(8)

Yield: 29%. mp 161-162 °C. HRFABMS: m/z 278.14331 [$\text{M} + \text{H}$]⁺ (calcd for $\text{C}_{13}\text{H}_{20}\text{N}_5\text{S}$, 278.14394). Elemental analysis: Calcd for $\text{C}_{13}\text{H}_{19}\text{N}_5\text{S}$; C, 56.29; H, 6.90; N, 25.25. S, 11.56%. Found; C, 56.62; H, 6.53; N, 25.51%. IR ν_{max} in KBr (selected bands) : cm^{-1} 3419 (m), 3267 (m), 3152 (m), 1674(s), 1613 (s), 1589 (s), 1497 (m), 1439 (s), 1076 (m), 856 (m), 629 (m); ^1H NMR (400 MHz, $\text{DMSO-}d_6$) : δ ppm 12.63 (1H, br s, HN-), 8.57 (1H, d, $J = 4.9$ Hz, H-6), 7.97 (1H, br s, H-3), 7.43 (1H, d, $J = 4.9$ Hz, H-5), 3.80 (4H, t, $J = 5.6$ Hz, H-1'), 2.39 (3H, br s, CH_3), 1.55 (2H, br s, H-3'), 1.41 (4H, br s, H-2'). ^{13}C NMR (100 MHz, $\text{DMSO-}d_6$) : δ ppm 79.6 (C-8), 150.1 (C-2), 149.8 (C-7), 145.1 (C-4), 144.4 (C-6), 127.6 (C-5), 122.6 (C-3), 47.8 (C-1'), 26.3 (C-2'), 25.4 (C-3'), 21.4 (CH_3).

4.3.2.9 4-Methyl-*N'*-(morpholine-1-carbonothioyl)picolinohydrazoneamide (9)

2-cyano-4-methyl-pyridine (2.942 g, 24.9 mmol) was reduced in the presence of thiosemicarbazide (**IIIc**) (4.015 g, 24.9 mmol) through general procedure and 4-methyl-*N'*-(morpholine-1-carbonothioyl)picolino hydrazoneamide (**9**) was obtained.

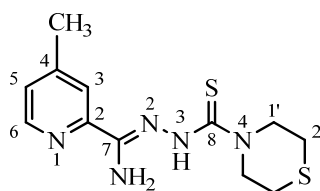


(9)

Yield: 41%. mp 183-185 °C. HRFABMS: m/z 280.12400 $[M + H]^+$ (calcd for $C_{12}H_{18}ON_5S$, 280.12321). Elemental analysis: Calcd for $C_{12}H_{17}ON_5S$; C, 51.59; H, 6.13; N, 25.07. S, 11.48 %. Found; C, 51.96; H, 5.83; N, 25.34%. IR ν_{max} in KBr (selected bands) : cm^{-1} 3419 (m), 3267 (m), 3240 (m), 1674 (s), 1615 (s), 1593 (s), 1466 (s), 1427 (s), 1022 (m), 839 (s), 627 (m); 1H NMR (400 MHz, DMSO- d_6) : δ ppm 12.52 (1H, br s, HN-), 8.61 (1H, d, $J = 4.9$ Hz, H-6), 8.01 (1H, br s, H-3), 7.47 (1H, d, $J = 4.9$ Hz, H-5), 3.80 (4H, br s, H-2'), 3.55 (4H, br s, H-1'), 2.41 (3H, br s, $\underline{CH_3}$). ^{13}C NMR (100 MHz, DMSO- d_6) : δ ppm 179.1 (C-8), 150.0 (C-2), 149.8 (C-7), 145.4 (C-4), 144.3 (C-6), 127.6 (C-5), 122.5 (C-3), 66.7 (C-2'), 47.2 (C-1'), 21.2 ($\underline{C}H_3$).

4.3.2.10 4-Methyl- N' -(thiomorpholine-1-carbonothioyl)picolinohydrazoneamide (10)

2-cyano-4-methyl-pyridine (2.942 g, 24.9 mmol) was reduced in the presence of thiosemicarbazide (**III d**) (4.415 g, 24.9 mmol) through general procedure and 4-methyl- N' -(thiomorpholine-1-carbonothioyl) picolinohydrazoneamide (**10**) was obtained.



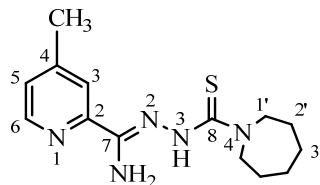
(10)

Yield: 32%. mp 166-168 °C. HRFABMS: m/z 296.09644 $[M + H]^+$ (calcd for $C_{12}H_{18}N_5S_2$, 296.10037). Elemental analysis: Calcd for $C_{12}H_{17}N_5S_2$; C, 48.79; H, 5.80; N, 23.71. S, 21.71%. Found; C, 49.06; H, 5.47; N, 24.04%. IR ν_{max} in KBr (selected bands) : cm^{-1} 3456 (s), 3244 (m), 3222 (m), 1672(s), 1610 (m), 1566 (s), 1459 (s), 1430 (s), 953 (m), 831 (s), 617 (m); 1H NMR (400 MHz, DMSO- d_6) : δ ppm 12.54 (1H, br s, HN-), 8.60 (1H, d, $J = 5.7$ Hz, H-6), 8.01 (1H, br s, H-3), 7.47 (1H, d, $J = 5.7$ Hz, H-5), 4.15 (4H, br s, H-1'), 2.51 (4H, br s, H-2'), 2.42 (3H, br s, $\underline{CH_3}$). ^{13}C

NMR (100 MHz, DMSO- d_6) : δ ppm 178.1 (C-8), 150.0 (C-2), 149.7 (C-7), 145.2 (C-4), 144.3 (C-6), 127.6 (C-5), 122.5 (C-3), 49.1 (C-1'), 26.6 (C-2'), 21.2 ($\underline{\text{C}}\text{H}_3$).

4.3.2.11 4-Methyl-*N'*-(azepane-1-carbonothioyl)picolinohydrazoneamide (11)

2-cyano-4-methylpyridine (2.942 g, 24.9 mmol) was reduced in the presence of thiosemicarbazide (**IIIe**) (4.315 g, 24.9 mmol) through general procedure and 4-methyl-*N'*-(azepane-1-carbonothioyl)picolino hydrazoneamide (**11**) was obtained.

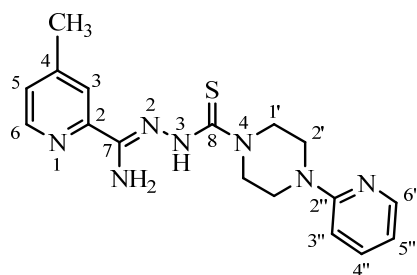


(11)

Yield: 45%. mp 160-162 °C. HRFABMS: m/z 292.16063 [$\text{M} + \text{H}$]⁺ (calcd for $\text{C}_{14}\text{H}_{22}\text{N}_5\text{S}$, 292.15959). Elemental analysis: Calcd for $\text{C}_{14}\text{H}_{21}\text{N}_5\text{S}$; C, 57.70; H, 7.26; N, 24.03. S, 11.00%. Found; C, 58.09; H, 7.07 N, 24.20%. IR ν_{max} in KBr (selected bands) : cm^{-1} 3429 (m), 3287 (m), 3152 (m), 1674 (m), 1612 (s), 1585 (s), 1470 (s), 1411 (s), 1076 (m), 860 (m), 629 (m); ^1H NMR (400 MHz, DMSO- d_6) : δ ppm 12.65 (1H, br s, HN-), 8.57 (1H, d, $J = 5.1$ Hz, H-6), 7.96 (1H, br s, H-3), 7.42 (1H, d, $J = 5.1$ Hz, H-5), 3.78 (4H, t, $J = 6.1$, H-1'), 2.39 (3H, br s, $\underline{\text{C}}\text{H}_3$); 1.66 (4H, br s, H-3'), 1.42 (4H, br s, H-2'). ^{13}C NMR (100 MHz, DMSO- d_6) : δ ppm 179.2 (C-8), 150.2 (C-2), 149.9 (C-7), 145.1 (C-4), 144.8 (C-6), 127.9 (C-5), 123.0 (C-3), 50.2 (C-1'), 28.3 (C-2'), 273(C-3'), 214 ($\underline{\text{C}}\text{H}_3$).

4.3.2.12 4-Methyl-*N'*-(4-(pyridin-2-yl)piperazine-1-carbonothioyl)picolinohydrazoneamide (12)

2-cyano-4-methyl-pyridine (2.942 g, 24.9 mmol) was reduced in the presence of thiosemicarbazide (**III f**) (4.339 g, 24.9 mmol) through general procedure and 4-methyl-*N'*-(4-(pyridin-2-yl)piperazine -1-carbonothioyl)picolinohydrazoneamide (**12**) was obtained.

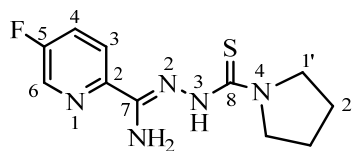


(12)

Yield: 63%. mp 175-177 °C. HRFABMS: m/z 356.16527 $[M + H]^+$ (calcd for $C_{17}H_{22}N_7S$, 356.16573). Elemental analysis: Calcd for $C_{17}H_{21}N_7S$; C, 57.44; H, 5.95; N, 27.58. S, 9.02%. Found; C, 57.72; H, 5.63; N, 27.52%. IR ν_{max} in KBr (selected bands) : cm^{-1} 3416 (m), 3261 (m), 3231 (m), 1672(s), 1594 (s), 1562 (s), 1485 (s), 1427 (s), 1019 (m), 873 (m), 626 (m); 1H NMR (400 MHz, DMSO- d_6) : δ ppm 12.57 (1H, br s, HN-), 8.62 (1H, br s, H-6), 8.12 (1H, br. s., H-6''), 8.05 (1H, br. s., H-3), 7.54 (1H, br s, H-4''), 7.48 (1H, br s, H-5), 6.85 (1H, br s, H-3''), 6.64 (1H, br s, H-5''), 3.96 (4H, br s, H-1'), 3.49 (4H, br s, H-2'), 2.43 (3H, br. s., $\underline{C}H_3$). ^{13}C NMR (100 MHz, DMSO- d_6) : δ ppm 178.9 (C-8), 159.6 (C-2''), 151.5 (C-2), 150.1 (C-7), 148.1 (C-6''), 145.3 (C-4), 144.3 (C-6), 138.1 (C-4''), 127.6 (C-5), 122.6 (C-3), 113.5 (C-5''), 107.7 (C-3''), 46.1 (C-1'), 45.1 (C-2'), 21.2 ($\underline{C}H_3$).

4.3.2.13 5-Fluoro-*N'*-(pyrrolidine-1-carbonothioyl)picolinohydrazoneamide (13)

2-cyano-5-fluoropyridine (3.040 g, 24.9 mmol) was reduced in the presence of thiosemicarbazide (**IIIa**) (3.616 g, 24.9 mmol) through general procedure and 5-fluoro-*N'*-(pyrrolidine-1-carbonothioyl)picolino hydrazoneamide (**13**) was obtained.



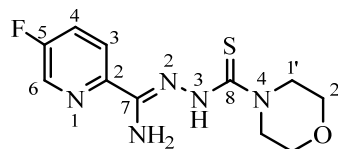
(13)

Yield: 45%. mp 161-163 °C. HRFABMS: m/z 268.10061 $[M + H]^+$ (calcd for $C_{11}H_{15}FN_5S$, 268.10322) Elemental analysis: Calcd for $C_{11}H_{14}FN_5S$; C, 49.42; H, 5.28; N, 26.20. Found; C, 49.87; H, 4.90; N, 26.56%. IR ν_{max} in KBr (selected bands) : cm^{-1} 3396 (m), 3271 (m), 3223(m), 1666 (s), 1605 (s), 1582 (s), 1470 (s), 1435 (s), 1093(m), 843 (m), 626 (m). 1H NMR (400MHz, $CDCl_3$) : δ ppm 12.87 (1H, H-N3), 8.43 (1H, br s, H-6), 8.05 (1H, d, $J = 4.9$ Hz, H-3), 7.49 (1H, br s, H-4), 6.63 (2H, br s, $\underline{N}H_2$), 3.81 (4H, br s, H-1'), 1.93 (4H, br s, H-2'); 1H -NMR (400 MHz, DMSO- d_6) :

δ ppm 12.48, 9.22 (1H, br s, HN-, *E* and *Z'* geometrical isomers); 8.55, 8.80 (1H, br s, H-6, *E* and *Z'* geometrical isomers); 8.06, (d, $J = 5.4$ Hz) 8.21 (1H, br s, H-3, *E* and *Z'* geometrical isomers); 7.78, (br s) 8.09 (1H, d, $J = 10.3$ Hz, H-4, *E* and *Z'* geometrical isomers); 6.76 (2H, br s, NH_2); 3.55, 3.72 (4H, br s, H-1', *E* and *Z'* geometrical isomers); 1.83 (4H, br s, H-2'). ^{13}C NMR (100 MHz, $\text{DMSO-}d_6$) : δ ppm 177.9 (C-8), 158.0 (C-5), 146.6 (C-7), 141.3 (C-2), 139.6 (C-6), 125.5 (C-3), 123.3 (C-4), 52.6 (C-1'), 25.2 (C-2')

4.3.2.14 5-Fluoro-*N'*-(morpholine-4-carbonothioyl)picolinohydrazoneamide (14)

2-cyano5-fluoropyridine (3.040 g, 24.9 mmol) was reduced in the presence of thiosemicarbazide (**IIIc**) (4.015 g, 24.9 mmol) through general procedure and 5-fluoro-*N'*-(morpholine-1-carbonothioyl) picolinohydrazoneamide (**14**) was obtained.

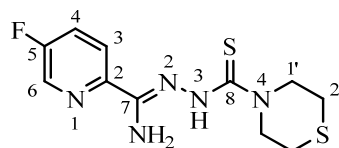


(14)

Yield: 50%. mp 181-183 °C. HRFABMS: m/z 306.08203 $[\text{M} + \text{Na}]^+$ (calcd for $\text{C}_{11}\text{H}_{14}\text{FN}_5\text{OSNa}$, 306.080008) Elemental analysis: Calcd for $\text{C}_{11}\text{H}_{14}\text{FN}_5\text{OS}$; C, 46.63; H, 4.98; N, 24.72. Found; C, 46.83; H, 4.85; N, 24.53%. IR spectrum in KBr (selected bands) : cm^{-1} 3429(m), 3304 (s), 3159 (m), 1678 (s), 1585 (s), 1506 (s), 1462 (s), 1418 (s), 1024 (m), 855 (m), 622 (m); ^1H NMR (400 MHz, $\text{DMSO-}d_6$) : δ ppm 12.48 (1H, br s, H-N3), 8.81 (1H, br s, H-6), 8.23 (1H, d, $J = 9.7$ Hz, H-3), 8.06 (1H, d, $J = 9.7$ Hz, H-4), 3.80 (4H, br s, H-2'), 3.55 (4H, br s, H-1'). ^{13}C NMR (100 MHz, $\text{DMSO-}d_6$) : δ ppm 179.2 (C-8), 159.5 (C-5), 144.4 (C-7), 141.0 (C-2), 139.4 (C-6), 125.5 (C-3), 123.6 (C-4), 66.7 (C-2'), 47.1 (C-1')

4.3.2.15 5-Fluoro-*N'*-(thiomorpholine-4-carbonothioyl)picolinohydrazoneamide (15)

2-cyano5-fluoropyridine (3.040 g, 24.9 mmol) was reduced in the presence of thiosemicarbazide (**IIIId**) (4.415 g, 24.9 mmol) through general procedure and 5-fluoro-*N'*-(thiomorpholine-1-carbonothioyl) picolinohydrazoneamide (**15**) was obtained.

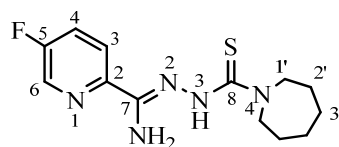


(15)

Yield: 52%. mp 156-158 °C. HRFABMS: m/z 300.07414 $[M + H]^+$ (calcd for $C_{11}H_{15}FN_5S_2$, 300.07530) Elemental analysis: Calcd for $C_{11}H_{14}FN_5S_2$; C, 44.13; H, 4.71; N, 23.39. Found; C, 44.36; H, 4.44; N, 23.15%. IR ν_{max} in KBr (selected bands) : cm^{-1} 3372 (m), 3256 (m), 3163(m), 1666 (s), 1604 (s), 1581 (s), 1465 (s), 1412 (s), 1092 (m), 825 (m), 632 (m); 1H NMR (400 MHz, DMSO- d_6) : δ ppm 12.48 (1H, br s, HN-), 8.79 (1H, br s, H-6), 8.21 (1H, m, H-3), 8.04 (1H, t, $J = 9.3$ H-4), 4.14 (4H, br s, H-1'), 2.49 (4H, br s, H-2'). ^{13}C NMR (100 MHz, DMSO- d_6) : δ ppm 178.2 (C-8), 159.7 (C-5), 144.5 (C-7), 141.2 (C-2), 139.3 (C-6), 125.4 (C-3), 123.7 (C-4), 49.3 (C-1'), 26.9 (C-2').

4.3.2.16 5-Fluoro-*N'*-(azepane-1-carbonothioyl)picolinohydrazoneamide (16)

2-cyano-5-fluoropyridine (3.040 g, 24.9 mmol) was reduced in the presence of thiosemicarbazide (**IIIe**) (4.315 g, 24.9 mmol) through general procedure and 5-fluoro-*N'*-(azepane-1-carbonothioyl)picolinohydrazoneamide (**16**) was obtained.

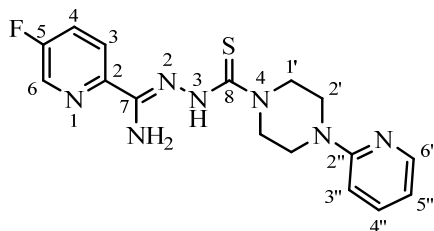


(16)

Yield: 40%. mp 150-152 °C. HRFABMS: m/z 296.13661 $[M + H]^+$ (calcd for $C_{13}H_{19}FN_5S$, 296.13452) Elemental analysis: Calcd for $C_{13}H_{18}FN_5S$; C, 52.86; H, 6.14; N, 23.71. Found; C, 52.23; H, 5.91; N, 24.05%. IR ν_{max} in KBr (selected bands) : cm^{-1} 3454 (m), 3360 (m), 3227(m), 1670(s), 1608 (s), 1582 (m), 1480 (s), 1417 (s), 1100 (m), 841 (m), 630 (m); 1H NMR (400 MHz, DMSO- d_6) : δ ppm 12.65 (1H, br s, H-N3), 8.80 (1H, br s, H-6), 8.19 (1H, d, $J = 9.3$ Hz, H-3), 8.05 (1H, d, $J = 9.3$ Hz, H-4), 3.81 (4H, br s, H-1'), 1.69 (4H, br s, H-3'), 1.48 (4H, br s, H-2'). ^{13}C NMR (100 MHz, DMSO- d_6) : δ ppm 178.5 (C-8), 159.3 (C-5), 142.9 (C-7), 141.3 (C-2), 139.4 (C-6), 125.4 (C-3), 123.3 (C-4), 57.6 (C-1'), 27.9 (C-2'), 27.1 (C-3')

4.3.2.17 5-Fluoro-*N'*-(4-(pyridin-2-yl)piperazine-1-carbonothioyl)picolinohydrazonamide (17)

2-cyano-5-fluoropyridine (3.040 g, 24.9 mmol) was reduced in the presence of thiosemicarbazide (**IIIc**) (4.339 g, 24.9 mmol) through general procedure and 5-fluoro-*N'*-(4-(pyridin-2-yl)piperazine-1-carbonothioyl)picolinohydrazonamide (**17**) was obtained.

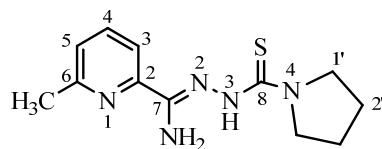


(17)

Yield: 61%. mp 193-195 °C. HRFABMS: m/z 359.14438 $[M + H]^+$ (calcd for $C_{16}H_{19}FN_7S$, 359.14542) Elemental analysis: Calcd for $C_{16}H_{18}FN_7S$; C, 53.47; H, 5.05; N, 27.28. Found; C, 53.69; H, 4.71; N, 27.01%. IR ν_{max} in KBr (selected bands) : cm^{-1} 3424 (m), 3299 (m), 3157(m), 1677 (s), 1604 (s), 1580 (s), 1482 (s), 1418 (s), 1018 (m), 841 (m), 625 (m); 1H NMR (400 MHz, DMSO- d_6) : δ ppm 12.53 (1H, H-N3), 8.82 (1H, br s, H-6), 8.24 (1H, br s, H-3), 8.12 (1H, br s, H-6''), 8.07 (1H, br s, H-4), 7.53 (1H, m, H-4''), 6.85 (1H, d, $J = 8.3$ Hz, H-3''), 6.64 (1H, m, H-5''), 3.96 (4H, br s, H-1'), 3.48 (4H, br s, H-2'). ^{13}C NMR (100 MHz, DMSO- d_6) : δ ppm 178.9 (C-8), 159.5 (C-5), 156.9 (C-2''), 148.0 (C-6''), 144.3 (C-7), 141.0 (C-2), 138.1 (C-4''), 138.0 (C-6), 125.5 (C-3), 123.5 (C-4), 113.5 (C-5''), 107.7 (C-3''), 46.1 (C-1'), 45.1 (C-2').

4.3.2.18 6-Methyl-*N'*-(pyrrolidine-1-carbonothioyl)picolinohydrazonamide (18)

2-cyano-6-methylpyridine (2.942 g, 24.9 mmol) was reduced in the presence of thiosemicarbazide (**IIIb**) (3.965 g, 24.9 mmol) through general procedure and 6-methyl-*N'*-(piperidine-1-carbonothioyl)picolino hydrazonamide (**18**) was obtained.

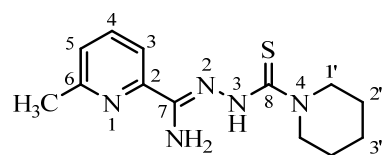


(18)

Yield: 26%. mp 152-154 °C. HRFABMS: m/z 264.12962 $[M + H]^+$ (calcd for $C_{12}H_{18}N_5S$, 264.12829) Elemental analysis: Calcd for $C_{12}H_{17}N_5S$ ($M_r = 263.4$ gm/mol); C, 54.73; H, 6.51; N, 26.59. Found; C, 55.12; H, 6.24; N, 26.76%. IR ν_{max} in KBr (selected bands) : cm^{-1} 3387 (m), 3249 (m), 3221 (m), 1667 (s), 1599 (s), 1569 (s), 1493 (s), 1431 (s), 1105 (m), 841 (m), 624 (m). 1H NMR (400 MHz, $CDCl_3$) : δ ppm 12.95 (1H, br s, HN-), 7.79 (1H, br s, H-5), 7.71 (1H, br s, H-4), 7.27 (1H, br s, H-3), 6.63 (2H, br s, NH_2), 3.76 (4H, br s, H-1'), 2.59 (3H, br s, CH_3), 1.92 (4H, br s, H-2'); 1H -NMR (400 MHz, $DMSO-d_6$) : δ ppm 12.52, 9.22 (1H, br s, HN-, *E* and *Z'* geometrical isomers), 7.82, 7.93 (1H, br s, H-3, *E* and *Z'* geometrical isomers), 7.72, 7.92, (1H, br s, H-4, *E* and *Z'* geometrical isomers), 7.29, 7.48 (1H, br s, H-5, *E* and *Z'* geometrical isomers); 6.74 (2H, br s, NH_2); 3.56, 3.74 (4H, br s, H-1', *E* and *Z'* geometrical isomers); 1.83 (4H, br s, H-2'). ^{13}C NMR (100 MHz, $DMSO-d_6$) : δ ppm 178.9 (C-8), 160.7 (C-6), 148.4 (C-7), 143.9 (C-2), 138.8 (C-4), 126.4 (C-5), 118.6 (C-3), 48.6 (C-1'), 25.2 (C-2'), 24.3 (CH_3).

4.3.2.19 6-Methyl-*N'*-(piperidine-1-carbonothioyl)picolinohydrazoneamide (19)

2-cyano-6-methylpyridine (2.942 g, 24.9 mmol) was reduced in the presence of thiosemicarbazide (**IIIb**) (3.965 g, 24.9 mmol) through general procedure and 6-methyl-*N'*-(piperidine-1-carbonothioyl)picolino hydrazoneamide (**19**) was obtained.

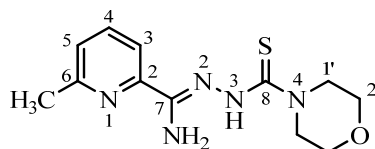


(19)

Yield: 21%. mp 150-151 °C. Anal.Calc. for $C_{13}H_{19}N_5S$ ($M_r = 277.4$ gm/mol); C, 56.29; H, 6.90; N, 25.25. Found; C, 56.11; H, 7.22; N, 25.53%. IR ν_{max} in KBr (selected bands) : cm^{-1} 3353 (m), 3234 (m), 3157(m), 1673 (s), 1603 (s), 1583(s), 1468 (s), 1427 (s), 1025 (m), 881 (m), 636 (m); 1H NMR (400 MHz, $DMSO-d_6$) : δ ppm 12.67 (1H, br s, HN-), 7.95 (1H, br s, H-5), 7.93 (1H, br s, H-4), 7.49 (1H, d, 4.9 Hz, H-3), 3.83 (4H, br s, H-1'), 2.56 (3H, s, CH_3), 1.58 (2H, br s, H-3'), 1.44 (4H, br s, H-2'). ^{13}C NMR (100 MHz, $DMSO-d_6$) : δ ppm 178.6 (C-8), 158.9 (C-6), 144.4 (C-7), 143.9 (C-2), 138.7 (C-4), 126.5 (C-5), 118.7 (C-3), 47.4 (C-1'), 26.1 (C-2'), 25.3 (C-3'), 24.6 (CH_3).

4.3.2.20 6-Methyl-*N'*-(morpholine-4-carbonothioyl)picolinohydrazoneamide (20)

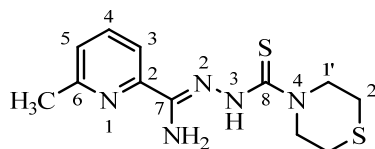
2-cyano-6-methylpyridine (2.942 g, 24.9 mmol) was reduced in the presence of thiosemicarbazide (**IIIc**) (4.015 g, 24.9 mmol) through general procedure and 6-methyl-*N'*-(morpholine-1-carbonothioyl)picolino hydrazoneamide (**20**) was obtained.

**(20)**

Yield: 54%. mp 164-166 °C. HRFABMS: m/z 280.12227 $[M + H]^+$ (calcd for $C_{12}H_{18}ON_5S$, 280.12321) Elemental analysis: Calcd for $C_{12}H_{17}ON_5S$; C, 51.59; H, 6.13; N, 25.07. Found; C, 51.86; H, 5.97; N, 24.90%. IR ν_{max} in KBr (selected bands) : cm^{-1} 3329 (s), 3240 (s), 3163(s), 1672 (s), 1614 (s), 1594 (s), 1465 (s), 1421 (s), 1019 (m), 842 (m), 621 (s); 1H NMR (400 MHz, $DMSO-d_6$) : δ ppm 12.53 (1H, br s, H-N3), 8.02 (1H, br s, H-5), 7.81 (1H, br s, H-4), 7.48 (1H, d, 5.1 Hz, H-3), 3.81 (4H, t, $J = 4.86$ Hz, H-2'), 3.56 (4H, t, 4.86 Hz, H-1'), 2.42 (3H, s, $\underline{CH_3}$); ^{13}C NMR (100 MHz, $DMSO-d_6$) : δ ppm 179.1 (C-8), 158.7 (C-6), 144.3 (C-7), 143.8 (C-2), 138.8 (C-4), 126.7 (C-5), 118.7 (C-3), 66.7 (C-2'), 47.2 (C-1'), 24.5 ($\underline{CH_3}$).

4.3.2.21 6-Methyl-*N'*-(thiomorpholine-4-carbonothioyl)picolinohydrazoneamide (21)

2-cyano-6-methylpyridine (2.942 g, 24.9 mmol) was reduced in the presence of thiosemicarbazide (**IIIId**) (4.415 g, 24.9 mmol) through general procedure and 6-methyl-*N'*-(thiomorpholine-1-carbonothioyl) picolinohydrazoneamide (**21**) was obtained.

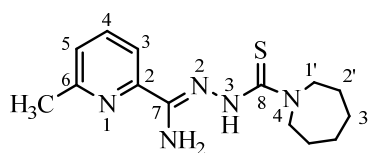
**(21)**

Yield: 41%. mp 157-158 °C. HRFABMS: m/z 296.09827 $[M + H]^+$ (calcd for $C_{12}H_{18}N_5S_2$, 296.10037) Elemental analysis: Calcd for $C_{12}H_{17}N_5S_2$; C, 48.79; H, 5.80; N, 23.71. Found; C, 49.15; H, 5.51; N, 23.45%. IR ν_{max} in KBr (selected bands): cm^{-1} 3410 (s), 3279 (s), 3140(s), 1658 (s), 1597 (s), 1581 (s), 1481 (s), 1466 (s), 1065 (s), 856 (s), 620 (s); 1H NMR (400 MHz, $DMSO-d_6$) : δ ppm 12.52 (1H, br s, HN-),

7.93(1H, br s, H-5), 7.92 (1H, br s, H-4), 7.48 (1H, d, $J = 5.1$ Hz, H-3), 4.14 (4H, br s, H-1'), 2.53 (3H, br s, $\underline{\text{CH}}_3$), 2.50 (4H, t, $J = 5.1$ Hz, H-2'). ^{13}C NMR (100 MHz, DMSO- d_6) : δ ppm 178.9 (C-8), 158.9 (C-6), 149.1 (C-7), 143.5 (C-2), 139.1 (C-4), 124.7 (C-5), 116.8 (C-3), 50.8 (C-1'), 26.8 (C-2'), 24.7 ($\underline{\text{C}}\text{H}_3$).

4.3.2.22 6-Methyl- N' -(azepane-1-carbonothioyl)picolinohydrazonamide (22)

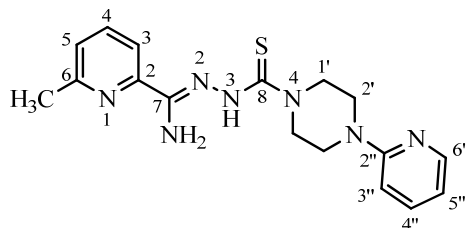
2-cyano-6-methylpyridine (2.942 g, 24.9 mmol) was reduced in the presence of thiosemicarbazide (**IIIe**) (4.315 g, 24.9 mmol) through general procedure and 6-methyl- N' -(azepane-1-carbonothioyl)picolino hydrazonamide (**22**) was obtained.



Yield: 20%. mp 139-141 °C. HRFABMS: m/z 292.15681 $[\text{M} + \text{H}]^+$ (calcd for $\text{C}_{14}\text{H}_{22}\text{N}_5\text{S}$, 292.15959) Elemental analysis: Calcd for $\text{C}_{14}\text{H}_{21}\text{N}_5\text{S}$; C, 57.70; H, 7.26; N, 24.03. Found; C, 58.02; H, 7.07; N, 24.18% ; IR ν_{max} in KBr (selected bands) : cm^{-1} 3357 (s), 3240 (s), 3156(s), 1672 (s), 1603 (s), 1581 (s), 1453 (s), 1410 (s), 1105 (m), 855 (m), 629 (m); ^1H NMR (400 MHz, DMSO- d_6) : δ ppm 12.68 (1H, br s, HN-), 7.94 (1H, br s, H-5), 7.92 (1H, br s, H-4), 7.47 (1H, br s, H-3), 3.82 (4H, br s, H-1'), 2.55 (3H, br s, $\underline{\text{C}}\text{H}_3$); 1.69 (4H, br s, H-3'), 1.45 (4H, br s, H-2'). ^{13}C NMR (100 MHz, DMSO- d_6) : δ ppm 178.2 (C-8), 158.8 (C-6), 143.9 (C-7), 143.8 (C-2), 138.7 (C-4), 126.3 (C-5), 118.6 (C-3), 49.3 (C-1'), 28.4 (C-2'), 27.1 (C-3'), 24.6 ($\underline{\text{C}}\text{H}_3$).

4.3.2.23 6-Methyl- N' -(4-(pyridin-2-yl)piperazine-1-carbonothioyl)picolinohydrazonamide (23)

2-cyano-6-methylpyridine (2.942 g, 24.9 mmol) was reduced in the presence of thiosemicarbazide (**IIIf**) (4.339 g, 24.9 mmol) through general procedure and 6-methyl- N' -(4-(pyridin-2-yl)piperazine-1-carbonothioyl)picolinohydrazonamide (**23**) was obtained.



(23)

Yield: 42%. mp 149-150 °C. HRFABMS: m/z 355.17386 $[M + H]^+$ (calcd for $C_{17}H_{22}N_7S$, 355.17050) Elemental analysis: Calcd for $C_{17}H_{21}N_7S$; C, 57.44; H, 5.95; N, 27.58. Found; C, 57.84; H, 5.62; N, 27.22% ; IR ν_{max} in KBr (selected bands): cm^{-1} 3431 (m), 3301 (m), 3228(m), 1666 (s), 1593 (s), 1562 (s), 1477 (s), 1417 (s), 1020 (m), 871 (s), 629 (m); 1H NMR (400 MHz, DMSO- d_6) : δ ppm 12.57 (1H, br s, H-N3), 8.12 (1H, br s, H-6''), 7.97 (1H, br s, H-5), 7.96 (1H, m, H-4), 7.54 (1H, br s, H-4''), 7.51 (1H, m, H-3), 6.85 (1H, d, $J = 7.3$ Hz, H-3''), 6.64 (1H, d, $J = 7.3$ Hz, H-5''), 3.96 (4H, br s, H-1'), 3.48 (4H, br s, H-2'), 2.57 (3H, br s, CH_3). ^{13}C NMR (100 MHz, DMSO- d_6) : δ ppm 178.9(C-8), 159.6 (C-6), 159.0 (C-2''), 148.0 (C-6''), 145.2 (C-7), 143.7 (C-2), 138.8 (C-4), 138.0 (C-4''), 126.7 (C-5), 118.9 (C-3), 113.5 (C-5''), 107.7 (C-3''), 46.1 (C-1'), 45.1(C-2'), 24.6 (CH_3).

4.4. Cell viability assay against HeLa cells

HeLa cells were grown initially in 75 cm^2 culture flask with Dulbecco's Modified Eagle's Medium (DMEM) at 37 °C under 5% CO_2 and 95% air. The supernatant from each well was removed and set aside. The cells were trypsinized and counted using hemocytometer.

2000 cells/well were seeded in 96 well plate in 100 μ l of DMEM. After 24 h pre-culture, the medium was aspirated off, and exchanged for that containing synthesized compounds at various concentrations (0.000, 0.001, 0.010, 0.100 10.000 and 100.000 μ mol/L) in DMEM. Blank controls (containing only media) and low controls (containing untreated cells) were included on each plate. After 72 h incubation at 37 °C, 100 μ L of DMEM containing 10% WST-8 cell counting kit solution was added to the each wells directly and incubated further for 3 h. The absorbance at 450 nm was measured with a reference wave-length of 630 nm using (Perkin Elmer EnSpire Multilabel Reader). The 50% growth inhibitory concentration (IC_{50}) of synthesized compounds were estimated by using the software GraphPad prism[®].

4.5 Preferential Cytotoxic Activity against PANC-1 Cells in Nutrient-Deprived Medium (NDM)

The *in vitro* preferential cytotoxicity of the synthesized compounds was determined by a previously described procedure with a slight modification.²¹⁹ Human pancreatic cancer cells were seeded in 96-well plates (1.5×10^4 /well) and incubated in fresh DMEM at 37 °C under 5% CO₂ and 95% air for 24 h. The supernatant from each well was removed and set aside. 2 mL trypsin (0.2 mg/mL) was added to each well and incubated at 37 °C under 5% CO₂ and 95% air for 5 min. The trypsinised cells were added to the supernatant removed from same well. The combined mixture was then centrifuged at 200 g for 5 min and the cells were resuspended in fresh medium (10 mL). An aliquot of cell suspension was diluted (100 µL of cell suspension added to 100 µL of medium) before counting cells using a haemocytometer. Once the concentration of cells per mL was known, the dilution factor could be calculated based on total number of cells and total volume of medium required.

Serial dilutions of synthesized compounds in both DMEM and NDM were prepared at 0.000, 0.001, 0.010, 0.100, 10.000 and 100.000 µmol/L. Blank controls (containing only media) and low controls (containing untreated cells) were included on each plate. DMEM was removed from the wells and the cells were washed with warm PBS buffer before adding serial dilution (100 µL per well). Each concentration was assayed in triplicate. After 24 h incubation, 100 µL of DMEM containing 10% WST-8 cell counting kit solution was added to the each wells directly. After 3 h incubation, the absorbance at 450 nm was measured (Perkin Elmer EnSpire Multilabel Reader). Cell viability was calculated from the mean values of data from three wells.

Preferential cytotoxicity was expressed as the concentration at which 50% cells died preferentially in NDM (PC₅₀)

4.6. Morphological Assessment of PANC-1 Cells

Cells for the morphological change study were seeded in 60 mm dishes (1×10^6) and incubated in humidified CO₂ incubator for 24 h for the cell attachment. The dishes were centrifuged at 1000 rpm, and 8 µL of staining solution (0.1 mg/mL for both Acridine Orange (AO) and Ethidium Bromide (EB) in Phosphate Buffered Saline

(PBS)) was added to each well. After 10 min, the cells were washed twice with PBS, and treated with 25 μ M of synthesized compound in DMEM, NDM, and the controls. After 24 h incubation, cell morphology was observed using an inverted Nikon Eclipse TS 100 microscope (40 \times objective) with phase-contrast. Microscopic images were taken with a Nikon DS-L-2 camera directly attached to the microscope.

4.7 Western Blot Analysis

The proteins were separated by gel electrophoresis on a polyacrylamide gel containing 0.1% SDS i.e., Sodium dodecyl sulphate polyacrylamide gel electrophoresis (SDS-PAGE) and then transferred to Polyvinylidene Difluoride (PVDF) membranes. The membranes were blocked with Block Ace (DS Pharma Medical, Suita, Japan), washed with PBS containing 0.1% polyoxyethylene (20) sorbitan monolaurate (Wako Pure Chemical), then incubated overnight at room temperature with primary antibodies diluted Can Get Signal (Toyobo, Osaka, Japan). After washing, the membranes were incubated for 45 min at room temperature with horseradish peroxidase (HRP)-conjugated anti-rabbit, mouse or goat immunoglobulins as the second antibody. The bands were detected with an enhanced chemiluminescence solution (PerkinElmer., Waltham, MA, USA).

4.8. Annexin V/PI staining assay

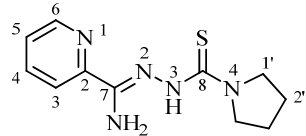
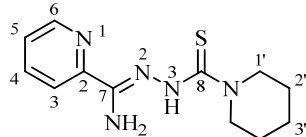
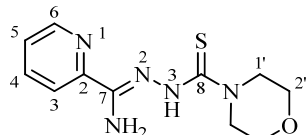
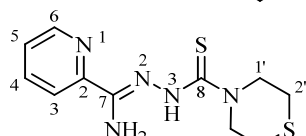
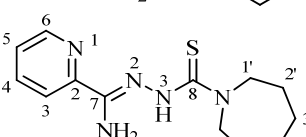
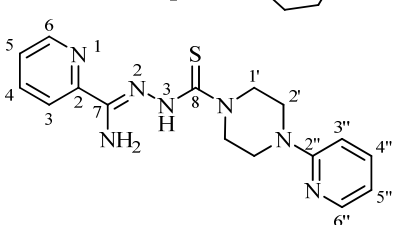
PANC-1 cells were seeded in 60 mm dishes (1×10^6 cells) and incubated in DMEM at 37 $^{\circ}$ C under 5% CO₂ for 24 h. The cells were then washed twice with PSB, and treated with 1 μ M of **6** in NDM and incubated for 12 h. Cells were then stained with Annexin-V (AV)-FLUOS Staining Kit (Roche Diagnostics GmbH, Penzberg, Germany) according to manufacturer's protocol, and incubated for 20 minutes at room temperature in dark. The cells were then visualized by Nikon Eclipse TS 100 microscope (40 \times objective) in fluorescent mode. Microscopic images were taken with a Nikon DS-L-2 camera directly attached to the microscope. During apoptosis, plasma membrane alteration occurs, leading to the translocation of phosphatidylserine (PS) to the external surface of the cell. AV specifically binds with exposed PS, and detected as green fluorescence. The dead cells are stained with propidium iodide (PI) and gives red fluorescence.

5.1 SYNTHESIS, CHARACTERIZATION AND BIOLOGICAL ACTIVITY OF 2-PYRIDINEFORMAMIDE *N*(4)-RING INCORPORATED THIOSEMICARBAZONES

5.1.1 General Discussions

Thiosemicarbazides were synthesized by the method described by Scovill.²⁷ The 2-pyridineformamide thiosemicarbazones with variations in *N*(4)-ring incorporation were prepared by reducing 2-cyanopyridine or substituted 2-cyanopyridine with sodium in dry methanol in the presence of desired thiosemicarbazide. Synthesis and characterization of compounds **2** and **5** have been reported earlier.^{37,220}

Table 5.1: Physical Properties of Compounds 1-6

Compd	Molecular formula	Molecular mass	Colour	Yield (%)	M. P. (°C)	
1		C ₁₁ H ₁₅ N ₅ S	249.34	Yellow	46	159-160
2		C ₁₂ H ₁₇ N ₅ S	263.36	Yellow	21	154-155
3		C ₁₁ H ₁₅ ON ₅ S	265.33	Yellow	60	173-175
4		C ₁₁ H ₁₅ N ₅ S ₂	281.40	Yellow	59	162-163
5		C ₁₃ H ₁₉ N ₅ S	277.39	Yellow	24	153-155
6		C ₁₆ H ₁₉ N ₇ S	341.43	Yellow	45	151-152

The thiosemicarbazones were obtained in low to moderate yield (21- 60%) having melting point in the range of 151-175 °C. The thiosemicarbazones were stable in air at room temperature, slightly soluble in CHCl₃, Me₂CO and more soluble in polar solvents such as EtOH, MeOH, DMF and DMSO, and slightly soluble in water. The synthesized compounds were characterized by elemental analysis, IR, ¹H and ¹³C-NMR spectroscopic techniques. The molecular structures were further confirmed by HRFAB mass spectrometry. The synthesized compounds were found highly active against HeLa cervical cancer and PANC-1 human pancreatic cancer cell lines. The physical characteristics of the compounds are compiled in table 5.1.

The elemental analyses results (Table 5.2) showed that the experimental data were in accordance to the calculated values within the limits of experimental error.

Table 5.2: Elemental Analysis Data of Compounds **1-6** (Calculated Data)

Compound	C	H	N
1	53.45 (52.99)	5.69 (6.06)	27.72 (28.09)
2	55.27 (54.73)	6.26 (6.51)	26.83 (26.59)
3	50.29 (49.79)	5.58 (5.70)	26.10 (26.39)
4	47.21 (46.95)	5.03 (5.37)	24.62 (24.89)
5	56.77 (56.29)	6.63 (6.90)	25.59 (25.25)
6	56.67 (56.28)	5.38 (5.61)	28.41 (28.72)

5.1.2 Spectral Studies

5.1.2.1 IR Spectra

The assignments of IR spectral bands are most useful in establishing the structural identity of the synthesized compounds **1-6** and are listed in Table 5.3.

The synthesized compounds exhibited characteristic bands corresponding to the various functional groups in their specific energy region. The compounds displayed three medium to strong intensity bands at around 3424 to 3389 cm⁻¹, 3277 to 3229 cm⁻¹, and 3234 to 3216 cm⁻¹ assignable to the asymmetric and symmetric stretching frequencies of the -NH₂ chromophore and N(3)H stretch, respectively.²²¹ Additional bands in this high frequency region can arise from intramolecular hydrogen bonding. The presence of N(3) stretching vibration in the range 3234 to 3216 cm⁻¹ suggest the thione formulation of the thiosemicarbazones in its solid state.²²² In principle, the

TSCs can exhibit thione – thiol tautomerism since it contains a thioamide –NH–C =S, functional group. The $\nu(\text{S-H})$ band at 2600 to 2500 cm^{-1} was absent in the IR spectrum of compounds but $\nu(\text{N-H})$ band was present, indicating that in the solid state, the TSC remains as the thione tautomer.^{223,224}

Table 5.3 Diagnostic Bands in the IR Spectra of Compounds 1-6

Group↓	Compound					
	1	2	3	4	5	6
$\nu(\text{NH}_2)$	3389(m), 3260(m)	3411(m), 3263(m)	3403(m), 3276(m)	3404(m), 3275(m)	3424(m), 3229(m)	3418(w), 3277(w)
$\nu(\text{NH})$	3216(m)	3219(m)	3231(m)	3234(m)	3131(m)	3229(m)
$\delta(\text{NH})$	1672(s)	1667(s)	1670(s)	1669(s)	1673(s)	1673(s)
$\nu(\text{C}=\text{C})$	1597(s), 1579(s), +	1601(s), 1582(s), 1465(s),	1605(s), 1583(s), 1460(s),	1604(s), 1584(s), 1461(s),	1595(s), 1585(s), 1476(s),	1602(s), 1566(s), 1462(s),
$\nu(\text{C}=\text{N})$	1428(s)	1425(s)	1431(s)	1428(s)	1413(s)	1427(s)
$\nu(\text{N-N})$	1090(m)	1074(m)	1025(m)	1067(m)	1097(m)	1020(m)
$\nu(\text{C}=\text{S})$	849(m)	884(m)	892(m)	861(m)	861(m)	877(m)
$\rho(\text{Py})$	635(m)	636(m)	627(m)	628(s)	631(m)	628(m)

s : strong, m : medium, w : weak

Likewise, the IR spectra of the compounds exhibited a strong band in the range 1605 to 1595 cm^{-1} assignable to $\nu(\text{C} = \text{N})$ stretching vibration of imine nitrogen, which was in a good agreement with the previous observations.^{225,226} Assignment of $\nu(\text{C} = \text{N})$ was complicated by the differences in the thiosemicarbazone moieties (i.e. the bifurcated *Z'* and the *E*) which was involved in hydrogen bonding, as well as the partial double bond character possessed by all of the C–N bonds of the molecule. Further, the $\nu(\text{C} = \text{N})$ appears along with the ring breath and N-H deformation bands that create ambiguity for its isolation with certainty.

A strong band found at 1097 to 959 cm^{-1} was due to the $\nu(\text{N-N})$ group of the thiosemicarbazone.⁴⁷ The compounds show the thioamide IV band of medium to strong intensity, which possesses considerable contribution from $\nu(\text{C}=\text{S})$, in the 892 to 790 cm^{-1} range.²²⁰ The in-plane deformation vibrations were observed in the region 635 to 616 cm^{-1} .¹⁶⁸ Slight difference in the vibrational frequencies of the TSCs throughout the series were observed due to the difference in nature of *N*(4) substituent.

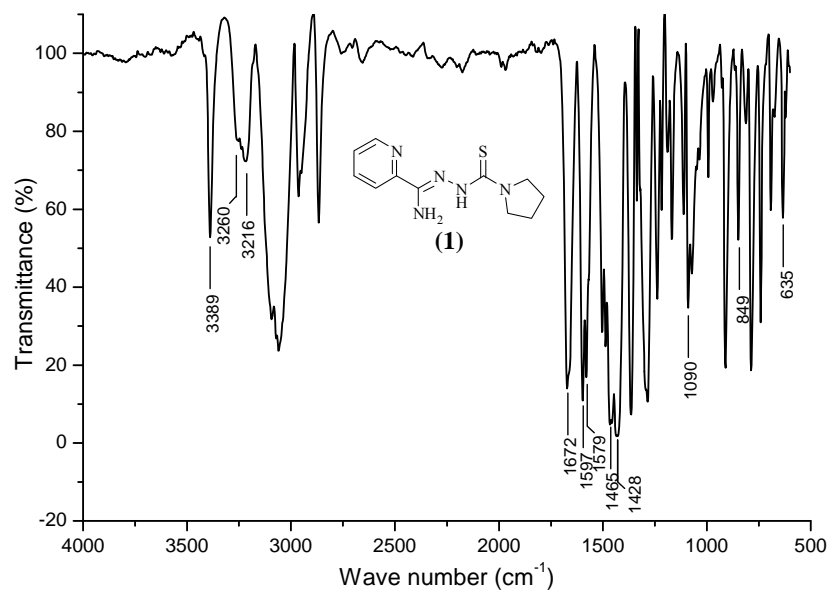


Figure 5.1: IR spectrum of compound 1

5.1.2.2 NMR Spectra

The ^1H -NMR spectral data for the synthesized compounds are listed in Table 5.4

The NMR spectra of the compounds confirm that in solution it exists as the neutral form. The absence of a signal at *ca.* δ 4 ppm that can be ascribed to $-\text{SH}$ was consistent with the idea that in solution, as in the solid state (also confirmed by IR) the TSCs exist as the thione tautomers.²²⁷ In $\text{DMSO-}d_6$, the signals of the aromatic protons of the compounds appeared at δ 7.42 to 8.77 ppm, and the resonance lines were found to correspond to the calculated multiplicity. $\text{C}(5)\text{H}$ of the pyridyl ring was easily identified in the spectra of the compounds as a doublet of doublet at about δ 7.6 ppm. $\text{C}(3)\text{H}$ and $\text{C}(4)\text{H}$ appeared as doublet at 7.84 to 8.16 ppm.

Compound 1 was found to exist as the *E*-isomer with intramolecular hydrogen bonding in CDCl_3 as indicated by a signal at a low field of δ 12.95 ppm in ^1H -NMR. In $\text{DMSO-}d_6$ there was a mixture of *E* isomer, *Z* isomer with hydrogen bonding to the solvent and a bifurcated tautomer *Z'* in which the $\text{N}(3)\text{H}$ was transferred to $\text{N}(2)$, resulting in a conjugated thiosemicarbazone moiety and yellow colour. The signal at low field δ 12.55 ppm was due to $\text{N}(3)\text{H}$ intramolecularly hydrogen bonded to pyridine nitrogen, whereas the signal at high field δ 9.23 was $\text{N}(3)\text{H}$ hydrogen bonded in DMSO solution.²²⁸ Downfield shifts to greater than δ 14.00 ppm have been observed for this proton when hydrogen bonded to the heterocyclic ring nitrogen

of the thiosemicarbazones, particularly when *N*(4) was bonded to bulky groups or was a part of a ring.²²⁹

Table 5.4: ¹H-NMR Spectral Assignments (ppm) of Compounds **1** – **6** (400 MHz)

Compd →		1	2	3	4	5	6
Solvent →		DMSO- <i>d</i> ₆	DMSO- <i>d</i> ₆	DMSO- <i>d</i> ₆	DMSO- <i>d</i> ₆	DMSO- <i>d</i> ₆	DMSO- <i>d</i> ₆
Proton ↓		CDCl ₃	DMSO- <i>d</i> ₆	DMSO- <i>d</i> ₆	DMSO- <i>d</i> ₆	DMSO- <i>d</i> ₆	DMSO- <i>d</i> ₆
3	7.99, d (8.1 Hz)	8.01, d (6.5 Hz), 8.10, d (6.5 Hz)	8.10, d (8.1 Hz)	8.14, d (7.3 Hz)	8.14, d (7.3 Hz)	8.09, d (8.1 Hz)	8.16, d (7.3 Hz)
4	7.80, br s	7.84, br d (6.5 Hz) 8.06, br d (6.5 Hz)	8.06, dd (8.1, 6.5 Hz)	8.09, br d (7.3 Hz)	8.08, m	8.06, dd (8.1, 6.5 Hz)	8.08, d (7.3 Hz)
5	7.39, br s	7.42, br s 7.61, dd (6.5, 4.9 Hz)	7.61, dd (6.5, 4.9 Hz)	7.64, dd (7.3, 5.7 Hz)	7.63, d (4.9 Hz)	7.60, dd (6.5, 4.1 Hz)	7.64, dd (6.5, 5.7 Hz)
6	8.61, br s	8.55, d (4.9 Hz) 8.74, d (4.9 Hz)	8.75, br d (4.9 Hz)	8.77, d (5.7 Hz)	8.77, d (4.9 Hz)	8.75, br d (4.1 Hz)	8.77, d (5.7 Hz)
1'	3.78, br s	3.55, br s 3.73, br s	3.83, t (4.9 Hz)	3.56, br s	4.17, br s	3.81, br s	3.96, br s
2'	1.92, br s	1.83, br s	1.44, br s	3.81, br s	2.52, br s	1.45, br s	3.48, br s
3'			1.57, br s			1.69, br s	
3"							6.85, d (8.9 Hz)
4"							7.53, dd (8.9, 6.5 Hz)
5"							6.64, dd (6.5, 5.7 Hz)
6"							8.14, d (5.7 Hz)
Me							
<i>N</i> (3)H	12.95, br s	12.55, br s 9.23 br s	12.69, br s	12.55, br s	12.57, br s	12.71, br s	12.59, br s

s: singlet, d: doublet, dd: doublet of doublet, t: triplet, m: multiplet

(*JJ* values)

¹H-NMR data of the synthesized compounds were consistent with the analogous TSCs. It was reported that compounds having the arylidene-hydrazide structure may

exist as *E/Z* geometrical isomers about the $-N=CH$ double bond and *cis/trans* amide conformers at the $SC-NH$ single bond.²³⁰ (Fig. 5.2). Compounds containing an imine bond were present in higher percentages in $DMSO-d_6$ solution in the form of *Z* isomer about the $-C=N$ bond. The *E* isomer can be stabilized in less polar solvents by an intramolecular hydrogen bond. In case where $N(4)$ bears no H-atoms, the molecule converts to the *Z'* tautomeric form.²³¹

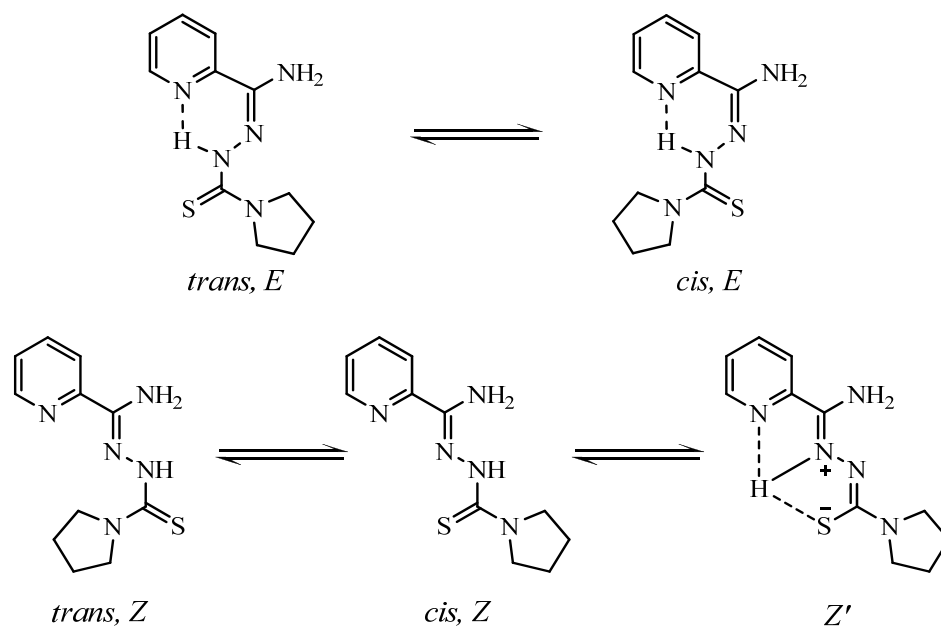


Figure 5.2: *E, Z* and *Z'* geometrical isomers and *cis, trans* conformers of compound **1**

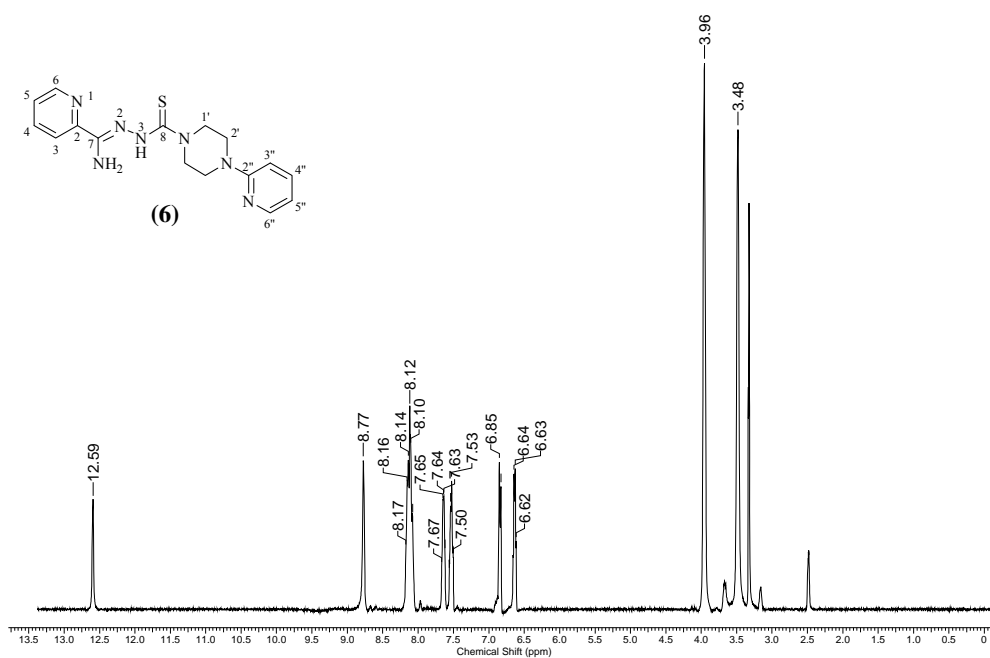


Figure 5.3: 1H -NMR spectrum (400 MHz, $DMSO-d_6$) of compound **6**

There were two pyridyl rings, in the compound **6**, one as the parent ring and another as a part of 2-pyridyl piperazinyl moiety substituted at *N*(4) position. The signals for parent pyridyl protons appeared downfield compared to those of 2-pyridyl piperazinyl group.²³² The structure of the compounds was further supported by ¹H-COSY spectrum of compound **6**. (Fig. 5.4)

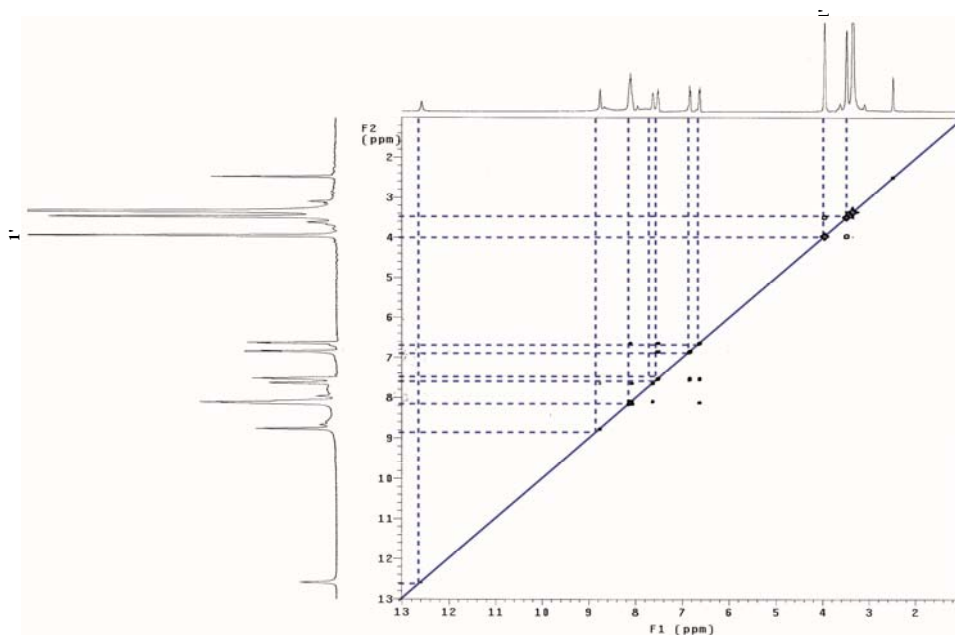


Figure 5.4: ¹H-COSY Spectrum (400 MHz, DMSO-*d*₆) of compound **6**

The ¹H-NMR spectra of the compound **1** in CDCl₃ revealed single signal for each proton suggesting the existence of only *E* isomer with the intramolecular hydrogen bonding of *N*(3)H with the pyridine ring. But in DMSO-*d*₆ solution, compound **1** shows existence of a mixture of *Z*-isomer, hydrogen bonded *E*-isomer and the bifurcated tautomer *Z'* as revealed by a pair of signals for each proton of the pyridine ring. The two hydrogen bonded isomers (*E* and *Z'*) together contribute the major percentage.²³³

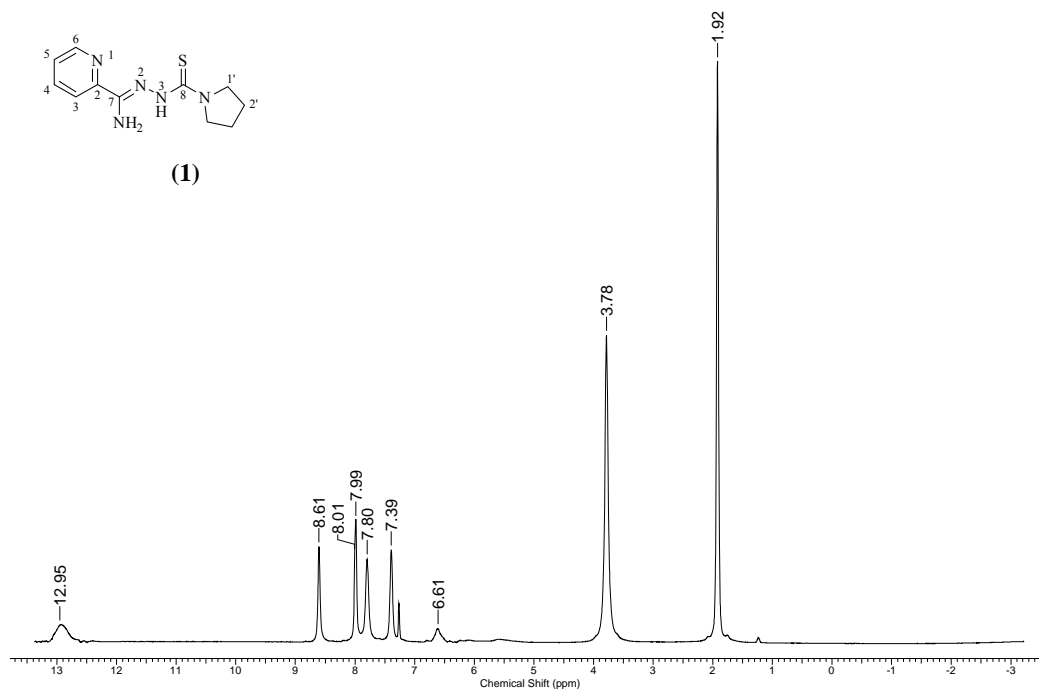


Figure 5.5: $^1\text{H-NMR}$ spectrum (400 MHz, CDCl_3) of compound **1**

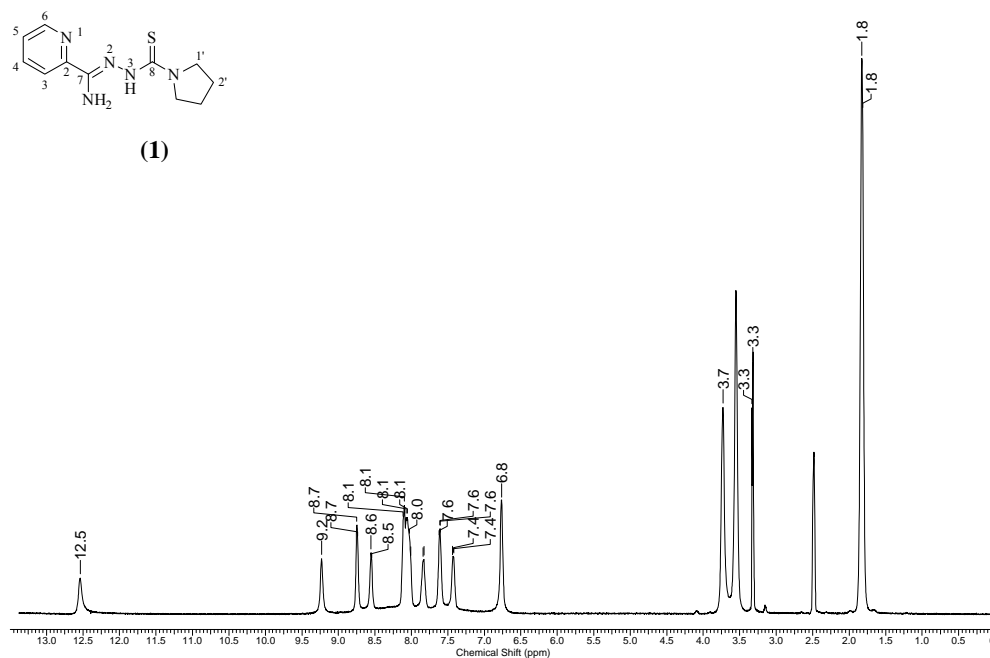


Figure 5.6: $^1\text{H-NMR}$ spectrum (400 MHz, $\text{DMSO-}d_6$) of compound **1**

The $^1\text{H-NMR}$ results were supported by those of the $^{13}\text{C-NMR}$ spectra. The $^{13}\text{C-NMR}$ spectral data of the compounds **1-6** are listed in Table 5.5.

Table 5.5: ^{13}C -NMR Spectral Assignments (ppm) of Compounds **1** – **6** (100 MHz, DMSO-*d*₆)

Compound	1	2	3	4	5	6
2	144.6	144.1	145.2	145.8	144.6	146.0
3	121.4	121.5	121.7	122.4	121.3	122.6
4	138.7	138.7	138.7	139.5	138.6	139.7
5	126.8	126.8	127.1	127.8	126.7	128.0
6	150.3	150.2	150.3	151.1	150.3	151.3
7	143.8	143.4	144.4	145.2	143.6	145.4
8	176.5	178.7	179.1	178.9	178.3	179.9
1'	48.6	47.4	47.2	49.9	48.6	47.0
2'	25.2	26.2	66.7	27.4	28.4	46.0
3'		25.3			27.1	
2''						160.5
3''						108.6
4''						138.9
5''						114.4
6''						149.0

The ^{13}C -NMR of the synthesized compounds were similar to the analogous compounds.²³² The number of signals in the ^{13}C -NMR spectra corresponds to the number of magnetically non-equivalent carbon atoms in the synthesized compounds. The aromatic carbons were observed between 121.3 to 151.3 ppm. The high frequency signal near 180 ppm was due to thioamide carbon. In the ^{13}C -NMR spectra, the carbon resonance signals of the C=N group appeared at δ 143.4 to 145.4 ppm. The C=S signals observed at δ 176.5 to 179.9 are characteristic for this group.

The ^{13}C -NMR spectra of the compounds showed that the nature of the *N*(4)-substituent had a small effect on the positions of the ring carbons. The formamide carbon, *C*(7), was little affected by substitution at the *N*(4) position. Of note is that there was a single peak for C=S in the spectra of the compounds suggesting that the thione form was present in solution.

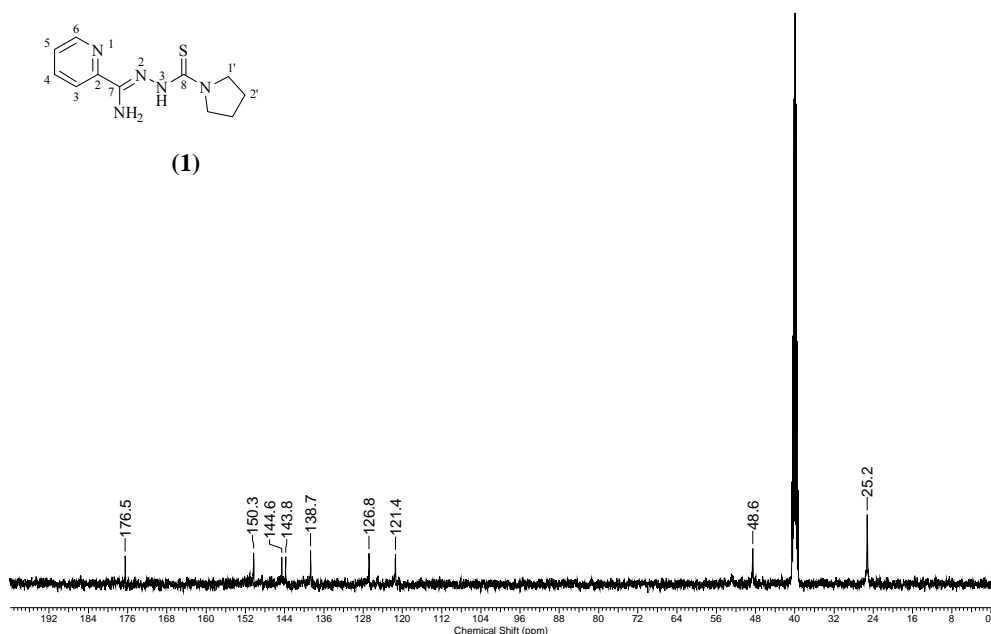


Figure 5.7: ^{13}C -NMR Spectrum (100 MHz, DMSO- d_6) of compound **1**

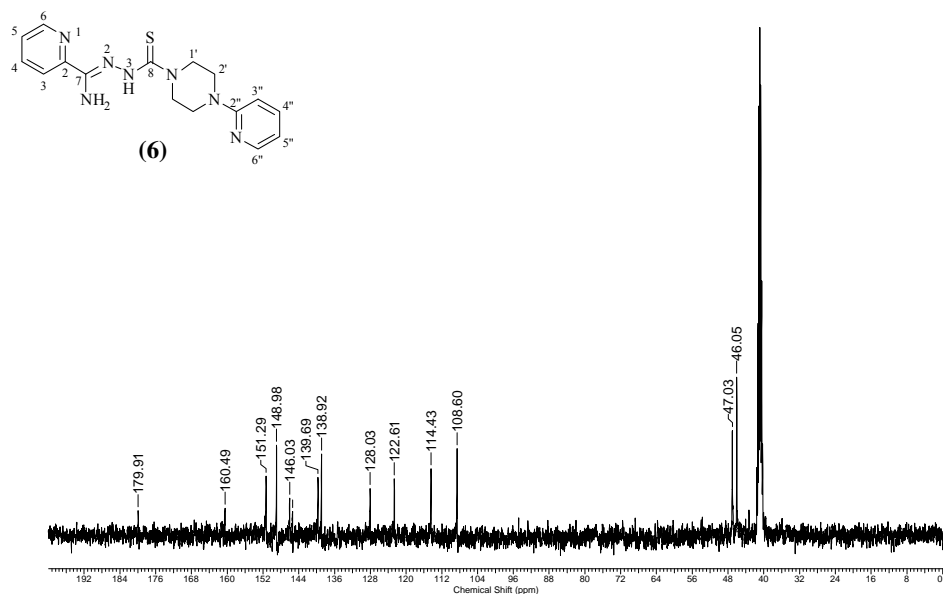


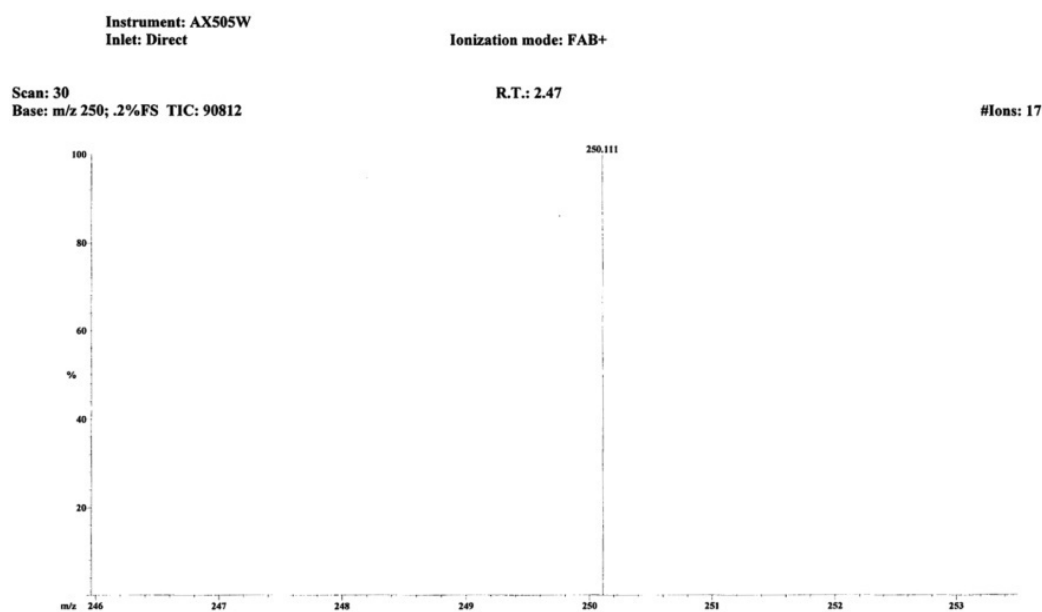
Figure 5.8: ^{13}C -NMR Spectrum (100 MHz, DMSO- d_6) of compound **6**

5.1.2.3 Mass spectrometry

The mass spectral data of the synthesized compounds are summarized in Table 5.7. The high resolution FAB mass spectrometry (HRFABMS) confirmed the protonated molecular ion, $[\text{M}+\text{H}]^+$ peaks of the synthesized compounds.

Table 5.6 Mass Spectrometric Data of Compounds 1-6

Compound No.	m/z $[M + H]^+$	
	Found	Calculated
1	250.11096	250.11264
2	264.13186	264.12829
3	266.10846	266.10756
4	282.08509	282.08472
5	278.14220	278.14394
6	342.15103	342.15008

**Figure 5.9:** HRFABMS of compound 1

5.1.3 Biological Activity of 2-Pyridineformamide *N*-(4) Ring Incorporated Thiosemicarbazones

5.1.3.1 Antineoplastic Activity against HeLa Cervical Cancer Cell Line

Cervical cancer is a major cause of cancer-related death in women worldwide. The cytotoxicity activities of compounds against HeLa cervical cell line were determined following standard WST (water soluble tetrazolium) colorimetric assays. WST-8 is a tetrazolium salt which can be converted to formazan by living cells. Metabolically active cells can oxidize NADH to NAD which in turn reduces WST-8 to formazan (Fig. 5.10).²³⁴ Increases in the production of formazan dye is therefore directly linked to the number of viable cells present in each well of the plate. WST-8 reagent is colourless and formazan is orange red so the absorbance can be measured to

determine how much formazan has been produced using an ELISA microplate reader at 450 nm.

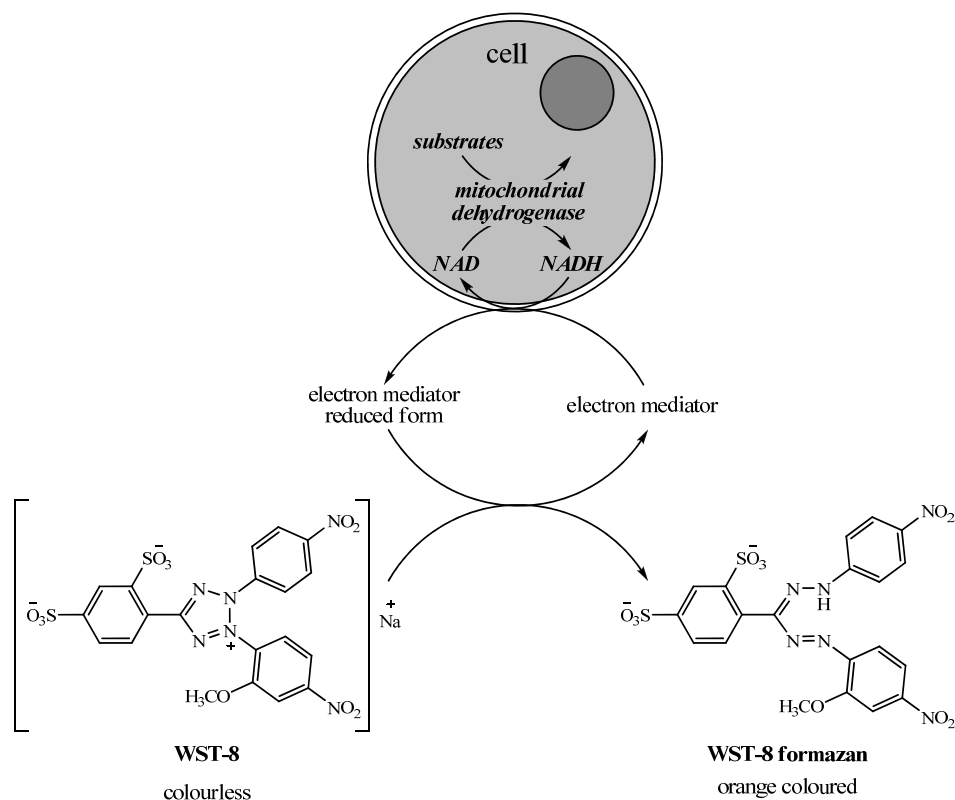


Figure 5.10: Principle of the cell viability detection with Cell Counting Kit-8 (CCK-8)

Despite there being an abundance of other available and widely used assays, the WST-8 assay has the advantage that the formazan compound produced is water soluble and therefore dissolves in the culture media. In contrast, other assays such as MTT²³⁵ involve additional steps in the assay where the crystals formed must be redissolved in DMSO for analysis. The WST-8 assay avoids these additional steps which reduces the time required for the assay and also avoids additional sources of error.

The *in vitro* cytotoxicities of the synthesized compounds were tested against HeLa (human cervical carcinoma cell line) cells using paclitaxel as a positive control. The concentration at which 50% of the cells were killed (IC_{50}) were also presented in fig. 5.11. Paclitaxel showed IC_{50} value of 0.0031 μ M.

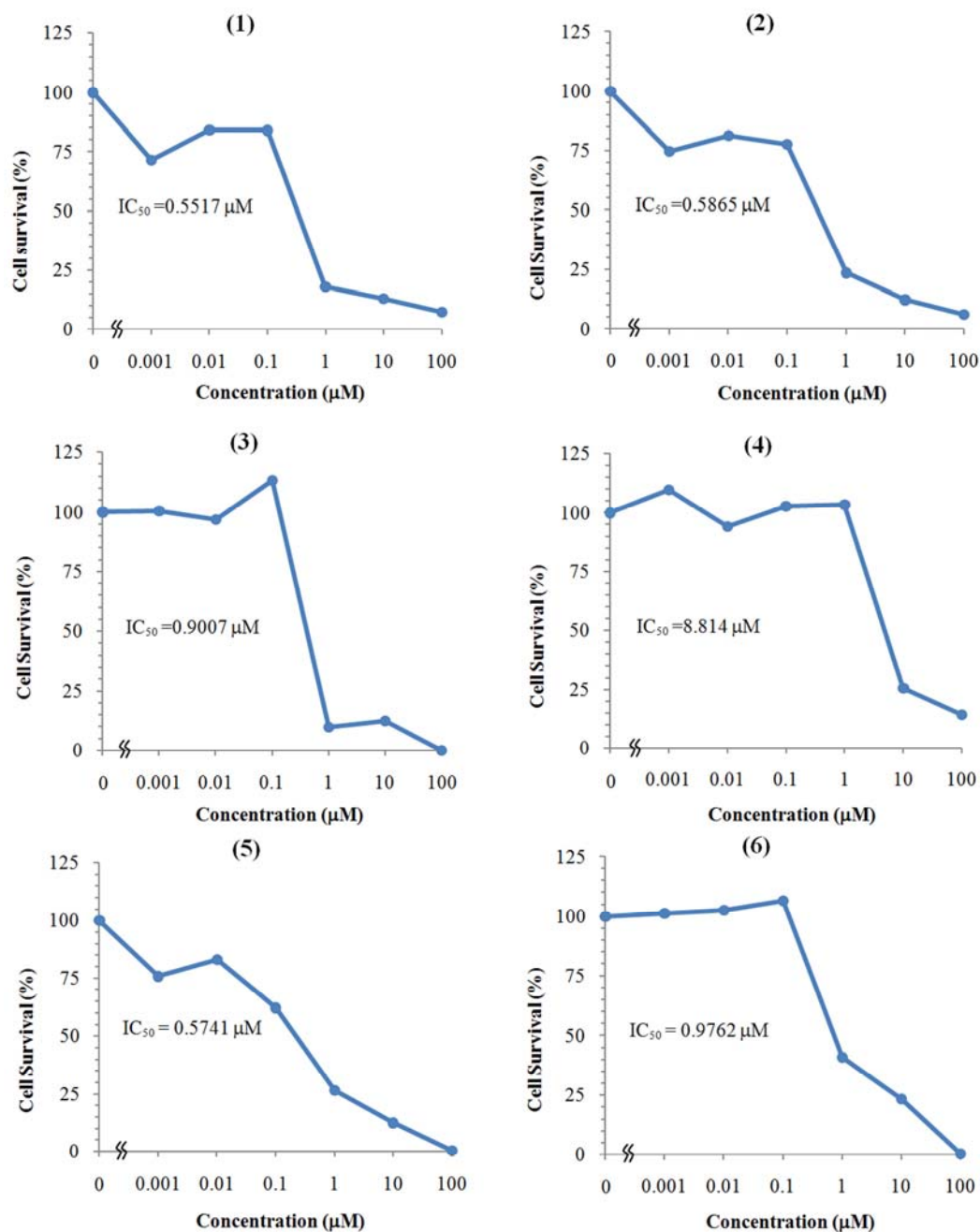


Figure 5.11: Antineoplastic activities of the compounds **1-6** against the HeLa cervical cancer cell line

All the thiosemicarbazones (**1-6**) were highly active against HeLa cervical cancer cell line (Table 5.7). Except for compound **4**, no significant different in cytotoxicities observed for the compounds. All the compounds exhibited potency less than the positive control paclitaxel (IC₅₀, 0.0031 µM).

Table 5.7: IC₅₀ Values of Compounds **1-6** against HeLa

Compound	IC ₅₀ , μ M
1	0.5517
2	0.5865
3	0.9007
4	8.814
5	0.5741
6	0.9762

5.1.3.2 Preferential Cytotoxic Activity against PANC-1 Human Pancreatic Cancer Cell Line in Nutrient-Deprived Medium (NDM)

Pancreatic cancer is one of the most deadly forms of cancer. It is associated with the lowest 5-year survival rate known for human cancers (<5%).²³⁶ Almost all patients with pancreatic cancer rapidly develop metastases and die within a short period after diagnosis.²³⁷ It is resistant to conventional chemotherapeutic agents, including paclitaxel, doxorubicin, cisplatin, and camptothecin, and there are currently no reliable chemotherapeutic agents available to treat this disease. Pancreatic cancers are hypovascular in nature, which causes an inadequate supply of nutrition and oxygen to aggressively proliferating tumor cells.²³⁸ However, these tumor cells show an extraordinary tolerance to nutrient starvation for a prolonged period of time, enabling them to survive in the hypovascular (austere) tumor microenvironment.¹⁹⁰ Development of drugs that specifically target the resistance of tumor cells to nutrient starvation has been termed as the antiausterity therapeutic strategy.¹⁹¹

The antiausterity effect of compounds was determined following the procedures and NDM composition described by Esumi¹⁹² but cell viability was measured using WST (water soluble tetrazolium) colourimetric assays.

All of the synthesized compounds were tested for their cytotoxic activity against human pancreatic cell line, PANC-1, in nutrient-rich medium (Dulbecco's modified Eagle medium, DMEM) and nutrient-deprived medium (NDM), utilizing antiausterity strategy. (Fig 5.12) PANC-1 cell is highly resistant to nutrient starvation, and can survive in NDM even after 48 h of starvation.²³⁹ Compounds possessing cytotoxicity in NDM without toxicity in DMEM are considered to be preferentially cytotoxic agents (antiausterity agents). The concentration at which 50% of the cells were

preferentially killed in the nutrient deprived medium (PC_{50}) are also presented in Fig. 5.12.

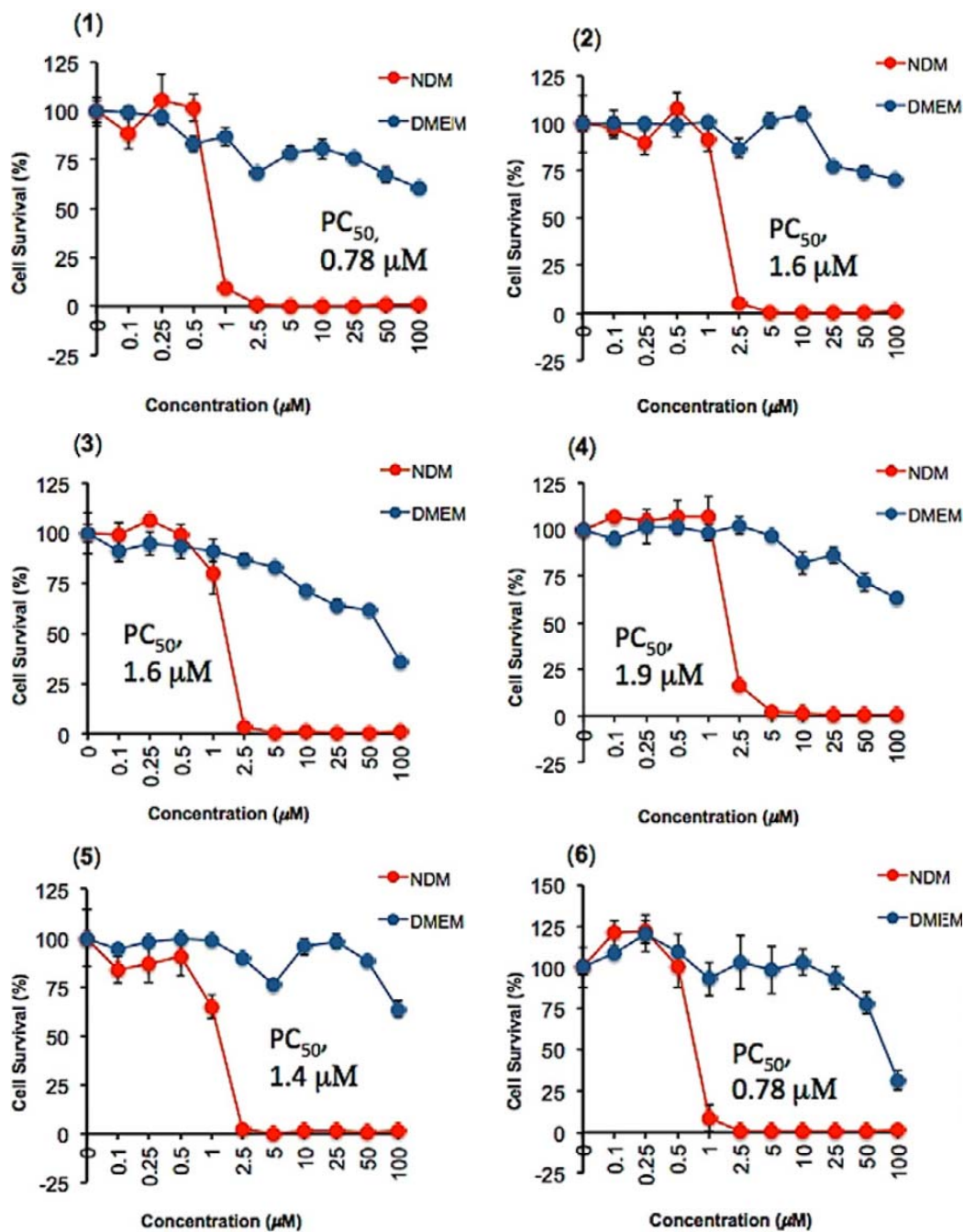


Figure 5.12: (a) Preferential cytotoxic activity of the compounds 1-6 against the PANC-1 human pancreatic cancer cell line in nutrient deprived medium (NDM) and Dulbecco's modified Eagle medium (DMEM).

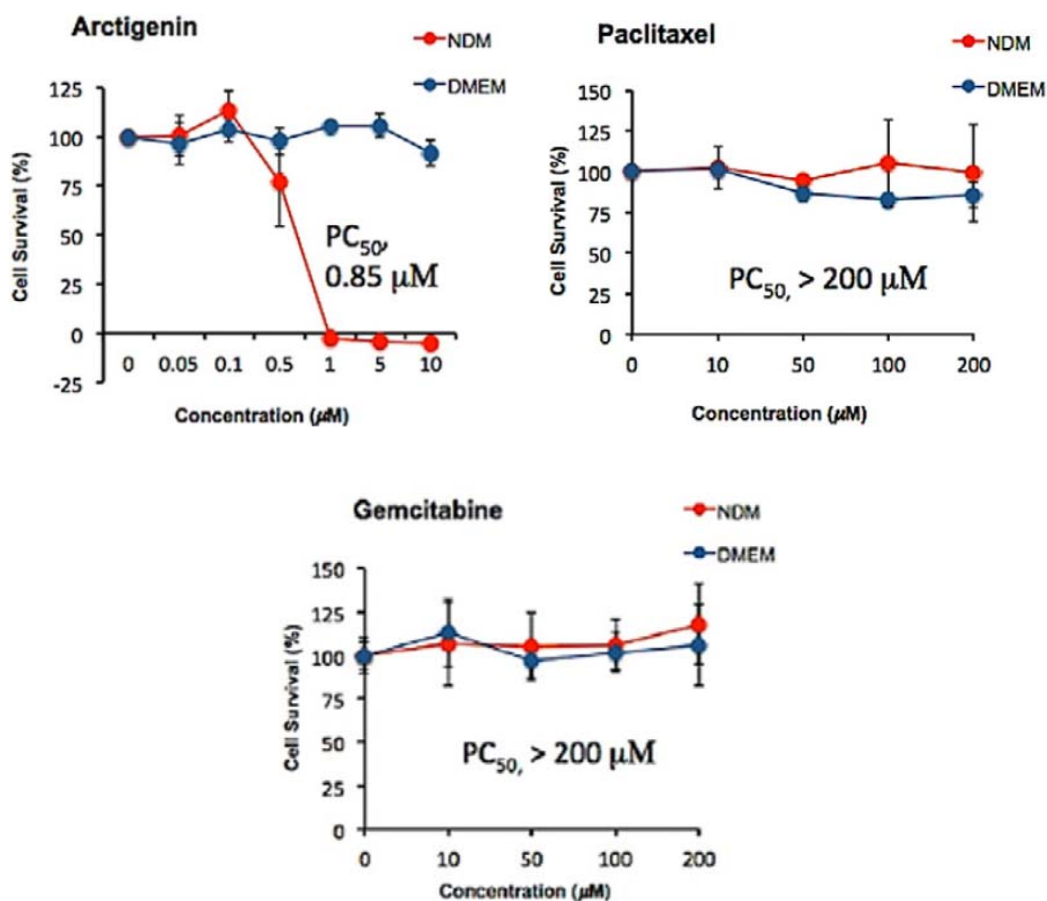


Figure 5.12: (b) Preferential cytotoxic activity of Arctigenin, Gemcitabine and Paclitaxel against the PANC-1 human pancreatic cancer cell line in nutrient deprived medium (NDM) and Dulbecco's modified Eagle medium (DMEM).

Arctigenin, (Fig. 5.13, a) an antiausterity strategy-based anticancer agent, was used as a positive control. It showed preferential cytotoxicity with a PC_{50} value of 0.85 μM . Of interest, the thiosemicarbazones (**1-6**) were highly active against PANC-1 human pancreatic cancer cell line (Table 5.8). Compounds **1** and **6** showed the most potent preferential cytotoxicity with a PC_{50} of 0.78 μM , more potent than the positive control arctigenin (PC_{50} , 0.85 μM). Paclitaxel, (Fig. 5.13, b) a well known anti cancer agent, was virtually inactive. Similarly, gemcitabine, (Fig. 5.13, c) a clinically used anticancer drug for the treatment of pancreatic cancer, was virtually inactive after 24 h in both NDM and DMEM at the maximum tested dose, with $\text{PC}_{50} > 200 \mu\text{M}$ (Fig. 5.12). This finding suggests that thiosemicarbazones are powerful lead candidates for antipancreatic cancer drug development and demand urgent further investigation.

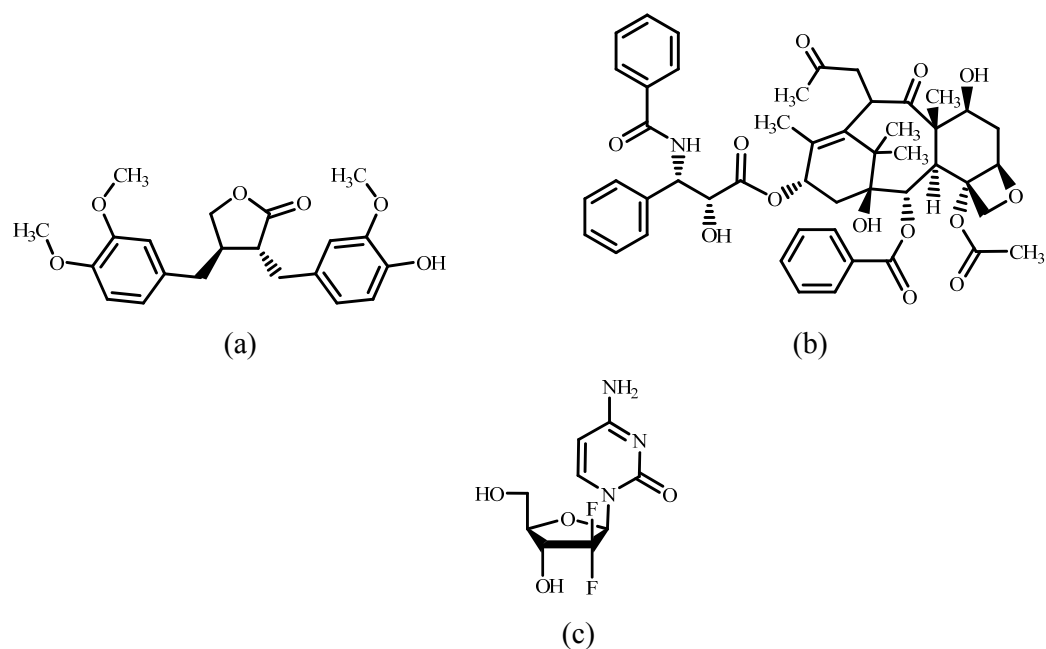


Figure 5.13: Structures of (a) Arctigenin, (b) Paclitaxel and (c) Gemcitabine

Table 5.8: Preferential Cytotoxicity Data of Compounds **1-6** against PANC-1

Compound	PC ₅₀ , μM
1	0.78
2	1.6
3	1.6
4	1.9
5	1.4
6	0.78

5.1.3.3 Morphological Assessment of Cancer Cells

Among the synthesized compounds, compound **6** was selected for further study.

5.1.3.3.1 Ethidium bromide (EB)/ Acridine orange (AO) staining assay

PANC-1 cells were treated with 1 μM of the compound **6** for 24 h in NDM, stained with ethidium bromide/acridine orange (EB/AO) reagent, and then visualized under fluorescent and phase contrast modes of the microscope. AO is a cell permeable dye that emits bright green fluorescence in viable cells. EB is impermeable and does not stain viable cells. In late apoptotic and necrotic cells, the integrity of the plasma and nuclear membranes decreases, allowing EB to pass through the membranes, intercalate into DNA and other nucleic acids, and emits red fluorescence. As shown in

Figure 5.14 a, control cells showed intact cell morphology with bright green AO fluorescence, suggesting the cells were viable. However, cells treated with 1 μM of the compound **6** showed exclusively red fluorescence due to EB, indicative of nonviable cells (Fig. 5.14, b). Phase contrast microscopic observation of the treated cells showed a dramatic alteration in the PANC-1 cell morphology (Fig. 5.14, c), including swelling, rupture of cell membranes, and disruption of cellular organelles.

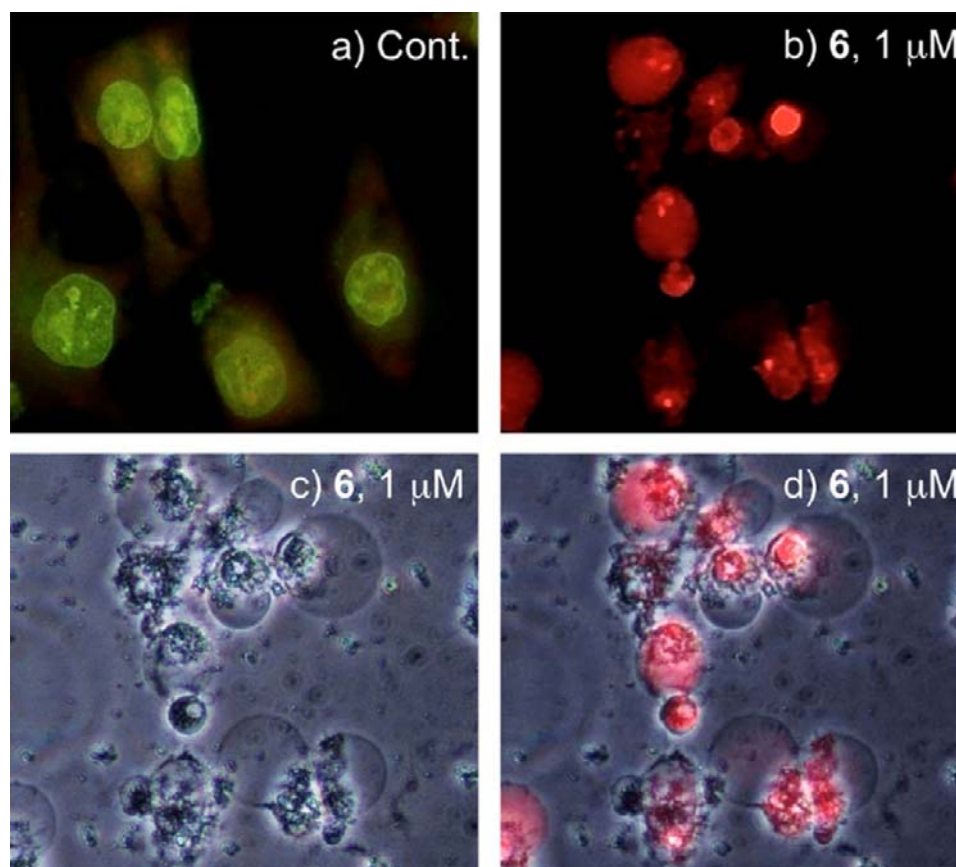


Figure 5.14: Fluorescent [ethidium bromide (EB)/acridine orange (AO)] and phase contrast images of PANC-1 cells at 24 h. (a) Control, live cells stained only with AO emitted bright green fluorescence, (b) treatment with compound **6** (1 μM) led to total death of PANC-1 cells within 24 h; cells stained with EB emitted red fluorescence, (c) phase contrast image of PANC-1 cells treated with compound **6** (1 μM) showing morphological alteration. (d) Merged image of phase contrast and red fluorescence image of PANC-1 cells treated with compound **6** (1 μM).

5.1.3.3.2 Western Blot Analysis

Further to check whether compound **6** modulated the key proteins involved in cell survival mechanisms western blot analysis was performed (Fig. 5.15). The western blot analysis is a widely accepted technique used to detect specific proteins in the given sample of tissue homogenate. It uses gel electrophoresis to separate native proteins by 3-D structure. The proteins were then transferred to a PVDF membrane where they were stained with antibodies specific to the target protein. The unbound antibody was washed off leaving only the bound antibody to the protein of interest. The bound antibodies were then detected by developing the film in a dark room. As the antibodies only bind to the protein of interest, only one band becomes visible. The thickness of the band corresponds to the amount of protein present.

A number of antiausterity agents have been found to inhibit protein kinase B (also known as Akt) activation, leading to preferential cell death under nutrient deprived conditions (NDM).¹⁹¹ However, in present study, compound **6** was not found to inhibit p-Akt (S437) or p-Akt (T308), suggesting that Akt signaling is unlikely to be a target of the compound **6**. However, compound **6** was found to activate apoptosis, resulting in the cleavage of caspase-3 even at a very short exposure time of 4 h in a concentration dependent manner (Fig. 5.15). Therefore, much stronger effect at lower concentration could be expected with increase in the exposure time period.

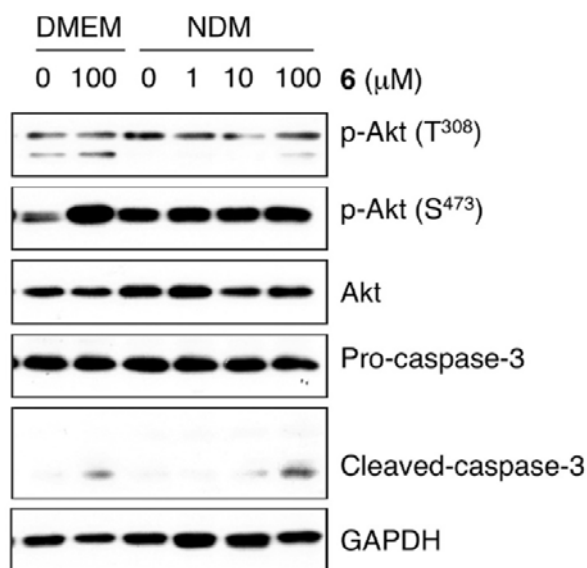


Figure 5.15: Western blot of the effect of compound **6** for 4 h against Akt, pAkt, pro-caspase 3, and cleaved-caspase 3.

5.1.3.3.3 Annexin V/Propidium Iodide Staining Assay

The evidence for apoptosis was further confirmed using an annexin V (AV) and propidium iodide (PI) staining assay. During apoptosis, alterations in the plasma membrane lead to the translocation of phosphatidylserine (PS), which was exposed at the external surface of the cell. AV specifically binds to the exposed PS, which was detected by green fluorescence (Fig. 5.16).

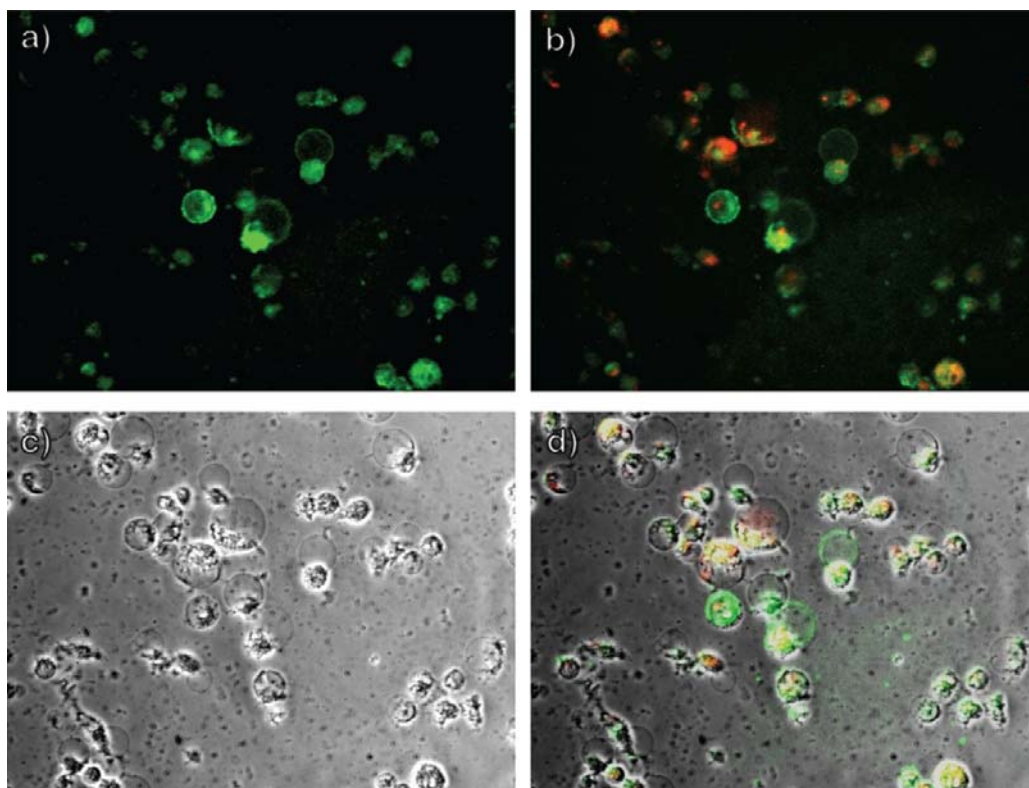


Figure 5.16: Fluorescent [Annexin v (AV)/propidium iodide (PI)] and phase contrast images of PANC-1 cells treated with 1 μM of compound **6** in NDM and incubated for 12 h. a) cells stained with AV emitted bright green fluorescence, b) cells stained with AV/PI emitted green fluorescence and red fluorescence, c) phase contrast image of PANC-1 cells treated with compound **6** (1 μM) showing morphological alteration, d) merged image of phase contrast and fluorescent image of PANC-1 cells treated with compound **6** (1 μM).

After 24 hours of *in vitro* culture, cells were analyzed for phosphatidylserine exposure. Slides for morphological analysis were prepared by cytocentrifugation and stained with May-Grunwald-Giemsa staining and the morphology was analyzed by light microscopy. To measure the phosphatidylserine exposure on the outer leaflet of the cell membrane, the cells were stained by the AV and cell necrosis was detected by PI method. Double staining with AV and PI gives the opportunity to distinguish early

apoptotic (AV+/PI-), late apoptotic/necrotic (AV+/PI+), and necrotic cell (AV-/PI+). The cells could therefore be divided into 4 populations according to AV and PI positivity and negativity and the proportion out of the entire cell population was calculated.

Pancreatic cancer cells are known to be resistant to apoptosis, which is one of the key reasons for the failure of chemotherapy, and lead to aggressive growth and metastasis. In the present study, apoptosis induced by compound **6** indicated that 2-pyridineformamide thiosemicarbazones are potential candidates for antipancreatic cancer drug development.

5.1.4 Conclusion

All the synthesized compounds (**1-6**) displayed cytotoxicity against both HeLa and PANC-1 cells. The potency of the tested compounds were found to vary only slightly with variation at *N*(4)-substitution. Compound **1** with *N*(4)-pyrrolidinyl substituent displayed the most potent cytotoxicity while compound **4** with *N*(4)-thiomorpholyl substituent displayed the least potent preferential cytotoxicity against both the cell lines. The cytotoxic activity against HeLa cells of the compounds with different *N*(4) substituents was found in the following order:

Pyrrolydinylyl > hexamethyleneiminyl > piperidyl > morpholyl > 2-pyridyl piperazinylyl
> thiomorpholyl.

The cytotoxic activity against PANC-1 cells of the compounds with different *N*(4) substituents was found in following order:

Pyrrolydinylyl = 2-pyridyl piperazinylyl > hexamethyleneiminyl > piperidyl = morpholyl
> thiomorpholyl.

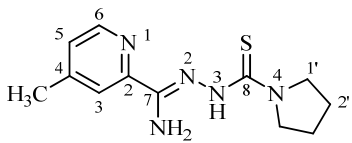
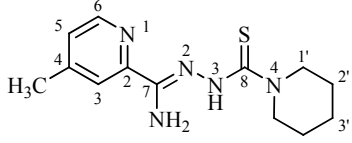
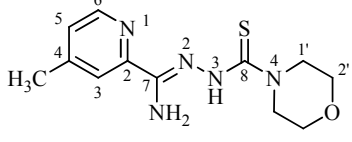
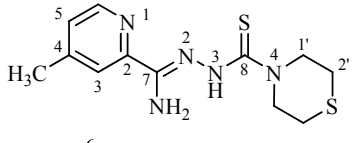
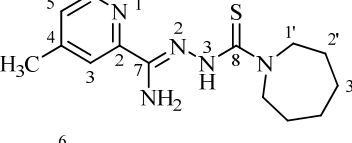
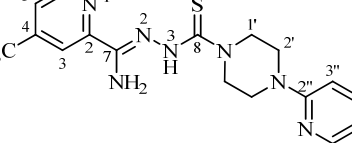
Microscopic observation of PANC-1 cells treated with compound **6** showed dramatic alteration in the PANC-1 cell morphology indicative of apoptic cell death. Therefore, 2-pyridineformamide thiosemicarbazones can be considered as potential candidates for antipancreatic cancer drug development. Inhibition of Akt signaling is unlikely to be a major antitumor mechanism of compound **6** in PANC-1 cells.

5.2 SYNTHESIS, CHARACTERIZATION AND BIOLOGICAL ACTIVITY OF 4-METHYL-2-PYRIDINEFORMAMIDE *N*(4)-RING INCORPORATED THIOSEMICARBAZONES.

5.2.1 General Discussion

A second series *N*(4) ring incorporated 2-pyridineformamide thiosemicarbazones with methyl group at 4 position of pyridine ring were prepared by reducing 2-cyano-4-methylpyridine with sodium in dry methanol followed by subsequent reaction with the corresponding thiosemicarbazide. Thiosemicarbazides were synthesized by the method described by Scovill.²⁷

Table 5.9: Physical Properties of Compounds 7-12

Compd	Molecular formula	Molecular mass	Colour	Yield (%)	M. P. (°C)	
7		C ₁₂ H ₁₇ N ₅ S	263.36	Yellow	24	164-166
8		C ₁₃ H ₁₉ N ₅ S	277.39	Yellow	29	161-162
9		C ₁₂ H ₁₇ ON ₅ S	279.36	Yellow	41	183-185
10		C ₁₂ H ₁₇ N ₅ S ₂	295.43	Yellow	32	166-168
11		C ₁₄ H ₂₁ N ₅ S	291.42	Yellow	45	160-162
12		C ₁₇ H ₂₁ N ₇ S	355.46	Yellow	63	175-177

The thiosemicarbazones were obtained in low to moderate yield (24 - 63%) having melting point in the range of 160 - 185 °C. The thiosemicarbazones were stable in air at room temperature, slightly soluble in CHCl₃, Me₂CO and more soluble in polar solvents such as EtOH, MeOH, DMF and DMSO, and slightly soluble in water. The synthesized compounds were characterized by elemental analysis, IR, ¹H and ¹³C-NMR and high resolution FAB mass spectrometry. All the synthesized compounds were found to have high cytotoxic effects against both HeLa and PANC-1 cell lines. The physical characteristic data of the compounds (**7-12**) are listed in Table 5.9. The elemental analyses results (Table 5.10) of the compounds were in close agreement with the calculated values.

Table 5.10: Elemental Analysis Data of Compounds **7-12** (Calculated Data)

Compound	C	H	N
7	55.14 (54.73)	6.18 (6.51)	26.79 (26.59)
8	56.62 (56.29)	6.53 (6.90)	25.51 (25.25)
9	51.96 (51.59)	5.83 (6.13)	25.34 (25.07)
10	49.06 (48.79)	5.47 (5.80)	24.04 (23.71)
11	58.09 (57.70)	7.07 (7.26)	24.20 (24.03)
12	57.72 (57.44)	5.63 (5.95)	27.52 (27.58)

5.2.2 Spectral Studies

5.2.2.1 IR Spectra

Selected IR bands of the compounds **7-12** are listed in Table 5.11. The IR spectral analysis supports the presence of characteristic groups in the synthesized compounds. A pair of bands for stretching vibrations (asymmetric and symmetric) due to NH₂ were observed in the region 3456 to 3416 cm⁻¹ and 3287 to 3244 cm⁻¹ respectively, while the stretching vibrations due to NH group were observed in the region 3222 to 3143 cm⁻¹.²²¹ These IR peaks in this region for ν(N-H) stretch were medium to strong in intensity which is inherent character of this functionally.

Pyridine ring vibrations that have been considered mainly were ring breathing vibrations and in-plane deformations. The pyridine ring breathing vibrations were observed as two pairs of bands in the region 1615 to 1411cm⁻¹.

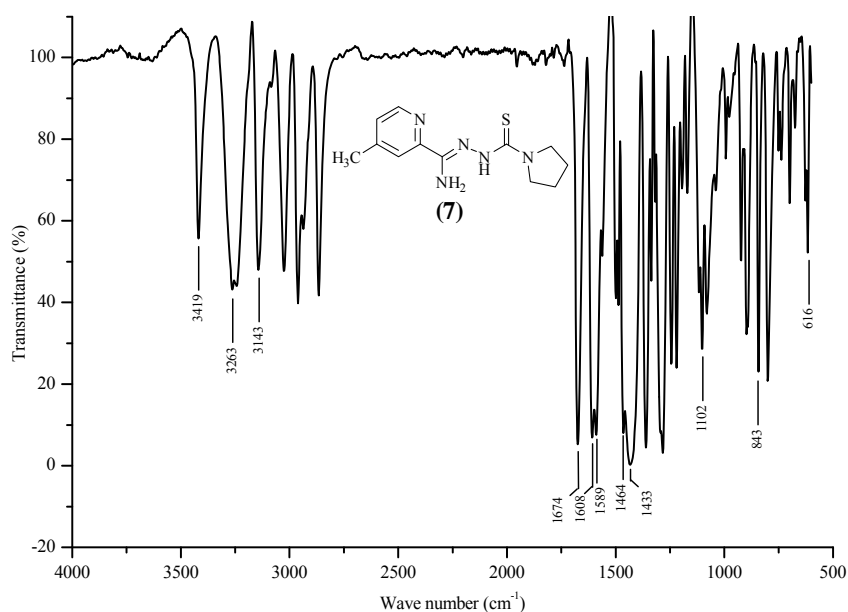
Table 5.11: Diagnostic Bands in the IR Spectra of Compounds 7-12

Group↓	Compound					
	7	8	9	10	11	12
$\nu(\text{NH}_2)$	3419(m), 3263(m)	3426(m), 3267(m)	3419(m), 3267(m)	3456(s), 3244(m)	3429(m), 3287(m)	3416(m), 3261(m)
$\nu(\text{NH})$	3143(m)	3152(s)	3240(m)	3222(m)	3152(m)	3231(m)
$\delta(\text{NH})$	1674(s)	1674(s)	1674(s)	1672(s)	1674(m)	1672(s)
$\nu(\text{C}=\text{C})$	1608(s), 1589(s), 1464(s), 1433(s)	1613(s), 1589(s), 1497(m), 1439(s)	1615(s), 1593(s), 1466(s), 1427(s)	1610(m), 1566(s), 1459(s), 1430(s)	1612(s), 1585(s), 1470(s), 1411(s)	1594(s), 1562(s), 1485(s), 1427(s)
$\nu(\text{C}=\text{N})$	1433(s)	1439(s)	1427(s)	1430(s)	1411(s)	1427(s)
$\nu(\text{N}-\text{N})$	1102(m)	1076(m)	1022(m)	953(m)	1076(m)	1019(m)
$\nu(\text{C}=\text{S})$	843(s)	856(m)	839(s)	831(m)	860(m)	873(m)
$\rho(\text{Py})$	616(m)	629(m)	627(m)	617(m)	629(m)	626(m)

s : strong, m : medium, w : weak

Of the four thioamide bands I, II, III and IV, the IV band, which has a substantive contribution due to thiocarbonyl stretching and bending vibration has been observed for all the compounds. The thioamide IV bands for the synthesized compounds were observed in the region 873 to 831 cm^{-1} .¹⁶⁵ The in-plane deformation vibrations were observed as medium intensity bands in the region 629 to 616 cm^{-1} .¹⁷¹

Lack of the band at approximately 2200 to 2500 cm^{-1} indicates the absence of thiol form (SH) suggesting that these compounds existed dominantly in their thione form (Fig. 1.8) in the solid state.²⁴⁰

**Figure 5.17:** IR spectrum of compound 7

5.2.2.2 NMR Spectra

The $^1\text{H-NMR}$ spectral data of the synthesized compounds are listed in Table 5.12

Table 5.12: $^1\text{H-NMR}$ Spectral Assignments (ppm) of Compounds **7 - 12** (400 MHz)

Compound	7	8	9	10	11	12	
Solvent→ proton↓	CDCl_3	$\text{DMSO-}d_6$	$\text{DMSO-}d_6$	$\text{DMSO-}d_6$	$\text{DMSO-}d_6$	$\text{DMSO-}d_6$	
3	7.77, br s	7.85, 7.99	7.97, br s	8.01 br. s.	8.01, br s	7.96, br s	8.05, br s
5	7.26, br s	7.27, 7.45	7.43, d (4.9 Hz)	7.47 d (4.9 Hz)	7.47, d (5.7 Hz)	7.42, d (5.1 Hz)	7.48, br s
6	8.47, br s	8.41, 8.59	8.57, d (4.9 Hz)	8.61 br d (4.9 Hz)	8.60, d (5.7 Hz)	8.57, d (5.1 Hz)	8.62, br s
1'	3.75, br s	3.55, 3.72	3.80, t (5.6 Hz)	3.55, br s	4.15, br s	3.78, t (6.1 Hz)	3.96, br s
2'	1.93, br s	1.83	1.41, br s	3.80, br s	2.51, br s	1.42, br s	3.49, br s
3'			1.55, br s			1.66, br s	
3"							6.85, br s
4"							7.54, br. s.
5"							6.64, br s
6"							8.12, br s
Me	2.45, br s		2.39, br s	2.41, br s	2.42, br s	2.39, br s	2.43, br s
N(3)H	12.94, br s	12.52, 9.12	12.63, br s	12.52, br s	12.54, br. s.	12.65, br s	12.57, br s

s: singlet, d: doublet, t: triplet (JJ values)

The $^1\text{H-NMR}$ of the compounds **7-12** showed typical patterns for a thiosemicarbazone molecules. The $^1\text{H-NMR}$ spectra for compound **9** was shown in Fig 5.18.

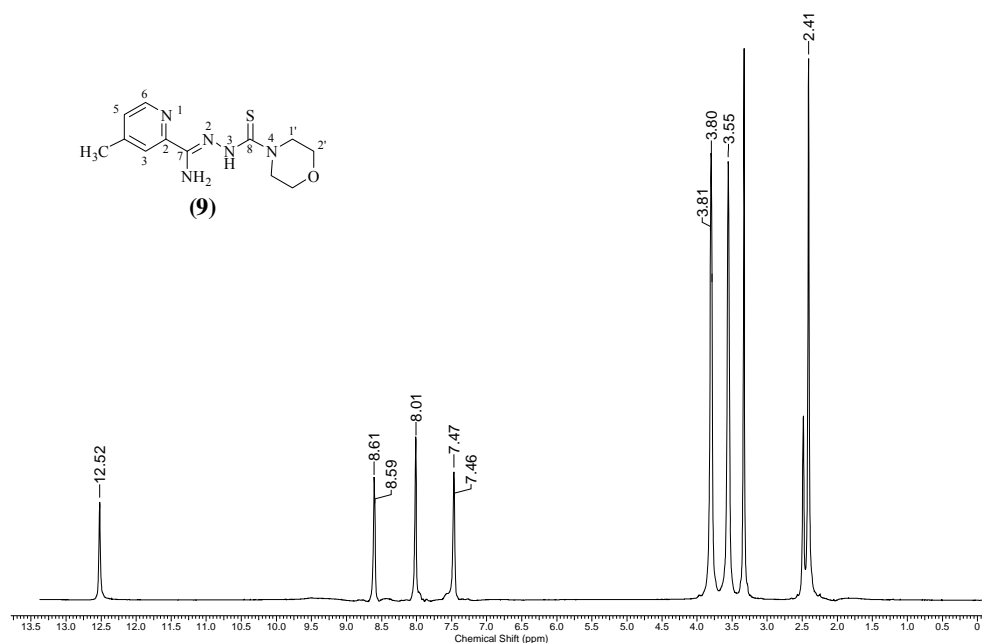


Figure 5.18: $^1\text{H-NMR}$ spectrum (400MHz, $\text{DMSO-}d_6$) of compound **9**

It revealed diagnostic $N(3)H$ proton signals as a broad singlets at $\delta = 12.52$ ppm. There was no signal at approximately at $\delta = 4$ ppm which was attributable to $-SH$ of thiol tautomer.²²⁷ The proton signals unequivocally demonstrated the predominant thione form of all the compounds in solution state. The peaks in the aliphatic region, 4.15 to 1.41, were assignable to the $H(1')$, $H(2')$ and $H(3')$ of the group incorporated at $N(4)$. In compound **9**, the incorporation of morpholyl group at $N(4)$ was indicated by the appearance of peaks in the aliphatic region $\delta = 3.80$ ppm and 3.55 ppm respectively for $H(2')$ and $H(1')$ respectively. The peak at $\delta = 2.45$ to 2.41 ppm was attributable to methyl proton. For the aromatic hydrogens, the broad doublet at 8.62 to 8.47 ppm was assigned to $H(6)$ which lie close to pyridyl nitrogen, broad singlet at 8.05 to 7.77 ppm was assigned to $H(3)$ and doublet at 7.48 to 7.26 ppm was assigned to $H(5)$.

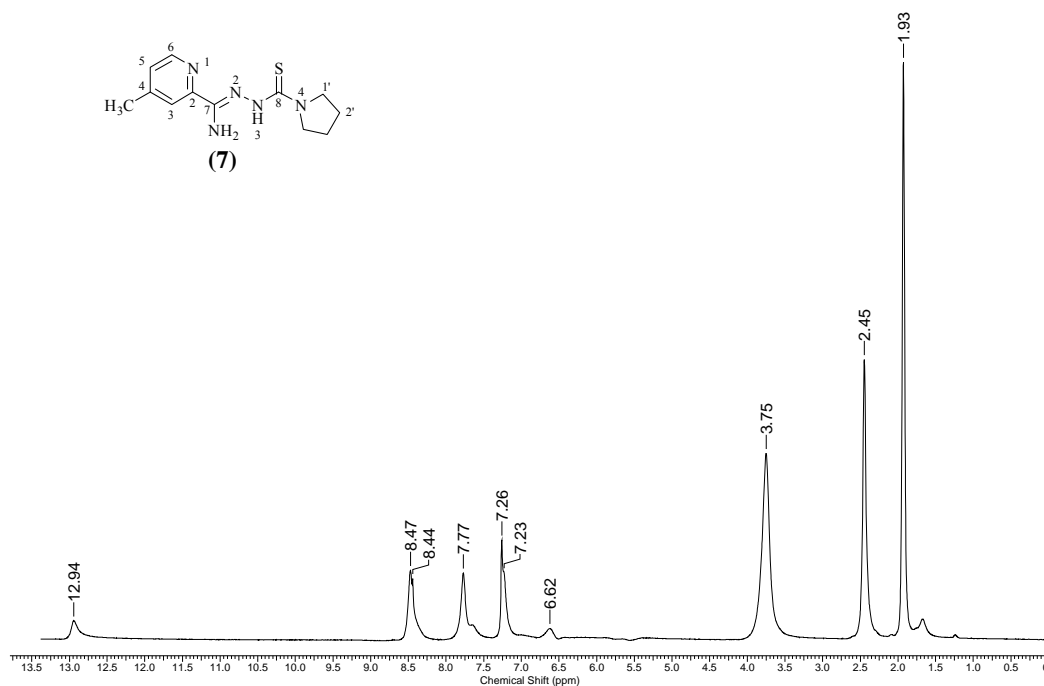


Figure 5.19: 1H -NMR spectrum (400MHz, $CDCl_3$) of compound **7**

In 1H -NMR spectra of the compound **7** in $CDCl_3$ (Fig. 5.19) only one signal was observed for each proton indicative of existence of only E isomer with the proton $N(3)H$ hydrogen bonded to pyridyl nitrogen. However, its 1H -NMR spectrum in $DMSO-d_6$ (Fig. 5.20) revealed a pair of signals for each proton indicating the existence of a mixture of E , Z and Z' -isomers in the solution.²³³ The $N(3)H$ chemical shift at $\delta = 9.12$ was indicative of Z configuration in which $N(3)H$ was hydrogen

bonded to the solvent and the chemical shift at $\delta = 12.52$ was indicative of *E* configuration with intramolecular H-bonding and bifurcated hydrogen bonded form (*Z'*) in which *N*(3)H was actually shifted to the azomethine nitrogen, *N*(2) creating formal charges on *N*(2) and the thiol sulphur.

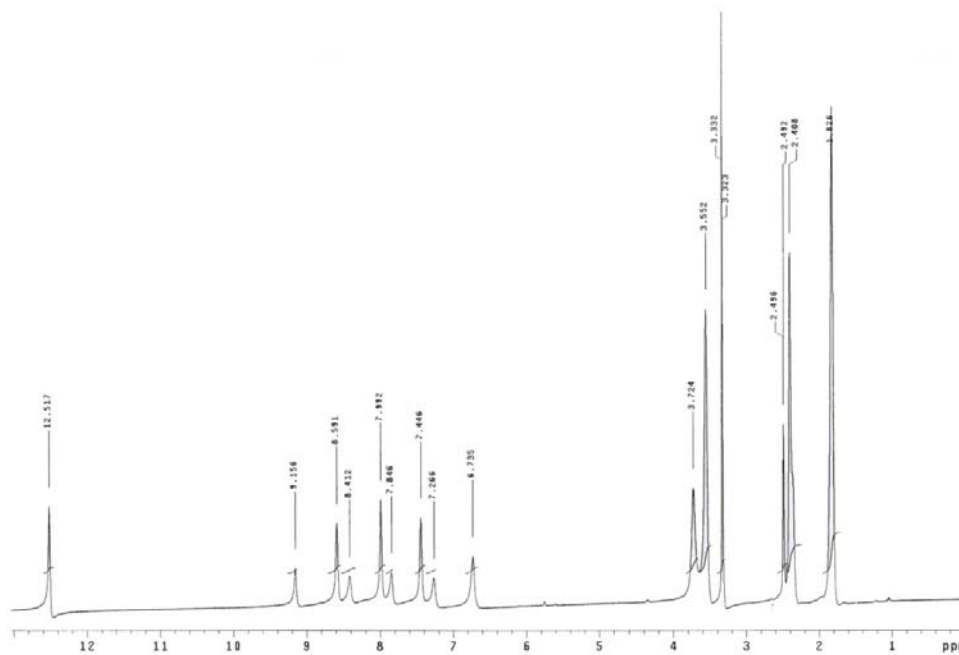


Figure 5.20: $^1\text{H-NMR}$ spectrum (400MHz, $\text{DMSO-}d_6$) of compound **7**

The $^{13}\text{C-NMR}$ spectral data of the synthesized compounds are listed in Table 5.13.

Table 5.13: $^{13}\text{C-NMR}$ Spectral Assignments (ppm) of Compounds **7 – 12** (100 MHz, $\text{DMSO-}d_6$)

Compound	7	8	9	10	11	12
2	150.1	150.1	150.0	150.0	150.2	151.5
3	118.7	122.6	122.5	122.5	123.0	122.6
4	143.9	145.1	145.4	145.2	145.1	145.3
5	126.5	127.6	127.6	127.6	127.9	127.6
6	138.7	144.4	144.3	144.3	144.8	144.3
7	148.8	149.8	149.8	149.7	149.9	150.1
8	178.6	179.6	179.1	178.1	179.2	178.9
1'	47.4	47.8	47.2	49.1	50.2	46.1
2'	26.1	26.3	66.7	26.6	28.3	45.1
3'		25.4			27.3	
2''						159.6
3''						107.7
4''						138.1
5''						113.5
6''						148.1
Me	24.6	21.4	21.2	21.2	21.4	21.2

The appearance of a peak at $\delta = 179.6$ to 178.1 ppm indicates the C=S carbon atom. Incorporation of substituent at $N(4)$ revealed with the appearance of signals in the aliphatic region 66.7 to 47.2 ppm for $C(1')$, $C(2')$ and $C(3')$. The peak at 145.3 to 143.9 ppm for aromatic carbon and 24.6 to 21.2 ppm for methyl carbon suggest the presence of methyl group at 4-position of pyridine ring. Other signals at 151.5 to 150.0 , 127.9 to 126.5 and 123.0 to 118.7 were attributed to aromatic carbons $C(2)$, $C(5)$ and $C(3)$ respectively.²³²

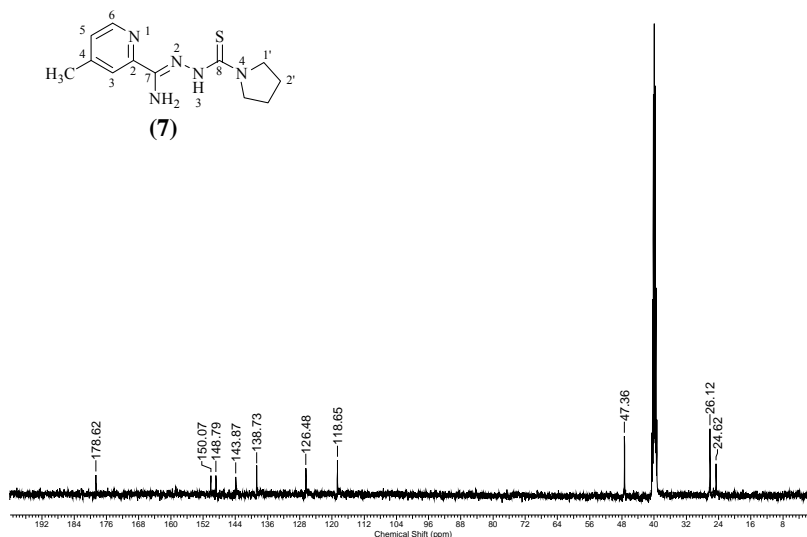


Figure 5.21: ^{13}C -NMR spectrum (100 MHz, $\text{DMSO-}d_6$) of compound 7

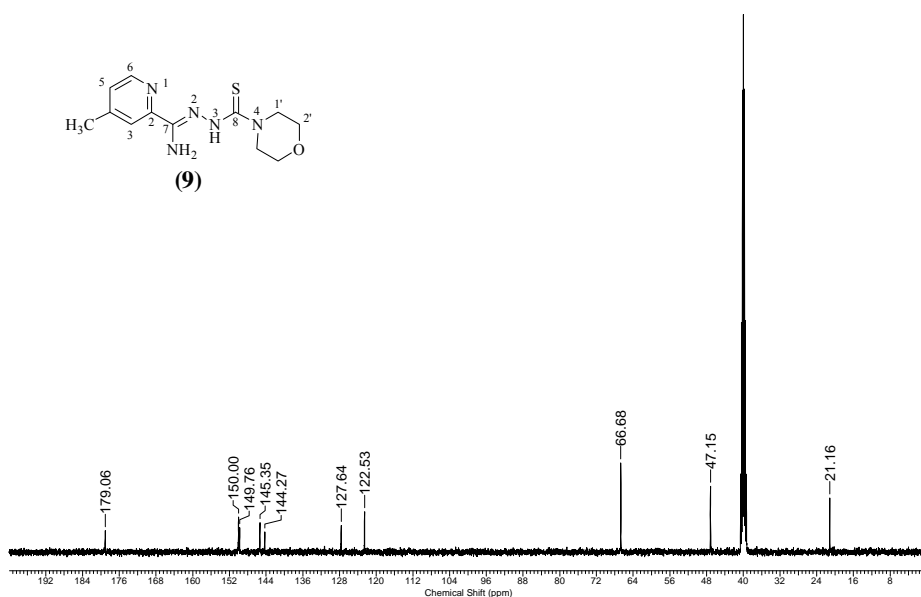


Figure 5.22: ^{13}C -NMR Spectrum (100 MHz, $\text{DMSO-}d_6$) of compound 9

5.2.2.3 Mass spectrometry

The mass spectral data of the synthesized compounds are summarized in Table 5.14. The high resolution FAB mass spectrometry (HRFABMS) provided further confirmation of The molecular structures with the presence of expected molecular ion $[M+H]^+$ peaks of the compounds.

Table 5.14: Mass Spectrometric Data of Compounds 7 – 12

Compound No.	$m/z [M + H]^+$	
	Found	Calculated
7	264.12711	264.12829
8	278.14331	278.14394
9	280.12400	280.12321
10	296.09644	296.10037
11	292.16063	292.15959
12	356.16527	356.16673

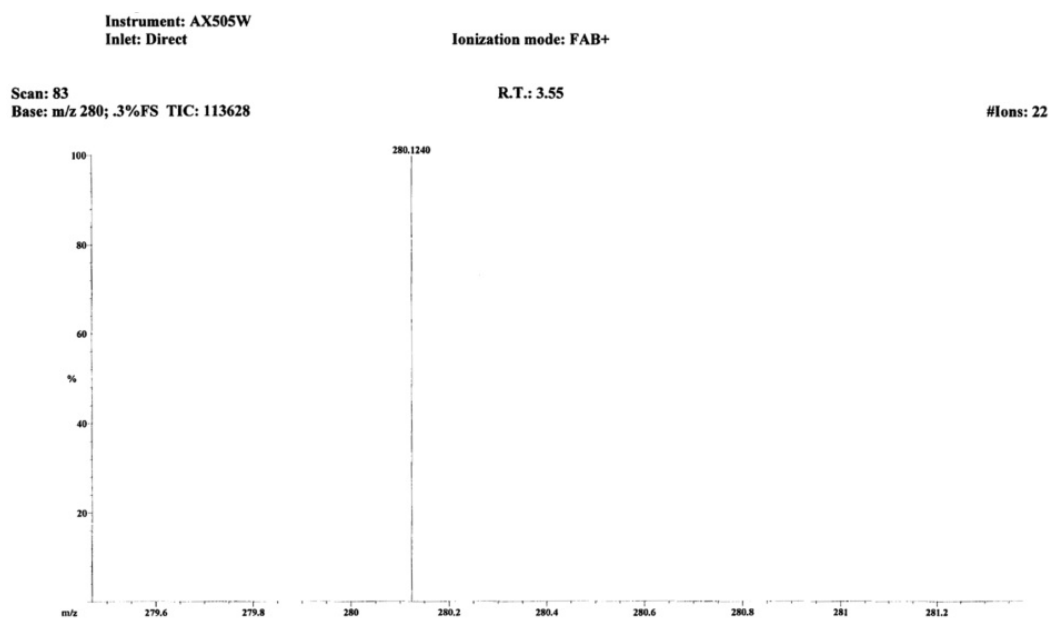


Figure 5.23: HRFABMS of compound 9

5.2.3 Biological Activity of 4-Methyl-2-Pyridineformamide *N*-(4) Ring Incorporated Thiosemicarbazones

5.2.3.1 Antineoplastic Activity against HeLa Cervical Cancer Cell Line

Cytotoxicity of all the synthesized compounds was evaluated against HeLa. The concentration at which 50% of the cells were killed (IC_{50}) are also presented in Fig. 5.24.

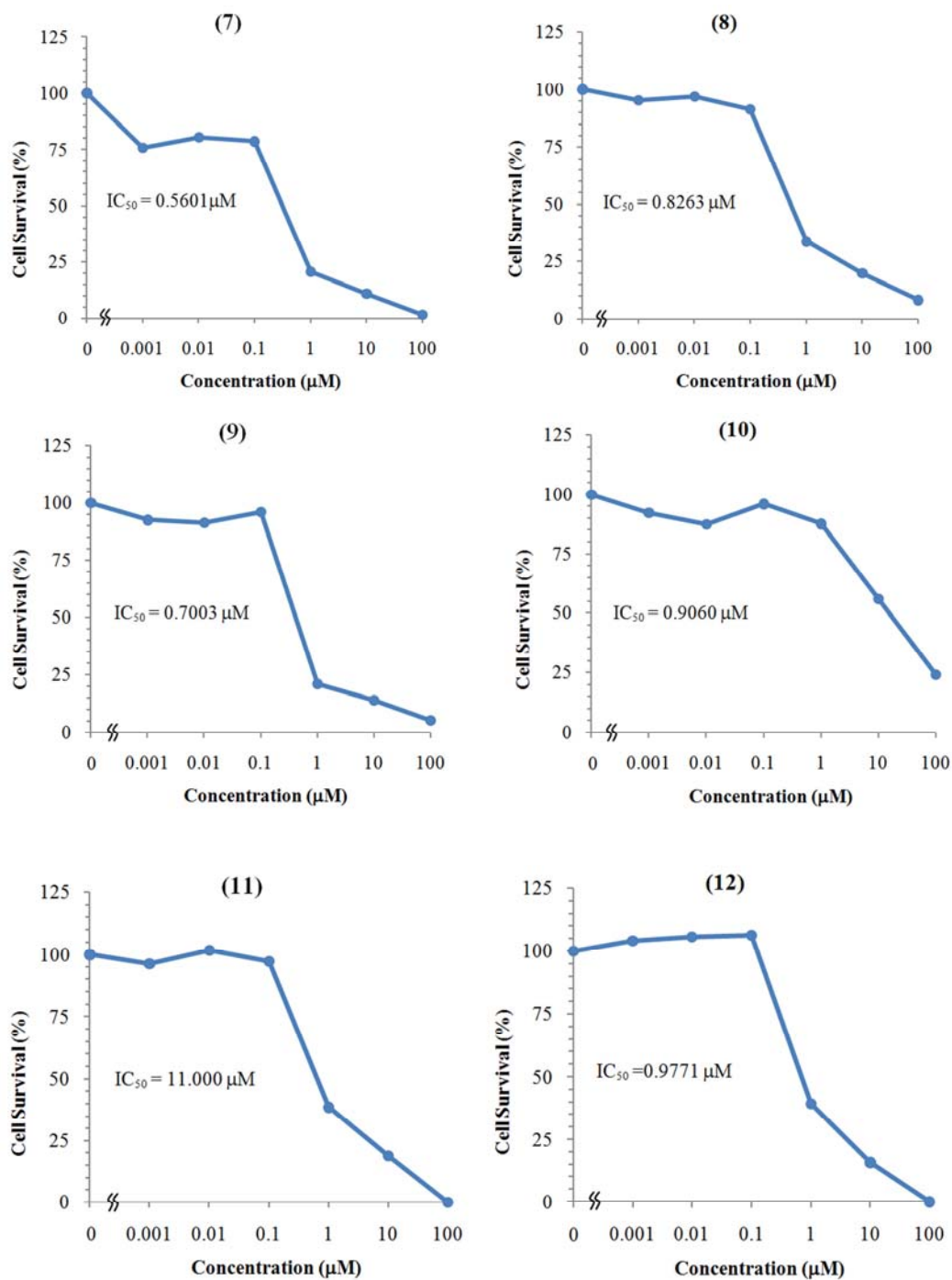


Figure 5.24: Antineoplastic activity of the compounds 7-12 against the HeLa cervical cancer cell line.

Table 5.15: IC₅₀ Values of Compounds **7-12** against HeLa

Compound	IC ₅₀ , μM
7	0.5601
8	0.8263
9	0.7003
10	0.9060
11	11.000
12	0.9771

Among this series compound **7** with *N*(4)-pyrrolidinyl substituent was the most potent showing a IC₅₀ value at 0.5601 μM. Activities of the other compounds were observed in the following order: **9** > **8** > **10** > **12** > **11**. Paclitaxel was used as a positive control in this study (PC₅₀ at 0.0031 μM).

5.2.3.2 Preferential Cytotoxic Activity against PANC-1 Human Pancreatic Cancer Cell Line in Nutrient-Deprived Medium (NDM)

Preferential cytotoxicity of all the synthesized compounds was evaluated against PANC-1 human pancreatic cancer cell line under both nutrient-rich and nutrient-deprived conditions, utilizing an antiausterity strategy (Fig. 5.25). The concentration at which 50% of the cells were preferentially killed in the nutrient deprived medium (PC₅₀) are also presented in Fig. 5.25. All the compounds exhibited very potent activity in a concentration dependent manner. (Table 5.16). Among this series compound **7** was the most potent showing a PC₅₀ value at 0.37 μM. Activities of the other compounds were observed in the following order: **12** > **11** > **8** = **9** > **10**. Arctigenin, an antiausterity strategy-based anticancer agent, was used as a positive control in this study (PC₅₀ at 0.85 μM) (Fig. 5.12, b).

Table 5.16: Preferential Cytotoxicity Data of Compounds **7-12** against PANC-1

Compound	PC ₅₀ , μM
7	0.37
8	1.8
9	1.8
10	1.9
11	1.7
12	0.68

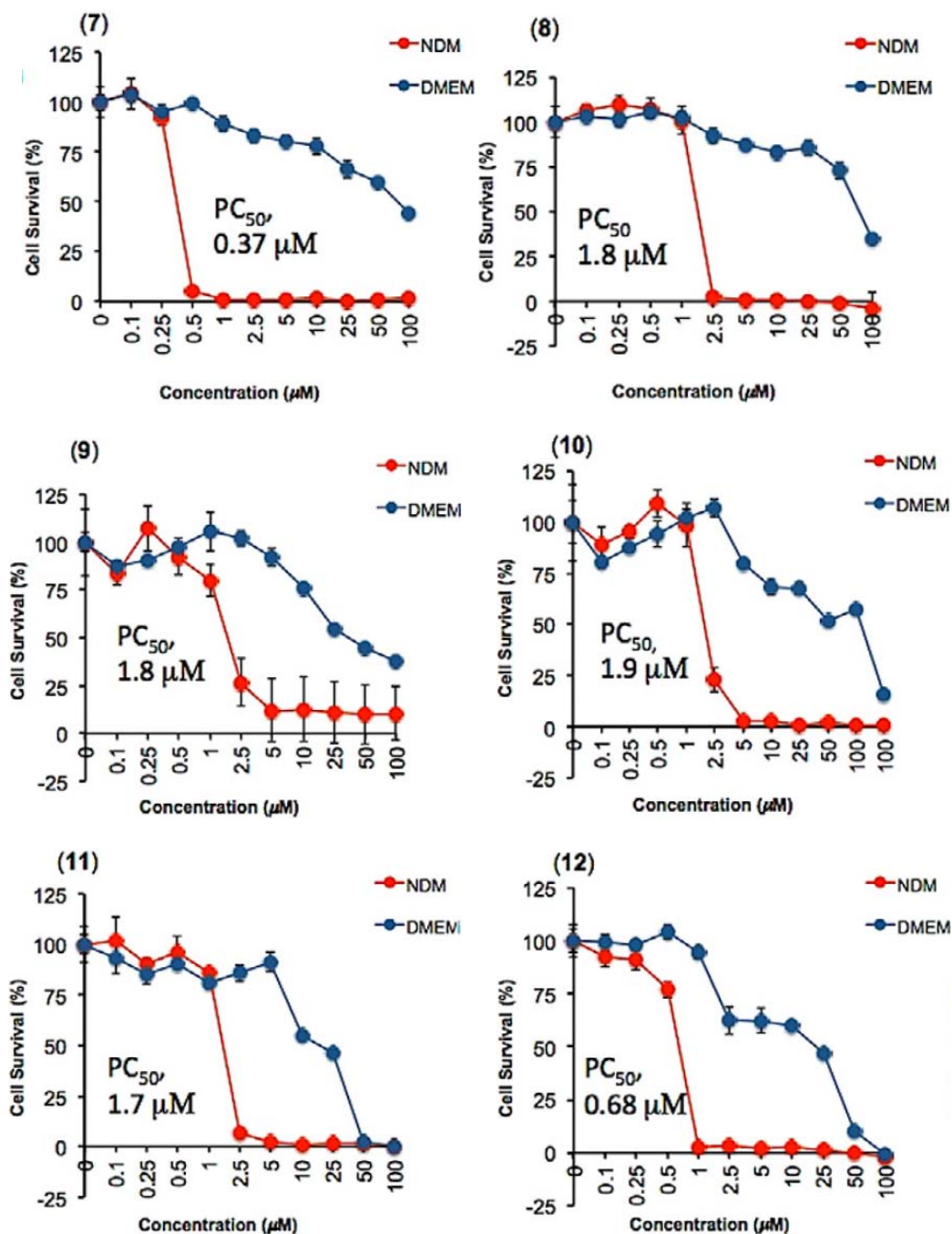


Figure 5.25: Preferential cytotoxic activity of the compounds 7-12 against the PANC-1 human pancreatic cancer cell line in nutrient deprived medium (NDM) and Dulbecco's modified Eagle medium (DMEM).

5.2.4 Conclusion

The potency of the tested compounds against both HeLa and PANC-1 cells were found to vary slightly with variation in *N*(4)-substitution. Compound 7 with *N*(4)-

pyrrolidinyl substituent displayed the most potent cytotoxicity while compound **11** with *N*(4)- hexamethyleneiminyl substituent displayed the least potent preferential cytotoxicity against both the cell lines.

The activity of the compounds against HeLa was found in the following order:

Pyrrolydinylyl > morpholyly > piperidyl > thiomorpholyly > 2-pyridyl piperazinyly > hexamethyleneiminyl.

The activity of the compounds was found in the following order:

Pyrrolydinylyl > 2-pyridyl piperazinyly > hexamethyleneiminyl > piperidyl = morpholyly > thiomorpholyly.

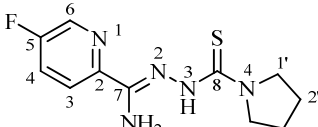
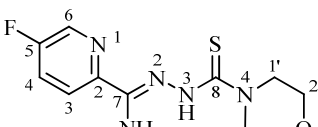
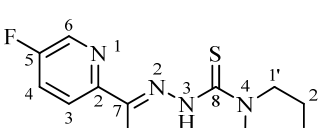
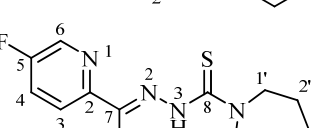
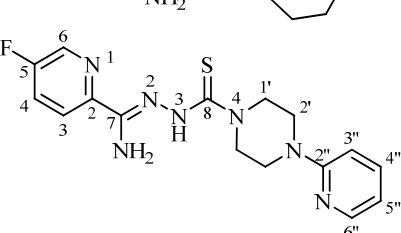
Compound **1** with pyrrolidinyl group and compound **12** with 2-pyridyl piperazinyl group at *N*(4) were found to be the more potent even than the positive control, arctigenin.

5.3 SYNTHESIS, CHARACTERIZATION AND BIOLOGICAL ACTIVITY OF 5-FLUORO-2-PYRIDINEFORMAMIDE *N*(4)-RING INCORPORATED THIOSEMICARBAZONES

5.3.1 General Discussions

A series of 5-fluoro-2-pyridineformamide thiosemicarbazones with variations in *N*(4) ring incorporation were prepared by reducing 2-cyano-5-fluoropyridine with sodium in dry methanol in the presence of desired thiosemicarbazide. The required thiosemicarbazides were synthesized by the method described by Scovill.²⁷

Table 5.17: Physical Properties of Compounds 13-17

Compd	Molecular formula	Molecular mass	Colour	Yield (%)	M. P. (°C)	
13		C ₁₁ H ₁₄ FN ₅ S	267.33	Yellow	45	161-163
14		C ₁₁ H ₁₄ FN ₅ O S	283.33	Yellow	50	181-183
15		C ₁₁ H ₁₄ FN ₅ S ₂	299.39	Yellow	52	156-158
16		C ₁₃ H ₁₈ FN ₅ S	295.38	Yellow	40	150-152
17		C ₁₆ H ₁₈ FN ₇ S	359.42	Yellow	61	193-195

The thiosemicarbazones were obtained in moderate yield (40 - 61%) having melting point in the range of 150–183 °C. The thiosemicarbazones were stable in air at room temperature, slightly soluble in CHCl₃, Me₂CO and more soluble in polar solvents such as EtOH, MeOH, DMF and DMSO, and slightly soluble in water. The

synthesized compounds were characterized by elemental analysis, IR, ^1H and ^{13}C -NMR spectroscopic techniques. The molecular structures of the compounds were further confirmed by mass spectrometry. All the synthesized compounds displayed potent cytotoxicity against HeLa human cervical cancer cells and PANC-1 human pancreatic cells in a concentration dependent manner. The physical characteristic data of the compounds are given in table 5.17.

The elemental analyses data were in accordance to the calculated values within the limits of experimental error.

Table 5.18: Elemental Analysis Data of Compounds **13-17** (Calculated Data)

Compound	C	H	N
13	49.87 (49.42)	4.90 (5.28)	26.56 (26.20)
14	46.83 (46.63)	4.85 (4.98)	24.53 (24.72)
15	44.36 (44.13)	4.44 (4.71)	23.15 (23.39)
16	52.53 (52.86)	5.91 (6.14)	24.05 (23.71)
17	53.69 (53.47)	4.71 (5.05)	27.01 (27.28)

5.3.2 Spectral Studies

5.3.2.1 IR Spectra

The characteristic bands of the synthesized compounds recorded are listed in Table 5.19.

Table 5.19: Diagnostic Bands in the IR Spectra of Compounds **13-17**

Group↓	Compound				
	13	14	15	16	17
$\nu(\text{NH}_2)$	3396(m), 3271(m)	3429(m), 3304(s)	3372(m), 3256(m)	3454(m), 3360(m)	3424(m), 3299(m)
$\nu(\text{NH})$	3223(m)	3159(m)	3163(m)	3227(m)	3157(m)
$\delta(\text{NH})$	1666(s)	1678(s)	1666(s)	1670(s)	1677(s)
$\nu(\text{C}=\text{C})$	1605(s), 1582(s)	1607(s), 1585(s)	1604(s), 1581(s)	1608(s), 1582(m)	1604(s), 1580(s)
$\nu(\text{C}=\text{N})$	1470(s), 1435(s)	1462(s), 1418(s)	1465(s), 1412(s)	1480(s), 1417(s)	1482(s), 1418(s)
$\nu(\text{N}-\text{N})$	1093(m)	1024(m)	1072(m)	1100(m)	1018(m)
$\nu(\text{C}=\text{S})$	843(m)	855(s)	825(m)	841(m)	841(m)
$\rho(\text{Py})$	626(m)	622(m)	632(m)	630(m)	625(m)

s : strong, m : medium, w : weak

The IR spectral analysis of the compounds **13-17** have differences in peak positions of respective functionality due to the presence of different substituent on the $N(4)$ position. These spectroscopic data agree with the structural properties of the compounds. Each compound presented three bands in the range of 4000 to 3000 cm^{-1} ,

a pair of which was due to the stretching frequencies of $\nu(\text{NH}_2)$, asymmetric and symmetric stretches, respectively, at 3454 to 3372 and 3227 to 3157 cm^{-1} , and one due to hydrazinic $\nu(\text{NH})$ at 3227 to 3157 cm^{-1} . A strong band was present at 1678 to 1666 cm^{-1} due to bending vibration of hydrazinic NH. The two pairs of strong bands at 1608 to 1585, 1582 to 1506, 1482 to 1462 and 1435 to 1412 cm^{-1} were assigned to the superimposed stretching frequencies of ring breath, $\nu(\text{C}=\text{C})$ and $\nu(\text{C}=\text{N})$. Medium intensity band was observed at 1100 to 1018 cm^{-1} for the hydrazinic (N-N) bond.²⁴¹ The thioamide IV band which has a large $\nu(\text{C}=\text{S})$ contribution appeared at 855 to 825 cm^{-1} .²²⁰ In-plane deformation vibrations characteristic of pyridyl ring $\rho(\text{py})$ was observed at 632 to 622 cm^{-1} .¹⁶⁸

The IR spectra of the compounds did not exhibit any $\nu(\text{SH})$ band in the region 2500 to 2200 cm^{-1} indicating that the thiol tautomer (Fig. 1.8, b) was absent in the solid state but exhibited $\nu(\text{NH})$ band at 3227 to 3157 cm^{-1} indicating the existence of only the thione tautomer (Fig. 1.8, a).^{223,224}

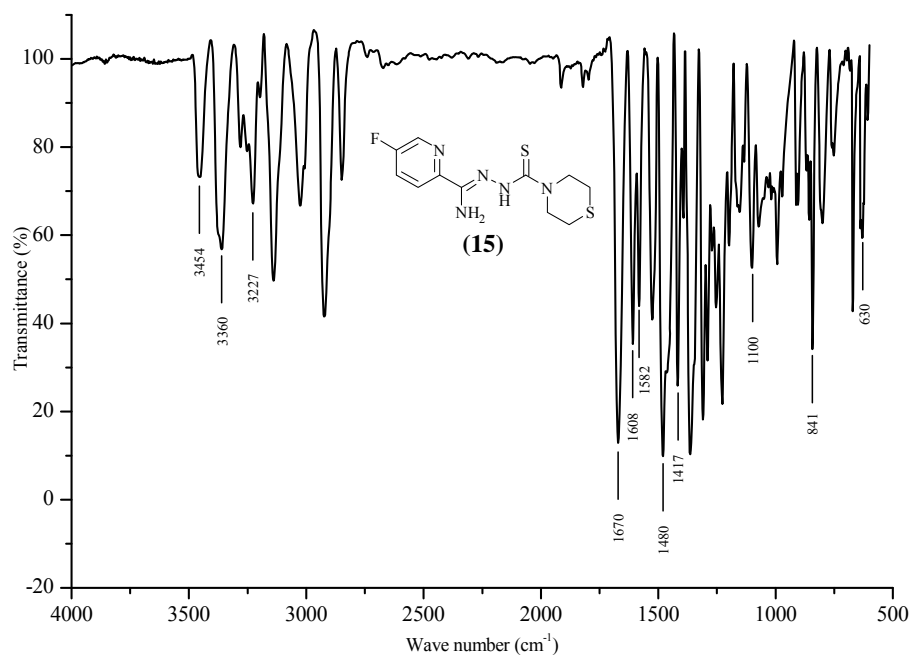


Figure 5.26: IR spectrum of compound 15

5.3.2.2 NMR Spectra

The ^1H -NMR spectral data of the synthesized compounds (**13-17**) are listed in Table 5.20.

Table 5.20: ^1H -NMR Spectral Assignments (ppm) of Compounds **13 – 17** (400 MHz)

Compound	13	13	14	15	16	17
Solvent→ proton↓	CDCl_3	$\text{DMSO-}d_6$	$\text{DMSO-}d_6$	$\text{DMSO-}d_6$	$\text{DMSO-}d_6$	$\text{DMSO-}d_6$
3	8.05, d (4.9 Hz)	8.06, d (5.4 Hz) 8.21 br s	8.23, d (9.7 Hz)	8.21, m	8.19, d (9.3 Hz)	8.24, br s
4	7.49, br s	7.78, br s 8.09, d (10.3 Hz)	8.06, d (9.7 Hz)	8.04, t (9.3 Hz)	8.05, d (9.3 Hz)	8.07, br s
6	8.43, br s	8.55, br s 8.80, br s	8.81, br s	8.79, br s	8.80, br. s.	8.82, br. s.
1'	3.81, br s	3.55, br s 3.72, br s	3.55, br s	4.14, br s	3.81, br s	3.96, br. s.
2'	1.93, br s	1.83, br s	3.80, br s	2.49, br s	1.45, br. s.	3.48, br. s.
3'					1.69, br s	
3"						6.85, d (8.3 Hz)
4"						7.53, m
5"						6.64, m
6"						8.12, br s
$N(3)\text{H}$	12.87, br. s.	12.48, 9.22 br. s.	12.48, br. s.	12.48, br s	12.65, br. s.	12.53, br. s.

s: singlet, d: doublet, t: triplet, m: multiplet (*JJ* values)

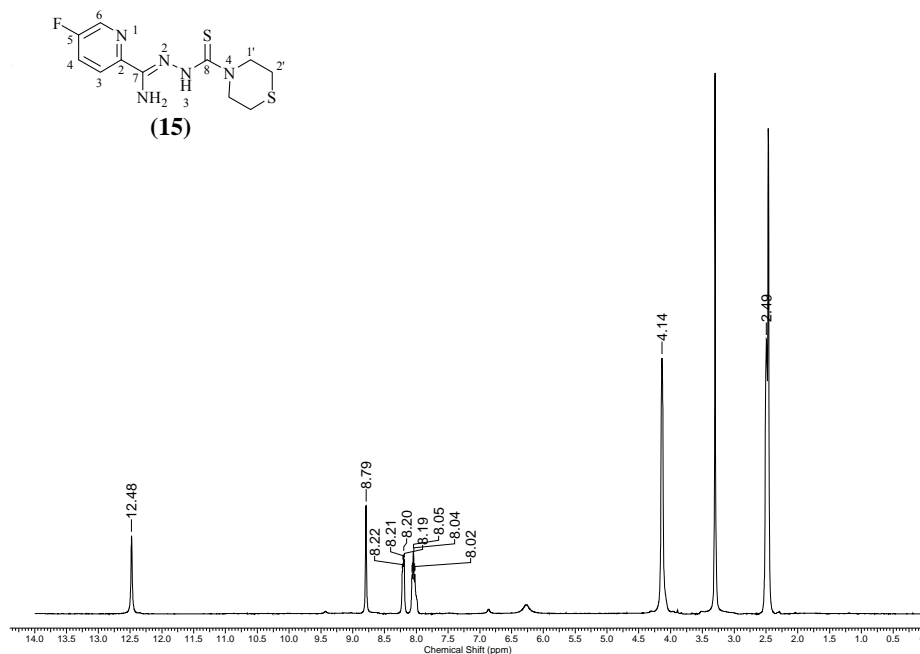


Figure 5.27: ^1H -NMR spectrum (400MHz, $\text{DMSO-}d_6$) of compound **15**

The $^1\text{H-NMR}$ spectra of the synthesized compounds were consistent with the analogous TSCs. The $^1\text{H-NMR}$ spectra of the compounds displayed broad singlets in the range δ 12.48 to 12.87 ppm corresponding to $N(3)\text{H}$ proton which was much deshielded due to hydrogen bonding to the pyridine nitrogen. This demonstrated the predominant thione form of all the compounds in solution state. In the compound **17** the peaks in the aromatic region between δ 7.49 to 8.82 ppm corresponded to the protons of the parent pyridine ring while those between δ 6.64 to 8.12 ppm corresponded to the protons of pyridine ring of pyridyl piperazinyl moiety at $N(4)$. The low frequency broad singlets at the regions between δ 1.45 to 4.14 ppm were observed for the methylene protons of the piperazinyl moiety at $N(4)$ position.

The presence of single signal for each proton in $^1\text{H-NMR}$ spectra of the compound **13** in CDCl_3 (Fig. 5.28) was indicative of existence of only *E* isomer with the proton $N(3)\text{H}$ hydrogen bonded to the pyridyl nitrogen.

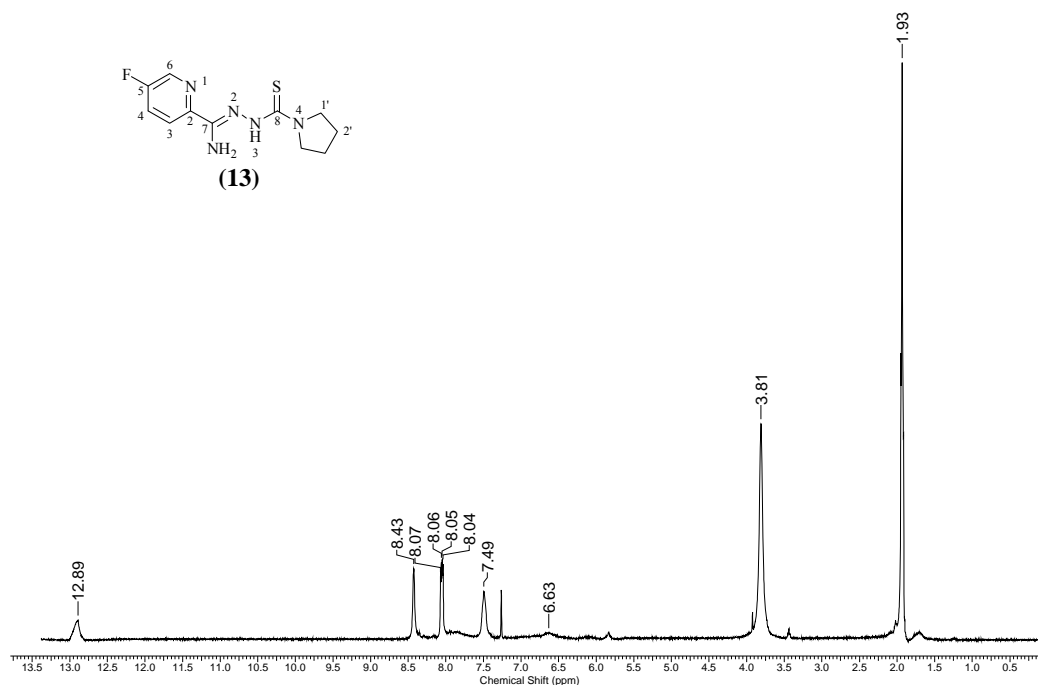


Figure 5.28: $^1\text{H-NMR}$ spectrum (400MHz, CDCl_3) of compound **13**

However, paired signals were observed for all the proton in the $^1\text{H-NMR}$ spectra of the compound **13** (Fig. 5.29) indicating the existence of a mixture of *E*-, *Z*- and *Z'*-isomers in the DMSO-solution.

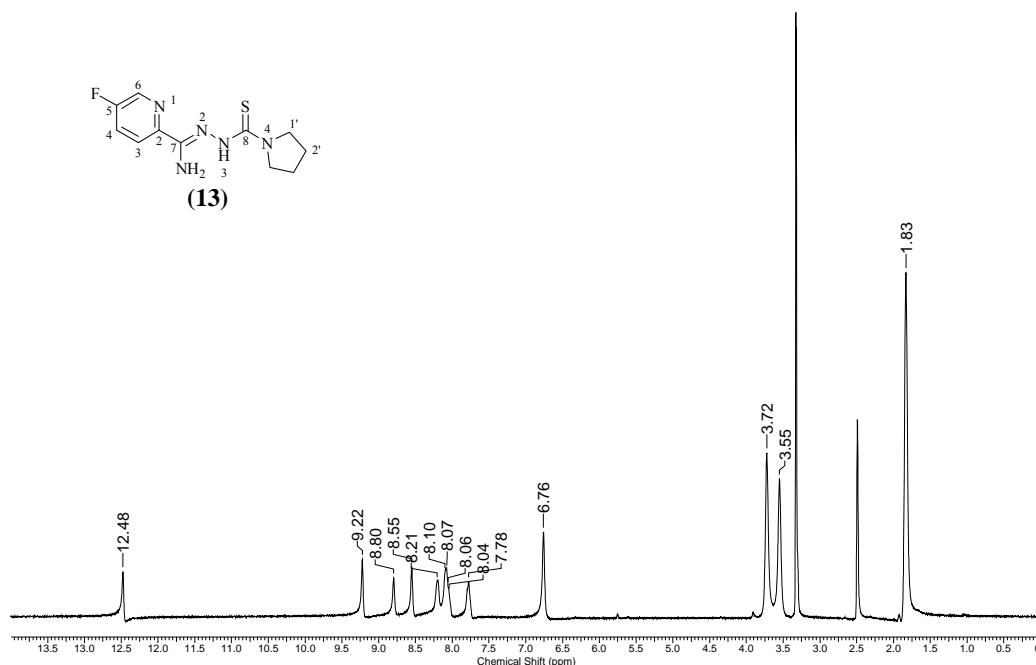


Figure 5.29: ^1H -NMR spectrum (400MHz, $\text{DMSO-}d_6$) of compound **13**

The ^{13}C -NMR spectral data for the synthesized compounds are listed in Table 5.21.

Table 5.21: ^{13}C Spectral Assignments (ppm) of Compounds **13** – **17** (100 MHz, $\text{DMSO-}d_6$)

Compound	13	14	15	16	17
2	141.3	141.0	141.2	141.3	141.0
3	125.5	125.5	125.4	125.4	125.5
4	123.3	123.6	123.7	123.3	123.5
5	158.0	159.5	159.7	159.3	159.5
6	139.6	139.4	139.3	139.4	138.0
7	146.6	144.4	144.5	142.9	144.3
8	177.9	179.2	178.2	178.5	178.9
1'	52.6	47.1	49.3	57.6	46.1
2'	25.2	66.7	26.9	27.9	45.1
3'				27.1	
2''					156.9
3''					107.7
4''					138.1
5''					113.5
6''					148.0

^{13}C -NMR spectroscopy of the compounds **13-17** further confirmed the molecular structure of the compounds. The chemical shifts of imine ($\text{C}=\text{N}$) carbon, $\text{C}(7)$,

observed at δ 146.6 to 142.9 ppm. The signal of thiocarbonyl (C=S) group in all of the proposed structures appeared at δ 179.2 to 177.9 ppm. This signal was very downfield because this carbon was most deshielded due to extensive electron delocalization along the conjugated framework of thiosemicarbazone skeleton reducing the electron density around the carbon atom.³⁷

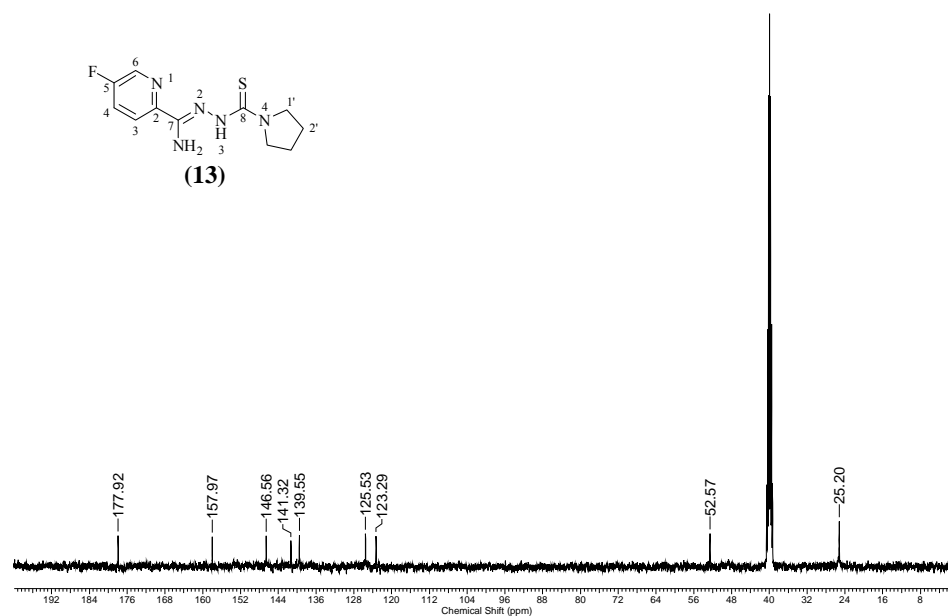


Figure 5.30: ¹³C-NMR spectrum (100 MHz, DMSO-*d*₆) of compound 13

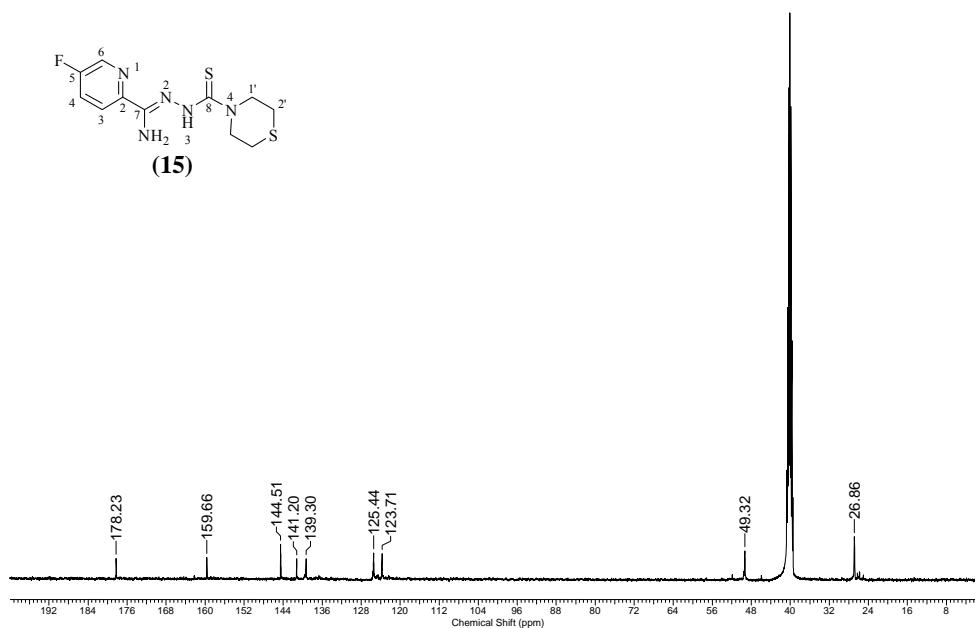


Figure 5.31: ¹³C-NMR Spectrum (100 MHz, DMSO-*d*₆) of compound 15

The signals in the range $\delta = 159.7$ to 125.4 ppm were assigned to aromatic carbons of the pyridine ring. Among the aromatic carbons, C(5) was more deshielded due to the presence of a fluorine atom attached to this carbon. At 66.7 to 25.2 ppm the signals were ascribed to the aliphatic carbons of the piperazinyl moiety at N(4) in compound **17**.

5.3.2.3 Mass Spectrometry

The mass spectra of the synthesized compounds are summarized in Table 5.22. The high resolution FAB mass spectrometry (HRFABMS) revealed $[M+Na]^+$ for compound **14**, and the protonated molecular ion, $[M+H]^+$ peaks for rest of the compound confirming their molecular structure.

Table 5.22: Mass Spectrometric Data of Compound **13** – **17**

Compound No.	<i>m/z</i>		Peak
	Found	Calculated	
13	268.10061	268.10322	$[M + H]^+$
14	306.08203	306.08008	$[M + Na]^+$
15	300.07414	300.07530	$[M + H]^+$
16	296.13661	296.13452	$[M + H]^+$
17	359.14438	359.14542	$[M + H]^+$

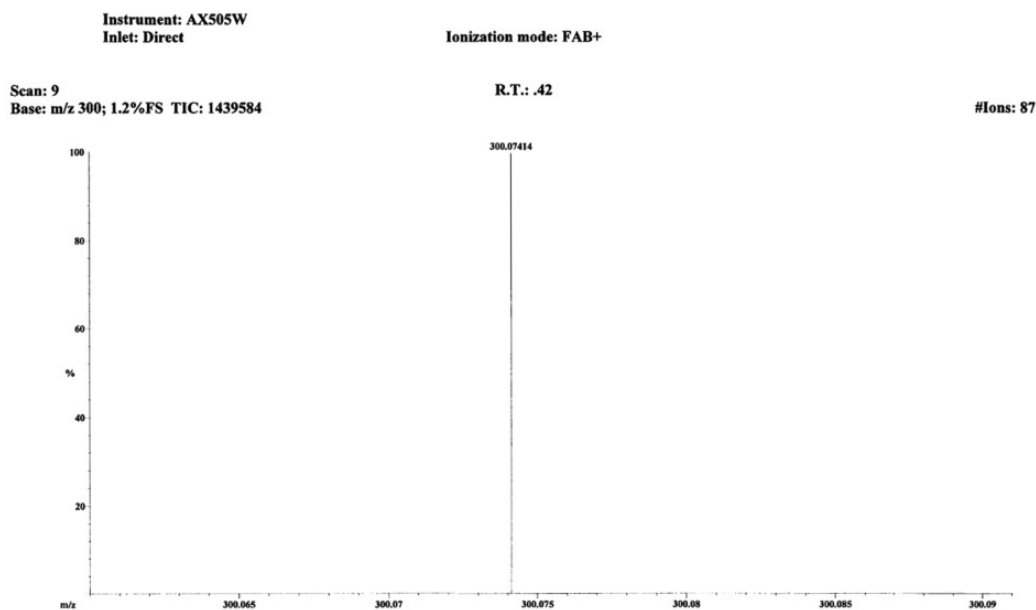


Figure 5.32: HRFABMS of compound **15**

5.3.3 Biological Activity of 5-Fluoro-2-Pyridineformamide N-(4) Ring Incorporated Thiosemicarbazones

5.3.3.1 Antineoplastic Activity against HeLa Cervical Cancer Line

The effect of all the synthesized compounds on HeLa cell viability was determined *in vitro*. (Fig. 5.33)

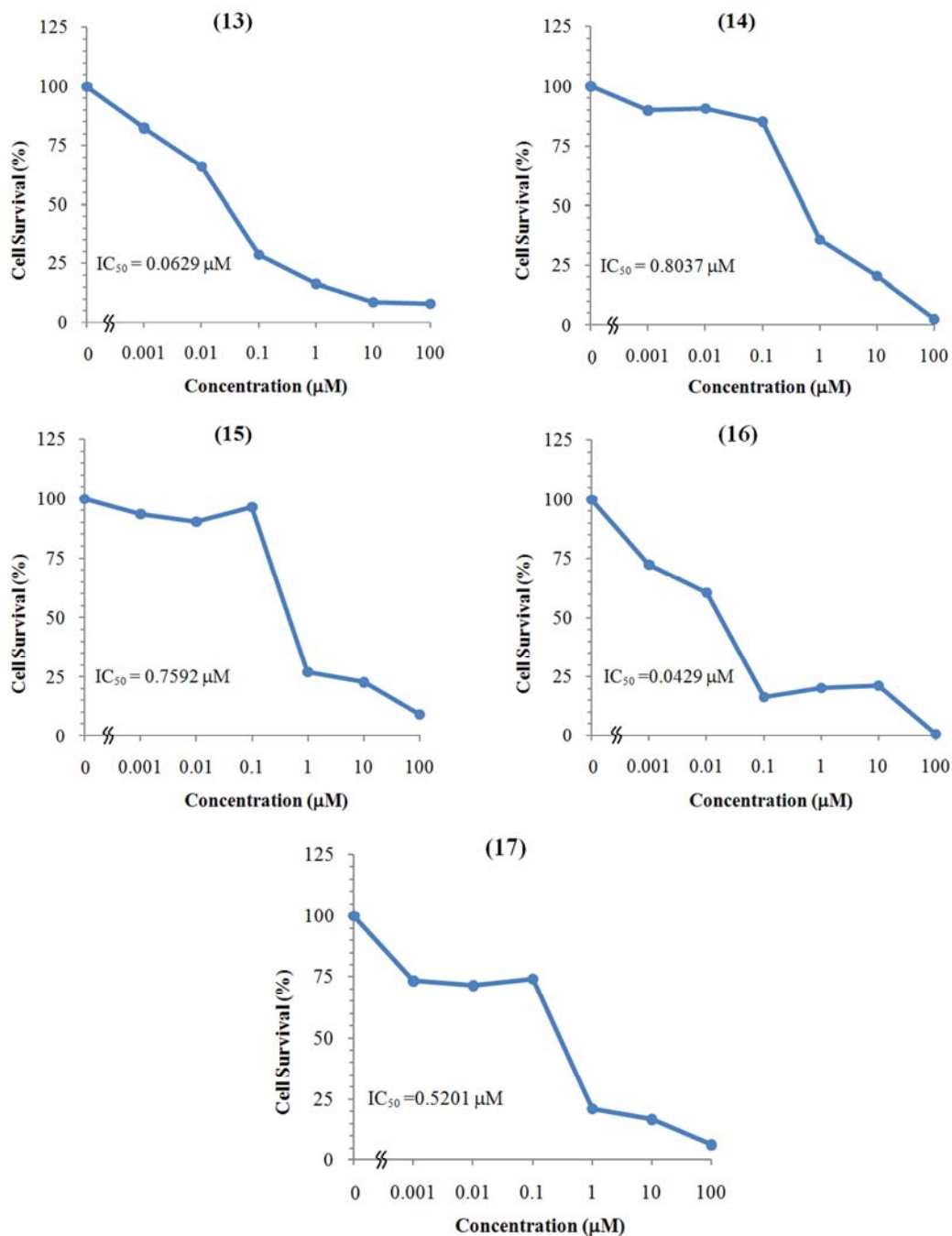


Figure 5.33: Antineoplastic activity of the compounds 13-17 against the HeLa human cervical cancer cell line

The cytotoxicity (IC_{50}) is summarized in table 5.24. The compound **16** was found to be the most potent with IC_{50} of 0.0429 μ M. The order of potency of other synthesized compounds was **13** > **17** > **15** > **14**.

Table 5.23: IC_{50} Values of Compounds **13-17** against HeLa

Compound No.	IC_{50} , μ M
13	0.0629
14	0.8037
15	0.7592
16	0.0429
17	0.5201

5.3.3.2 Preferential Cytotoxic Activity against PANC-1 Cells in Nutrient-Deprived Medium (NDM)

The effect of all the synthesized compounds on PANC-1 cell viability under nutrient deprived medium conditions was determined *in vitro* (Fig. 5.34). The preferential cytotoxicity (PC_{50}) is summarized in Table 5.24. The compound **13** was found to be the most potent with PC_{50} of 0.68 μ M. The order of potency of other synthesized compounds was **17** > **16** > **15** > **14**. Compound **13** and **17** were found to be more potent than the positive control, arctigenin.

Table 5.24: Preferential Cytotoxicity Data of Compounds **13-17** against PANC-1

Compound No.	PC_{50} , μ M
13	0.68
14	1.84
15	1.61
16	0.99
17	0.70

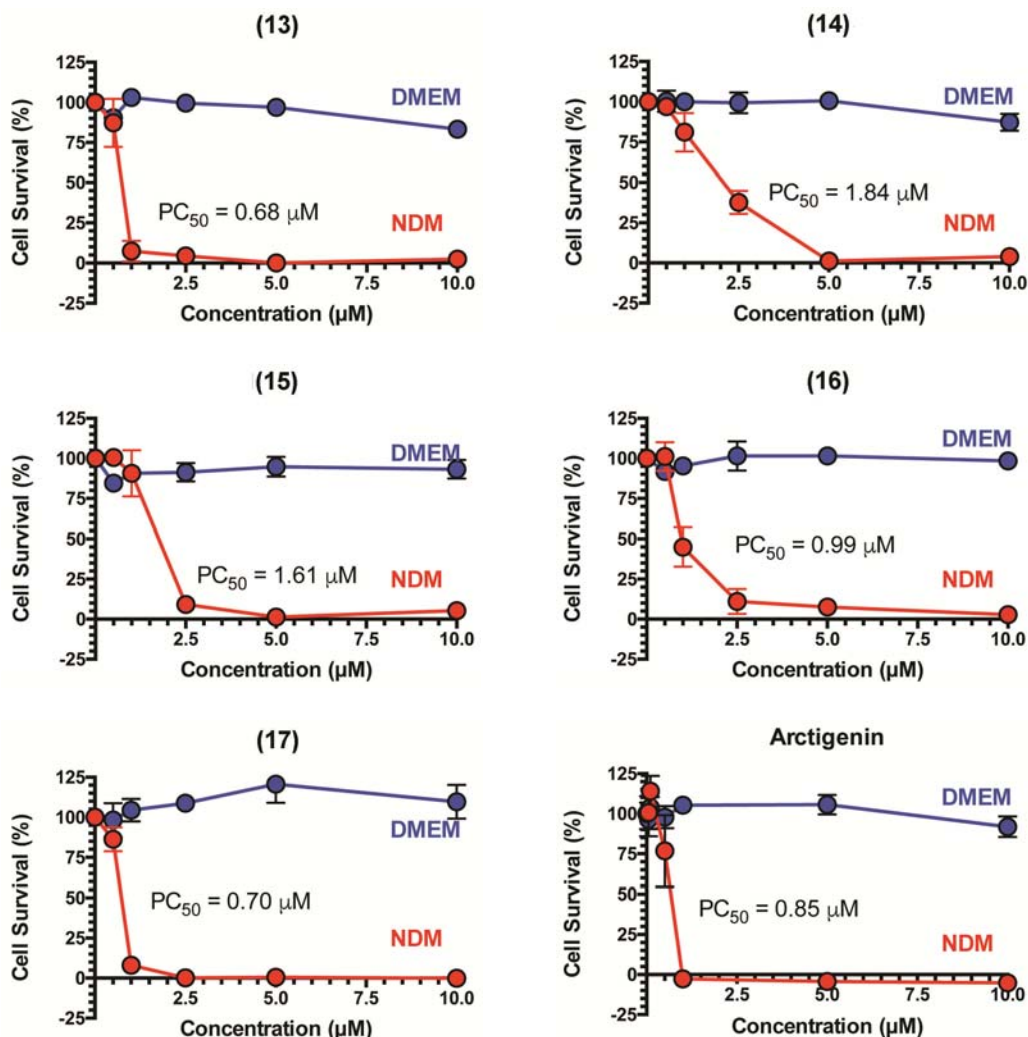


Figure 5.34: Preferential cytotoxic activity of the compounds **13-17** and arctigenin against the PANC-1 human pancreatic cancer cell line in nutrient deprived medium (NDM).

5.3.4 Conclusion

All the synthesized compounds of this series (**13-17**) were evaluated for their cytotoxicity against HeLa and PANC-1 cell lines. Against HeLa, compound **13** with pyrroldinyl group and compound **16** with hexamethyleneiminyl group at *N*(4) displayed activity comparable to the positive control, paclitaxel. While, against PANC-1 cells under nutrient-deprived condition, compound **13** with pyrroldinyl group and compound **17** with pyridyl piperazinyl group at *N*(4) displayed more potent activity even than the positive control, arctigenin.

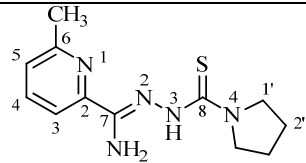
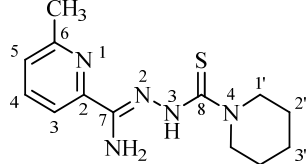
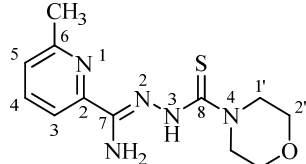
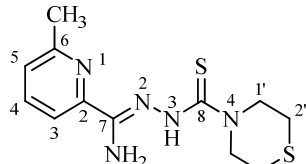
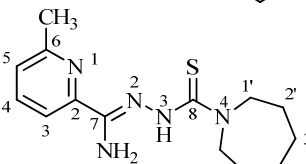
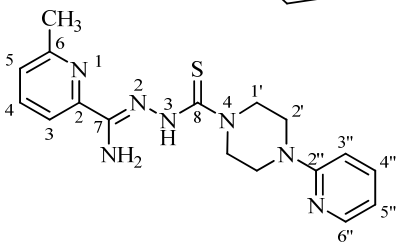
Compound **14** with piperidyl group at *N*(4) displayed the least cytotoxicity against both HeLa and PANC-1 cell lines.

5.4. 6-METHYL-2-PYRIDINEFORMAMIDE *N*(4)-RING INCORPORATED THIOSEMICARBAZONES

5.4.1 General Discussions

Thiosemicarbazides were synthesized by the method described by Scovill.²⁷ The 6-methyl-2-pyridineformamide *N*(4)-ring incorporated thiosemicarbazones were prepared by reducing 2-cyano-6-methylpyridine with sodium in dry methanol in the presence of desired thiosemicarbazides.

Table 5.25: Physical Properties of Compounds 18-23

Compd	Molecular formula	Molecular mass	Colour	Yield (%)	M. P. (°C)	
18		C ₁₂ H ₁₇ N ₅ S	263.36	Yellow	26	152-154
19		C ₁₃ H ₁₉ N ₅ S	277.39	Yellow	21	150-151
20		C ₁₂ H ₁₇ ON ₅ S	279.36	Yellow	54	164-166
21		C ₁₂ H ₁₇ N ₅ S ₂	295.43	Yellow	41	157-158
22		C ₁₄ H ₂₁ N ₅ S	291.42	Yellow	20	139-141
23		C ₁₇ H ₂₁ N ₇ S	355.46	Yellow	42	149-150

The thiosemicarbazones were obtained in low to moderate yield (20 - 54%) having melting point in the range of 139 - 166 °C. The thiosemicarbazones were stable in air at room temperature, slightly soluble in CHCl₃, Me₂CO and more soluble in polar solvents such as EtOH, MeOH, DMF and DMSO, and slightly soluble in water. The synthesized compounds were characterized by elemental analysis, IR, ¹H and ¹³C-NMR spectroscopic techniques. The molecular structures were further confirmed by high resolution FAB mass spectrometry (HRFAB). All the synthesized compounds were found to exhibit potent cytotoxicity against HeLa human cervical cancer cell lines and PANC-1 human pancreatic cancer cell lines. The physical characteristic data of the compounds are presented in Table 5.25.

The elemental analyses data were in agreement with the calculated values within the limits of experimental error.

Table 5.26: Elemental Analysis Data of Compounds **18-23** (Calculated Data)

Compound	C	H	N
18	55.12 (54.73)	6.24 (6.51)	26.76 (26.59)
19	56.11 (56.29)	7.22 (6.90)	25.53 (25.25)
20	51.86 (51.59)	5.97 (6.13)	24.90 (25.07)
21	49.15 (48.79)	5.51 (5.80)	23.45 (23.71)
22	58.02 (57.70)	7.07 (7.26)	24.18 (24.03)
23	57.84 (57.44)	5.62 (5.95)	27.22 (27.58)

5.4.2 Spectral Studies

5.4.2.1 IR Spectra

The significant IR bands of the compounds **18-23** and their assignments are given in Table 5.27. In the synthesized compounds **18-23**, medium absorption bands in the range 3431 to 3329 cm⁻¹ and 3301 to 3234 cm⁻¹ were attributable to asymmetric stretching and symmetric stretching vibrations respectively of NH₂ group.²²¹ The band corresponding to stretching of -NH group appeared at 3228 to 3140 cm⁻¹ while strong band corresponding to bending of -NH group appeared at 1673 to 1666 cm⁻¹.²⁴² Absence of absorption bands corresponding to enol group in the region 2200 to 2500 cm⁻¹ revealed the presence of only the thione form in the solid state.²⁴⁰ The 1600 to 1400 cm⁻¹ region of the spectra was complicated by the presence of azomethine

(C=N) and pyridine ring breathing vibrations. The ν (C=N) stretch should appear at higher energy than the peaks for ring breath.²²⁵ Medium absorption bands observed at 1105 to 1019 cm^{-1} for the compounds were assigned to hydrazinic N–N bonds. All the compounds exhibited medium bands in the 881 to 841 cm^{-1} range ascribed to amide IV bands with large contribution from C=S.¹⁶⁵ Medium absorption bands were observed in the region 636 to 620 cm^{-1} of the spectra due to in-plane deformations of pyridine ring.²⁴³

Table 5.27: Diagnostic Bands in the IR Spectra of Compounds **18-23**

Group↓	Compound					
	18	19	20	21	22	23
$\nu(\text{NH}_2)$	3387(m), 3249(m)	3353(m), 3234(m)	3329(s), 3240(s)	3410(s), 3279(s)	3357(s), 3240(s)	3431(m), 3301(m)
$\nu(\text{NH})$	3221(m)	3157(m)	3163(s)	3140(s)	3156(s)	3228(m)
$\delta(\text{NH})$	1667(s)	1673(s)	1672(s)	1658(s)	1672(s)	1666(s)
$\nu(\text{C}=\text{C})$ +	1599(s), 1569(s), 1493(s), 1431(s)	1603(s), 1583(s), 1468(s), 1427(s)	1614(s), 1594(s), 1465(s), 1421(s)	1597(s), 1581(s), 1481(s), 1466(s)	1603(s), 1581(s), 1453(s), 1410(s)	1593(s), 1562(s), 1477(s), 1417(s)
$\nu(\text{C}=\text{N})$	1105(m)	1025(m)	1019(m)	1065(s)	1105(m)	1020(m)
$\nu(\text{C}=\text{S})$	841(m)	881(m)	842(m)	856(s)	855(m)	871(m)
ρ (Py)	624(m)	636(m)	621(s)	620(s)	629(m)	629(m)

s : strong, m : medium, w : weak

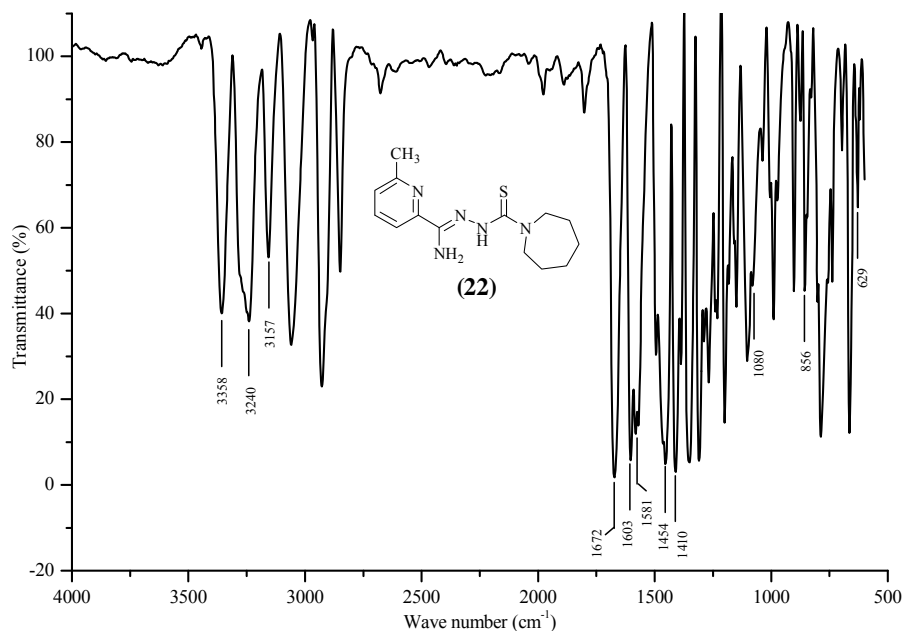


Figure 5.35: IR spectrum of the compound **22**

5.4.2.2 NMR Spectra

The ^1H -NMR spectral data of the compounds **18-23** are presented in Table 5.28

Table 5.28: ^1H -NMR Spectral assignments (ppm) of compounds **18 – 23** (400 MHz)

Compound	18	18	19	20	21	22	23
Solvent→ proton↓	CDCl_3	$\text{DMSO-}d_6$	$\text{DMSO-}d_6$	$\text{DMSO-}d_6$	$\text{DMSO-}d_6$	$\text{DMSO-}d_6$	$\text{DMSO-}d_6$
3	7.27, br s	7.29 br s, 7.48 br s	7.49, d (4.9 Hz)	7.48, d (5.1 Hz)	7.48, d (5.1 Hz)	7.47, br s	7.51, br s
4	7.71, br s	7.72 br s, 7.92 br s	7.93, br s	7.81, br. s.	7.92, br s	7.92, br s	7.96, br s
5	7.79, br s	7.82 br s, 7.93 br s	7.95, br s	8.02, br s	7.93, br s	7.94, br s	7.97, br s
1'	3.76, br s	3.56 br s, 3.74 br s	3.83, br s	3.56, t (4.864 Hz)	4.14, br s	3.82, br s	3.96, br. s.
2'	1.92, br s	1.83 br s	1.44, br s	3.81, t (4.864 Hz)	2.50, br s	1.45, br s	3.48, br. s.
3'			1.58, br s			1.69, br s	
3''							6.85, d (7.3 Hz)
4''							7.54, br s
5''							6.64, m
6''							8.12, br s
Me	2.59, s	2.50 s, 2.55 s	2.56, s	2.49, s	2.53, br s	2.55, s	2.57, s
N(3)H	12.95, br s	12.52 br s, 9.22 br s	12.67, br s	12.53, br s	12.52, br s	12.68, br s	12.57, br. s.

s: singlet, d: doublet, m: multiplet (JJ values)

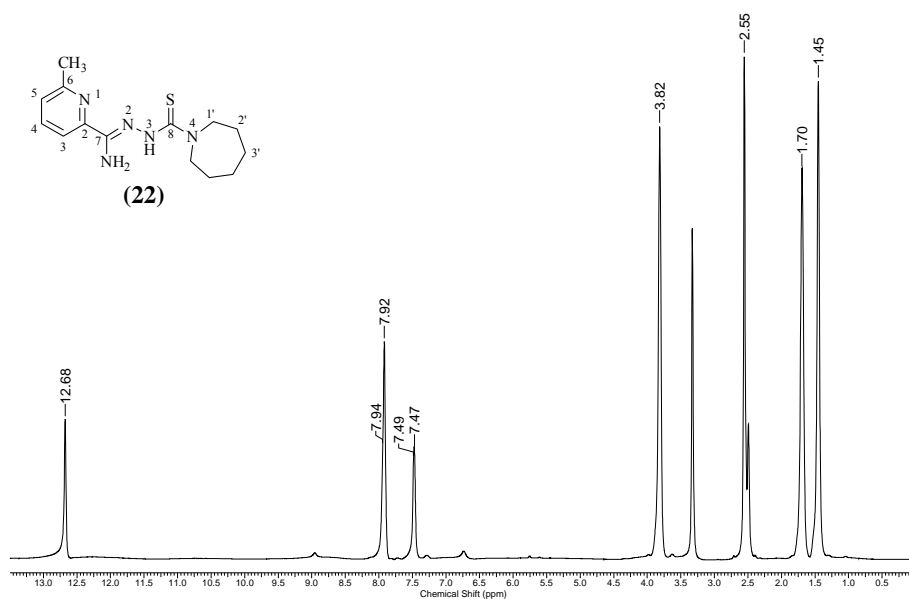


Figure 5.36: ^1H -NMR spectrum (400MHz, $\text{DMSO-}d_6$) of compound **22**

The $^1\text{H-NMR}$ spectra of the compounds, exhibited the aromatic proton signals appearing at 8.12 to 6.64 ppm, methylene protons of the $N(4)$ substituted ring at 4.14 to 1.44 ppm, methyl protons at 2.59 to 2.53 ppm and the azomethine proton at 12.95 to 12.52 ppm respectively.

However, the $^1\text{H-NMR}$ spectra of the compound **18** in $\text{DMSO-}d_6$ (Fig 5.38) revealed a pair of signals for each of the proton indicating existence of a mixture of E -, Z - and Z' -isomers in the solution.²⁴⁴

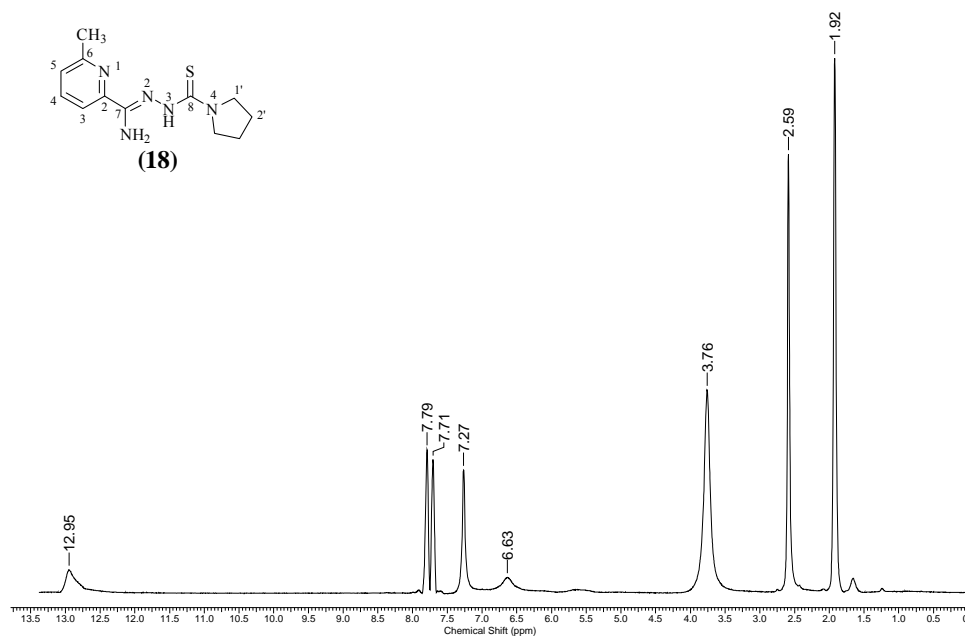


Figure 5.37: $^1\text{H-NMR}$ spectrum (400MHz, CDCl_3) of compound **18**

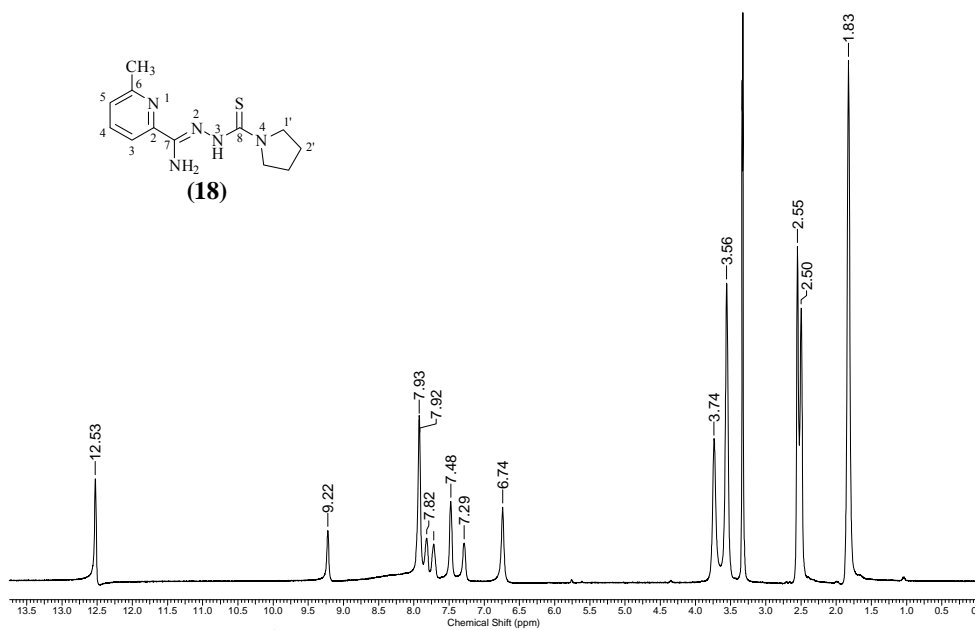


Figure 5.38: $^1\text{H-NMR}$ spectrum (400MHz, $\text{DMSO-}d_6$) of compound **18**

The ^{13}C -NMR spectral data for the synthesized compounds are listed in Table 5.29.

Table 5.29: ^{13}C Spectral Assignments (ppm) of compounds **18** – **23** (100 MHz, DMSO- d_6)

Compound	18	19	20	21	22	23
2	143.9	143.9	143.8	143.5	143.8	143.7
3	118.6	118.7	118.7	116.8	118.6	118.9
4	138.8	138.7	138.8	139.1	138.7	138.8
5	126.4	126.5	126.7	124.7	126.3	126.7
6	160.7	158.9	158.7	158.9	158.8	159.6
7	148.4	144.4	144.3	149.1	143.9	145.3
8	178.9	178.6	179.1	178.9	178.2	178.9
1'	48.6	47.4	47.2	50.8	49.3	46.1
2'	25.2	26.1	66.7	26.8	28.4	45.1
3'		25.3			27.1	
2''						159.0
3''						107.7
4''						138.0
5''						113.5
6''						148.0
Me	24.3	24.6		24.7	24.6	24.6

In the ^{13}C -NMR spectra, the carbon resonance signals of the C=N group appeared at δ 149.1 to 143.9 ppm. The results were similar to the chemical shifts found for other 2-pyridineformamide thiosemicarbazones. The C=S signals observed at δ 178.9 to 178.2 ppm are characteristic for this group, while the aromatic carbons were observed at δ 160.7 to 116.8 ppm. The signals for two methylene carbons were observed at δ 50.8 to 46.1 ppm and 45.1 to 25.2 for C-1' and C-2' respectively and the for methyl carbon it was observed at δ 24.7 to 24.6 ppm.

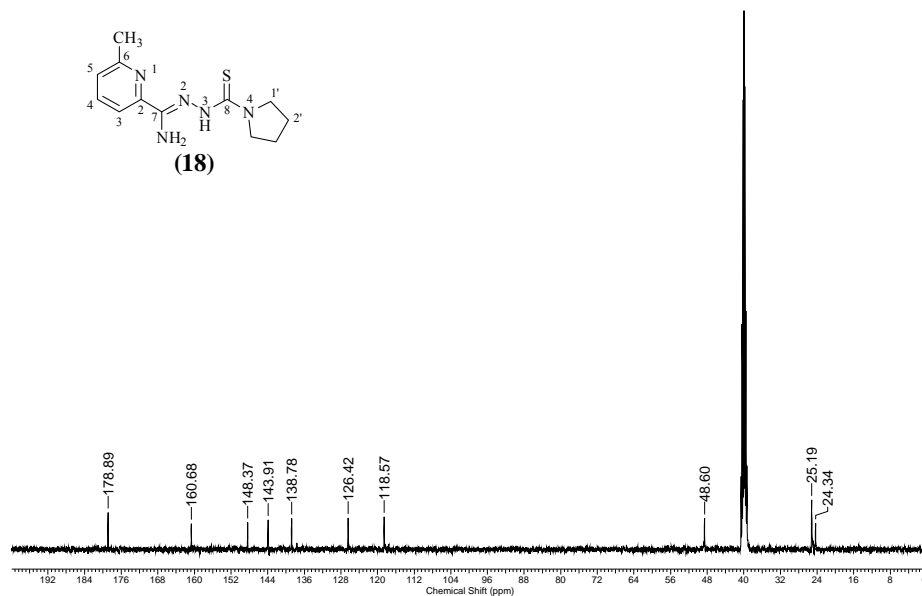


Figure 5.39: ^{13}C -NMR spectrum (100 MHz, $\text{DMSO-}d_6$) of compound **18**

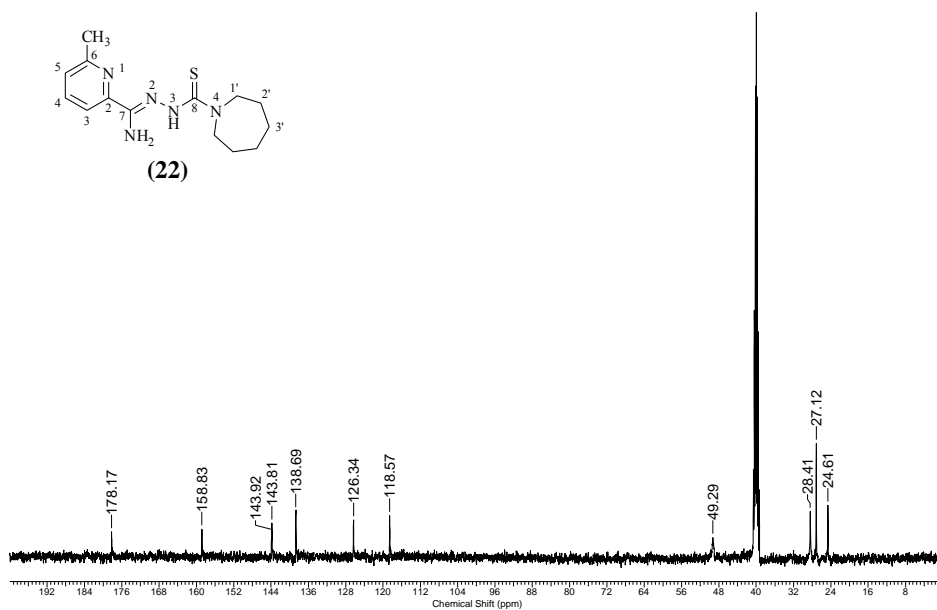


Figure 5.40: ^{13}C -NMR spectrum (100 MHz, $\text{DMSO-}d_6$) of compound **22**

5.4.2.3 Mass Spectrometry

The mass spectra of synthesized compounds are summarized in Table 5.30. The high resolution FAB mass spectral data confirmed the molecular structures of the synthesized compounds as indicated by the protonated molecular ion peak, $[M+H]^+$.

Table 5.30: Mass Spectrometric Data of Compounds **18 – 23**

Compound No.	$m/z [M + H]^+$	
	Found	Calculated
18	264.12962	264.12829
20	280.12227	280.12321
21	296.09827	296.10037
22	292.15681	292.15959
23	355.17386	355.17050

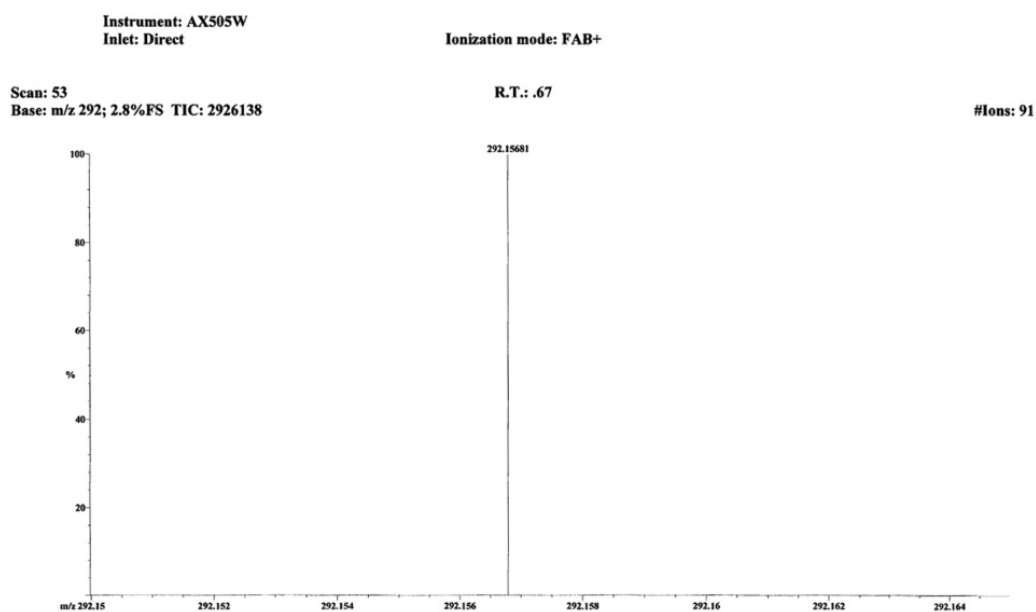


Figure 5.41: HRFABMS of compound **22**

5.4.3 Biological Activity of 6-Methyl-2-Pyridineformamide *N*(4)-Ring Incorporated Thiosemicarbazones

5.4.3.1 Antineoplastic Activity against HeLa Cervical Cancer Cell Line

All the synthesized compounds **18-23** were evaluated for *in vitro* cytotoxicity against HeLa cervical cancer cell line, (Fig. 5.42). The results are summarized in Table 5.31. Among this series, compound **22** exhibited most potent activity with IC_{50} at

0.3681 μM . The activities of the compounds were found in the order : **22** > **21** > **18** > **23** > **20** > **19**.

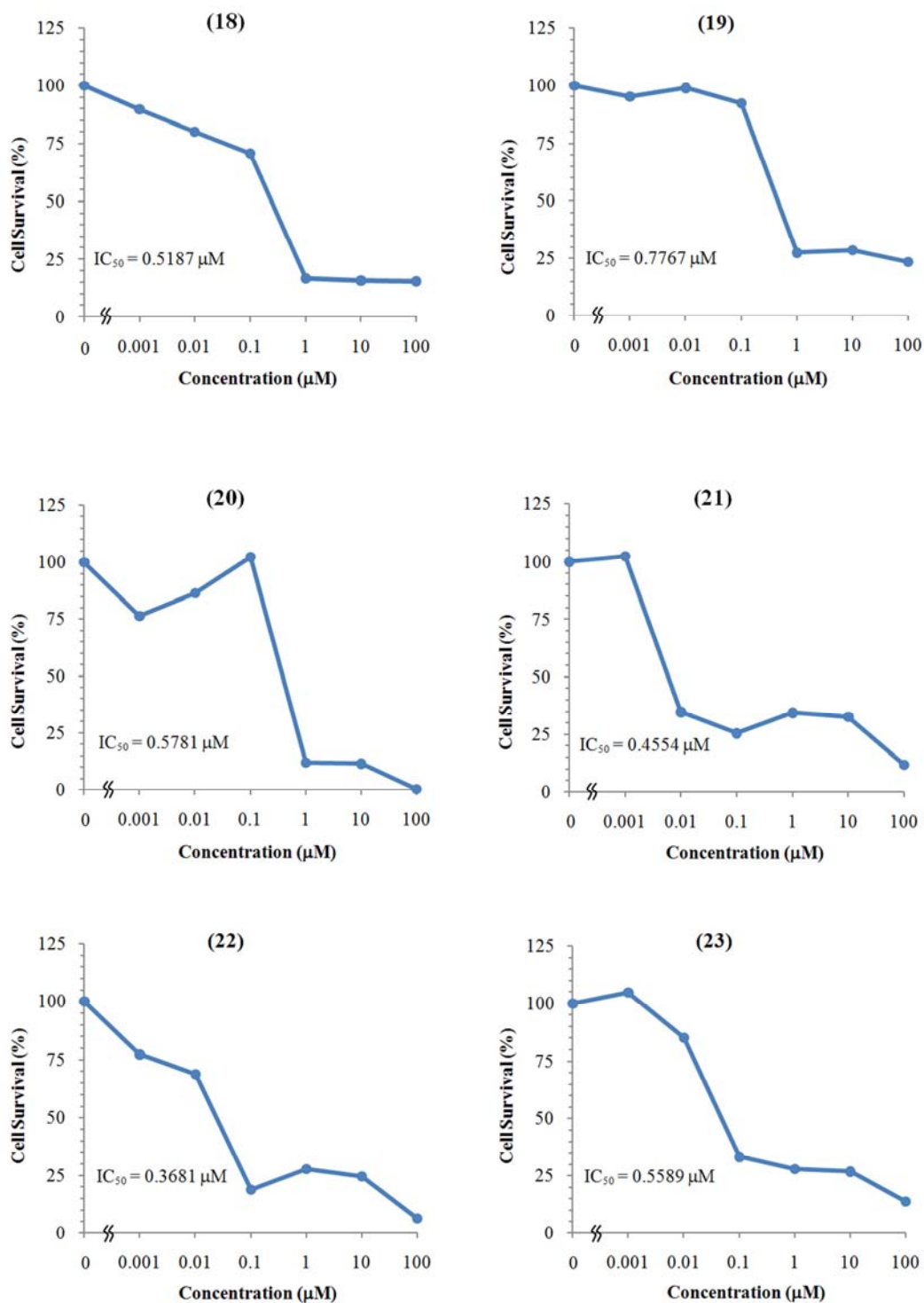


Figure 5.42: Antineoplastic activity of compounds 19-24 against the HeLa cervical cancer cell line.

Table 5.31: IC₅₀ Values against HeLa cells of Compounds **18-23**

Compound No.	IC ₅₀ , μM
18	0.5187
19	0.7767
20	0.5781
21	0.4554
22	0.3681
23	0.5589

5.4.3.2 Preferential Cytotoxic Activity against PANC-1 Cells in Nutrient-Deprived Medium (NDM)

Following antiausterity strategy, all the synthesized compounds **18-23** were evaluated for *in vitro* preferential cytotoxicity against PANC-1 human pancreatic cancer cell line under nutrient-deprived conditions, (Fig. 5.43). The results are summarized in Table 5.32. Among this series, compound **22** exhibited most potent activity with PC₅₀ at 0.70 μM. The positive control Arctigenin displayed preferential cytotoxicity of PC₅₀ at 0.85 μM (Fig. 5.34). The activities of the compounds were found in the order of : **22 > 21 > 23 > 19 > 20 > 18**.

Table 5.32: Preferential Cytotoxicity Data of Compounds **19-24** against PANC-1

Compound No.	PC ₅₀ , μM
18	1.9
19	0.95
20	1.00
21	0.77
22	0.69
23	0.79

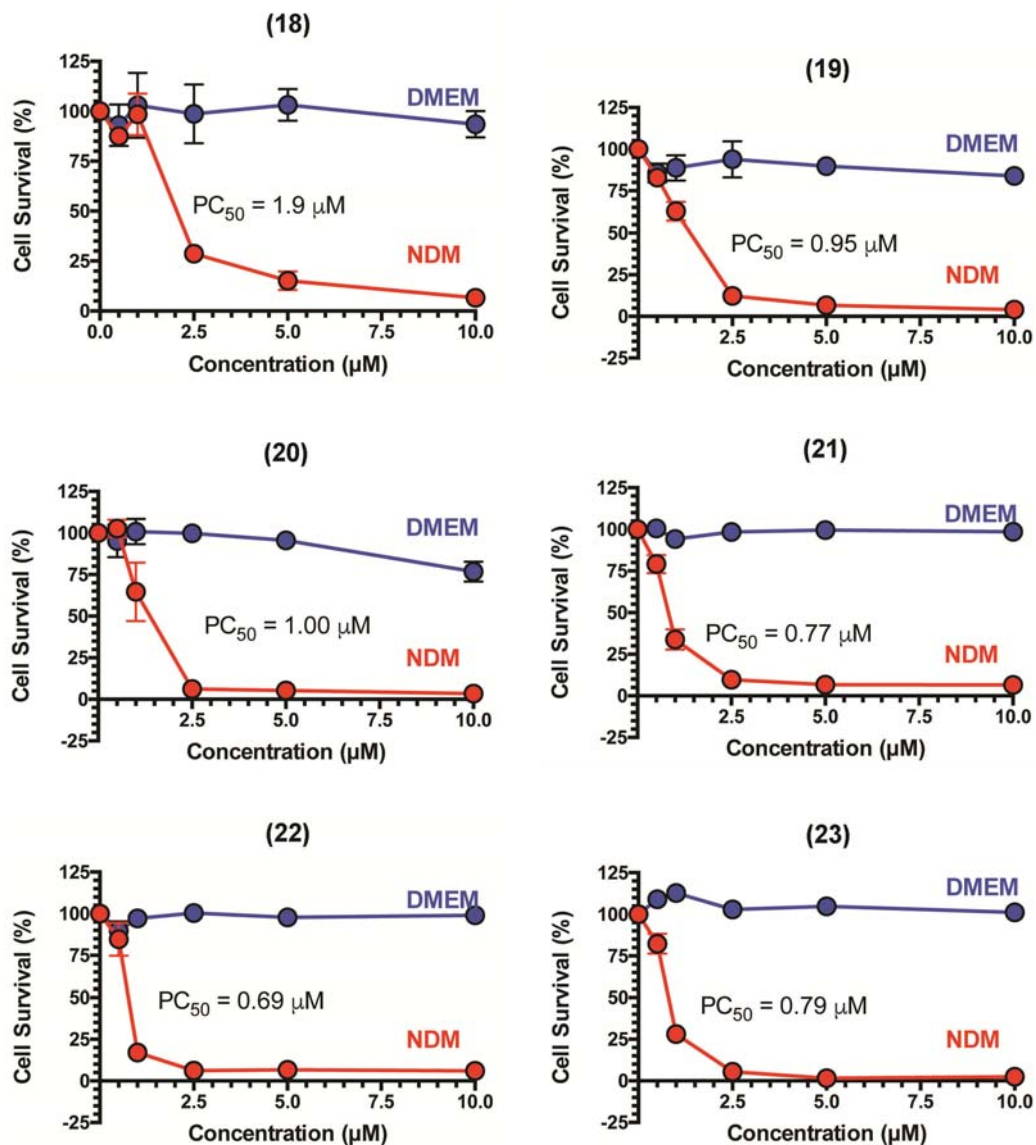


Figure 5.43: Preferential cytotoxic activity of compounds **18-23** against the PANC-1 human pancreatic cancer cell line in nutrient deprived medium (NDM).

5.4.4 Conclusion

The synthesized compounds were evaluated for their cytotoxicity against HeLa and PANC-1 cells. Among them compounds **22** with hexamethyleneiminyl group at *N*(4) displayed most potent activity against both HeLa and PANC-1 cells. Against PANC-1 it showed even more potent than the positive control, arctigenin. The least potent cytotoxicity effect was exhibited by compound **19** with piperidyl group at *N*(4) against HeLa while by compound **18** with pyrroldinyl group at *N*(4) against PANC-1.

6. CONCLUSION AND RECOMMENDATIONS

6.1 Conclusion

All the synthesized 2-pyridineformamide thiosemicarbazones displayed cytotoxicity against both HeLa and PANC-1 cells. The potency of the tested compounds against these cell lines were found to vary slightly with variation in *N*(4)-substitution and substitution at parent pyridine ring. The evaluation of the compounds against HeLa revealed that 2-pyridineformamide thiosemicarbazones are less potent than the positive control paclitaxel, a well known anticancer agent, however their potency against PANC-1 was superior to the control. *N*(4)-Pyrrolidinyl substituted compounds **1** (PC₅₀ of 0.78), **7** (PC₅₀ of 0.37), and **13** (PC₅₀ of 0.68), and *N*(4)-(2-pyridyl)piperazinyl substituted compounds **6** (PC₅₀ of 0.78), **12** (PC₅₀ of 0.68), and **17** (PC₅₀ of 0.70), from 2-pyridineformamide, 4-methyl-2-pyridineformamide and 5-fluoro-2-pyridineformamide respectively exhibited preferential cytotoxicity more potent than the positive control arctigenin (PC₅₀ of 0.085). Conversely, thiosemicarbazones derived from 6-methyl-2-pyridineformamide with *N*(4)-thiomorpholinyl, *N*(4)-hexamethyleneiminy and *N*(4)-(2-pyridyl)piperazinyl substitution compounds **21** (PC₅₀ of 0.77), **22** (PC₅₀ of 0.69) and **23** (PC₅₀ of 0.79) respectively exhibited potency higher than the control arctigenin.

Compound **6** was selected for Ethidium bromide (EB)/Acridine orange (AO) staining assay, Western Blot Analysis and Annexin V/Propidium Iodide Staining Assay. In EB/AO staining assay, phase contrast microscopic observation of the treated cells showed a dramatic alteration in the PANC-1 cell morphology, including swelling, rupture of cell membranes, and disruption of cellular organelles. In Western Blot Analysis, compound **6** was found to activate apoptosis, resulting in the cleavage of caspase-3 even at a very short exposure time of 4 h in a concentration dependent manner. Therefore, much stronger effect at lower concentration could be expected with increase in the exposure time period. Inhibition of Akt signaling is unlikely to be a major antitumor mechanism of compound **6** in PANC-1 cells. The evidence for apoptosis was further confirmed using an annexin V (AV) and propidium iodide (PI) staining assay. During apoptosis, alterations in the plasma membrane lead to the translocation of phosphatidylserine (PS), which was exposed at the external surface of

the cell. AV specifically binds to the exposed PS, which was detected by green fluorescence.

Pancreatic cancer cells are known to be resistant to apoptosis, which is one of the key reasons for the failure of chemotherapy, and lead to aggressive growth and metastasis. In the present study, apoptosis induced by compound **6** indicated that 2-pyridineformamide thiosemicarbazones are effective antipancreatic cancer agent.

So far only compounds extracted from medicinal plants have been studied for anticancer activity against pancreatic cancer utilizing antiausterity strategy. This is the first study to investigate the anticancer activity of synthetic compounds against pancreatic cancer utilizing antiausterity strategy. The activity of 2-pyridineformamide thiosemicarbazones were comparable with Arctigenin, an antiausterity strategy based anticancer agent that has successfully completed phase II clinical trial and showed remarkable survival benefit to the cancer patients in real clinical trials. Our present study indicated that 2-pyridineformamide thiosemicarbazones could be powerful drug candidates for the treatment of pancreatic cancer.

6.2 Recommendation for further work

The recommendation for further research concerning its impact gives new directions in this field of research. This dissertation work has established that 2-pyridineformamide thiosemicarbazones are novel powerful antiausterity agents and further work needs to explore their mechanism of action and its *in vivo* activity. From the study of mechanism the factors that influence the anticancer activity can be identified and addressed in the design of more potent molecule. Substitution of $-NH_2$ or $-OH$ group at the 3 or 5-position of the parent pyridine ring leads to considerable anticancer activity. Therefore, anticancer activity of 2-pyridineformamide thiosemicarbazones with $-NH_2$ or $-OH$ group at the 3- or 5-position of the parent pyridine ring and substitution at $N(4)$ position should explore. In majority of the cases activity of the ligands greatly enhanced by the presence of metal ion. Study of coordination chemistry of 2-pyridineformamide thiosemicarbazones in reference to anticancer activity deserves equal importance.

SUMMARY

The thesis is structured under 5 chapters. In the first three chapters, the theoretical underpinnings for this research are presented in a concise form and the rest of the chapters cover the experiments and findings.

Chapter-1. This chapter presents a short overview of thiosemicarbazones; its types (Mono, bis and di-thiosemicarbazones), general synthetic procedure mainly by condensation of aldehyde or ketones and reduction of cyano functionality with thiosemicarbazides, different isomeric form *Z*, *E* and *E'* it exhibits where bulkier *N*(4)-substitution impose *Z* isomer, monodentate, bidentate and polydentate coordination properties are described. The rationale behind the study is the anticancer activity of α -(*N*) heterocyclic thiosemicarbazones and the observed significant effects on the activity with structural modifications. The objectives of the study are synthesis, characterization of 2-pyridineformamide thiosemicarbazones and evaluation of their anticancer activity.

Chapter-2. This chapter deals with an extensive literature review related to the biological activity of thiosemicarbazones. The literature reports reveals that the thiosemicarbazone possess wide spectrum of biological activities like antitrypanosomal activity, antimalarial activity, antibacterial activity including antitubercular activity, antifungal activity, antiviral activity and antitumor activity. Hence, the present research work envisages towards development of novel thiosemicarbazones and evaluates their anticancer activity. A series of comparative studies from the literature are presented. *p*-Acetamidobenzaldehyde thiosemicarbazone, also known as Thiacetazone is the most widely used drug for the treatment of tuberculosis. Another successful example of thiosemicarbazone drug is *N*-methyl- β -isatin TSC, better known as methisazone (Marboran), which was used to treat smallpox. 3-Aminopyridine-2-carboxaldehyde thiosemicarbazone (Triapine, 3-AP) has been in clinical trials for the treatment of cancer.

Chapter-3. A description of the mechanism of anticancer action of thiosemicarbazone has been realized and discussed in this chapter.

Chemotherapeutic agents can act in either of three ways: Stop the synthesis of pre DNA molecule building blocks (eg. methotrexate, fluorouracil); Directly damage the DNA in the nucleus of the cell (eg. cisplatin, doxorubicin etc.); Effect the synthesis or breakdown of the mitotic spindles (paclitaxel, vinblastine etc.).

The major effects associated with the anticancer activity of thiosemicarbazone includes RR inhibition, topoisomerase II inhibition, mitochondria disruption, reactive oxygen species (ROS) production and multidrug resistance protein (MDR1) inhibition. RR catalyzes the synthesis of deoxyribonucleotides from their ribonucleotide precursors. Thiosemicarbazones are among the most potent inhibitors of RR activity which is due to binding iron at the active site of enzyme or by preformation of an iron chelate which then inhibits the enzyme by directly destroying the tyrosyl radical in the R2 subunit of RR. Thelander and Graslund demonstrated for the first time that destruction of the tyrosyl radical by $\alpha(N)$ -TSC requires iron and oxygen.

Chapter-4. This chapter describes about the synthesis, characterization and anticancer screening of thiosemicarbazones. The thiosemicarbazides with *N*(4)-substitution were synthesized by the method developed by Scovill through transamination reaction.

2-Pyridineformamide thiosemicarbazones were synthesized by the reduction of 2-cyanopyridine/ substituted 2-cyanopyridine with sodium in dry methanol in the presence of desired thiosemicarbazide.

Chapter 5. This chapter comprises results and discussion about the characterization and anticancer activity of the synthesized compounds.

IR study:

The synthesized compounds exhibited characteristic bands corresponding to the various functional groups. Asymmetric and symmetric stretching for -NH₂ moiety were observed at 3460 to 3229 cm⁻¹ and acidic *N*(3)H exhibited stretch at 3240 to 3130 cm⁻¹. Absence of band at 2600 to 2500 cm⁻¹ correspond to ν (S-H) confirmed the existence of thiosemicarbazone in thione tautomer form in the solid state. Strong

band in the range of 1616 to 1593 cm^{-1} assigned to $\nu(\text{C}=\text{N})$ stretching further conformed the formation thiosemicarbazone molecule.

The in-plane deformation vibrations due to pyridine ring were observed as strong and very distinguishable band at 636 to 616 cm^{-1} . Nature of substituent at $N(4)$ position was found to influence the peak position of different functionality.

NMR Study

The ^1H -NMR spectra of the compounds were consistent with the analogous thiosemicarbazones and confirm that in solution it exists as the neutral molecule. The absence of a signal at *ca.* δ 4 ppm corresponding to $-\text{SH}$ confirmed that thiosemicarbazone exists as the thione tautomer in solution also. Aromatic protons of the compounds appeared at δ 7.26 to 8.77, with calculated multiplicity.

Some compounds were found to exist as the mixture of *E*, *Z* and *Z'* isomers. In *Z* isomer, there exists intramolecular hydrogen bond of $N(3)\text{H}$ with pyridine nitrogen. Much downfield shifts of about δ 12.00 ppm have been observed for $N(3)\text{H}$ proton when $N(4)$ was substituted with bulky group.

In the ^{13}C -NMR spectra the aromatic carbons were observed between 116.8 to 159.7 ppm. Thioamide carbon peak was observed at characteristic high frequency near 180 ppm and the carbon resonance signals of the $\text{HC}=\text{N}$ group appeared at δ 142.9 to 150.1 ppm. From ^{13}C -NMR spectra it was observed that the nature of the $N(4)$ -substituent had no significant effect on the position of the carbons peak.

Mass Spectrometry

The high resolution FAB mass spectrometry (HRFABMS) confirmed the molecular structures with the presence of expected molecular ion $[\text{M}+\text{H}]^+$ peaks of the compounds.

Anticancer Screening

Evaluation of the synthesized compounds against HeLa cells with paclitaxel as positive control revealed that these compounds are less potent than the control. Preferential cytotoxicity of all the synthesized compounds was also evaluated against

PANC-1 human pancreatic cancer cell line utilizing an antiausterity strategy in reference to arctigenin, an antiausterity strategy-based anticancer agent (PC_{50} at 0.85 μM), as a positive control. The activity of the compounds was found very potent in a concentration dependent manner and influenced by substitution on pyridine ring and $N(4)$ position. The antitumor activity of thiosemicarbazone is extremely differentiated and dependent on the typology of tumor cells.

$N(4)$ -Pyrrolidinyl and $N(4)$ -(2-pyridyl)piperazinyl substituted compounds from 2-pyridineformamide and 4-methyl-2-pyridineformamide exhibited the cytotoxicity more potent than the positive control arctigenin. While $N(4)$ -thiomorpholinyl, $N(4)$ -hexamethyleneiminyl and $N(4)$ -(2-pyridyl)piperazinyl substituted compounds from 6-methyl-2-pyridineformamide were also found to be more potent than the control arctigenin.

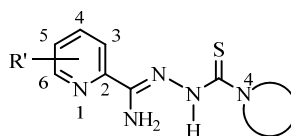


Table : Cytotoxic activity of synthesized compounds against HeLa (IC_{50} , μM)

$N(4)$ -substituent ↓	$R' \rightarrow$	H-	4-Me	5-F	6-Me
Pyrrolidinyl		0.5517	0.5601	0.0629	0.5187
Piperidyl		0.5865	0.8263	-	0.7767
Morpholinyl		0.9007	0.7003	0.8037	0.5781
Thiomorpholinyl		8.814	0.9060	0.7592	0.4554
Hexamethyleneiminyl		0.5741	11.000	0.0429	0.3681
2-Pyridyl piperazinyl		0.9762	0.9771	0.5201	0.5589

Table : Cytotoxic activity of synthesized compounds against PANC-1 (PC_{50} , μM)

$N(4)$ -substituent ↓	$R' \rightarrow$	H-	4-Me	5-F	6-Me
Pyrrolidinyl		0.78	0.37	0.68	1.90
Piperidyl		1.60	1.80	-	0.95
Morpholinyl		1.60	1.80	1.84	1.00
Thiomorpholinyl		1.90	1.90	1.61	0.77
Hexamethyleneiminyl		1.40	1.70	0.99	0.69
2-Pyridyl piperazinyl		0.78	0.68	0.70	0.79

Morphological Assessment of Cancer Cells

Among the synthesized compounds, compound *N'*-(4-(pyridin-2-yl)piperazine-1-carbonothioyl)picolinohydrazoneamide (compound **6**) was selected for further study.

i) Ethidium bromide (EB)/ Acridine orange (AO) staining assay

PANC-1 cells were treated with 1 μ M of the compound **6** for 24 h in NDM, stained with ethidium bromide/acridine orange (EB/AO) reagent. Phase contrast microscopic observation of the treated cells showed a dramatic alteration in the PANC-1 cell morphology, including swelling, rupture of cell membranes, and disruption of cellular organelles.

ii) Western Blot Analysis

Further to check whether compound **6** modulated the key proteins involved in cell survival mechanisms western blot analysis was performed. A number of antiausterity agents have been found to inhibit Akt activation, leading to preferential cell death under nutrient deprived conditions (NDM). However, in present study, compound **6** was not found to inhibit p-Akt (S437) or p-Akt (T308), suggesting that Akt signaling is unlikely to be a major antitumor mechanism of 2-pyridineformamide thiosemicarbazone in PANC-1 cells. However, compound **6** was found to activate apoptosis, resulting in the cleavage of caspase-3 even at a very short exposure time of 4 h in a concentration dependent manner.

iii) Annexin V/PI staining assay

The evidence for apoptosis was further confirmed using an annexin V (AV) and propidium iodide (PI) staining assay. During apoptosis, alterations in the plasma membrane lead to the translocation of phosphatidylserine (PS), which is exposed at the external surface of the cell. AV specifically binds to the exposed PS, which is detected by green fluorescence. Pancreatic cancer cells are known to be resistant to apoptosis, which is one of the key reasons for the failure of chemotherapy, and lead to aggressive growth and metastasis. In the present study, apoptosis induced by compound **6** indicated that 2-pyridineformamide thiosemicarbazones are potential candidates for antipancreatic cancer drug development.

REFERENCES

1. IARC, WHO press release, 12 Dec **2013** (accessed Dec 15, 2013).
2. Shao, J.; Zhou, B.; Chu, B.; Yen, Y. *Mol. Cancer Ther.* **2006**, *5*, 586.
3. Moore, E. C.; Sartorelli, A. C. *Inhibitors of Ribonucleoside Diphosphate Reductase Activity*, Cory, J. G.; Cory, A. H., Pergamon Press; Oxford, **1989**, vol 12; p 203.
4. Brockman, R. W.; Thomson, J. R.; Bell, M. J.; Skipper, H. E. *Cancer Res.*, **1956**, *16*, 167.
5. French, F. A.; Blanz, E. J. Jr. *J. Med. Chem.* **1966**, *9*, 585.
6. Liu, M. C.; Lin, T. S.; Sartorelli, A. C. *Prog. Med. Chem.* **1995**, *32*, 1.
7. French, F. A.; Blanz, E. J. Jr. *J. Med. Chem.* **1966**, *26*, 1638.
8. DeConti, R. C.; Toftness, B. R.; Agrawal, K. C.; Tomchick, R.; Mead, J. A. R.; Bertino, J. R.; Sartorelli, A. C.; Creasey, W. A. *Cancer Res.* **1972**, *32*, 1455.
9. Yu, Y.; Wong, J.; Lovejoy, D. B.; Kalinowski, D. S.; Richardson, D. R. *Clin. Cancer Res.* **2006**, *12*, 6876.
10. Mackenzie, M. J.; Saltman, D.; Hirte, H.; Low, J.; Johnson, C.; Pond, G.; Moore, M. J. *Invest. New Drugs* **2007**, *25*, 553.
11. Knox, J. J.; Hotte, S. J.; Kollmannsberger, C.; Winqvist, E.; Fisher, B.; Eisenhauer, E. A. *Invest. New Drugs* **2007**, *25*, 471.

-
12. Ma, B.; Goh, B. C.; Tan, E. H.; Lam, K. C.; Soo, R.; Leong, S. S.; Wang, L. Z.; Mo, F.; Chan, A. T. C.; Zee, B.; Mok, T. *Invest. New Drugs* **2008**, *26*, 169.
 13. Karp, J. E.; Giles, F. J.; Gojo, I.; Morris, L.; Greer, J.; Johnson, B.; Thein, M.; Sznol, M.; Low, J. *Leuk. Res.* **2008**, *32*, 71.
 14. Domagk, G.; Behnisch, R.; Mietzsch, F.; Schmidt, H. *Naturwissenschaften*, **1946**, *33*, 315.
 15. E.A.B.M.R. Council, *Tubercle* **1963**, *44*, 301.
 16. Hamre, D., Bernstein, J., and Donovan, R. *Proc. Soc. Exp. Biol. Med.* **1950**, *73*, 275.
 17. Hamre, D., Brownlee, K.A., and Donovan, R. *J. Immunology* **1951**, *67*, 305.
 18. Bauer, D.J.; Kempe, C.H.; Downie, A.W. *Lancet* **1963**, *ii*, 494.
 19. Casas, J. S.; M. S. Garcia-Tasende; Sordo, J. *Coord. Chem. Rev.* **2000**, *209*, 197.
 20. Kizilcikli, I.; Ulkuseven, B.; Dasdemir, Y.; Akkurt, B. **2004**, *34*, 653.
 21. Mishra, D.; Naskar, S.; Michael, G.; Chattopadhyay, S. K. **2006**, *359*, 585.
 22. *IUPAC Nomenclature of Organic Compounds*, Panico, R., Powell, W. H., Richer, J. C., Eds; Blackwell, London; **1993**; p 105.
 23. Chattopadhyay, D.; Mazumdar, S. K.; Banerjee, T.; Sheldrick, W. S. *Acta Crystallogr., Sect. C: Crystallogr.* **1989**, *C45*, 314.

-
24. Palenik, G.J.; Rendle, D.F.; Carter, W.S. *Acta Crystallogr.* **1974**, *B30*, 2390.
 25. Bahr, G. V.; Schleizer, G. *Z. Anorg. Chem.* **1955**, *280*, 161.
 26. Tenorio, R. P.; Goes, A. J. S.; de Lima, J.G.; de Faria, A. R.; Alves, A. J.; Aquino, T. M. *Quim. Nova* **2005**, *28*, 1030.
 27. Scovill, J. P. *Phosphorus Sulfur Silicon* **1991**, *60*, 15.
 28. Van Koningsbruggen, P. J.; Haasnoot, J. G.; de Graalf, R. A. G.; Reedijk, J.; *Inorg. Chim. Acta.* **1995**, *234*, 87.
 29. Aguirre, M. C.; Borrás, J.; Castineiras, A.; Garcia, J. M.; Garcia, I.; Niclos, J.; West, D. X.; *Eur. J. Inorg. Chem.* **2006**, *6*, 1231.
 30. Steed, J. W.; Turner, D.R.; Wallace, K.J. *Core Concepts in Supramolecular Chemistry and Nanochemistry* Wiley: Chichester, **2007**.
 31. West, D. X.; Bain, G. A.; Butcher, R. J.; Jasinski, J. P.; Pozdniakiv, R. Y.; Lee, Y.; Valdes-Martines, J.; Toscano, R. A.; Hernandez-Ortega, S. *Polyhedron* **1996**, *15*, 665.
 32. Valdes-Martines, J.; Hernandez-Ortega, S.; West, D. X.; Stark, A. M.; Bain, G. *A. J. Chem. Crystallogr.* **1996**, *26*, 861.
 33. Valdes-Martines, J.; Hernandez-Ortega, S.; West, D. X.; Ives, J. S.; Bain, G. A. *Z. Kristallogr.* **1998**, *213*, 246.
 34. West, D. X.; Ahrweiler, P.; Ertem, G.; Scovill, J. P.; Klayman, D. L.; Flippen-Anderson, J. L.; Gilardi, R.; George, C.; Pannell, L. K. *Transition Met. Chem.* **1985**, *10*, 264.

-
35. Usman, A.; Razak, I. A.; Chantrapromma, S.; Fun, H. K.; Philip, V.; Sreekanth, A.; Kurup, M. R. P. *Acta Crystallogr., Sect. C: Cryst. Struct. Commun.* **2002**, C58, 652.
 36. Sreekanth, A.; Kurup, M. R. P. Synthesis, *Polyhedron* **2004**, 23, 969.
 37. Ketcham, K. A.; Swearingen, J. K.; Castineiras, A.; Garcia, I.; Bermejo, E.; West, D. X. *Polyhedron* **2001**, 20, 3265.
 38. Bermejo, E.; Castifieiras, A.; Fostiak, L. M.; Garcia, I.; Llamas-Saiz, A. L.; Swearingen, J. K.; West, D. X. *Z. Naturforsch., B: Chem. Sci.* **2001**, 56, 1297.
 39. Richardson, D. R.; Kalinowski, D. S.; Richardson, V.; Sharpe, P. C.; Lovejoy, D. B.; Islam, M.; Bernhardt, P. V. *J. Med. Chem.* **2009**, 52, 1459.
 40. Yu, Y.; Kalinowski, D. S.; Kovacevic, Z.; Siafakas, A. R.; Jansson, P. J.; Stefani, C.; Lovejoy, D. B.; Sharpe, P. C.; Bernhardt, P. V.; Richardson, D. R. *J. Med. Chem.* **2009**, 52, 5271.
 41. Pessoa, M. M. B.; Andrade, G. F. S.; Monteiro, V. R. P.; Temperini, M. L. A. *Polyhedron* **2001**, 20, 3133.
 42. Richardson, D. R.; Sharpe, P. C.; Lovejoy, D. B.; Senaratne, D.; Kalinowski, D. S.; Islam, M.; Bernhardt, P. V. *J. Med. Chem.* **2006**, 49, 6510.
 43. Kalinowski, D. S.; Sharpe, P. C.; Bernhardt, P. V.; Richardson, D. R. *J. Med. Chem.* **2007**, 50, 6212.
 44. Sartorelli, A. C.; Booth, B. A. *Cancer Res.* **1967**, 27, 1614.
 45. Sartorelli, A. C.; Agrawal, K. C.; Tsiftoglou, A. S.; Moore, E. C. *Adv. Enzyme Regul.* **1976**, 15, 117.
-

-
46. Mohan, M.; Kumar, M.; Kumar, A.; Madhuranath, P. H.; Jha, N. K. *J. Inorg. Biochem.* **1988**, *33*, 121.
 47. Joseph, M.; Kuriakose, M.; Kurup, M. R. P.; Suresh, E.; Kishore, A.; Bhat, S. G. *Polyhedron* **2006**, *25*, 61.
 48. Bernhardt, P. V.; Caldwell, L. M.; Chaston, T. B.; Chin, P.; Richardson, D. R. *J. Biol. Inorg. Chem.* **2003**, *8*, 866.
 49. Bernhardt, P. V.; Chin, P.; Sharpe, P. C.; Richardson, D. R. *Dalton Trans.* **2007**, *30*, 3232.
 50. Bernhardt, P. V.; Wilson, G. J.; Sharpe, P. C.; Kalinowski, D. S.; Richardson, D. R. *J. Biol. Inorg. Chem.* **2008**, *13*, 107.
 51. Klayman, D.L.; Scovill, J.P.; Bartosevich, J.F.; Bruce, J. *J. Med.Chem.* **1983**, *26*, 35.
 52. Johnson, C. W.; Joyner, J. W.; Perry, R. P. *Antibiotics & Chemotherapy* **1952**, *2*, 636.
 53. Dobek, A. S.; Klayman, D. L.; Dickson, E. T.; Scovill, J. P.; Tramont, E. C. *Antimicrob. Agents Chemother.* **1980**, *18*, 27.
 54. Usman, A.; Razak, I. A.; Chantrapromma, S.; Fun, H. K.; Sreekanth, A.; Sivakumar, S.; Kurup, M. R. P. *Acta. Crystallogr., Sect. C: Cryst. Struct. Commun.Cryst.* **2002**, *C58*, 461.
 55. Klayman, D. L.; Lin, A. J.; McCall, J. W.; Wang, S. Y.; Townson, S.; Grogl, M.; Kinnamon, K. E. *J. Med. Chem.* **1991**, *34*, 1422.

-
56. Shipman, C. Jr.; Smith, S. H.; Drach, J. C.; Klayman, D. L. *Antiviral Res.* **1986**, *6*, 197.
57. Mishra, V.; Pandeya, S. N.; Pannecouque, C.; Witvrouw, M.; De Clercq E. *Arch. Pharm. Pharm. Med. Chem.* **2002**, *335*, 183.
58. Padhye S.; Kauffman, G.B. *Coord. Chem. Rev.* **1985**, *63*, 127.
59. Agrawal, K. C.; Sartorelli, A. C. *Prog. Med. Chem.*; Ellis, G. P.; West, G.B., Eds.; Elsevier: Amsterdam, **1978**, *15*, 321.
60. Klayman, D. L.; Scovill, J. P.; Bartosevich, J. F.; Mason, C. J. *J. Med. Chem.* **1979**, *22*, 1367.
61. Jain, S. K.; Garg, B. S.; Bhoon, Y. K. *Spectrochim. Acta A* **1986**, *42*, 959.
62. Hu, W.; Zhou, W.; Xia, C.; Wen, X. *Bioorg. & Med. Chem. Lett.* **2006**, *16*, 2213.
63. Cerecetto, H.; Gonzalez, M. *Mini Rev. Med. Chem.* **2008**, *8*, 1355.
64. Donnici, C. L.; Araújo, M. H.; Oliveira, H. S.; Moreira, D. R. M.; Pereira, V. R. A.; Souza, M. de A.; De Castro, M. C. A. B.; Leite, A. C. L. *Bioorg. Med. Chem.* **2009**, *17*, 5038.
65. Rebolledo, A. P.; Vieites, M.; Gambino, D.; Piro, O. E.; Castellano, E. E.; Zani, C. L.; Souza-Fagundes, E. M.; Teixeira, L. R.; Batista, A. A.; Beraldo, H. J. *Inorg. Biochem.* **2005**, *99*, 698.
66. Bernhardt, P. V.; Sharpe, P. C.; Islam, M.; Lovejoy, D. B.; Kalinowski, D. S.; Richardson, D. R. *J. Med. Chem.* **2009**, *52*, 407.
-

-
67. Wilson, H. R.; Revankar, G. R.; Tolman, R. L. *J. Med. Chem.* **1974**, *17*, 760.
68. Casero, R. A., Jr.; Klayman, D. L.; Childs, G. E.; Scovill, J. P.; Desjardins, R. E. *Antimicrob. Agents Chemother.*, **1980**, *18*, 317.
69. Du, X.; Guo, C.; Hansell, E.; Doyle, P. S.; Caffrey, C. R.; Holler, T. P.; McKerrow, J. H.; Cohen, F. E. *J. Med. Chem.* **2002**, *45*, 2695.
70. Chibale, K.; Musonda, C. C. *Curr. Med. Chem.* **2003**, *10*, 1863.
71. Cohen, F.E.; Du, X.; Guo, Ch.; McKerrow, J. H.: US20056897240 (**2005**).
72. Greenbaum, D. C.; Mackey, Z.; Hansell, E.; Doyle, P.; Gut, J.; Caffrey, C. R.; Lehman, J.; Rosenthal, P. J.; McKerrow, J. H.; Chibale, K. *J. Med. Chem.* **2004**, *47*, 3212.
73. Fujii, N.; Mallari, J. P.; Hansell, E. J.; Mackey, Z.; Doyle, P.; Zhou, Y. M.; Gut, J.; Rosenthal, P. J.; McKerrow, J. H.; Guy, R. K. *Bioorg. Med. Chem. Lett.* **2005**, *15*, 121.
74. Leite, A.C.; de Lima, R.S.; Moreira, D.R.; Cardoso, M.V.; Gouveia de Brito, A.C.; Farias Dos Santos, L.M.; Hernandez, M.Z.; Kiperstok, A.C.; de Lima, R.S.; Soares, M.B. *Bioorg. Med. Chem.* **2006**, *14*, 3749.
75. Porcal, W.; Hernández, P.; Boiani, L.; Boiani, M.; Ferreira, A.; Chidichimo, A.; Cazzulo, J. J.; Olea-Azar, C.; González, M.; Cerecetto, H. *Bioorg. Med. Chem.* **2008**, *16*, 6995.
76. Otero, L.; Vieites, M.; Boiani, L.; Denicola, A.; Rigol, C.; Opazo, L.; Olea-Azar, C.; Maya, J. D.; Morello, A.; Krauth-Siegel, R. L.; Piro, O. E.; Castellano, E.; Gonzalez, M.; Gambino, D.; Cerecetto, H. *J. Med. Chem.* **2006**, *49*, 3322.
-

-
77. Pérez-Rebolledo, A.; Teixeira, L. R.; Batista, A. A.; Mangrich, A. S.; Aguirre, G.; Cerecetto, H.; González M.; Hernández, P.; Ferreira, A. M.; Speziali, N. L.; Beraldo, H. *Eur. J. Med. Chem.* **2008**, *43*, 939.
78. Vieites, M.; Otero, L.; Santos, D.; Toloza, J.; Figueroa, R.; Norambuena, E.; Olea-Azar, C.; Aguirre, G.; Cerecetto, H.; González, M.; Morello, A.; Maya, J. D.; Garat, B.; Gambino, D. *J. Inorg. Biochem.* **2008**, *102*, 1033.
79. Vieites, M.; Otero, L.; Santos, D.; Olea-Azar, C.; Norambuena, E.; Aguirre, G.; Cerecetto, H.; González, M.; Kemmerling, U.; Morello, A.; Diego Maya, J.; Gambino, D. *J. Inorg. Biochem.* **2009**, *103*, 411.
80. Duschak, V. G.; Couto, A. S. *Recent Patents on Anti-Infective Drug Discovery* **2007**, *2*, 19.
81. Duschak, V. G.; Couto, A. S. *Current Med. Chem.* **2009**, *16*, 3174.
82. Lessa, J. A.; Reis, D. C.; Mendes, I. C.; Speziali, N. L.; Rocha, L. F.; Pereira, V. R. A.; Melo, C. M. L.; Beraldo, H. *Polyhedron* **2011**, *30*, 372.
83. Klayman, D. L.; Bartosevich, J. F.; Griffin, T. S.; Mason, C. J.; Scovill, J. P. *J. Med. Chem.* **1979**, *22*, 855.
84. Biot, C.; Dessolin, J.; Ricard, I.; Dive, D. *J. Organomet. Chem.* **2004**, *689*, 4678.
85. Biot, C.; Pradines, B.; Sergeant, M.; Gut, J.; Rosenthal, P. J.; Chibale, K. *Bioorg. Med. Chem. Lett.* **2007**, *17*, 6434.
86. Scovill, J. P.; Klayman, D. L.; Lambros, C.; Childs, G. E.; Notsch, J. D. *J. Med. Chem.* **1984**, *27*, 87.
-

-
87. Chellan, P.; Naser, S.; Vivas, L.; Chibale, K., Smith, G. S. *J. Organometallic Chem.* **2010**, *695*, 2225.
 88. Khanye, S. D.; Gut, J.; Rosenthal, P. J.; Chibale, K.; Smith, G. S. *J. Organomet. Chem.* **2011**, *696*, 3296.
 89. Dobek, A. S.; Klayman, D. L.; Dickson, E. T., Jr.; Scovill, J. P.; Oster C. N. *Arzneimittelforschung* **1983**, *33*, 1583.
 90. Klayman, D. L.; Lin, A. J.; Hoch, J. M.; Scovill, J. P.; Lambros, C.; Dobek, A. S. *J. Pharm. Sci.* **1984**, *73*, 1763.
 91. Dobek, A. S.; Klayman, D. L.; Scovill, J. P.; Dickson, E. T. Jr. *Chemotherapy* **1986**, *32*, 25.
 92. Demertzi, K. D.; Demertzis, M. A.; Miller, J. R.; Papadopoulou, C.; Dodorou, C.; Filousis, G. *J. Inorg. Biochem.* **2001**, *86*, 555.
 93. Maiti, A.; Guha, A. K.; Ghosh, S. *J. Inorg. Biochem.* **1988**, *33*, 57.
 94. Dittes, U.; Diemer, R.; Lenz, O.; Keppler, B.K. *J. Inorg. Biochem.* **1995**, *59*, 215.
 95. Singh, S. K.; Pandeya, S. N. *Boll. Chim. Farm.* **2001**, *140*, 238.
 96. Kolocouris, A.; Dimas, K.; Pannecouque, C.; Witvrouw, M.; Foscolos, G. B.; Stamatiou, G.; Fytas, G.; Zoidis, G.; Kolocouris, N.; Andrei, G.; Snoeck, R.; De Clerq, E. *Bioorg. Med. Chem. Lett.*, **2002**, *12*, 723.
 97. Hoggarth, E.; Martin, A.R.; Storey, N.E.; Young, H.P. *Brit. J. Pharmacol* **1949**, *4*, 248.

98. Donovick, R.; Pansy, F.; Stryker, G.; Bernstein, J. *J. Bacteriol.* **1950**, *59*, 667.
99. Hamre, D.; Bernstein, J.; Donovick, R. *J. Bacteriol.* **1950**, *59*, 675.
100. Mascitelli-Coriandoli, E.; Maiocchi, G. *Igiene e sanita Pubblica* (Rome), **1955**, *11*, 11.
101. Sensi, P.; Grassi, G. G. *Burger's Medicinal Chemistry and Drug Discovery*, 6th Ed., Vol. 5, *Chemotherapeutic Agent*, Abraham, D. J., Ed.; John Wiley & Sons, Inc. **2003**, p 832.
102. Benns, B. G.; Gingras, B. A.; Bayley, C. H. *Appl. Microbiology* **1960**, *8*, 353.
103. Sensi, P. *Antimicrobial Agents*, In *Burger's Medicinal Chemistry and Drug Discovery* 6th Ed., Vol. 5: *Chemotherapeutic Agents*, Abraham, D.J., Ed.; John Wiley & Sons, Inc., **2003**, p 834.
104. Sriram, D.; Yogeeswari, P.; Basha, J. S.; Radha, D. R.; Nagaraja, V. *Bioorg. Med. Chem.* **2005**, *13*, 5774.
105. Sriram, D.; Yogeeswari, P.; Thirumurugan, R.; Pavana, R. K. *J. Med. Chem.* **2006**, *49*, 3448.
106. Sriram, D.; Yogeeswari, P.; Dhakla, P.; Senthilkumar, P.; Banerjee, D. *Bioorg. Med. Chem. Lett.* **2007**, *17*, 1881.
107. Güzel, Ö.; Karali, N.; Salman, A. *Bioorg. Med. Chem.* **2008**, *16*, 8976.
108. Merlani, M. I.; Amiranashvili, L. Sh.; Mulkidzhanyan, K. G.; Shelar, A. R.; Manvi, F. V. *Chem. Nat. Comp.* **2008**, *44*, 618.

109. Bermudez, L. E.; Reynolds, R.; Kolonoski, P.; Aralar, P.; Inderlied, C. B.; Young, L. S. *Antimicrob. Agents Chemother.* **2003**, *47*, 2685.
110. Tute, M. S. *Adv. Drug Res.* **1971**, *6*, 1.
111. Pavan, F. R.; Maia, P. I. da S.; Leite, S. R. A.; Deflon, V. M.; Batista, A. A.; Sato, D. N.; Franzblau, S. G.; Leite, C. Q. F. *Eur. J. Med. Chem.* **2010**, *45*, 1898.
112. Thimmaiah, K. N.; Chandrappa, G. T.; Lloyd, W. D.; Parkanyi, C. *Trans. Met. Chem.* **1985**, *10*, 299.
113. Parwana, H. K.; Singh, G. *Inorg. Chim. Acta* **1985**, *108*, 87.
114. West, D. X.; Carlson, C. S.; White, A. C.; Liberta, A. *Transition Met. Chem.* **1990**, *15*, 43.
115. West, D. X.; White, A. C.; Sharif, F. D.; Gebremedhin, H.; Liberta, A. E. *Transition Met. Chem.* **1993**, *18*, 238.
116. West, D. X.; Carlson, C. S.; Liberta, A. E.; Albert, J. N.; Daniel, C. R. *Transition Met. Chem.* **1990**, *15*, 341.
117. Bermejo, E.; Caballo, R.; Castiñeras, A.; Domínguez, R.; Liberta, A. E.; Maichle-Mössmer, C.; Salberg, M. M.; West, D. X. *Eur. J. Inorg. Chem.* **1999**, *54*, 965.
118. West, D. X.; Ives, J.; Krejci, J.; Salberg, M.; Zumbahlen, T. L.; Bain, G. A.; Liberta, A. E.; Valdes-Martinez, J.; Hernandez-Ortega, S.; Toscano, R. A. *Polyhedron* **1995**, *14*, 2189.

119. West, D. X.; Yang, Y.; Klein, T. L.; Goldberg, K. I.; Liberta, A. E. *Polyhedron* **1995**, *14*, 3051.
120. Opletlová, V.; Kalinowski, D. S.; Vejsová, M.; Kuneš, J.; Pour, M.; Jampílek, J.; Buchta, V.; Richardson, D. R. *Chem. Res. Toxicol.* **2008**, *21*, 1878.
121. Thompson, R. L.; Minton, S. A., Jr.; Officer, J. E.; Hitchings, G. H. *J. Immunol.* **1953**, *70*, 229.
122. Thompson, R. L.; Davis, J.; Russell, P. B.; Hitchings, G. H. *Soc. Exp. Biol. Med.* **1953**, *84*, 496.
123. Heiner, G. G.; Fatima, N.; Russell, P. K.; Haase, A. T.; Ahmad, N.; Mohammed, N.; Thomas, D. B.; Mack, T. M.; Khan, M. M.; Knatterud, G. L.; Anthony, R. L.; McCrumb, F. R., Jr. *Am. J. Epidemiol.* **1971**, *94*, 435.
124. Ronen, D.; Nir, E.; Teitz, Y. *Antiviral Research* **1985**, *5*, 249.
125. Teitz, Y.; Ronen, D.; Vansover, A.; Stematsky, T.; Riggs, J. L. *Antiviral Research* **1994**, *24*, 305.
126. Sidwell, R. W.; Arnett, G.; Dixon, G. J.; Schabel, F. M., Jr. *Proc. Soc. Exp. Biol. Med.* **1969**, *13*, 1223.
127. Brockman, R. W.; Sidwell, R. W.; Arnett, G.; Shaddix, S. *Proc. Soc. Exp. Biol. Med.* **1970**, *133*, 609.
128. Shipman, C., Jr.; Smith, S. H.; Drach, J. C.; Klayman, D. L. *Antimicrob. Agents Chemother.* **1981**, *19*, 682.
129. Turk, S. R.; Shipman, C.; Drach, J. C. *Biochem. Pharmacol.* **1986**, *35*, 1539.

130. Bal, T. R.; Anand, B.; Yogeeswari, P.; Sriram, D. *Bioorg. Med. Chem. Lett.* **2005**, *15*, 4451.
131. French, F. A.; Blanz, E. J., Jr. *Cancer Res.* **1965**, *25*, 1454.
132. Agrawal, K. C.; Sartorelli, A. C. *J. Med. Chem.* **1969**, *12*, 771.
133. Blanz, E. J., Jr.; French, F. A. *J. Med. Chem.* **1968**, *28*, 2419.
134. French, F. A.; Blanz, E. J., Jr.; DoAmaral, J. R.; French, D. A. *J. Med. Chem.* **1970**, *13*, 1124.
135. Creasey, W. A.; Agrawal, K. C.; Capizzi, R. L.; Stinson, K. K.; Sartorelli, A. C. *Cancer Res.* **1972**, *32*, 565.
136. Krakoff, I. H.; Etcubanas, E.; Tan, C.; Mayer, K.; Bethune, V.; Burchenal, J. H. *Cancer Chemother. Rep.* **1974**, *58*, 207.
137. Richardson, D. R. *Crit. Rev. Oncol. Hematol.* **2002**, *42*, 267.
138. Kolberg, M.; Strand, K. R.; Graff, P.; Kristoffer Andersson, K. *Structure, Biochim. Biophys. Acta.* **2004**, *1699*, 1.
139. Liu, M. C.; Lin, T. S.; Sartorelli, A. C. *J. Med. Chem.* **1992**, *35*, 3672.
140. Wang, Y.; Liu, M. C.; Lin, T. S.; Sartorelli, A. C. *J. Med. Chem.* **1992**, *35*, 3667.
141. Finch, R. A.; Liu, M.-C.; Cory, A. H.; Cory, J. G.; Sartorelli, A. C. *Adv. Enzyme Reg.* **1999**, *39*, 3.

142. Finch, R. A.; Liu, M.-C.; Grill, S. P.; Rose, W. C.; Loomis, R.; Vasquez, K. M.; Cheng, Y. C.; Sartorelli, A. C. *Biochem. Pharmacol.* **2000**, *59*, 983.
143. Chaston, T. B.; Lovejoy, D. B.; Watts, R. N.; Richardson, D. R. *Clin. Cancer Res.* **2003**, *9*, 402.
144. Antholine, W.; Knight, J.; Whelan, H.; Petering, D. H. *Mol. Pharmacol.* **1977**, *13*, 89.
145. Becker, E.; Richardson, D. R. *J. Lab. Clin. Med.* **1999**, *134*, 510.
146. Richardson, D. R. *J. Lab. Clin. Med.* **2001**, *137*, 324.
147. Lovejoy, D. B.; Richardson, D. R. *Blood* **2002**, *100*, 666.
148. Attia, S.; Kolesar, J.; Mahoney, M. R.; Pitot, H. C.; Laheru, D.; Heun, J.; Huang, W.; Eickhoff, J.; Erlichman, C.; Holen, K. D. *Invest New Drugs* **2008**, *26*, 369.
149. Yuan, J.; Lovejoy, D. B.; Richardson, D. R. *Blood* **2004**, *104*, 1450.
150. Becker, E. M.; Lovejoy, D. B.; Greer, J. M.; Watts, R. N.; Richardson, D. R. *Br. J. Pharmacol.* **2003**, *138*, 819.
151. Whitnall, M.; Howard, J.; Ponka, P.; Richardson, D. R. *Proc. Natl. Acad. Sci. U.S.A.* **2006**, *103*, 14901.
152. Lovejoy, D. B.; Sharp, D. M.; Seebacher, N.; Obeidy, P.; Prichard, T.; Stefani, C.; Basha, M. T.; Sharpe, P. C.; Jansson, P. J.; Kalinowski, D. S.; Bernhardt, P. V.; Richardson, D. R. *J. Med. Chem.* **2012**, *55*, 7230.
153. Whitnall, M.; Richardson, D. R. *Sem. Pediatric Neurology* **2006**, *13*, 186.
-

-
154. Kovacevic, Z.; Chikhani, S.; Lovejoy, D. B.; Richardson, D. R. *Mol. Pharmacol.* **2011**, *80*, 598.
155. Kalinowski, D. S.; Richardson, D. R. *Pharmacol. Rev.* **2005**, *57*, 547.
156. Richardson, D. R.; Kalinowski, D. S.; Lau, S.; Jansson, P. J.; Lovejoy, D. B. *Biochim. Biophys. Acta* **2009**, 1790, 702.
157. Kalinowski, D. S.; Yu Y; Sharpe, P. C.; Islam, M.; Liao, Y. T.; Lovejoy, D. B.; Kumar, N.; Bernhardt, P. V.; Richardson, D. R. *J. Med. Chem.* **2007**, *50*, 3716.
158. Yu, Y.; Rahmanto, Y. S.; Richardson, D. R. *Br. J. Pharmacol.* **2012**, *165*, 148.
159. Stariat, J.; Kovarikova, P.; Klimes, J.; Lovejoy, D. B.; Kalinowski, D. S.; Richardson, D. R. *J. Chromatogr. B. Analyt. Technol. Biomed. Life Sci.* **2009**, *877*, 316.
160. Agrawal, K. C.; Mooney, P. D.; Sartorelli, A. C. *J. Med. Chem.* **1976**, *19*, 970.
161. Serda, M.; Kalinowski, D. S.; Mrozek-Wilczkiewicz, A.; Musiol, R.; Szurko, A.; Ratuszna, A.; Pantarat, N.; Kovacevic, Z.; Merlot, A. M.; Richardson, D. R.; Polanski, J. *Bioorg. Med. Chem. Lett.* **2012**, *22*, 5527.
162. Buss, J. L.; Greene, B. T.; Turner, J.; Torti, F. M.; Torti, S. V. *Curr. Top. Med. Chem.* **2004**, *4*, 1623.
163. Li, Q. Y.; Zu, Y. G.; Shi, R. Z.; Yao, L. P. *Curr. Med. Chem.* **2006**, *13*, 2021.
164. Liberta, A. E.; West, D. X. *Biometals* **1992**, *5*, 121.
165. West, D. X.; Ooms, C. E.; Saleda, J. S.; Gebremedhin, H.; Liberta, A. E. *Trans. Met. Chem.* **1994**, *19*, 553.
-

166. Miller, M. C.; Stineman, C. N.; Vance, J. R.; West, D. X.; Hall, I. H. *Anticancer Res.* **1998**, *18*, 4131.
167. Castineiras, A.; Garcia I.; Bermejo, E.; West D. X. *Polyhedron* **2000**, *19*, 1873.
168. Mendes, I. C.; Moreira, J.P.; Ardisson, J.D.; Santos, R.G.; da Silva, P.R.; Garcia, I.; Castiñeiras, A.; Braldo, H. *Eur J Med Chem* **2008**, *43*, 1454.
169. Mendes, I. C.; Costa, F.B.; de Lima, G.M.; Ardisson, J. D.; Garcia-Santos, I.; Castiñeiras, A.; Beraldo, H. *Polyhedron* **2009**, *28*, 1179.
170. Graminha, A. E.; Vilhena, F. S.; Batista, A. A.; Louro, S. R.W.; Ziolli, R. L.; Teixeira, L. R.; Beraldo, H. *Polyhedron* **2008**, *27*, 547.
171. Ferraz, K. O.; Wardell, S. M. S. V.; Wardell, J. L.; Louro, S. R.W.; Beraldo, H.; *Spectrochimica Acta Part A* **2009**, *73*, 140.
172. Mendes, I. C.; Soares, M. C.; dos Santos, R. G.; Pinheiro, C.; Beraldo, H. *Eur. J. Med. Chem.* **2009**, *44*, 1870.
173. Bastos T. T. de L.; Soares, B. M.; Cisalpino, P. S.; Mendes, I. C.; dos Santos, R. G.; Beraldo, H.; *Microbiol. Res.* **2010**, *165*, 573.
174. Pal, S.; Barik, A. K.; Aich, P.; Peng, S.M.; Lee, G. H.; Kar, S. K. *Struct. Chem.* **2007**, *18*, 149.
175. Mullar, A.; Krebs, B. *Sulfur, its singnificance for chemistry, for the geo- and comosphere and technology, Studies in organic chemistry*, Elsevier Sciences Publishers: Amsterdam, **1984**, vol 5.
176. Panja, A.; Campana, C.; Leavitt, C.; van Stipdonk, M. J.; Eichhorn, D. M. *Inorg. Chim. Acta* **2009**, *362*, 1348.

-
177. Lim, S. C.; Price, K. A.; Chong, S. F.; Paterson, B. M.; Caragounis, A.; Barnham, K. J.; Crouch, P. J.; Peach, J. M.; Dilworth, J. R.; White, A. R.; Donnelly, P. S. *J. Biol. Inorg. Chem.* **2010**, *15*, 225.
178. Lim, S. C.; Paterson, B. M.; Fodero-Tavoletti, M. T.; O'Keefe, G. J.; Cappai, R.; Barnham, K. J.; Villemagne, V. L.; Donnelly, P. S. *Chem. Commun.* **2010**, *46*, 5437.
179. Yu, M. D.; Green, M. A.; Mock, B. H.; Shaw, S.M. *J. Nucl. Med.* **1989**, *30*, 920.
180. Anderson, C. J.; Welch, M. J. *J. Chem. Rev.* **1999**, *99*, 2219.
181. Takahashi, N.; Fujibayashi, Y.; Yonekura, Y.; Welch, M. J.; Waki, A.; Tsuchida, T.; Sadato, N.; Sugimoto, K.; Itoh, H. *Ann. Nucl. Med.* **2000**, *14*, 323.
182. Lewis, J. S.; Sharp, T. L.; Laforest, R.; Fujibayahsi Y.; Welch, M. J. *J. Nucl. Med.* **2001**, *42*, 655.
183. Lewis, J. S.; Laforest, R.; Buettner, T. L.; Song, S. K.; Fujibayahsi, Y.; Connet J. M.; Welch, M. J. *Proc. Natl. Acad. Sci. USA*, **2001**, *98*, 1206.
184. Cowley, A. R.; Dilworth, J. R.; Donnelly, P. S.; Labisbal E.; Sousa, A. *J. Am. Chem. Soc.* **2002**, *124*, 5270.
185. Borges, R.H.U.; Paniago, E.; Beraldo, H. *J. Inorg. Biochem.* **1997**, *65*, 268.
186. Nicolaou, A.; Waterfield, C.; Kenyon, S.; Gibbons, W.; Kepper, E. *Eur. J. Biochem.* **1997**, *244*, 8876.
187. Southerland, R. M. *Science* **1988**, *240*, 178.
188. Helmlinger, G.; Yuan, F.; Dellian, M.; Jain, R. K. *Nat. Med.* **1997**, *3*, 177.
-

189. Dang, C.V.; Semenza, G.L. *Trends Biochem. Sci.* **1999**, *24*, 68.
190. Izuishi, K.; Kato, K.; Ogura, T.; Kinoshita, T.; Esumi, H. *Cancer Res.* **2000**, *60*, 6201.
191. Lu, J.; Kunimoto, S.; Yamazaki, Y.; Kaminishi, M.; Esumi, H. *Cancer Sci.* **2004**, *95*, 547.
192. Esumi, H.; Lu, J.; Kurashima, Y.; Hanaoka, T. *Cancer Sci.* **2004**, *95*, 685.
193. Yuan, H. Studies on The Chemistry of Paclitaxel, Ph.D. Dissertation, Virginia Polytechnic Institute and State University, Blacksburg, Virginia **1998**.
194. Hall, I. H.; Lackey, C. B.; Kistler, T. D.; Durham, R. W., Jr.; Jouad, E. M.; Khan, M.; Thanh, X. D.; Djebbar-Sid, S.; Benali-Baitich, O.; Bouet, G. M. *Pharmazie* **2000**, *55*, 937.
195. Ludwig, J. A.; Szakács, G.; Martin, S. E.; Chu, B. F.; Cardarelli, C.; Sauna, Z. E.; Caplen, N. J.; Fales, H. M.; Ambudkar, S. V.; Weinstein, J. N. *Cancer Res.* **2006**, *66*, 4808.
196. Wu, C.; Shukla, S.; Calcagno, A. M.; Hall, M. D.; Gottesman, M. M.; Ambudkar, S. V. *Mol. Cancer Ther.* **2007**, *6*, 3287.
197. Thelander, L.; Reichard, P. *Annu. Rev. Biochem.* **1979**, *48*, 136.
198. Nelson, D. L.; Cox, M. M. *Lehninger Principles of Biochemistry*, 5th ed.; W. H. Freeman and Company, **2008**.
199. Weber, G. *Cancer Res.* **1983**, *43*, 3466.

-
200. Eklund, H.; Uhlin, U.; Farnegardh, M.; Logan, D. T.; Nordlund, P. *Prog. Biophys. Mol. Biol.* **2001**, *77*, 177.
201. Michael, W. K. The medical biochemistry page; <http://the.medicalbiochemistrypage.org>, (accessed Nov 28, **2011**).
202. Chitambar, C. R.; Matthaeus, W. G.; Antholine, W. E.; Graff, K.; O'Brien, W. *J. Blood* **1988**, *72*, 1930.
203. Matesanz, A. I.; Souza, P. *Mini-Rev. Med. Chem.* **2009**, *9*, 1389.
204. French, F. A.; Blanz, E. J., Jr.; Shaddix, S. C.; Brockman, R. W. *J. Med. Chem.* **1974**, *17*, 172.
205. Yu, Y.; Rahmanto, Y. S.; Hawkins, C. L.; Richardson, D. R.; *Mol. Pharmacol.* **2011**, *79*, 921.
206. Saryan, L. A.; Ankel, E.; Krishnamurti, C.; Petering, D. H. *J. Med. Chem.* **1979**, *22*, 1218.
207. Preidecker, P. J.; Agrawal, K. C.; Sartorelli, A. C.; Moore, E. C. *Mol. Pharmacol.* **1980**, *18*, 507.
208. Moore, E. C.; Sartorelli, A. C. *Pharmac. Ther.* **1984**, *24*, 439.
209. Thelander, L.; Graslund, A. *J. Biol. Chem.* **1983**, *258*, 4063.
210. Nyholm, S.; Mann, G. J.; Johansson, A. G.; Bergeron, R. J.; Graeslund, A.; Thelander, L. *J Biol Chem.* **1993**, *268*, 26200.
211. Cooper, C.E.; Lynagh, G. R.; Hoyes, K. P.; Hider, R. C.; Cammack, R.; Porter, J. B. *J. Biol. Chem.* **1996**, *271*, 20291.
-

-
212. Green, D. A.; Antholine, W. E.; Wong, S. J.; Richardson, D. R.; Chitambar, C. R. *Clin. Cancer Res.* **2001**, *11*, 2574.
213. Dilovic, I.; Rubcic, M.; Vrdoljak, V.; Kraljevic, P. S.; Kralj, M.; Piantanida, I.; Cindric, M. *Bioorg. Med. Chem.* **2008**, *16*, 5189.
214. Hancock, C. N.; Stockwin, L. H.; Han, B.; Divelbiss, R. D.; Jun, J. H.; Malhotra, S. V.; Hollingshead, M. G.; Newton, D. L. *Free Radic. Biol. Med.* **2011**, *50*, 110.
215. Holmberg, B.; Psilanderhielm, B. *J. Prakt. Chem.* **1910**, *82*, 440.
216. Stanovnik, B.; Tisler, M. *J. Org. Chem.* **1960**, *25*, 2234.
217. Castineiras, A.; Garcia, I.; Bermejo, E.; West, D. X. *Z. Naturforsch* **2000**, *55b*, 511.
218. Armarego, W. L., Chai, C. L. L. *Purification of Laboratory Chemicals*, 6th ed.; Butterworth–Heinemann publications, **2009**, p 159.
219. Awale, S.; Nakashima, E. M. N.; Kalauni, S. K.; Tezuka, Y.; Kurashima, Y.; Lu, J.; Esumi, H.; Kadota, S. *Bioorg. Med. Chem. Lett.* **2006**, *16*, 581.
220. Bermejo, E.; Castineiras, A.; Garcia-Santos, I.; West, D. X. *Z. Anorg. Allg. Chem.* **2004**, *630*, 1096.
221. Garcia, I.; Bermejo, E.; El Sawaf, A. K.; Castineiras, A.; West, D. X. *Polyhedron* **2002**, *21*, 729.
222. Khan, S. A.; Asiri, A. M.; Al-Amry K.; Malik M. A. *The Scientific World Journal*, **2014**, <http://dx.doi.org/10.1155/2014/592375>.

-
223. Mostafa, M.M.; El-Hammid, A.; Shallaby M.; El-Asmay, A. A. *Transition Met. Chem.*, **1981**, *6*, 303.
224. West, D. X.; Liberta, A. E.; Padhye, S. B., Chikate, R. C.; Sonawane, P. B.; Kumbhar, A. S.; Yerande, R. G. *Coord. Chem. Rev.* **1993**, *123*, 49.
225. Philip, V.; Suni, V.; Kurup, M. R. P.; Nethaji, M. *Polyhedron*, **2006**, *25*, 1931.
226. Bindu, P.; Kurup, M. R. P.; Satyakeerty, T.R. *Polyhedron* **1999**, *18*, 321.
227. Beckford, F. A.; Shaloski, M. Jr.; Leblanc, G.; Thessing J.; Lewis-Alleyne, L. C.; Holder, A. A.; Li, L.; Seeram N. P.; *Dalton Trans.* DOI: 10.1039/b915081a, **2009**, 10757.
228. Afrasiabi, Z.; Sinn, E.; Kulkarni, P.; Ambike, V.; Padhye, S.; Deobagakar, D.; Heron, M.; Gabbutt, C.; Anson, C.; Powell, A. *Inorg. Chim. Acta* **2005**, *358*, 2023.
229. Philip, V.; Suni, V.; Kurup, M. R. P. *Acta Crystallogr. C60* **2004**, *08*, 56.
230. Wyrzykiewicz, E.; Prukah, D. *J. Heterocyclic Chem.* **1998**, *35*, 381.
231. Galic, N.; Peric, B.; Kojic-Prodic, B.; Cimerman, Z. *J. Mol. Struct.* **2001**, *559*, 187.
232. Demertzi, D. K.; Alexandratos, A.; Papageorgiou, A.; Yadav, P. N.; Dalezis P.; Demertzis M. A. *Polyhedron* **2008**, *27*, 2731.
233. West, D. X.; Tnientanavanich, I.; Liberta, A. E. *Transition Met. Chem.* **1995**, *20*, 303.

234. Ishiyama, M.; Shiga, M.; Sasamoto, K.; Mizoguchi, M.; He, P. G. *Chem. Pharm. Bull.* **1993**, *41*, 1118.
235. Mosmann, T.; *J. Immunol. Method*, **1983**, *65*, 55.
236. Asuthkar, S.; Rao, J. S.; Gon di, C. S. *Expert Opin. Invest. Drugs* **2012**, *21*, 143.
237. Hidalgo, M. N. *Engl. J. Med.* **2010**, *362*, 1605.
238. Sakamoto, H.; Kitano, M.; Suetomi, Y.; Maekawa, K.; Takeyama, Y.; Kudo, M. *Ultrasound Med. Biol.* **2008**, *34*, 525.
239. Awale, S.; Lu, J.; Kalauni, S. K.; Kurashima, Y.; Tezuka, Y.; Kadota, S.; Esumi, H. *Cancer Res.* **2006**, *66*, 1751.
240. Chandra, S.; Kumar, U. *Spectrochimica Acta Part A*, **2005**, *62*, 940.
241. Bermejo, E.; Casteneiras, A.; Dominguez, R.; Carballo, R.; Mossmer, C. M.; Strahle, J.; West, D. X. *Z. Anorg. Allg. Chem.* **1999**, *625*, 961.
242. El-Sawaf, A. K.; West, D. X., El-Saied, F. A.; El-Bahnasawy, R. M. *Transition Met. Chem.* **2006**, *23*, 649.
243. West, D.X.; Jasinski, I., Jasinski, J. M., Butcher, R. J. *Trans. Met. Chem.* **1998**, *23*, 209.
244. Lessa, J. A.; Mendes, I. C.; da Silva, P. R. O.; Soares, M. A. Santos, R. G.; Speziali, N. L.; Romeiro, N. C.; Barreiro, E. J.; Beraldo, H. *Eur. J. Med. Chem.* **2010**, *45*, 5671.

LIST OF PUBLICATIONS

1. Shakya, B.; Yadav, P. N. Synthesis and Characterization of 2-Pyridineformamide 3-Pyrrolidinyl Thiosemicarbazone, *J. Nep. Chem. Soc.*, **2012**, 29 (1), 28-33.
2. Shakya, B.; Adhikari, S.; Lamichhane, J.; Yadav, P. N. Synthesis of *N'*-(4-Methylpiperazine-1-carbonothioyl)picolinohydrazonamide as an Antineoplastic Agent, *J. Nep. Chem. Soc.*, **2013**, 32, 11-18.
3. Shakya, B.; Yadav, P. N.; Ueda, J-Y.; Awale, S. Discovery of 2-Pyridineformamide Thiosemicarbazones as Potent Antiausterity Agents, *Biorg. Med. Chem. Lett.*, **2014**, 24, 458-461.

LIST OF PRESENTATIONS

Oral Presentations

1. Synthesis and Characterization of *N*(4) Substituted 2-Pyridineformamide Thiosemicarbazones, Bhushan Shakya, Paras Nath Yadav; ***International Conference, Kathmandu Symposia on Advanced Materials (KαSAM-2012)***, Nepal Polymer Institute, Kathmandu, May 9-12, 2012.
2. Synthesis of *N*(4) Substituted 2-Pyridineformamide Thiosemicarbazones as Potential Antiausterity Agents, Bhushan Shakya, Paras Nath Yadav, Jun-ya Ueda, Suresh Awale ***Bangladesh Chemical Congress (BCC 2012)***, Bangladesh Chemical Society, Dhaka, December 07-09, 2012.
3. Synthesis of *N*{4-(Pyridin-2-yl)piperazine-1-carbonothioyl}picolinohydrazonamides and Their Preferential Cytotoxicity Against Human Pancreatic Cancer Cell Line, Bhushan Shakya, Paras Nath Yadav, Jun-ya Ueda, Suresh Awale ***Second International Conference, Kathmandu Symposia on Advanced Materials (KαSAM-2014)***, Nepal Polymer Institute, Kathmandu, September 7-10, 2014.
4. Discovery of 2-Pyridineformamide Thiosemicarbazones as Potent Antiausterity Agents Bhushan Shakya, Paras Nath Yadav, Jun-ya Ueda, Suresh Awale ***International Conference on Advanced Materials and Nanotechnology for Sustainable Development***, Nepal Chemical Society, Kathmandu, November 4-6, 2014.
5. Synthesis of 5-Fluoro and 6-Methyl-2-Pyridineformamide Thiosemicarbazones as Potent Preferentially Cytotoxic Agents Against Human Pancreatic Cancer, Bhushan Shakya, Paras Nath Yadav, Jun-ya Ueda, Suresh Awale ***The 16th International Symposium on Eco-Materials Processing and Design (ISEPD 2015)***, International Materials Society, Kathmandu, January 12-15, 2015.